NUMERICAL APPROXIMATIONS OF FRACTIONAL DIFFERENTIAL EQUATIONS: A CHEBYSHEV PSEUDO–SPECTRAL APPROACH

A THESIS SUBMITTED TO THE UNIVERSITY OF KWAZULU-NATAL

FOR THE DEGREE OF DOCTOR OF PHILOSOPHY

IN THE COLLEGE OF AGRICULTURE, ENGINEERING & SCIENCE

by

Ṣhina Daniel Ọlọniiju

School of Mathematics, Statistics and Computer Science

July 2020

To my best ever, my mum, M. B. Ajayi–Ọlọniiju.

To the loving memory of my dad, F. B. Ọlọniiju.

Preface

The work described in this thesis was carried out under the supervision of Prof. P. Sibanda and Dr. S. P. Goqo in the School of Mathematics, Statistics and Computer Science, College of Agriculture, Engineering and Science, University of KwaZulu-Natal, Pietermaritzburg from June 2018 to July 2020.

I hereby declare that except where due credit and reference is given, no portion of this work has been submitted wholly or in part for the award of any degree or qualification at this university or any other institution of learning.

[redacted] 15/02/2021

Ṣhina Daniel Ọlọniiju Date

[redacted] 16/02/2021

Prof. P. Sibanda Date

[redacted] 16/02/2021

Dr. S. P. Goqo Date

Declaration 1 – Plagiarism

I, **Ṣhina Daniel Ọlọniiju** declare that:

1. the work reported in this thesis, except where otherwise indicated or acknowledged, represents my original effort;
2. this thesis has not been submitted in full or in part for any degree or examination at any other university;
3. this thesis does not contain data, pictures, graphs or other information that belongs to someone else, unless specifically acknowledged;
4. this thesis does not contain other persons' writing, unless specifically acknowledged as being sourced from other researchers. Where other written sources have been quoted, then:
   (a) their words have been rewritten but the general information attributed to them has been referenced;
   (b) where their exact words have been used, their writing has been placed inside quotation marks, and duly referenced;
5. this thesis does not contain text, graphics or tables copied and pasted from the internet, unless specifically acknowledged, and the source being detailed in the thesis and in the References sections.

..... [redacted] ..... 15/02/2021 .....

Ṣhina Daniel Ọlọniiju Date

Declaration 2 – Publications

All the publications, which include publications in preparation, submitted, in press or published, that form part of or include research presented in this thesis are a combined efforts of all the authors. The first drafts of all these publications were written by the student under the supervision of Prof. P. Sibanda and Dr. S. P. Goqo

1. **Oloniiju, S.**, Goqo, S., & Sibanda, P. (2019). A Chebyshev Spectral Method for Heat and Mass Transfer in MHD Nanofluid Flow with Space Fractional Constitutive Model. Frontiers in Heat and Mass Transfer, 13, 19, 8 pages. http://dx.doi.org/10.5098/hmt.13.19.

2. **Oloniiju, S. D.**, Goqo, S. P., & Sibanda, P. (2020). A Chebyshev pseudo-spectral method for the multi–dimensional fractional Rayleigh problem for a generalized Maxwell fluid with Robin boundary conditions. Applied Numerical Mathematics, 152, 253–266. https://doi.org/10.1016/j.apnum.2019.12.001.

3. **Oloniiju, S.D.**, Goqo, S.P., Sibanda, P. (2020). A Chebyshev based spectral method for solving boundary layer flow of a fractional-order Oldroyd–B fluid. Mathematical Modelling of Engineering Problems, 7(3), 377–386. https://doi.org/10.18280/mmep.070307.

4. **Oloniiju, S. D.**, Nkomo, N. S., Goqo, S. P., & Sibanda, P. Shifted Chebyshev Spectral Method for Two–dimensional Space–time Fractional Partial Differential Equations. *Submitted* to Azerbaijan Journal of Mathematics.

5. **Oloniiju, S. D.**, Goqo, S. P., Sibanda, P. A Geometrically Convergent Pseudo–spectral Method for Multi–dimensional Two–sided Space Fractional Partial Differential Equations. *Submitted* to Journal of Applied Analysis and Computation.

6. **Oloniiju, S. D.**, Goqo, S. P., Sibanda, P. A Chebyshev Pseudo–spectral Method for the Numerical Solutions of Distributed Order Fractional Ordinary Differential Equations. *Submitted* to Applied Mathematics E–Notes.

7. **Oloniiju, S. D.**, Goqo, S. P., Sibanda, P. A Pseudo–spectral Method for Multidimensional Time Distributed Order Two–sided Space Fractional Differential Equations. *Submitted* to Applied Numerical Mathematics.

Ṣhina Daniel Ọlọniiju

15/02/2021

Date

Acknowledgments

I am most grateful to Almighty God, the giver of life, for His guidance and undeserved kindness throughout the period of this study.

Many thanks go to my supervisors Prof. P. Sibanda and Dr. S. P. Goqo. Their support, insightful comments and constructive criticism have fostered the success of this study. I would like to recognize and appreciate Prof. Sibanda's guidance, expertise and patience. Thank you for always keeping the door to your office open. I am grateful for the opportunity to be under your tutelage. I am so grateful for the time you took to read this thesis, and thank you for the constructive comments. I have not only gained scientific knowledge; I have also learnt to become better at scientific writing. I will forever be grateful to you and your wife for making South Africa feel like home to me.

I am appreciative of my co–supervisor's contribution to the success of this research. I am grateful for all your support, right from the moment you agreed to co–supervise my masters thesis. Thank you for not just being a co–supervisor, but also a friend and a mentor. I am grateful for your genuine and invaluable support.

I am grateful to the University of KwaZulu–Natal for providing fees remission, a conducive environment and the facilities needed during the period of this study. My sincere appreciation also goes to the academic staff of the School of Mathematics, Statistics and Computer Science, UKZN. To the school administrators, Ms. Barnard, Ms. Shangase and Ms. Bonhomme, thank you for taking the effort to make me comfortable throughout the course of my study.

To my mum and my siblings; Oluwasegunfunmi, Oluwakemisola and Oluwaseyifunmi, words alone cannot describe how grateful I am for your support; emotionally, morally and

spiritually. What and where would I be without you guys? I am indebted to you for your unwavering support and prayers. Thank you for listening to my frustrations and fears, and offering moral support. To my aunt, O. I. Fati, thanks for being such an amazing mentor, thank you for the academic advices. To my aunt, Mrs Osatuyi and her family, your love and support did not go unnoticed; I am sincerely grateful. To the rest of my uncles, aunts and cousins: I would not have made it this far without your love; thank you for being my family.

To my colleagues, and by extension my friends, in the School of Mathematics, Statistics and Computer Science, I say a huge *thanks* to all of you. My wholehearted thanks especially to Ibukun Oyelakin, Muyiwa Otegbeye, Izu Okoye–Ogbalu, Titi Agbaje and her family, Lolu Aluko, Alex Somto, Kevin Igwe, Fidelis Joseph, Hammed Ogunseye, Carlson and Nicolette Boucher, Nondumiso Mbhele, Precious Mtshatsha and my Sudanese friends, for making South Africa home to me; thank you for not making me feel the burn of being far from home. I am grateful to the AIMS–Ghana 2016 family, my friends Innocenter Amima, Suzy Maepe, Tolu Babalola, Micah Michael, Jeph Ojo, Ebenezer James, Abimbola Bamisaye and Eunice Iwakin, thank you for being such a pillar of moral support even though we are miles apart.

To everyone who was or has been part of my journey, I say, *ẹ ṣeun gán án*, thank you all.

Abstract

This study lies at the interface of fractional calculus and numerical methods. Recent studies suggest that fractional differential and integral operators are well suited to model physical phenomena with intrinsic memory retention and anomalous behaviour. The global property of fractional operators presents difficulties in finding either closed–form solutions or accurate numerical solutions to fractional differential equations. In rare cases, when analytical solutions are available, they often exist only in terms of complex integrals and special functions, or as infinite series. Similarly, obtaining an accurate numerical solution to arbitrary order differential equation is often computationally demanding. Fractional operators are non–local, and so it is practicable that when approximating fractional operators, non–local methods should be preferred. One such non–local method is the spectral method. In this thesis, we solve problems that arise in the flow of non–Newtonian fluids modelled with fractional differential operators. The recurrent theme in this thesis is the development, testing and presentation of tractable, accurate and computationally efficient numerical schemes for various classes of fractional differential equations. The numerical schemes are built around the pseudo–spectral collocation method and shifted Chebyshev polynomials of the first kind. The literature shows that pseudo–spectral methods converge geometrically, are accurate and computationally efficient. The objective of this thesis is to show, among other results, that these features are true when the method is applied to a variety of fractional differential equations. A survey of the literature shows that many studies in which pseudo–spectral methods are used to numerically approximate the solutions of fractional differential equations often to do this by expanding the solution in terms of certain orthogonal polynomials and then simultaneously solving for the coefficients of expansion. In this study, however, the orthogonality condition of the Chebyshev polynomials of the first kind and the Chebyshev–Gauss–Lobatto quadrature are used to numerically find the coefficients of the series expansions. This approach is

then applied to solve various fractional differential equations, which include, but are not limited to time–space fractional differential equations, two–sided fractional differential equations and distributed order differential equations. A theoretical framework is provided for the convergence of the numerical schemes of each of the aforementioned classes of fractional differential equations. The overall results, which include theoretical analysis and numerical simulations, demonstrate that the numerical method performs well in comparison to existing studies and is appropriate for any class of arbitrary order differential equations. The schemes are easy to implement and computationally efficient.

Keywords

Fractional calculus, pseudo–spectral method, fractional constitutive relations, Chebyshev polynomials of the first kind, Chebyshev–Gauss–Lobatto quadrature, one– and two–sided fractional differential equations, distributed order fractional differential equations, convergence analysis.

Contents

Chapter 1

Introduction

In this chapter, we give context to this thesis by reviewing literature concerned with the historical development of fractional calculus, applications of fractional operators and methods of solution of fractional differential equations. This chapter motivates the choice of the fractional operators and numerical technique used in this study, and provides a description of the main mathematical concepts on which Chapters 2 to 8 will draw. For the development of numerical schemes, we focus on the Chebyshev polynomials of the first kind.

1.1 Historical development of fractional calculus

The term calculus refers to the analysis of continual change or amassing of quantities [1]. Fractional calculus is the generalization of classical differential and integral calculus to arbitrary real order [2]. The study of infinitesimal calculus dates back to as early as 500 BC. However, the history of calculus of arbitrary order only goes back to the late seventeenth century. By the end of the nineteenth century, the theory of fractional derivatives and integrals had taken root, partially due to the work of Euler, Fourier, Grünwald, Heaviside, Lacroix, Laplace, Letnikov, Liouville and Riemann [3, 4]. It was during this period that Lacroix defined the nth derivative of the power function x^m, with m being a positive integer, using mathematical induction and the Gamma Γ function to generalize the factorial. The result obtained by Lacroix through induction is similar to that obtained through a differential operator, whose definition was later formalized by

Riemann and Liouville in their study of fractional operators [5, 6]. Lacroix's work focused on generalizing from integer to fractional orders.

Laplace and Fourier proposed the definition of derivatives of arbitrary order using their respective integral operators [3, 7]. Nonetheless, it was Liouville who made the first real progress on fractional calculus by successfully applying his definition to problems in potential theory [5]. Liouville assumed that the fractional derivative of a function can be expanded in series form and so extended known results for derivatives of integer order to real order. The result is now known as Liouville's first formula for fractional derivatives [3, 5]. However, this first formula has the disadvantage that the arbitrary order must be restricted to certain values for the series to converge. It was due to this limitation that Liouville proposed a second definition of a fractional differential operator using the Euler Gamma integral [3].

The theory of fractional integration was expanded in Riemann [6], through a generalization of Taylor's series. There are, however, disagreements over the inclusion of a complementary function in Riemann's definition. The most commonly used definition of integration of arbitrary order is Riemann's fractional integral without the complementary function [3]. The Riemann–Liouville fractional integral is, in fact, a result of the work of Sonin [8], Letnikov [9] and Laurent [10]. In fact, Laurent [10] obtained the Riemann–Liouville integral by applying contour integration to Cauchy's integral formula. The same representation of fractional integration was obtained by Nekrassov [11] and Krug [12]; albeit, using different integration contours. Unlike classical differentiation, fractional differentiation is defined through the fractional integral, which explains why most of the earlier work on fractional calculus is on fractional integral operators. This body of work culminated in the introduction of the Riemann–Liouville differential operator and later, the Grünwald–Letnikov derivative. Under certain conditions, the latter is equivalent to

the Riemann–Liouville definition.

The development of the theory of fractional operators was accelerated by Heaviside's application of fractional operators to the transmission of electrical current in cables [13]. Many other alternative definitions of fractional operators have been proposed, one of which is the Caputo fractional differential operator, whose Laplace transform does not contain limits of the fractional derivatives at the lower terminal [14, 15]. This limitation is often encountered when the Riemann–Liouville fractional differential operator is used. When the Laplace transform of the Riemann–Liouville operator is taken, it often leads to differential equations with initial or boundary conditions that contain limits of the Riemann–Liouville fractional derivative. During the early development of the theory of fractional calculus, it was assumed that no physical interpretation can be given for such initial conditions, and so the solutions of such differential equations are meaningless and impractical, even if they can be solved mathematically [2]. However, recent development in applied fractional calculus has shown that differential equations with such non–local boundary conditions often emerge in applied sciences, especially in the quasi–static theory of thermoelasticity and reaction–diffusion [16, 17]. Other limitations of the Riemann–Liouville fractional differential operator include the existence of a singularity at the lower terminal of the fractional derivatives of certain functions, such as the Mittag–Leffler and exponential functions, which limit the scope of application of the Riemann–Liouville operator in modelling physical and engineering processes. The Caputo derivative, on the other hand, also have its limitations, one of which is, as in the Riemann–Liouville derivative, the use of power–law kernel which sometimes cannot model the heterogeneities found in many physical phenomena.

Recently, Caputo and Fabrizio [18] introduced a new definition of a fractional derivative, which makes use of a non–singular exponential kernel. It was suggested that the new

definition could model material heterogeneities and fluctuations at different scales. These heterogeneities and fluctuations cannot normally be modelled by fractional models with singular kernels [19]. Atangana and Baleanu [20] have extended the Caputo–Fabrizio definition to a more general form. The differential operator introduced in Atangana and Baleanu [20] is a convolution of the generalized Mittag–Leffler function and the classical derivative of the given function [21]. Despite the nuances that distinguish these various fractional differential operators, one distinctive feature among them is that their definitions all depend on classical calculus.

1.1.1 Applications of fractional calculus

Following Heaviside's studies on the applications of fractional calculus to the transmission of electrical currents, research into applications of fractional calculus remained dormant for nearly a century. This is, in part, due to the theory of fractional calculus being considered mainly from a purely theoretical perspective. It was Oldham and Spanier [4] who, in 1974, considered applications of fractional calculus to fields such as physics, engineering and chemistry. The field of applied fractional calculus has subsequently grown tremendously since then. For instance, Caputo [22] applied fractional calculus to study the flow of fluids in porous media, by modifying Darcy's law to introduce a memory term with arbitrary order derivative to capture the effect of reducing permeability over time. This was done by replacing the permeability–fluid viscosity ratio with a time fractional order derivative and pseudo–permeability; an approach that had been used a century before by Boltzmann [23] for heat flow models. In Caputo and Fabrizio [18], fractional derivatives with a temporal exponential kernel and spatial Gaussian kernel for both Laplacian and gradient operators were applied to the linear solid model that had been introduced for elasticity by Zener and Siegel [24] and Cole and Cole [25] in their electromagnetism model. The standard linear solid model was generalized to include memory terms by replacing classical derivatives with derivatives of arbitrary order in Caputo and Mainardi [26]. The

theoretical result from the fractional model proposed by Caputo and Mainardi [26] was found to be consistent with experimental data.

The idea of replacing the classical Fick's law by a formulation involving fractional derivatives was introduced in the study by Oldham and Spanier [27], in which, they suggested that introducing half–derivatives into the concentration conservation equation allows the concentration of electroactive species at the surface of an electrode to be correlated with the current density. It was found that this correlation is not restricted to a diffusion–modulated system and is true regardless of the degree of reversibility of the reaction. Jumarie [28] proposed a Malthusian growth model with arbitrary order random growth rate, in which the birth and death rates, and Poissonian processes are obtained as differential equations of fractional orders.

Following the introduction of Atangana and Baleanu's [20] derivative, the fractional differential operator as well as the Caputo [14] and Caputo–Fabrizio [18] operators were applied to chaotic and hyperchaotic systems; namely, the Labyrinth attractor in Atangana and Araz [29]. In the study, it was shown that the numerical results obtained for each of the operator are equivalent. A similar study was carried out in Riaz et al. [30], though in this case, the fractional differential operators were applied to heat and mass transfer in a generalized MHD Oldroyd–B fluid subjected to ramped wall temperature boundary conditions. The model equations used by Riaz et al. were shown to be equivalent to the classical model under appropriate conditions and certain asymptotic behaviours. The theoretical framework for a time fractional Keller–Segel model of chemotaxis with the Mittag–Leffler kernel was proposed in Atangana and Alqahtani [31]. This model captures the metamorphosis that occur during the diffusion process. Further, the fractional model does not only describe the change in state but also encapsulates the non–local fading memory of the diffusion process. Atangana and his colleagues have extended the use of

the Atangana–Baleanu fractional operator to models in neurobiology [32], autocatalytic reaction networks [33], groundwater transport [34] and disease dynamics [35, 36].

In diffusion processes, the theory of fractional calculus has been used to describe anomalous diffusion; a phenomenon that is usually observed in cell migration, continuous time random walks, turbulent plasma transport, long range correlations, photon diffusion and so on. The term 'anomalous diffusion' describes a process where there is a nonlinear relationship between time t and the mean square displacement σ^2 [37–39]. The anomalous diffusion is characterized by a power–law term $\sigma_r^2(t) \sim t^\alpha$. For $\alpha < 1$, there is subdiffusion, which is, diffusion that is slower than typical diffusion, while for $1 < \alpha < 2$, there is superdiffusion or fast diffusion [38]. In her study, Beghin [38] investigated some augmentations of the space fractional diffusion equations using the Riesz–Feller exponential and the Riesz logarithmic differential operators [40].

Jacobs and Harley [41] applied a time–fractional diffusion equation to binarize noisy grayscale images. The study examined a two–dimensional time–fractional diffusion equation with a nonlinear source term on a bounded domain with both Dirichlet and Neumann boundary conditions. The study suggested that the time fractional order defined in the domain $(0, 1]$ can serve as a control parameter in image binarization, and that the smaller value of the fractional order increases the brightness of the image background. A review of diffusion–advection and Fokker–Planck type equations of arbitrary order was carried out by Metzler and Klafter [42]. Other domains of application of fractional calculus include, but are not limited to, heat and mass transfer, viscoelasticity and wave propagation [43, 44].

1.1.2 Analytic and semi–analytic methods of solution

In light of the non–locality associated with fractional differential equations, it is typical that numerical methods are used to obtain solutions. However, some closed–form solutions to

arbitrary order differential equations have been found. For example, El-Kahlout et al. [45] derived the exact solution of a time fractional partial differential equation in terms of the complementary error function and the H–function using the Laplace transform as well as the Mellin transform. In Damor et al. [46], Laplace–Fourier transforms were used to find the solutions of space–time fractional Penes bioheat equations. Analytical solutions of special cases of the equation were obtained in terms of the Fox H–function. Pandir and Gurefe [47] obtained analytical solutions to the generalized fractional Zakharov–Kuznetsov equation using a travelling wave transformation and the extended trial equation method, while Pandir et al. [48] used the same approach for the time fractional nonlinear dispersive Korteweg–de Vries equation. The differential transform method was used in Arikoglu and Ozkol [49] to find closed–form solutions of some fractional differential equations such as the Bagley–Torvik, Ricatti and the composite fractional oscillation differential equations. Momani et al. [50] introduced the generalized differential transform method, which is a generalization of Taylor's expansion. This method has been extensively applied to different classes of fractional differential equations by Odibat and his collaborators [51–55].

Other methods that have been used to obtain closed–form solutions of fractional differential equations include, but are not limited to, the Adomian decomposition method, variational iteration method, fractional complex transform and exp–function method [56–60]. For instance, Jafari and Jassim [61] derived the exact solutions of coupled fractional partial differential equations using the local fractional variational iteration method. In Jafari et al. [62], the same method was used to obtain closed–form solution of the three–dimensional fractional diffusion model. The solution is identical to that obtained using the local fractional reduced differential transform method given in the same study. Some decomposition methods were used on time–fractional Klein–Gordon equation in Jafari [63]. The closed–form solutions were obtained as truncated series and/or in terms of special functions such as the one parameter Mittag–Leffler function. The methods are

effective and can be used to obtain analytical solutions of various fractional equations, although, treating nonlinearity might be tedious, or in some cases, impossible. A common feature of analytical solutions of differential equations of arbitrary order is the inclusion of special functions, special integrals and infinite series, which in certain instances, can be too elaborate for practical purpose.

A hybrid method for time–fractional differential equations, comprising the Laplace transform and compact finite difference method, was proposed in Jacobs [64]. The solution is semi–analytic, being continuous in time and discrete in the spatial dimension. On the one hand, the compact finite difference, which was applied to the spatial domain, is of fourth order convergence. On the other hand, results from the study indicated that the temporal convergence rate is geometric. The image binarization time–fractional diffusion model studied in Jacobs and Harley [41] was solved using a hybridization of the Laplace transform, Chebyshev collocation and quasilinearization methods. This hybrid technique had been used in earlier studies by Jacobs and Harley [65, 66]. In the earlier studies, the time–fractional derivative was evaluated using the Laplace transform and numerically inverted through a technique that had been proposed by Weideman and Trefethen [67], which defined an integral contour that maps the complex time domain of the Bromwich integral to a real space. The integral was then evaluated using the trapezoidal rule. The nonlinear term in the diffusion equation was linearized using the quasilinearization technique, and the equation was discretized using the Chebyshev collocation. The resulting solution is semi–analytic; being discrete in space and continuous in time. The use of the Laplace transform for the time derivative ensures that no error is incurred during algebraic representation of the temporal derivative. The error in the temporal dimension is attributable to the approximation of the inversion integral. Compared to time marching schemes, such as the Grünwald–Letnikov discretization, the computational time of the method is small, and unlike in the Grünwald–Letnikov difference scheme, as time advances,

the truncation error reduces. However, this method is not suitable for fractional partial differential equations with both temporal and spatial fractional differential operators. Also, owing to the Laplace transform being a linear operator, the method cannot be applied to fractional partial differential equations with nonlinear temporal component.

Semi–analytic solutions of the fractional models proposed in Riaz et al. [30] were obtained using the Laplace transform. The transformed solutions were numerically inverted using the Gaver–Stehfest algorithm [68, 69]. Although the solutions obtained are accurate and are consistent with known limiting cases of the model equations, and with the solutions of the corresponding classical equations, the transformed solutions contain complicated and special functions. Finding the inverse of the transformed functions is not straightforward and can be numerically demanding. Also, using the linear Laplace operator raises concerns when the fractional differential equation is nonlinear. The schemes presented in this study are robust for fractional partial differential equations with both spatial and temporal fractional derivatives, and using a linearization technique, the schemes can be adapted for fractional partial differential equations with nonlinear component.

1.1.3 Numerical methods for solving fractional differential equations

In this thesis, we focus on developing numerical schemes for differential equations of arbitrary real orders. Owing to challenges in handling the typical complexity presented by fractional differential equations, largely precluding the use of analytic methods, many studies of fractional differential equations have, instead, focused on developing accurate and efficient numerical schemes. In this regard, Podlubny [2] described an effective method for evaluating fractional order derivative, using the Grünwald–Letnikov definition and the fact that under certain conditions, and for a large number of real life and engineering applications, the Riemann–Liouville and the Caputo fractional derivatives are equivalent to the Grünwald–Letnikov definition. More recently, Zhang [70] presented an unconditionally

stable finite difference scheme for space–time fractional differential equations, in which he used the shifted Grünwald–Letnikov finite difference approximation, applied to space–time fractional convection–diffusion equations. He determined the accuracy and convergence of the scheme, using numerical solutions and concluded that the scheme is of first order accuracy.

Finite difference discretization of derivatives of arbitrary order using the orthodox Grünwald–Letnikov definition only leads to first order accuracy, so attempts have been made to improve the order of accuracy. One such attempt was by Tian et al. [71], who proposed a novel unconditionally stable class of second order finite difference schemes for space fractional differential equations. The method uses weighted and shifted Grünwald–Letnikov difference approximations. Chen et al. [72] extended the study by Tian et al. [71] by applying the method to differential equations of arbitrary order with endpoint singularities, in which they introduced correction terms to the shifted and weighted Grünwald–Letnikov difference scheme. They found that the accuracy and convergence of their method depended on the number of correction terms and starting weights.

Jacobs [73] proposed a Grünwald–Letnikov type difference formula that was of at least second order accuracy for fractional differential operator. The difference formula is a modification of the Grünwald–Letnikov approximation introduced in Podlubny [2]. The reconstructed difference scheme uses the shifted form of the conventional Grünwald–Letnikov finite difference formula. However, Jacobs' Grünwald–Letnikov approximation differs in the choice of the order of the difference formula and in being derived from the central difference scheme. The new scheme also improves the accuracy of the conventional shifted Grünwald–Letnikov scheme in approximating the limiting behaviour of fractional differential operators as the independent variables tends to zero. The result was a second order accurate difference scheme as opposed to first order

accuracy of orthodox Grünwald–Letnikov finite difference approximation. Albadarneha et al. [74] introduced a class of methods by fusing several finite difference formulas with the composite trapezoidal rule. They used the trapezoidal rule to approximate the integral and the difference formulas to approximate the integer order derivative in the fractional differential operator. This resulted in second order accurate difference schemes. An implicit difference scheme with second order accuracy using the method of splines was presented by Sousa [75]. The stability, consistency and convergence of a difference scheme using the shifted Grünwald–Letnikov formula was established by Tadjeran et al. [76]. However, only first order accuracy was obtained by directly applying the shifted Grünwald–Letnikov with the Crank–Nicolson discretization, but Tadjeran et al. [76] improved their result to second order accuracy by using Richardson's extrapolation. Shen et al. [77] proposed an explicit higher order accurate finite difference approximation of the Riesz fractional advection–dispersion equation. In their study, Fix and Roop [78] gave the least square element discretization of differential equations of fractional order. Deng [79] developed a finite element scheme of order $\mathcal{O}(k^{2-\alpha} + h^{\mu})$ for the space–time fractional Fokker–Planck equation, where k and h are the time and space step sizes respectively, α and μ are orders of arbitrary time and space derivatives, respectively.

Ghanbari and Atangana [80] proposed an implicit product–integration numerical technique for time–fractional diffusion equations. Their numerical results suggested that the numerical schemes are efficient with convergence rates of order $\mathcal{O}(\Delta t^{1+\alpha})$, α being the time–fractional order. Although the numerical schemes were only proposed for fractional partial differential equations with fractional derivative appearing in a single independent variable, the authors, nevertheless, suggested that the technique could be extended to a wide range of fractional differential equations. Atangana and Alqahtani [31] constructed accurate numerical schemes for the time–fractional Keller–Segel equation mentioned in Section 1.1.1. Their numerical approximation, which combines Lagrange polynomial

interpolation and forward/backward Euler formula, was found to have a truncation error of order $\mathcal{O}(l^n + h^\alpha)$, where l and h are the number of grid points in space and time, respectively, α is the time fractional order and n is the number of times the dependent variable is continuously differentiable in space. There are many other studies on the numerical approximation of the solutions of fractional differential equations, which use, among other approaches, the finite volume method, predictor–corrector method and block pulse method [81–84].

A major difficulty in developing numerical schemes for differential equations of arbitrary orders is the enormous computational expense associated with the intrinsic non–local property of fractional differential and integral operators. Nevertheless, it is important that non–local numerical methods are developed for this class of differential equations. Efforts to develop highly effective and accurate global methods that suit fractional differential equations have grown significantly. For example, spectral methods, because of their non–local characteristics, have shown great promise in evaluating numerical solutions of fractional differential equations, where they can accommodate the problematic non–local property of fractional operators.

1.2 Spectral methods

The underlying principle in spectral methods is the presumption that the solution of a differential equation can be expanded as a series [85]. The crucial elements of the series expansion are the trial function and corresponding weight function. What sets spectral methods apart from other methods, such as finite difference and finite element methods, is the choice of the basis functions. The approximating functions for spectral methods are mostly smooth or infinitely differentiable, non–local and predominantly orthogonal [85, 86].

In a typical spectral method, the approximating functions are generally the eigenvalue solutions of the singular Sturm–Liouville problems. For finite difference methods, the approximations are pointwise, and when viewed from the basis function standpoint, the basis functions are non–global. Analogously, in finite element approximations, the domain is subdivided into smaller domains called elements, and the unknowns are approximated in each element using non–global and non–smooth basis functions. This makes the finite element method suitable for problems with irregular domains [85].

Different spectral methods are characterized by the choice of the weight function used. The weight functions are chosen to guarantee that the differential equation and boundary conditions can be evaluated using a truncated series approximation. This may be done by ensuring that the residual error is either minimized or it satisfies a certain orthogonality condition with regard to the basis function [85, 87]. The three most common spectral approaches are the Galerkin, collocation and tau methods.

In the Galerkin technique, the weight and the basis functions are similar or the same. These are infinitely continuous and differentiable functions that satisfy the boundary conditions. For the collocation technique, the weight functions are the Dirac delta function centred at the collocation points. This method demands that the differential equations must be satisfied at the collocation points [87]. Boyd [86] noted that there are only two favourable sets of collocation points; namely, the Gauss–Lobatto points and the Gauss–Chebyshev points. The spectral tau approach is equivalent to the Galerkin method in the way the method is applied. The only difference is that in the tau method, the weight functions need not satisfy the boundary conditions. In that case, an extra system of algebraic equations is needed to satisfy the boundary conditions. Unlike finite element and finite difference methods, spectral methods lead to full and dense matrices. Nevertheless, relatively high accuracy is obtained, as a result of the high order of the trial functions.

Although, there is comparatively little literature published on spectral methods for fractional differential equations, significant results have been shown in this regard. In Doha et al. [88], a Jacobi polynomial spectral tau method was proposed for linear and nonlinear multi–term differential equations of arbitrary orders. To obtain the numerical solutions, the system of algebraic equations was interpolated using Jacobi–Gauss quadrature. In the case of nonlinear multi–term fractional differential equations, they applied Newton's iterative method to obtain the coefficients of the series expansion. A Chebyshev polynomial spectral tau method was presented in Doha et al. [89, 90]. In these studies, the Caputo derivative was obtained using shifted polynomials, from which differential operational matrices were obtained. Several examples were presented to demonstrate the accuracy of the numerical methods. Furthermore, results showed fast convergence using only a small number of interpolation points. Bhrawy et al. [91] developed a quadrature shifted Legendre tau method for multi–order differential equations of fractional order with variable coefficients. They presented an explicit formula for evaluating fractional derivatives using shifted Legendre polynomials and Caputo fractional differential operator. The entries of the discrete operational matrix were explicitly obtained using the shifted Legendre–Gauss–Lobatto quadrature. Zaky [92] applied the shifted Legendre tau method to the equation describing the fractional Stoke's problem for a heated fractional second grade fluid. Doha and his associates applied the tau method to solve different kinds of problems with derivatives of arbitrary order [93–97].

Li and Xu [98] gave a theoretical analysis of a space–time spectral Galerkin method for a time–fractional diffusion equation, in which they established that the convergence of the scheme is exponential. They observed that, despite the analysis failing when the order is unity, the scheme still gave high accuracy when the fractional order was close to unity. In a subsequent study, Li and Xu [99] sought to find a weak solution of the two–sided space–time fractional diffusion equations. They constructed an effective

spectral Galerkin scheme for the numerical approximations of the weak solution. They formulated a theoretical structure in which the variational problem for the fractional differential equation was rendered into an elliptic weak problem.

1.2.1 Spectral collocation techniques

Unlike the Galerkin and tau methods, spectral collocation schemes can be relatively easy to use when solving fractional differential equations. These schemes easily circumvent the challenges associated with nonlinearity and multiple fractional orders. A linear B–spline collocation scheme for the fractional order Ricatti differential equations was given by Jafari et al. [100]. These authors applied the collocation scheme to solve a particular class of fractional partial differential equations. This method gives accuracy and simplicity that are typically associated with a collocation method. However, this scheme was only developed for single spatial dimensional fractional partial differential equations. In subsequent studies by Jafari and his team, other collocation methods, which used alternative polynomials as basis functions, were proposed. A case in point is in Mahmoudi et al. [101], where a collocation scheme using Legendre polynomials as approximating functions was developed for delay fractional differential equations. Another example, where discretization using Laguerre polynomials as basis functions for the time–fractional Cahn–Hilliard equation was given in Pandey et al. [102]. The results evidently suggested that the schemes are accurate, efficient and clearly manifest the properties typical of spectral collocation techniques.

Zayernouri and Karniadakis [103] used the eigenvalue solutions of the fractional Sturm–Liouville problem, that is, the Jacobi polyfractonomials, as basis functions to construct a highly convergent spectral collocation method for fractional differential equations. In their study, the unknown functions were expanded in terms of fractional Lagrange interpolants. These interpolants satisfy the Kronecker delta property at the

interpolation points. The published numerical scheme was applied to, among others, the space–fractional advection–diffusion and space–fractional multi–term fractional ordinary differential equations. Exponential decay of the error using the L–infinity norm was observed. In Zayernouri and Karniadakis [104], the method was extended to be applicable for linear and nonlinear two–sided variable order fractional partial differential equations of the Riemann–Liouville and Riesz types. The method was shown to give accurate solutions for these equations. Khader [105] proposed an approximate fractional derivative of a function in the Caputo sense using Chebyshev polynomials, and applied that approximation to fractional diffusion equations. Other studies that have used spectral collocation methods for fractional differential equations include Baseri et al. [106], Esmaeili and Shamsi [107] and Sweilam et al. [108], and some references therein.

1.3 Preliminary concepts

Within the context of this study, we discuss the basic theory of fractional calculus and Chebyshev polynomial of the first kind. These form the foundation on which the numerical schemes in this study are constructed. The choice of fractional operators discussed here is determined by and restricted to those fundamental to this body of work. To this end, we begin the discussion with the generalization of integer order derivatives and integrals.

1.3.1 Fractional differential and integral operators

For a continuous and differentiable function $f : \mathbb{R} \mapsto \mathbb{R}$, the first order derivative of the function f is

$$f^{(\prime)}(x) = \frac{df}{dx} = \lim_{\Delta x \to 0} \frac{f(x) - f(x - \Delta x)}{\Delta x}, \tag{1.3.1}$$

where Δx is a small change in the variable x. By induction, the above expression can be generalized to the nth–order derivative

$$f^{(n)} = \frac{d^n f}{dx^n} = \lim_{\Delta x \to 0} \frac{1}{\Delta x^n} \sum_{k=0}^{n} (-1)^k \binom{n}{k} f(x - k\Delta x), \quad n \in \mathbb{Z}, \tag{1.3.2}$$

where $\binom{n}{k}$ is the notation for the binomial coefficients. To generalize Equation (1.3.2), we choose m, an arbitrary integer such that $m \leq n$, and define [2]

$$f^{(m)}(x) = \lim_{\Delta x \to 0} f^{(m)}_{\Delta x}(x), \tag{1.3.3}$$

where

$$f^{(m)}_{\Delta x}(x) = \frac{1}{\Delta x^m} \sum_{k=0}^{n} (-1)^k \binom{m}{k} f(x - k\Delta x). \tag{1.3.4}$$

For Equation (1.3.4) to hold when $m < 0$, we use the more general expression of the binomial coefficients,

$$\binom{m}{k} = \frac{m!}{(m-k)!k!} = \frac{\Gamma(m+1)}{\Gamma(m-k+1)\Gamma(k+1)}. \tag{1.3.5}$$

Here $\Gamma(\cdot)$ is the gamma function. The generalization on the right hand side of Equation (1.3.5) accepts any complex number as argument. This generalization of the binomial coefficients allows Equation (1.3.4) to hold for all $m \leq n$. However, if m is negative, Equation (1.3.4) tends to zero as $\Delta x \to 0$; a result that is unexciting. To obtain a limit that is non–zero, and consequently obtain the fractional integral operator, we assume that $n \to \infty$ as $\Delta x \to 0$ and as such define $n\Delta x = x - a$, where a is a real constant and the lower terminal of $f(x)$ [2]. We define the operator

$$ {}_{a^+}D_x^{-m} f(x) = \lim_{\Delta x \to 0} f_{\Delta x}^{(-m)}(x), \tag{1.3.6} $$

and consider the case when $m = 1$. Using the limit of the Riemann sum as a definition of the definite integral, we have

$$ \begin{aligned} {}_{a^+}D_x^{-1} f(x) = \lim_{\Delta x \to 0} f_{\Delta x}^{(-1)}(x) &= \lim_{\substack{\Delta x \to 0 \\ n\Delta x = x-a}} \Delta x \sum_{k=0}^{n} (-1)^{2k} f(x - k\Delta x) \\ &= \int_0^{x-a} f(x-y)dy = \int_a^x f(\varsigma)d\varsigma. \end{aligned} \tag{1.3.7} $$

It is obvious that ${}_{a^+}D_x^{-1} f(x)$ gives the 1–fold integral. As a matter of fact, a more general representation for an n–fold integral can be obtained by induction as shown in Podlubny [2]:

$$ \begin{aligned} {}_{a^+}D_x^{-m} f(x) &= \lim_{\substack{\Delta x \to 0 \\ n\Delta x = x-a}} \Delta x^m \sum_{k=0}^{n} (-1)^k \binom{m}{k} f(x - k\Delta x) \\ &= \frac{1}{\Gamma(m)} \int_a^x (x - \varsigma)^{m-1} f(\varsigma)d\varsigma. \end{aligned} \tag{1.3.8} $$

We note that Equation (1.3.2) allows for the generalization of the concept of nth order derivative and Equation (1.3.8) is the m–fold integral of a continuous function. We further note that these concepts are particular cases of

$$ {}_{a^+}D_x^m f(x) = \lim_{\substack{\Delta x \to 0 \\ n\Delta x = x-a}} \frac{1}{\Delta x^m} \sum_{k=0}^{n} (-1)^k \binom{m}{k} f(x - k\Delta x), \tag{1.3.9} $$

which generally lead to the notions of derivatives of order m for $m \geq 0$, and m–fold integral for $m < 0$. Here, m can be arbitrarily real or complex. If we restrict m to real numbers, we obtain the well–known Grünwald–Letnikov definition ${}^{GL}_{a^+}D_x^m$ [40]. This definition often serve as a fitting discrete representation of fractional differential and integral operators in applications [70]. However, the limit cannot easily be obtained, thereby making computations tedious. To correct this difficulty, in addition to the assumption that $f(x)$ be continuous, $f(x)$ must also be continuously differentiable i–times, $1 \leq i \leq r+1$ in $[a, x]$, where r is an integer such that $r < m < r+1$. This assumption holds in physical and mathematical applications, and thus for the m–fold integral, we have [2, 4]

$$ {}^{GL}_{a^+}D_x^{-m} f(x) = \sum_{i=0}^{r} \frac{f^{(i)}(a)(x-a)^{m+i}}{\Gamma(m+i+1)} + \frac{1}{\Gamma(m+r+1)} \int_a^x (x-\varsigma)^{m+r} f^{(r+1)}(\varsigma) d\varsigma, \tag{1.3.10} $$

and for mth order derivative, we have

$$ {}^{GL}_{a^+}D^m_x f(x) = \sum_{i=0}^{r} \frac{f^{(i)}(a)(x-a)^{-m+i}}{\Gamma(-m+i+1)} + \frac{1}{\Gamma(-m+r+1)} \int_a^x (x-\varsigma)^{r-m} f^{(r+1)}(\varsigma) d\varsigma. \tag{1.3.11} $$

Equation (1.3.11) can be obtained by repeated integration by parts and differentiation of

$$ {}^{RL}_{a^+}D^m_x f(x) = \left(\frac{d}{dx}\right)^{r+1} \int_a^x (x-\varsigma)^{r-m} f(\varsigma) d\varsigma, \tag{1.3.12} $$

provided $f(x)$ is continuously differentiable $(r+1)$ times [2]. Equation (1.3.12) is the well known Riemann–Liouville definition. Equation (1.3.12) can be written as nth order derivative of the $(n-m)$–fold integral. Therefore, for $m \in \mathbb{R}^+$ and $n \in \mathbb{N}$, we have

$$ {}^{RL}_{a^+}D^m_x f(x) = \left(\frac{d}{dx}\right)^n \left({}^{RL}_{a^+}I^{n-m}_x f(x)\right) = \frac{1}{\Gamma(n-m)} \left(\frac{d}{dx}\right)^n \int_a^x (x-\varsigma)^{n-m-1} f(\varsigma) d\varsigma, \quad n-1 \leq m < n, \tag{1.3.13} $$

where

$$ {}^{RL}_{a^+}I^m_x f(x) = \frac{1}{\Gamma(m)} \int_a^x (x-\varsigma)^{m-1} f(\varsigma) d\varsigma \tag{1.3.14} $$

is the Riemann–Liouville fractional integral operator. If, on the one hand, $m = n-1$, Equation (1.3.13) becomes the integer order derivative of order $n-1$:

$$ {}^{RL}_{a^+}D^{n-1}_x f(x) = \left(\frac{d}{dx}\right)^n \left({}^{RL}_{a^+}I_x f(x)\right) = \frac{d^{n-1}}{dx^{n-1}} f(x). \tag{1.3.15} $$

On the other hand, for $m = n \geq 1$, ${}^{RL}_{a^+}I^0_x f(x) \equiv {}^{RL}_{a^+}D^0_x f(x)$ and $x \geq a$:

$$ {}^{RL}_{a^+}D^m_x f(x) = \frac{d^n}{dx^n}\left({}^{RL}_{a^+}I^0_x f(x)\right) = \frac{d^n}{dx^n} f(x). \tag{1.3.16} $$

Equation (1.3.16) implies that for $x > a$, the Riemann–Liouville fractional differential operator of order $m = n \geq 1$ corresponds to classical derivative of order n. Properties and discussion of the Riemann–Liouville operator can be found in Podlubny [2] and Miller and Ross [43].

A limitation of the Riemann–Liouville fractional operator is the existence of initial or boundary conditions with fractional derivatives at the lower terminal $x = a$. While problems with such conditions might be solvable, they make no physical or mathematical sense. Hence, the formulation of the Caputo fractional operator becomes necessary [14]. In addition to ameliorating the aforesaid limitation, the Caputo fractional differential operator is better suited for description of physical problems. Caputo's definition, which we use throughout this study is defined as

$$ {}^{C}_{a^+}D^m_x f(x) = \frac{1}{\Gamma(n-m)} \int_a^x (x-\varsigma)^{n-m-1} f^{(n)}(\varsigma) d\varsigma, \quad n-1 < m < n. \tag{1.3.17} $$

Podlubny [2] gave an extensive review of the properties of this operator and some of the similarities and differences between it and the Riemann–Liouville definition.

1.3.2 Two–sided fractional derivatives

Another important concept in fractional calculus is the notion of left– and right–sided fractional derivatives. So far, we have only considered and assumed that $a < x$, which implies that ${}_{a^+}D_x^m f(x)$ has a moving upper terminal x and fixed lower terminal a. We can also have fractional derivatives with moving lower terminal x and fixed upper limit, say b. The left– and right–sided differential operators can be defined for all the differential operators; namely, Grünwald–Letnikov, Riemann–Liouville and Caputo. The fractional differential operators with fixed upper terminal are called right–sided derivatives. The right–sided Grünwald–Letnikov fractional derivative is defined by De Oliveira and Tenreiro Machado [40] as

$$ {}_{x}^{GL}D_{b^-}^m f(x) = \lim_{\substack{\Delta x \to 0 \\ n\Delta x = b-x}} \frac{1}{\Delta x^m} \sum_{k=0}^{n} (-1)^k \binom{m}{k} f(x + k\Delta x). \tag{1.3.18} $$

The right–sided Riemann–Liouville fractional differential operator is given by Podlubny [2] as

$$ {}_{x}^{RL}D_{b^-}^m f(x) = \frac{(-1)^n}{\Gamma(n-m)} \left(\frac{d}{dx}\right)^n \int_x^b (\varsigma - x)^{n-m-1} f(\varsigma) d\varsigma, \quad x < b. \tag{1.3.19} $$

And lastly, the right–sided Caputo definition is given by De Oliveira and Tenreiro Machado [40] as

$$ {}_{x}^{C}D_{b^-}^m f(x) = \frac{(-1)^n}{\Gamma(n-m)} \int_x^b (\varsigma - x)^{n-m-1} f^{(n)}(\varsigma) d\varsigma, \quad x < b. \tag{1.3.20} $$

If the function $f(x)$ is a time evolution function, one might view the left–sided fractional derivative at the point x as dependent on events occurring after the time a, while the right–sided fractional derivative at x is dependent on events leading up to time b. In a nutshell, for a time evolving process, the left–sided differential operator is used for past states of a process, while the right–sided differential operator is used for future states of a process. However, for a process changing in space, it is logical to consider non–local rates of change in both direction. Hence one might use left–, right– or, in some cases, two–sided fractional differential operators. However, in this study, whenever we have a time–fractional differential operator, we will use the left–sided derivative. Nevertheless, we also construct numerical schemes for two–sided space–fractional differential equations. A limited number of studies have presented numerical schemes for two–sided fractional differential equations. These include Samiee et al. [109], Kelly et al. [110], and Hejazi et al. [111] and some of the references therein.

1.3.3 Distributed order fractional derivative

Fractional calculus offers a robust tool in the mathematical modelling of physical phenomena. Another generalization of a derivative is the concept of the distributed order fractional operator. This operator provides a flexible instrument for modelling multiscale physics. In the distributed order fractional differential operator, arbitrary differential orders are distributed over a range of values rather than being just a single value as with conventional fractional derivatives. There has been massive interest in the application of distributed fractional calculus, specifically in its application to diffusion processes [112, 113]. The distributed order derivative is defined as

$$ {}^{DO}_{a^+}D^m_x f(x) = \int_{m_1}^{m_2} \rho(m) \, {}^{*}_{a^+}D^m_x f(x) dm, \tag{1.3.21} $$

where $m \in \mathbb{R}^+$, $f(x)$ is a continuously differentiable function and ${}^{*}_{a^+}D^m_x$ could be any of the left–sided differential operators defined earlier. Most studies on the approximation of distributed order fractional derivatives use difference schemes. Constructing an approximation for single order fractional differential operators can be computationally demanding, in terms of memory and CPU time. Additional cost may be incurred in the simulation of mathematical models with distributed order fractional derivatives. Further, unlike with fixed order derivatives where exact solutions can be forced by including a source term, in distributed order models such forcing might be difficult. Studies that have focused on the development of numerical schemes for distributed order fractional differential equations include Diethelm and Ford [114], Gao and Sun [115] and Katsikadelis [116].

1.3.4 Chebyshev polynomials of the first kind

Spectral methods are developed through expansion of a function as an infinite series of orthogonal polynomials, the most popular series for such an approximation being the Fourier series [87]. Most of the numerical schemes developed in this study are constructed using Chebyshev polynomials of the first kind. The Chebyshev polynomials, as defined by Abramowitz and Stegun [117] are given as

$$T_n(x) = \cos(n \arccos x), \quad n = 0, 1, 2, \ldots, \tag{1.3.22}$$

with recurrence relation

$$T_{n+1}(x) = 2xT_n(x) - T_{n-1}(x), \quad n \geq 1, \tag{1.3.23}$$

where $T_0(x) = 1$ and $T_1(x) = x$ are eigenvalue solutions of the singular Sturm–Liouville problem

$$\left(\sqrt{1-x^2}T_n'(x)\right)' + \frac{n^2}{\sqrt{1-x^2}}T_n(x) = 0, \quad -1 \leq x \leq 1, \tag{1.3.24}$$

with weight function $w(x) = 1/\sqrt{1-x^2}$. The polynomials can be expanded in series form as

$$T_n(x) = \frac{n}{2}\sum_{j=0}^{\lfloor n/2 \rfloor}(-1)^n \frac{(n-j-1)!}{(n-2j)!j!}(2x)^{n-2j}. \tag{1.3.25}$$

The Chebyshev polynomials are defined in $[-1, 1]$. Many physical problems are defined in the positive upper half domain, so we transform $[-1, 1]$ to $[0, L]$ by using the affine mapping

$$T_{L,n}(x) = T_n\left(\frac{2x}{L} - 1\right). \tag{1.3.26}$$

Applying the transformation above to Equation (1.3.23), we obtain the recursive formula for the shifted form of the first kind Chebyshev polynomials,

$$T_{L,n+1}(x) = 2\left(\frac{2x}{L} - 1\right)T_{L,n}(x) - T_{L,n-1}(x), \quad n \geq 1, \tag{1.3.27}$$

where $T_{L,0}(x) = 1$ and $T_{L,1}(x) = {}^{2x}/_{L} - 1$. The shifted Chebyshev polynomials are defined as

$$T_{L,n}(x) = n \sum_{j=0}^{n} (-1)^{n-j} \frac{(n+j-1)! 2^{2j}}{(n-j)!(2j)!} x^j, \tag{1.3.28}$$

with shifted weight function $w_L(x) = 1/\sqrt{Lx - x^2}$. The shifted form satisfies the orthogonality condition

$$\int_0^L T_{L,n}(x) T_{L,m}(x) w_L(x) = \delta_{mn} h_n, \tag{1.3.29}$$

where

$$h_n = \begin{cases} \pi & n = 0 \\ \frac{\pi}{2} & n \geq 1. \end{cases} \tag{1.3.30}$$

If $f(x)$ is a continuous and integrable function defined in the domain $[0, L]$, the shifted Chebyshev series of $f(x)$ is given as

$$f_N(x) = \sum_{n=0}^{\infty} f_n T_{L,n}(x), \tag{1.3.31}$$

where the coefficients f_n are defined as

$$f_n = \frac{2}{\pi c_n} \int_0^L f(x) T_{L,n} \frac{1}{\sqrt{Lx - x^2}} dx, \quad c_n = \begin{cases} 2 & n = 0 \\ 1 & n \geq 1. \end{cases} \tag{1.3.32}$$

The above expansion forms the basis upon which the numerical schemes in this study are constructed.

1.4 Aims and structure of the thesis

Many pseudo–spectral schemes developed for fractional differential equations using Chebyshev polynomials are appropriate for solving fractional ordinary differential equations. In instances when fractional partial differential equations were considered, the fractional order is often only in one of the variables. It is evident that applying this technique to fractional differential equations of varying degree and dimensionality has received limited attention. The aim of this study is to bridge this gap, by constructing pseudo–spectral schemes for fractional differential equations of varying degree and dimensionality. To address this aim, we introduce, describe and present accurate and computationally efficient numerical schemes for fractional differential equations, including those that range from one–dimensional equations to two–dimensional equations, those with nonlinear terms, and those with multiple and distributed fractional orders. The numerical scheme is developed to solve fractional ordinary differential equations, as in Chapter 2, and further extended to solve other classes of fractional differential equations.

The remainder of the thesis is organized as follows. We begin in Chapter 2 by studying a system of nonlinear fractional ordinary differential equations describing heat and mass

transfer in a non–Newtonian fluid using fractional constitutive relation. The solutions to the system of equations are approximated using shifted Chebyshev polynomials of the first kind. We give a comparison between the solutions of these new equations and the classical form of the equations. The accuracy of the numerical scheme is established.

In Chapter 3, we include nonlinearity by considering the non–isothermal model for the boundary layer flow of a fractional Oldroyd–B fluid model. A numerical discretization scheme is presented for the flow equations and a theoretical analysis of the error bound is presented.

In Chapter 4, we consider a multi–dimensional problem, where the focus is on the numerical solution of the fractional Rayleigh problem of a generalized Maxwell fluid with Robin boundary conditions. Unlike in Chapter 3, where all derivatives are approximated using shifted Chebyshev polynomials, in Chapter 4, arbitrary temporal derivatives are approximated using shifted Chebyshev polynomials of the first kind and spatial derivatives are approximated in terms of Lagrange polynomials. Analysis of convergence of the numerical scheme indicates that the absolute error vanishes for a sufficiently large number of grid points.

In Chapter 5, the numerical discretization method is extended by application to two–dimensional fractional differential equations with arbitrary orders in both space and time derivatives. Numerical solutions of both linear and nonlinear differential equations are presented. The nonlinear differential equation is linearized using the Newton–Raphson approach. Numerical results show that the scheme is accurate and computationally effective.

Chapter 6 presents a convergence analysis of the pseudo–spectral method for solving two–sided space–time fractional partial differential equations. We demonstrate the use

of the numerical scheme using selected two–sided space fractional partial differential equations. The numerical results indicate that the method is accurate.

In Chapter 7, we extend the pseudo–spectral method to distributed order fractional ordinary differential equations. Distributed order fractional differential equations serve as a robust instrument for modelling multiscale and memory dependent phenomena. However, the computational cost of obtaining numerical solutions of such differential equations is high. Chapter 7 gives the case of fractional differential equations with a single variable as a precursor to the work in Chapter 8.

In Chapter 8, we construct a computationally efficient and accurate numerical method for the solution of multidimensional two–sided space fractional partial differential equations with time distributed orders. The convergence analysis is presented, and examples are presented to establish the accuracy and computational efficiency of the numerical method.

Chapter 9 concludes the study by summarizing and outlining overall findings, and highlights possibilities for future research.

Chapter 2

A Chebyshev spectral method for heat and mass transfer in MHD nanofluid flow with space fractional constitutive model

In this chapter, we present a numerically accurate method for approximating the solution of a system of ordinary differential equations of arbitrary order. To this end, we consider heat and mass transfer in a magnetohydrodynamics nanofluid modelled using a spatially non–local velocity gradient. The shear stress is defined in terms of a space fractional constitutive model and a fractional dynamic viscosity coefficient. The system of differential equations describing the fluid flow is then transformed using Lie's symmetry group of transformations. We solve the system of ordinary differential equations of arbitrary order numerically by representing the solutions as a truncated series expansion of the shifted Chebyshev polynomials. An error bound for the numerical method is presented, and numerical solutions are compared with results from past studies and exact solutions of the reduced classical form of the system. The results indicate that the method is accurate for solving this form of equation. The results also show that the non–local velocity gradient is effective in modelling the flow of a non–Newtonian nanofluid.

Frontiers in Heat and Mass Transfer

Available at www.ThermalFluidsCentral.org

A CHEBYSHEV SPECTRAL METHOD FOR HEAT AND MASS TRANSFER IN MHD NANOFLUID FLOW WITH SPACE FRACTIONAL CONSTITUTIVE MODEL

Shina D. Oloniiju†, Sicelo P. Goqo, Precious Sibanda

School of Mathematics, Statistics and Computer Science, University of KwaZulu–Natal, Private Bag X01, Scottsville, Pietermaritzburg 3209, South Africa

ABSTRACT

In some recent studies, it has been suggested that non–Newtonian fluid flow can be modeled by a spatially non–local velocity, whose dynamics are described by a fractional derivative. In this study, we use the space fractional constitutive relation to model heat and mass transfer in a nanofluid. We present a numerically accurate algorithm for approximating solutions of the system of fractional ordinary differential equations describing the nanofluid flow. We present numerically stable differentiation matrices for both integer and fractional order derivatives defined by the one–sided Caputo derivative. The differentiation matrices are based on the series expansion of the unknown functions using a truncated Chebyshev polynomial of the first kind and interpolation using Gauss–Lobatto quadrature. We show that the proposed technique is highly effective for solving the fractional model equations.

Keywords: *Fractional constitutive equations, Spectral method, Chebyshev polynomials, Fractional differentiation matrix*

1. INTRODUCTION

The boundary layer flow of both Newtonian and non–Newtonian fluids has been explored extensively in the literature because of the many industrial and scientific uses of these fluids. Experimental and theoretical investigations of non–Newtonian fluids have shown that they exhibit anomalous behaviours and are generally more complex than viscous fluids. To describe these behaviours, several models have been proposed to mathematically describe and experimentally quantify the stress–strain relationship. These constitutive relations include but are not limited to the power–law, Ellis and Powell–Eyring fluids models. These models and several others have been subjected to experimental and theoretical investigations. In some recent studies, attempts have been made to reconstruct the constitutive relations to incorporate hereditary properties, memory retention and non–local properties of non–Newtonian fluids. The primary objective is to recast the velocity gradient in the momentum transport equation as a fractional derivative.

Fractional calculus can best describe physical models with long term memory and non–locality of the spatial domain. For instance, constitutive relations with time fractional derivative are used to describe memory dependence in dynamical systems (Tarasov, 2013). An investigation and summary of studies on fluid flow problems in which the rheological properties of the fluid are described using fractional calculus is given by Sun *et al.* (2018). In this study, the classical constitutive equation of a viscous fluid was reconstructed so that the velocity gradient is expressed using a non–local spatial derivative. This approach allows for the capture of the non–locality of non–Newtonian fluid and the correlation between the fluid particles. They conducted a theoretical analysis of a steady pipe flow of a laminar incompressible flow, obtaining the frictional head loss, velocity profile and yield stress in terms of the fractional Reynolds number. Chen *et al.* (2015) investigated the fractional boundary layer flow of a Maxwell fluid on an unsteady stretching surface. The constitutive equation was recast so as to introduce space–time dependent fractional derivatives. Research on classical boundary layer flow, heat and mass transfer in magnetohyrodynamics nanofluid has been carried out by, among others, Dhanai *et al.* (2015) and Khan and Pop (2010). By applying the implicit finite difference method, velocity, temperature and nanoparticle concentration profiles were obtained in the study of Dhanai *et al.* (2015) which investigated the combined effects of heat and mass transfer parameters on a steady boundary layer nanofluid flow and examined multiple solutions of the conservation equations. Critical review of literature shows that heat and mass transfer in viscous nanofluid with fractional constitutive relation has not been studied. In this study, a fractional system of equations describing heat and mass transport in an incompressible magnetohydrodynamic viscous nanofluid is developed and solved using a spectral technique that uses Chebyshev polynomials of the first kind as basis functions.

2. MATHEMATICAL FORMULATION

We consider a steady two–dimension boundary layer flow of an incompressible nanofluid with space fractional shear rate induced by an im-

†*Corresponding author. Email: shina@aims.edu.gh*

permeable horizontal wall along the plane $y = 0$, where the y–axis is perpendicular to the wall and the x–axis along the wall. It is assumed that the flow occurs at $y \geq 0$ and a constant magnetic field B is applied in the y–direction. The temperature and nanoparticle volume fraction at the wall (T_w, C_w) are constant and the ambient temperature and concentration are T_∞ and C_∞ respectively as in Fig. 1. By defining the shear stress associated with a fluid with fractional dynamic viscosity coefficient μ_α $(kg/m^{2-\alpha}/s)$ in the following form

$$\tau = \mu_\alpha \frac{\partial^\alpha u}{\partial y^\alpha}, \quad 0 < \alpha < 2, \tag{1}$$

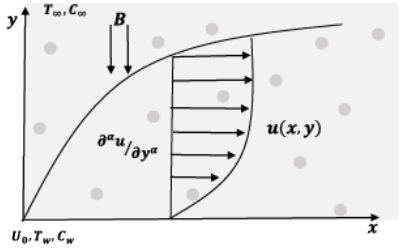

Fig. 1 Coordinate system and flow geometry.

where α is the order of the fractional space derivative, and $\partial^\alpha u/\partial y^\alpha$ denotes the fractional velocity gradient. A reclassification of non–Newtonian fluid based on the fractional constitutive equation (1) was given by (Sun *et al.*, 2018). In the aforementioned study, the case $< \alpha < 1$ was proposed to describe shear thickening fluids, $2 > \alpha > 1$ model shear thinning fluids and $\alpha = 1$, viscous fluids. The partially coupled system of equations describing the transport processes is given as (Chen *et al.*, 2015; Khan and Pop, 2010)

$$\frac{\partial u}{\partial x} + \frac{\partial v}{\partial y} = 0 \tag{2}$$

$$u\frac{\partial u}{\partial x} + v\frac{\partial u}{\partial y} = \nu_\alpha {}_0^C D_y^{\alpha+1} u - \frac{\sigma B^2}{\rho} u \tag{3}$$

$$(\rho c)_b \left(u\frac{\partial T}{\partial x} + v\frac{\partial T}{\partial y} \right) = k\frac{\partial^2 T}{\partial y^2} + (\rho c)_p \left(D_B \frac{\partial C}{\partial y}\frac{\partial T}{\partial y} + \frac{D_T}{T_\infty}\left(\frac{\partial T}{\partial y}\right)^2 \right) \tag{4}$$

$$u\frac{\partial C}{\partial x} + v\frac{\partial C}{\partial y} = D_B \frac{\partial^2 C}{\partial y^2} + \frac{D_T}{T_\infty}\frac{\partial^2 T}{\partial y^2}, \tag{5}$$

subject to the boundary conditions

$$\begin{aligned} &v = 0, \quad u = U_0, \quad T = T_w, \quad C = C_w \quad \text{at} \quad y = 0, \\ &u = 0, \quad T = T_\infty, \quad C = C_\infty \quad \text{as} \quad y \to \infty. \end{aligned}$$

Here ${}_0^C D_y^\alpha$ is the Caputo fractional operator of order α of the function $u(y) : (0, \infty) \to \mathbb{R}$, defined as

$${}_0^C D_y^\alpha u(y) = \begin{cases} \frac{1}{\Gamma(n-\alpha)} \int_0^y \frac{u^n(\tilde{y})}{(y-\tilde{y})^{\alpha+1-n}} d\tilde{y}, & n-1 \leq \alpha < n \in \mathbb{N} \\ \frac{d^n u(y)}{dy^n} & \alpha = n \in \mathbb{N}. \end{cases} \tag{6}$$

The Caputo fractional operator is the most popular in applications due to the ease in imposing conditions on the fractional differential equations. Other fractional operators include the Riemann-Liouville, Riesz and the Canavati fractional derivatives. We note that the Caputo fractional operator is a regularized form of the Riemann-Liouville fractional derivative. The definitions and properties of the Caputo derivative and the aforementioned arbitrary order derivatives can be found in Miller and Ross (1993); Podlubny (1998); Atanackovic *et al.* (2014).

We define u and v (m/s) as the horizontal and vertical velocity components respectively, $\nu_\alpha(m^{1+\alpha}/s) = \mu_\alpha/\rho_b$ is the fractional kinematic viscosity, ρ_b and ρ_p (kg/m^3) are constant basefluid and nanoparticle densities respectively. If we assume the reference length L and velocity U_0, we have the following dimensionless variables

$$(U, V, X, Y, \theta, \phi) = \left(uU_0^{-1}, vU_0^{-1}, xL^{-1}, yL^{-1}, \frac{T - T_\infty}{\Delta T}, \frac{C - C_\infty}{\Delta C} \right), \tag{7}$$

$$(Re_\alpha, M^2, Le, Pr, Nbt, Sc) = \left(\frac{U_0 L^\alpha}{\nu_\alpha}, \frac{\sigma B^2 L}{\rho U_0}, \frac{k}{(\rho c)_p D_B \Delta C}, \frac{LU_0(\rho c)_f}{k}, \frac{Nb}{Nt}, \frac{D_B}{LU_0} \right), \tag{8}$$

where Nb and Nt are respectively the Brownian diffusion and thermophoresis parameters, Re_α is the fractional Reynolds number, M is the magnetic parameter, Le is the Lewis number, Pr is the Prandtl number, and Sc is the Schmidt number (Dhanai *et al.*, 2015). Introducing the stream function ψ defined by $U = \partial\psi/\partial Y$ and $V = -\partial\psi/\partial X$, Eqs. (3) to (5) become

$$\frac{\partial \psi}{\partial Y}\frac{\partial^2 \psi}{\partial X \partial Y} - \frac{\partial \psi}{\partial X}\frac{\partial^2 \psi}{\partial Y^2} = \frac{1}{Re_\alpha}\frac{\partial^{\alpha+2}\psi}{\partial Y^{\alpha+2}} - M^2 \frac{\partial \psi}{\partial Y} \tag{9}$$

$$LePr\left[\frac{\partial \psi}{\partial Y}\frac{\partial \theta}{\partial X} - \frac{\partial \psi}{\partial X}\frac{\partial \theta}{\partial Y} \right] = Le\frac{\partial^2 \theta}{\partial Y^2} + \frac{\partial \phi}{\partial Y}\frac{\partial \theta}{\partial Y} + \frac{1}{Nbt}\left(\frac{\partial \theta}{\partial Y}\right)^2 \tag{10}$$

$$Sc\left[\frac{\partial \psi}{\partial Y}\frac{\partial \phi}{\partial X} - \frac{\partial \psi}{\partial X}\frac{\partial \phi}{\partial Y} \right] = \frac{\partial^2 \phi}{\partial Y^2} + \frac{1}{Nbt}\frac{\partial^2 \theta}{\partial Y^2}. \tag{11}$$

We perform a scaling transformation by introducing the new variables $x, y, \tilde{\psi}, \tilde{\theta}, \tilde{\phi}$ defined as

$$(X, Y, \psi, \theta, \phi) = \left(\lambda^{a_1} x, \lambda^{a_2} y, \lambda^{a_3}\tilde{\psi}, \lambda^{a_4}\tilde{\theta}, \lambda^{a_5}\tilde{\phi} \right). \tag{12}$$

Here, λ is the scaling parameter and a_i for $i = 1 \ldots 5$ are constants to be determined such that Eqs. (9) to (11) remain invariant under this group transformation. Upon substituting Eq. (12) into Eqs. (9) to (11), and dropping the tilde for convenience, we get

$$\lambda^{2a_3 - 2a_2 + a_1}\left[\frac{\partial \psi}{\partial y}\frac{\partial^2 \psi}{\partial x \partial y} - \frac{\partial \psi}{\partial x}\frac{\partial^2 \psi}{\partial y^2} \right] = \lambda^{a_3 - (\alpha+2)a_2}\frac{1}{Re_\alpha}\frac{\partial^{\alpha+2}\psi}{\partial y^{\alpha+2}} - \lambda^{a_3 - a_2} M^2 \frac{\partial \psi}{\partial y} \tag{13}$$

$$\lambda^{a_3 - a_2 + a_4 - a_1} LePr\left[\frac{\partial \psi}{\partial y}\frac{\partial \theta}{\partial x} - \frac{\partial \psi}{\partial x}\frac{\partial \theta}{\partial y} \right] = \lambda^{a_4 - 2a_2} Le\frac{\partial^2 \theta}{\partial y^2} + \lambda^{a_4 + a_5 - 2a_2}\frac{\partial \phi}{\partial y}\frac{\partial \theta}{\partial y} + \lambda^{2a_4 - 2a_2}\frac{1}{Nbt}\left(\frac{\partial \theta}{\partial y}\right)^2 \tag{14}$$

$$\lambda^{a_3 + a_5 - a_2 - a_1} Sc\left[\frac{\partial \psi}{\partial y}\frac{\partial \phi}{\partial x} - \frac{\partial \psi}{\partial x}\frac{\partial \phi}{\partial y} \right] = \lambda^{a_5 - 2a_2}\frac{\partial^2 \phi}{\partial y^2} + \lambda^{a_4 - 2a_2}\frac{1}{Nbt}\frac{\partial^2 \theta}{\partial y^2}. \tag{15}$$

For the system of equations to remain invariant, we set $a_1 = a_3 = a$ (arbitrary) and $a_2 = a_4 = a_5 = 0$. The characteristics equations associated with the transformation is given as

$$\frac{dx}{ax} = \frac{dy}{0} = \frac{d\psi}{a\psi} = \frac{d\theta}{0} = \frac{d\phi}{0}, \tag{16}$$

which give the similarity functions

$$y = \eta, \quad \psi(x,y) = xf(\eta), \quad \theta(x,y) = \theta(\eta), \quad \phi(x,y) = \phi(\eta). \tag{17}$$

Using the Caputo fractional operator to obtain the fractional derivative of the similarity function $\psi(x,y) = xf(\eta)$ and substituting Eq. (17) into Eqs. (9) to (11) gives the following similarity equations

$$f^{(\alpha+2)} - Re_\alpha M^2 f' - Re_\alpha f'^2 + Re_\alpha f f'' = 0 \tag{18}$$

$$Le\theta'' + \theta'\phi' + \frac{1}{Nbt}\theta'^2 + LePrf\theta' = 0 \tag{19}$$

$$\phi'' + \frac{1}{Nbt}\theta'' + Scf\phi' = 0, \tag{20}$$

with boundary conditions

$$\begin{aligned} &f(0) = 0, \quad f'(0) = 1, \quad \theta(0) = 1, \quad \phi(0) = 1, \\ &f'(\eta) = 0, \quad \theta(\eta) = 0, \quad \phi(\eta) = 0 \quad \text{as} \quad \eta \to \infty. \end{aligned} \tag{21}$$

We note here that setting $\alpha = 1$, $Re_\alpha = 1$ and $M = 0$, the system of equations reduces to the problem studied in Khan and Pop (2010).

3. NUMERICAL APPROXIMATION

Existing numerical methods for integer order differential equations have been extended to fractional order differential equations. Numerical and approximate methods such as the differential transform, homotopy, Adomian decomposition and finite difference methods have been used to solve fractional differential equations (Wang, 2006; Diethelm *et al.*, 2002; Erjaee *et al.*, 2011; El-Sayed *et al.*, 2010; Momani and Odibat, 2007a,b). Despite the fact that some of these methods are considered accurate and reliable, they have certain limitations. For example, due to the history dependence associated with fractional derivatives, approximations can be computationally expensive. Fractional derivatives are defined globally, hence numerical methods that discretize non–locally would be appropriate in approximating the derivative. One such method is the spectral method. Spectral methods are synonymous with exponential rate of convergence. We discretized the dependent variables and their arbitrary order derivatives using the spectral collocation methods. The Chebyshev spectral collocation method uses trial functions to represent the functions as truncated series expansions. The trial functions are usually orthogonal basis functions such as the Lagrange, Jacobi, Chebyshev and other polynomials. A crucial difference between spectral methods and other methods is that the test functions for spectral methods are inherently continuous and infinitely differentiable global functions. Some recent studies have demonstrated the use of the operational matrix for certain orthogonal polynomials. Ahmadi Darani and Saadatmandi (2017) introduced the operational matrix of a class of fractional order Chebyshev functions using classical Chebyshev polynomials of the first kind. Doha *et al.* (2011) and Atabakzadeh *et al.* (2013) presented a matrix operator for shifted Chebyshev polynomials and used it to approximate multi–order fractional ordinary differential equations and Doha *et al.* (2012) obtained the matrix operator of the Jacobi polynomials. In recent studies by Kazem *et al.* (2013) and Kayedi-Bardeh *et al.* (2014), the operational matrices of the fractional Legendre polynomials and fractional Jacobi polynomials are respectively obtained. Direct implementation of the operational matrices usually lead to accurate solutions. However, dealing with nonlinearity and coupling can be time consuming. Hence, in this study, we follow a different approach by using approximations based on the shifted Chebyshev polynomials of the first kind and integration on the Gauss–Lobatto quadrature to obtain the coefficients of expansion.

The series form of shifted Chebyshev polynomials $T_{l,n}$ of degree $n > 0$, where l is the truncation of the positive half domain, is defined (Abramowitz and Stegun, 1965; Doha *et al.*, 2011; Ahmadi Darani and Saadatmandi, 2017) as

$$T_{l,n} = n\sum_{j=0}^{n} \frac{(-1)^{n-j}(n+j-1)!2^{2j}}{(n-j)!(2j)!l^j}\eta^j, \tag{22}$$

and satisfies the orthogonality condition

$$\int_0^l T_{l,n}(\eta)T_{l,m}(\eta)w_l(\eta)d\eta = \delta_{mn}h_n. \tag{23}$$

We discretized the dependent variables using the shifted Chebyshev Gauss Lobatto grid points $\eta \in [0, l]$

$$\eta = \frac{l}{2}\left(1 - \cos\frac{\pi i}{N}\right), \qquad i = 0, \ldots, N. \tag{24}$$

The weight function $w_l(\eta)$ for the shifted Chebyshev polynomials is given by $1/\sqrt{l\eta - \eta^2}$ and $h_n = c_n\pi/2$, with $c_0 = 2$ and $c_n = 1$ for $n \geq 1$. If we assume $F(\eta) = \{f(\eta), \theta(\eta), \phi(\eta)\}$, to be a square integrable and smooth function defined over the truncated semi infinite interval $[0, l]$, then the function can be approximated as $N + 1$ terms of the shifted Chebyshev polynomials

$$F_N(\eta) = \sum_{n=0}^{N} F_n T_{l,n}(\eta), \tag{25}$$

the coefficients F_n satisfy the orthogonality condition

$$F_n = \frac{1}{h_n}\sum_{j=0}^{N}\frac{\pi}{c_j N}T_{l,n}(\eta_j)F(\eta_j), \quad n = 0, \ldots, N. \tag{26}$$

If $F(\eta)$ is approximated using the shifted Chebyshev polynomials and evaluated at the shifted Gauss-Lobatto collocation points, then any arbitrary order derivative of $F(\eta)$ is given as

$$\mathsf{D}^\alpha F_N(\eta_p) = \sum_{j=0}^{N} \mathsf{D}^\alpha_{j,p} F(\eta_j). \tag{27}$$

Here,

$$\mathsf{D}^\alpha_{j,p} = \frac{\pi}{c_j N}\sum_{n=0}^{N}\sum_{k=0}^{N}\frac{1}{h_n}T_{l,n}(\eta_j)\mathsf{D}^{(\alpha)}_{n,k}T_{l,k}(\eta_p), \quad j,p = 0, 1, \ldots, N. \tag{28}$$

and

$$\mathsf{D}^{(\alpha)}_{n,k} = n\sum_{j=0}^{n}\frac{(-1)^{n-j}(n+j-1)!2^{2j}}{(n-j)!(2j)!l^j}\frac{\Gamma(j+1)}{\Gamma(j-\alpha+1)}q_{j,k}, \tag{29}$$

where $q_{j,k}$ are entries of a matrix defined as (Ahmadi Darani and Saadatmandi, 2017; Ahmadi-Darani and Nasiri, 2013; Atabakzadeh *et al.*, 2013; Doha *et al.*, 2011)

$$q_{j,k} = \begin{cases} 0 & j = 0, 1, \ldots, \lceil \alpha \rceil - 1, \\ \frac{k\sqrt{\pi}}{h_k} \sum_{r=0}^{k} \frac{(-1))^{k-r}(k+r-1)!2^{2r}}{(k-r)!(2r)!} l^{j-\alpha} \frac{\Gamma(j-\alpha+r+1/2)}{\Gamma(j-\alpha+r+1)} & j = \lceil \alpha \rceil, \lceil \alpha \rceil + 1, \ldots, N; \\ & k = 0, 1, \ldots, N. \end{cases} \tag{30}$$

We note here that if $\alpha = 1$, Eq. (27) is equivalent to

$$\mathsf{D}F_N(\eta_k) = \sum_{j=0}^{N} \left[\frac{2w_{l,j}}{\pi} \sum_{n=1}^{N} \frac{n}{c_n} T_{l,n}(\eta_j) S_{l,n-1}(\eta_k) \right] F(\eta_j), \quad k = 0, \ldots, N, \tag{31}$$

where $S_{l,n}$ is the shifted second kind Chebyshev polynomials of degree $n \geq 1$. In order to approximate $f(\eta)$ in terms of the Chebyshev polynomials, it has been assumed that $f(\eta)$ is a smooth function, so it is safe to take advantage of the semi–group property of the Caputo fractional operator, therefore when approximating $f^{\alpha+2}(\eta)$, we can have (Matlob and Jamali, 2017; Dabiri and Butcher, 2018)

$$\frac{d^2}{d\eta^2} \left({}_0^C D_\eta^\alpha f(\eta) \right) = {}_0^C D_\eta^\alpha \left(\frac{d^2 f(\eta)}{d\eta^2} \right) = {}_0^C D_\eta^{2+\alpha} f(\eta). \tag{32}$$

3.1. Error bound estimation

If $F(\eta)$ is a square integrable function and $w_l(\eta)$ is a Lebesque integrable function defined in the interval $(0, l)$, we can define a $L^2_{w_l}$ space in which $F(\eta)$ is measurable and the norm of $F(\eta)$ associated with the space is defined as

$$\|F(\eta)\|_{w_l} = \left(\int_0^l |F(\eta)|^2 w_l(\eta) d\eta \right)^{\frac{1}{2}}, \quad \text{finite}, \tag{33}$$

and this norm is induced by the inner product

$$\langle F(\eta), \tilde{F}(\eta) \rangle = \int_0^l F(\eta) \tilde{F}(\eta) w_l(\eta) d\eta. \tag{34}$$

If we consider $\mathbf{T}_N$, the space of all Chebyshev polynomials of degree $\leq N$, such that $\mathbf{T}_N F(\eta)$ is the approximation of $F(\eta)$ on the shifted Chebyshev–Gauss–Lobatto nodes. Assume that the derivative $F^{N+1}(\eta)$ exist and is continuous on the interval $(0, l)$, and using the error term of the generalized Taylor's approximation of $F(\eta)$, for any η, the error bound is defined as

$$\|\varepsilon_N\|_{w_l} = \|F(\eta) - \mathbf{T}_N F(\eta)\|^2_{w_l} \tag{35}$$

$$\leq \frac{1}{(\Gamma(N+2))^2} Q_N \int_0^l \frac{\eta^{2N+2}}{\sqrt{l\eta - \eta^2}} d\eta \tag{36}$$

$$= \frac{1}{(\Gamma(N+2))^2} Q_N l^{2N+2} \frac{\Gamma(2N+5/2)}{\Gamma(2N+3)}, \tag{37}$$

where $Q_N = \left(\max_{0<\eta\leq l} F^{N+1}(\eta) \right)^2$. For sufficiently large N, we can see that $\|\varepsilon_N\|_{w_l} \to 0$.

4. NUMERICAL RESULTS

In this section, we obtain approximate solutions of the equations describing heat and mass transfer in a nanofluid with space fractional constitutive relation using the technique described in Section 3. The aim is to obtain approximate solutions of the system of differential Eqs. (18) to (20) rather than giving an analysis of the effects of the flow parameters. The parametric analysis of heat and mass transfer process has been given in studies such as Dhanai *et al.* (2015); Khan and Pop (2010); Fang and Zhang (2009); Chen *et al.* (2015). Some results obtained using the above scheme are compared with results in these studies. The nonlinear system is first linearized using quasilinearization as in Bellman and Kalaba (1965); Motsa *et al.* (2011, 2014) [see Appendix A for the discretization of the equations]. In developing numerical schemes, a pertinent question often asked centers around the accuracy of the numerical scheme. For an approximation method, it is expected that when the approximate solutions and their derivatives are substituted in Eqs. (18) to (20), the residual errors should vanish. That is, given the points $\eta_j \in [0, l]$ for $j = 0, \ldots, N$, we should expect

$$\varepsilon_f = \left| {}_0^C D_\eta^{\alpha+2} f(\eta_j) - Re_\alpha M^2 \frac{df}{d\eta}(\eta_j) - Re_\alpha \left(\frac{df}{d\eta}(\eta_j) \right)^2 + Re_\alpha f(\eta_j) \frac{d^2 f}{d\eta^2}(\eta_j) \right|_{L^2_{w_l}} \approx 0 \tag{38}$$

$$\varepsilon_\theta = \left| Le \frac{d^2\theta}{d\eta^2}(\eta_j) + \frac{d\theta}{d\eta}(\eta_j) \frac{d\phi}{d\eta}(\eta_j) + \frac{1}{Nbt} \left(\frac{d\theta}{d\eta}(\eta_j) \right)^2 + LePrf(\eta_j) \frac{d\theta}{d\eta}(\eta_j) \right|_{L^2_{w_l}} \approx 0 \tag{39}$$

$$\varepsilon_\phi = \left| \frac{d\phi}{d\eta}(\eta_j) + \frac{1}{Nbt} \frac{d^2\theta}{d\eta^2}(\eta_j) + Scf(\eta_j) \frac{d\phi}{d\eta}(\eta_j) \right|_{L^2_{w_l}} \approx 0. \tag{40}$$

Tables 1 to 3 show the solutions obtained for different values of N and α and the residual errors as defined in Eqs. (38) to (40). The approximate solutions are obtained with $Nt = Nb = 0.5, Le = Pr = 5, Re_\alpha = 1, M = 0$. It can be seen that the errors are bounded between 10^{-16} and 10^{-13}.

An analytic solution of the momentum equation for $\alpha = 1$ and $Re_\alpha = 1$ was obtained by Fang and Zhang (2009) as

$$f(\eta) = \frac{1}{\sqrt{1+M^2}} \left(1 - e^{-\sqrt{1+M^2}\eta} \right), \tag{41}$$

and so the skin friction is given as

$$f''(0) = -\sqrt{1+M^2}. \tag{42}$$

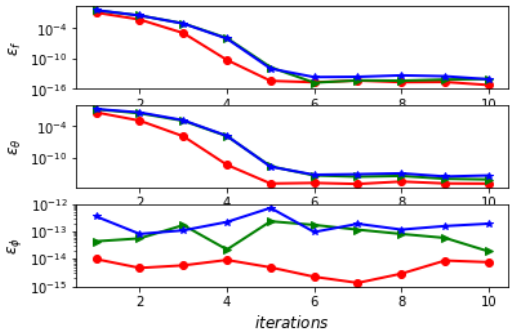

Fig. 2 The $L^2_{w_l}$ norm error of the numerical solutions to the model equations using different number of collocation points. The blue line corresponds to $N = 10$, green line to $N = 15$ and red line corresponds to $N = 20$ for $\alpha = 0.2$.

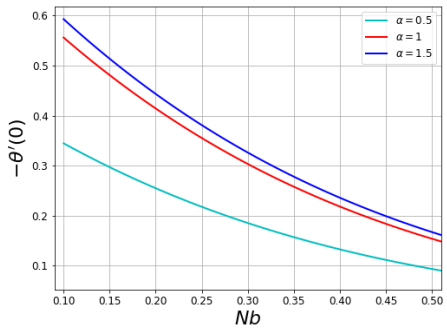

(a)

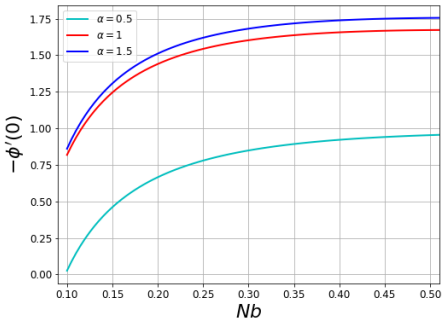

(b)

Fig. 3 Variation of heat and mass transfer rates with Nb for different values of fractional order α.

Table 3 Approximate solution of $\phi(\eta)$ and the maximum residual error for $l = 2$.

α	N	$\phi(\eta)$	ε_ϕ
0.5	4	$[1, 0.5661, 0.1631, 0.0565, 0]^T$	$5.55e^{-16}$
	6	$[1, 0.7769, 0.3273, 0.0650, -0.0047, -0.0107, 0]^T$	$1.54e^{-14}$
1	4	$[1, 0.5749, 0.2088, 0.0752, 0]^T$	$1.55e^{-15}$
	6	$[1, 0.7658, 0.3564, 0.1916, 0.0928, 0.0140, 0]^T$	$1.50e^{-14}$
1.5	4	$[1, 0.5443, 0.2174, 0.0348, 0]^T$	$2.66e^{-15}$
	6	$[1, 0.7457, 0.3362, 0.1917, 0.0665, 0.0010, 0]^T$	$7.55e^{-15}$

Table 4 Comparison of the shear stress at the wall $f^{(\alpha+1)}(0)$ for $\alpha = 1$ between the exact solution as obtained by Fang and Zhang, 2009 and approximate solutions based on the proposed method.

M	Exact	Approximate
0	-1.0000	-1.000039
0.1	-1.0049	-1.004979
0.2	-1.0198	-1.019658
0.3	-1.0440	-1.043674
0.4	-1.0770	-1.076404
0.5	-1.1180	-1.117066

Table 1 Computation results of $f'(\eta)$ and the maximum residual error for $l = 2$.

α	N	$f'(\eta)$	ε_f
0.5	4	$[1, 0.7111, 0.0007, -0.2103, 0]$	$1.33e^{-15}$
	6	$[1, 0.7734, 0.1885, -0.0036, -0.0526, -0.1339, 0]^T$	$1.09e^{-14}$
1	4	$[1, 0.7439, 0.3115, 0.0675, 0]^T$	$6.11e^{-16}$
	6	$[1, 0.8671, 0.5768, 0.3046, 0.1236, 0.0288, 0]^T$	$4.40e^{-14}$
1.5	4	$[1, 1.001, 0.6175, 0.1164, 0]^T$	$7.77e^{-16}$
	6	$[1, 0.9702, 0.7793, 0.4531, 0.18308, 0.0391, 0]^T$	$1.07e^{-13}$

Table 2 Numerical results of $\theta(\eta)$ and norm of the residual error for $l = 2$

α	N	$\theta(\eta)$	ε_θ
0.5	4	$[1, 0.9219, 0.5083, 0.1128, 0]^T$	$4.44e^{-16}$
	6	$[1, 0.9863, 0.8981, 0.6650, 0.3585, 0.1035, 0]^T$	$4.10e^{-15}$
1	4	$[1, 0.9052, 0.3961, 0.0301, 0]^T$	$8.05e^{-16}$
	6	$[1, 0.9770, 0.8048, 0.4140, 0.1170, 0.0214, 0]^T$	$6.14e^{-15}$
1.5	4	$[1, 0.8571, 0.2085, 0.0310, 0]^T$	$8.33e^{-16}$
	6	$[1, 0.9757, 0.7606, 0.3093, 0.0562, 0.0124, 0]^T$	$3.43e^{-15}$

Table 5 Comparison of the heat and mass transfer coefficients at the wall for different values of Nt and Nb with $\alpha = 1$ and fixed values for $Pr = Le = 10$, $Re_\alpha = 1$ and $M = 0$

Nt	Nb	$-\theta'(0)$		$-\phi'(0)$	
		Present Study	Khan and Pop (2010)	Present Study	Khan and Pop (2010)
0.2	0.2	0.36572	0.3654	2.49971	2.5152
	0.3	0.18262	0.1816	2.50181	2.5150
	0.4	0.08745	0.0859	2.46878	2.4807
0.3	0.2	0.27395	0.2371	2.63457	2.6555
	0.3	0.13639	0.1355	2.59230	2.6068
	0.4	0.06496	0.0641	2.53433	2.5486
0.4	0.2	0.21160	0.2110	2.75631	2.7818
	0.3	0.10507	0.1046	2.66824	2.6876
	0.4	0.04996	0.0495	2.58740	2.6038

Table 6 Numerical values of the shear stress at the wall, rate of heat and mass transfer coefficients for different values of the fractional order α, magnetic parameter M, and Prandtl number Pr when $Le = 5, Nt = Nb = 0.5$.

M	α	Pr	$f^{(\alpha+1)}(0)$	$-\theta'(0)$	$-\phi'(0)$
0	0.5	0.7	12.31787	0.37124	1.04856
		10	12.31714	0.00415	1.46487
	1	0.7	-1.05859	0.42433	1.59908
		10.	-1.06348	0.03665	1.81565
	1.5	0.7	-2.19141	0.44243	1.70113
		10	-2.17969	0.03934	1.95014
0.5	0.5	0.7	12.34448	0.36922	1.02365
		10	12.34473	0.00340	1.45313
	1	0.7	-1.16309	0.42146	1.58259
		10	-1.16406	0.03584	1.79791
	1.5	0.7	-2.38672	0.44005	1.69217
		10	-2.40234	0.03960	1.93226

To establish the accuracy of the numerical scheme, we compare Equation (42) with the approximate solutions. Table 4 shows the comparison between the exact and approximate values of the skin friction coef-

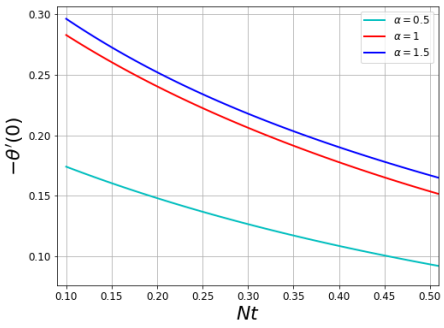

(a)

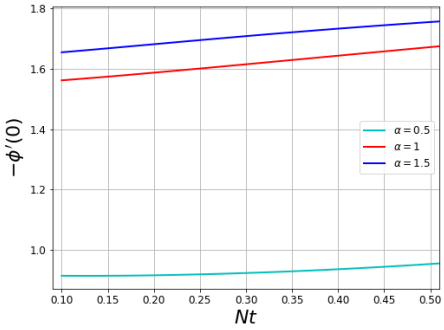

(b)

Fig. 4 Variation of heat and mass transfer rates with Nt for different values of fractional order α.

ficient for different values of M. The approximate values are found to be close to the exact values. The approximate values in Table 4 are obtained with $N = 10$ and $l = 5.9$. The heat and mass transfer coefficients $\{\theta'(0), \phi'(0)\}$ obtained using this method are compared with earlier results by Khan and Pop (2010). Table 5 shows that the new results are in agreement with the published data. Figure 2 shows that the solutions converge for different number of collocation points, especially in the equation where we have the fractional order. In Table 6, the approximate values of the skin friction and heat and mass transfer rates are presented. Figs. 3 and 4 respectively show the variation in the heat and mass transfer rates with the Brownian diffusion and thermophoresis parameters for different values of the fractional order α. It can be clearly seen that the heat and mass transfer rates increase as α increases. Fig. 3(a) shows that the heat transfer rate decreases as the mass diffusion parameter Nb increases, while Fig. 3(b) shows that the mass transfer rate is a monotonically increasing function of Nb. From Fig. 4, we can see that the mass transfer rate decreases as the thermal diffusion parameter increases, while the heat transfer rate strictly decreases. Previous studies have suggested that increasing the number of collocation points for spectral methods does not necessarily improves the accuracy (Dabiri and Butcher, 2017b,a; Zayernouri and Karniadakis, 2014).

5. CONCLUSION

This study proposed a new numerical technique for finding solutions of fractional differential equations. The method uses Chebyshev polynomials as basis function for the series solution and interpolating using Gauss–Lobatto quadrature. Differentiation matrices for fractional and integer order derivatives were introduced. To test its accuracy, the method was used to solve the model equations that describe momentum, heat and mass transfer in a nanofluid with fractional constitutive relation. The residual error norms in the solutions were found to be less or equal to 10^{-13}, thus demonstrating the accuracy and convergence of the method.

APPENDIX A: DISCRETIZATION OF THE MODEL EQUATIONS

In this appendix, we describe the full discretization of the coupled system of the equations (18) to (20). We obtain the numerical solution $f(\eta)$ by solving Eq. (18) independent of Eqs. (19) and (20) and then Eqs. (19) and (20) are solved as coupled system. In order to linearize each equation, we apply the quasilinearization method of Bellman and Kalaba (1965). The linearization method is a generalization method of the Newton–Raphson method and is constructed using the Taylor's series expansion about an initial guess of the solution. Applying the linearization on Eqs. (18), we have

$$f_{r+1}^{\alpha+1} + (Re_\alpha f_r) f''_{r+1} + (-2Re_\alpha f'_r - Re_\alpha M^2) f'_{r+1} + (Re_\alpha f''_r) f_{r+1} = R_r^f, \tag{43}$$

where $R_r^f = Re_\alpha f''_r f_r - Re_\alpha f'^2_r$ and f_r and f_{r+1} are solutions $f(\eta)$ at two successive iterations. The linearization method assumes that the difference between these solutions approaches zero as $r \to \infty$ (Bellman and Kalaba, 1965). If we now apply the Chebyshev approximation on the linearized Eq. (43) by substituting Eqs. (25), (27), and (31) where appropriate and using the semi–group property, so that we have

$$\left[\mathsf{D}^\alpha \mathsf{D}^2 + \mathit{diagflt}[Re_\alpha f_r]\mathsf{D}^2 + \mathit{diagflt}[-2Re_\alpha f'_r - Re_\alpha M^2]\mathsf{D} + \mathit{diagflt}[Re_\alpha f''_r]\right] f_{N,r+1} = \mathsf{R}_r^f, \tag{44}$$

in which *diagflt*[...] constructs a two–dimensional matrix with the input as a diagonal. upon obtaining the solution $f_{N,r+1}(\eta)$, we use the known solution in the linearization of Eqs. (19) and (20) which is solved as system. The linearized form of Eqs. (19) and (20) is given as

$$Le\theta''_{r+1} + (\phi'_r + (2/Nbt)\theta'_r + LePrf_{r+1})\theta'_{r+1} + (\theta'_r)\phi'_{r+1} = R_r^\theta \tag{45}$$

$$(1/Nbt)\theta''_{r+1} + \phi''_{r+1} + (Scf_{r+1})\phi'_{r+1} = 0, \tag{46}$$

where $R_r^\theta = \phi'_r\theta'_r + (1/Nbt)\theta'^2_r$. Again we apply the Chebyshev approximation to the linearized coupled system and this yields

$$\left[Le\mathsf{D}^2 + \mathit{diagflt}[\phi'_r + (2/Nbt)\theta'_r + LePrf_{r+1}]\mathsf{D}\right]\theta_{N,r+1} + \left[\mathit{diagflt}[\theta'_r]\mathsf{D}\right]\phi_{N,r+1} = \mathsf{R}_r^\theta \tag{47}$$

$$\left[(1/Nbt)\mathsf{D}^2\right]\theta_{N,r+1} + \left[\mathsf{D}^2 + \mathit{diagflt}[Scf_{r+1}]\mathsf{D}\right]\phi_{N,r+1} = \mathsf{O}, \tag{48}$$

where O is a zero matrix of size $(N+1)\times 1$. Note also that the right hand side of Eqs. (44) and (47) are expressed in terms of the $N+1$–truncated shifted Chebyshev approximation. As stated earlier, the semi–infinite domain $[0,\infty)$ has been truncated to $[0,l]$, therefore, the coupled linearized system of algebraic equations are solved subject to

$$f_{N,r+1}(\eta_0) = 0, \quad \mathsf{D}_{0,q} f_{N,r+1}(\eta_0) = 1, \quad \theta_{N,r+1}(\eta_0) = 1, \quad \phi_{N,r+1}(\eta_0) = 1$$
$$\mathsf{D}_{N,q} f_{N,r+1}(\eta_N) = 0, \quad \theta_{N,r+1}(\eta_N) = 0, \quad \phi_{N,r+1}(\eta_N) = 0 \tag{49}$$

to obtain a consistent system.

REFERENCES

Abramowitz, M., and Stegun, I.A., 1965, *Handbook of mathematical functions: with formulas, graphs, and mathematical tables*, vol. 55, Courier Corporation.
https://doi.org/10.1115/1.3625776.

Ahmadi-Darani, M., and Nasiri, M., 2013, "a fractional type of the Chebyshev polynomials for approximation of solution of linear fractional differential equations," *Computational Methods for Differential Equations*, **1**(2), 96–107.

Ahmadi Darani, M., and Saadatmandi, A., 2017, "the operational matrix of fractional derivative of the fractional-order Chebyshev functions and its applications," *Computational Methods for Differential Equations*, **5**(1), 67–87.

Atabakzadeh, M., Akrami, M., and Erjaee, G., 2013, "Chebyshev operational matrix method for solving multi-order fractional ordinary differential equations," *Applied Mathematical Modelling*, **37**(20-21), 8903–8911.
https://doi.org/10.1016/j.apm.2013.04.019.

Atanackovic, T.M., Pilipovic, S., Stankovic, B., and Zorica, D., 2014, *Fractional calculus with applications in mechanics: wave propagation, impact and variational principles*, John Wiley & Sons.
https://doi.org/10.1002/9781118909065.

Bellman, R.E., and Kalaba, R.E., 1965, "Quasilinearization and nonlinear boundary-value problems," .

Chen, S., Zheng, L., Shen, B., and Chen, X., 2015, "Time–space dependent fractional boundary layer flow of Maxwell fluid over an unsteady stretching surface," *Theoretical and Applied Mechanics Letters*, **5**(6), 262–266.
https://doi.org/10.1016/j.taml.2015.11.005.

Dabiri, A., and Butcher, E.A., 2017a, "Efficient modified Chebyshev differentiation matrices for fractional differential equations," *Communications in Nonlinear Science and Numerical Simulation*, **50**, 284–310.
https://doi.org/10.1016/j.cnsns.2017.02.009.

Dabiri, A., and Butcher, E.A., 2017b, "Stable fractional Chebyshev differentiation matrix for the numerical solution of multi-order fractional differential equations," *Nonlinear Dynamics*, **90**(1), 185–201.
https://doi.org/10.1007/s11071-017-3654-3.

Dabiri, A., and Butcher, E.A., 2018, "Numerical solution of multi-order fractional differential equations with multiple delays via spectral collocation methods," *Applied Mathematical Modelling*, **56**, 424–448.
https://doi.org/10.1016/j.apm.2017.12.012.

Dhanai, R., Rana, P., and Kumar, L., 2015, "Multiple solutions of MHD boundary layer flow and heat transfer behavior of nanofluids induced by a power-law stretching/shrinking permeable sheet with viscous dissipation," *Powder Technology*, **273**, 62–70.
https://doi.org/10.1016/j.powtec.2014.12.035.

Diethelm, K., Ford, N.J., and Freed, A.D., 2002, "a predictor-corrector approach for the numerical solution of fractional differential equations," *Nonlinear Dynamics*, **29**(1-4), 3–22.
https://doi.org/10.1023/A:1016592219341.

Doha, E., Bhrawy, A., and Ezz-Eldien, S., 2011, "Efficient Chebyshev spectral methods for solving multi-term fractional orders differential equations," *Applied Mathematical Modelling*, **35**(12), 5662–5672.
https://doi.org/10.1016/j.apm.2011.05.011.

Doha, E., Bhrawy, A., and Ezz-Eldien, S., 2012, "a new Jacobi operational matrix: an application for solving fractional differential equations," *Applied Mathematical Modelling*, **36**(10), 4931–4943.
https://doi.org/10.1016/j.apm.2011.12.031.

El-Sayed, A., El-Kalla, I., and Ziada, E., 2010, "Analytical and numerical solutions of multi-term nonlinear fractional orders differential equations," *Applied Numerical Mathematics*, **60**(8), 788–797.
https://doi.org/10.1016/j.apnum.2010.02.007.

Erjaee, G., Taghvafard, H., and Alnasr, M., 2011, "Numerical solution of the high thermal loss problem presented by a fractional differential equation," *Communications in Nonlinear Science and Numerical Simulation*, **16**(3), 1356–1362.
https://doi.org/10.1016/j.cnsns.2010.06.031.

Fang, T., and Zhang, J., 2009, "Closed-form exact solutions of MHD viscous flow over a shrinking sheet," *Communications in Nonlinear Science and Numerical Simulation*, **14**(7), 2853–2857.
https://doi.org/10.1016/j.cnsns.2008.10.005.

Kayedi-Bardeh, A., Eslahchi, M., and Dehghan, M., 2014, "a method for obtaining the operational matrix of fractional Jacobi functions and applications," *Journal of Vibration and Control*, **20**(5), 736–748.
https://doi.org/10.1177/1077546312467049.

Kazem, S., Abbasbandy, S., and Kumar, S., 2013, "Fractional-order Legendre functions for solving fractional-order differential equations," *Applied Mathematical Modelling*, **37**(7), 5498–5510.
https://doi.org/10.1016/j.apm.2012.10.026.

Khan, W., and Pop, I., 2010, "Boundary-layer flow of a nanofluid past a stretching sheet," *International journal of heat and mass transfer*, **53**(11-12), 2477–2483.
https://doi.org/10.1016/j.ijheatmasstransfer.2010.01.032.

Matlob, M.A., and Jamali, Y., 2017, "the concepts and applications of fractional order differential calculus in modelling of viscoelastic systems: A primer," *Critical ReviewsâĎć in Biomedical Engineering*.
https://doi.org/10.1615/CritRevBiomedEng.2018028368 .

Miller, K.S., and Ross, B., 1993, "an introduction to the fractional calculus and fractional differential equations," .

Momani, S., and Odibat, Z., 2007a, "Comparison between the homotopy perturbation method and the variational iteration method for linear fractional partial differential equations," *Computers & Mathematics with Applications*, **54**(7-8), 910–919.
https://doi.org/10.1016/j.camwa.2006.12.037.

Momani, S., and Odibat, Z., 2007b, "Homotopy perturbation method for nonlinear partial differential equations of fractional order," *Physics Letters A*, **365**(5-6), 345–350.
https://doi.org/10.1016/j.physleta.2007.01.046.

Motsa, S.S., Dlamini, P.G., and Khumalo, M., 2014, "Spectral relaxation method and spectral quasilinearization method for solving unsteady boundary layer flow problems," *Advances in Mathematical Physics*.
https://doi.org/10.1155/2014/341964.

Motsa, S., Sibanda, P., and Shateyi, S., 2011, "on a new quasi-linearization method for systems of nonlinear boundary value problems," *Mathematical Methods in the Applied Sciences*, **34**(11), 1406–1413.
https://doi.org/10.1002/mma.1449.

Podlubny, I., 1998, *Fractional differential equations: an introduction to fractional derivatives, fractional differential equations, to methods of their solution and some of their applications*, vol. 198, Elsevier.

Sun, H., Zhang, Y., Wei, S., Zhu, J., and Chen, W., 2018, "a space fractional constitutive equation model for non-Newtonian fluid flow," *Communications in Nonlinear Science and Numerical Simulation*, **62**, 409–417.
https://doi.org/10.1016/j.cnsns.2018.02.007.

Tarasov, V.E., 2013, "Review of some promising fractional physical models," *International Journal of Modern Physics B*, **27**(09), 1330005.
https://doi.org/10.1142/S0217979213300053.

Wang, Q., 2006, "Numerical solutions for fractional KdV–Burgers equation by Adomian decomposition method," *Applied Mathematics and Computation*, **182**(2), 1048–1055.
https://doi.org/10.1016/j.amc.2006.05.004.

Zayernouri, M., and Karniadakis, G.E., 2014, "Fractional spectral collocation method," *SIAM Journal on Scientific Computing*, **36**(1), A40–A62.
https://doi.org/10.1137/130933216.

Chapter 3

A Chebyshev based spectral method for solving boundary layer flow of a fractional order Oldroyd–B fluid

In Chapter 2, a space fractional ordinary differential equation was solved and we showed that approximating the solutions as a truncated series expansion of the Chebyshev polynomials of the first kind gives accurate results. In this chapter, we extend this method to time fractional one–dimensional nonlinear partial differential equations of arbitrary orders. The time–fractional partial differential equations model the boundary layer flow of an Oldroyd–B fluid. The solutions of these equations are represented as a linear combination of shifted Chebyshev polynomials of the first kind, and are then interpolated using the Gauss–Lobatto quadrature. The nonlinear terms are linearized using a Newton–Raphson like approach. We present error bound estimates for the numerical results. We also investigate the effect of the fractional order objective stress rate on the shear stress and fluid velocity.

IIETA International Information and Engineering Technology Association
Advancing the World of Information and Engineering

Mathematical Modelling of Engineering Problems
Vol. 7, No. 3, September, 2020, pp. 377-386
Journal homepage: http://iieta.org/journals/mmep

A Chebyshev Based Spectral Method for Solving Boundary Layer Flow of a Fractional-Order Oldroyd-B Fluid

Shina D. Oloniiju*, Sicelo P. Goqo, Precious Sibanda

School of Mathematics, Statistics and Computer Science, University of KwaZulu-Natal, Private Bag X01, Scottsville, Pietermaritzburg 3209, South Africa

Corresponding Author Email: shina@aims.edu.gh

https://doi.org/10.18280/mmep.070307

Received: 14 June 2020
Accepted: 5 September 2020

Keywords:
MHD fluid, non-isothermal flow, fractional calculus, Chebyshev – Gauss – Lobatto quadrature, fractional Oldroyd–B fluid

ABSTRACT

We focused on developing an accurate numerical scheme for the flow of a fractional-order Oldroyd–B fluid model with the non-isothermal property. In many cases, the direct application of the Chebyshev tau method using the operational matrix of the Chebyshev polynomials usually leads to an accurate solution. However, in some cases, dealing with non–linearity and coupling can be tedious. In this study, we present a numerical method based on Chebyshev polynomials of the first kind and interpolation using Gauss–Lobatto quadrature. The coefficients of the series expansion of the pseudospectral method are obtained through integration of the Chebyshev polynomials orthogonality condition. The numerical results show that the scheme is accurate and reliable. The effects of the fractional-order objective stress rate of the Oldroyd–B fluid on the velocity and shear stress are also presented. The error bound theorems presented in this study support the findings of the numerical computations.

1. INTRODUCTION

The Oldroyd–B fluid is a rate type model for viscoelastic fluids that have been studied extensively since its formulation by Oldroyd [1]. This model is part of a large class of rate type viscoelastic fluids models, which include, but are not limited to the upper convected Maxwell model, Jeffrey model and Burgers' model. The Oldroyd-B model gives a good representation of the rheological response of viscoelastic fluids in shear flow. The Cauchy stress tensor for the classical Oldroyd–B constitutive model has the form

$$S_{ij} = -p\delta_{ij} + \tau_{ij}, \tag{1}$$

$$\left[1 + \lambda \overset{\nabla}{\mathrm{D}}\right] \tau_{ij} = \mu \left[1 + \lambda_r \overset{\nabla}{\mathrm{D}}\right] e_{ij}, \tag{2}$$

where, τ_{ij} is the extra stress tensor, e_{ij} is the stress tensor. The material parameters μ, λ and λ_r are the viscosity, stress relaxation time and retardation time respectively and $\overset{\nabla}{\mathrm{D}}$ is the upper convected time derivative. The constitutive model of the Oldroyd–B is a generalization of the Maxwell fluid model [2]. Unlike the Maxwell model, the Oldroyd–B fluid uses the objective stress rate that takes into account frame indifference of the deformation rate. The deformation rate is represented by the upper convected derivative in Eq. (2). Because of the memory retention characteristics of viscoelastic fluids, recent studies have suggested using non–local time derivatives [3]. Non–local objective stress rate exhibits complex dynamical and viscoelastic behaviours. Taking advantage of the inherent non–locality and memory retention characteristics of fractional derivatives, we generalize the Oldroyd–B constitutive relation by replacing the local time derivatives in Eq. (2) with fractional time derivative [4]:

$$\left[1 + \lambda^{\alpha} \overset{\nabla}{\mathrm{D}}{}^{\alpha}\right] \tau_{ij} = \mu \left[1 + \lambda_r^{\beta} \overset{\nabla}{\mathrm{D}}{}^{\beta}\right] e_{ij}, \tag{3}$$

where,

$$\overset{\nabla}{\mathrm{D}}{}^{\alpha} = \frac{\partial^{\alpha} \tau}{\partial t^{\alpha}} + \mathbf{U} \cdot \nabla \tau - \tau \nabla \mathbf{U} - (\nabla \mathbf{U})^{\mathrm{T}} \tau. \tag{4}$$

In the constitutive model Eq. (3), $0<\alpha, \beta \leq 1$ and $\mu, \lambda, \lambda_r>0$. If $\alpha>\beta$, it should be noted that the model is physically unrealistic. This case corresponds to an increasing relaxation function [5]. Hence, the constraint on the order of the derivatives must satisfy $0<\alpha \leq \beta \leq 1$. It is evident that if $\alpha=\beta=1$, the constitutive relation is the classical Oldroyd–B fluid. Setting λ_r to zero in Eq. (3) corresponds to the fractional Maxwell fluid, if $\lambda=0$, the model is equivalent to the fractional second-grade fluid, if $0<\lambda_r<\lambda$, we obtain the fractional Jeffrey fluid [6] and when $\lambda=\lambda_r=0$, the model corresponds to the classical Newtonian fluid. If we consider an incompressible fluid with constant pressure and using established notation, the momentum conservation equation for an unsteady flow of a magnetohydrodynamic (MHD) fluid is:

$$\rho \left[\frac{\partial \mathbf{U}}{\partial t} + \mathbf{U} \cdot \nabla \mathbf{U}\right] = \nabla \tau_{ij} - \sigma B_0^2 \mathbf{U}, \tag{5}$$

where, ρ is the fluid density, σ is the electrical conductivity of the fluid and B_0 is the applied magnetic field. To write the conservation equation and the shear stress relation in non–dimensional form, we assume a reference length $\mathbf{L}$ and velocity $\mathbf{U}_0$, so that we define $t = \tilde{t}\mathbf{L}\mathbf{U}_0^{-1}$, $\mathbf{y} = \tilde{\mathbf{y}}\mathbf{L}$ for all $\mathbf{y}$ in

the domain of the flow, $\mathbf{U}(\mathbf{y},t)=\mathbf{U}_0\tilde{\mathbf{U}}(\tilde{\mathbf{y}},\tilde{t})$, $\tau_{ij}(\mathbf{y},t)=\mathbf{U}_0\mu\mathbf{L}^{-1}\tilde{\tau}_{ij}(\tilde{\mathbf{y}},\tilde{t})$, and $\lambda_r=\tilde{\lambda}_r\mathbf{L}\mathbf{U}_0^{-1}$. Therefore, we write Eq. (3) and Eq. (5) in the dimensionless form (dropping the tilde for convenience):

$$Re\left[\frac{\partial\mathbf{U}}{\partial t}+\mathbf{U}\cdot\nabla\mathbf{U}\right]=\nabla\tau_{ij}-Ha^2\mathbf{U} \tag{6}$$

$$\left[1+We^{\alpha}\overset{\triangledown}{\mathrm{D}}^{\alpha}\right]\tau_{ij}=\left[1+\lambda_r^{\beta}\overset{\triangledown}{\mathrm{D}}^{\beta}\right]e_{ij}. \tag{7}$$

Here, $Re=\rho\mathbf{L}\mathbf{U}_0\mu^{-1}$ is the Reynolds number, $Ha=B_0\mathbf{L}(\sigma/\mu)^{1/2}$ is the Hartmann number, $We=\mathbf{U}_0\lambda\mathbf{L}^{-1}$ is the Weissenberg number, λ_r is a dimensionless retardation parameter. Some special cases of interest include the Jeffrey fluid ($0<\lambda_r<We$), Maxwell fluid ($\lambda_r=0$), second-order fluid ($We=0$), Newtonian fluid ($We=\lambda_r=0$) and hydrodynamic fluids ($Ha=0$).

Exact solutions to fractional partial differential equations are, in general, challenging to find. Even when found, the solution may contain complicated integrals and special functions that have to be approximated numerically. Several studies have proposed various methods, both numerical and analytic, for solving fractional differential equations [7-12]. However, recent studies have identified spectral methods as efficient for approximating solutions of fractional partial differential equations. Spectral methods are favoured because of their spectral rate of convergence and accuracy, especially for differential equations with sufficiently smooth solutions. Doha et al. [13] and Atabakzadeh et al. [14] presented the operational matrix of the shifted Chebyshev polynomial and used the polynomial to approximate multi-order fractional ordinary differential equations. Liu et al. [15] presented numerical solutions to multiterm variable-order fractional ordinary differential equations using the Chebyshev polynomial of the second kind as the basis function. Operational matrices of the shifted Chebyshev wavelets, generalized Laguerre polynomials, and Bernstein polynomials are presented in the studies of Benattia and Belghaba [16], Bhrawy and Alghamdi [17], Baseri et al. [18] respectively. These matrices are used to approximate the solutions of fractional differential equations. The numerical results that were reported in the studies as mentioned earlier are typical of spectral method, and they exhibit the spectral convergence property of spectral methods. From literature, many authors have used the spectral tau method to solve fractional differential equations with different orthogonal polynomials as basis functions. In this study, we propose a spectral method that uses the shifted Chebyshev polynomials of the first kind as basis functions and interpolates using Gauss–Lobatto quadrature. We obtain the coefficients of the series expansion in the spectral method by integrating the orthogonal condition of the Chebyshev polynomials using Chebyshev-Gauss-Lobatto quadrature. We then apply the resulting fractional differentiation matrix to solve fractional partial differential equations that describe the unsteady boundary layer flow of a generalized MHD Oldroyd–B fluid and a non–isothermal flow of an Oldroyd–B fluid (see Section 4). We also investigate the effects of derivatives of arbitrary order in Eq. (6) and Eq. (7) on fluid velocity and shear stress.

2. FRACTIONAL ORDER DIFFERENTIATION MATRIX

The most used definitions of fractional operators are the Riemann-Liouville and Caputo fractional operators. In the Riemann-Liouville case, we have the definition

$${}^{RL}\mathrm{D}_y^{\alpha}H(y)=\frac{1}{\Gamma(n-\alpha)}\frac{d^n}{dy^n}\int_0^y\frac{H(\varsigma)}{(y-\varsigma)^{\alpha+1-n}}d\varsigma \tag{8}$$

and the Caputo case is defined as

$${}_0^C\mathrm{D}_y^{\alpha}H(y)=\begin{cases}\dfrac{1}{\Gamma(n-\alpha)}\displaystyle\int_0^y\frac{H^{(n)}(\varsigma)}{(y-\varsigma)^{\alpha+1-n}}d\varsigma, & n-1<\alpha<n\\ \dfrac{d^nH}{dy^n}, & \alpha=n.\end{cases} \tag{9}$$

In both cases, n-1<α<n, and $n\in\mathbb{N}$ and $H(y)$ is a continuously bounded function with n derivatives in [0, L], for χ>0. For an in-depth exploration of these definitions, see Podlubny [19], Atangana [20]. Using the Caputo operator, the following holds

$${}^{C}\mathrm{D}^{\alpha}\ K=0,\qquad \mathrm{K\ is\ a\ constant}, \tag{10}$$

$${}^{C}\mathrm{D}^{\alpha}y^{j}=\begin{cases}0 & \text{for } \mathrm{j}\in\mathbb{N}_0 \text{and } \mathrm{j}<\lceil\alpha\rceil\\ \dfrac{\Gamma(j+1)}{\Gamma(j+1-\alpha)}y^{j-\alpha} & \text{for } \mathrm{j}\in\mathbb{N}_0, \mathrm{j}\geq\lceil\alpha\rceil.\end{cases} \tag{11}$$

Considering that most physical problems are defined in [0, L], L being a truncation of the semi-infinite domain, we define the series form of the shifted Chebyshev polynomials $T_{L,n}$ of degree n>0 as ([21, 22])

$$T_{L,n}=n\sum_{j=0}^{n}\frac{(-1)^{n-j}(n+j-1)!\,2^{2j}}{(n-j)!\,(2j)!\,L^j}y^j, \tag{12}$$

which satisfies the orthogonality condition

$$\int_0^L T_{L,n}(y)T_{L,m}(y)w_L(y)dy=\delta_{mn}h_n. \tag{13}$$

Here, the weight function of the shifted Chebyshev polynomials is given by $w_L(y)=1/\sqrt{Ly-y^2}$ and $h_n=c_n\,\pi/2$, with c_0=2 and c_n=1 for n≥1.

At this point, we discuss some lemmas and theorems that are used in developing the approximation of the fractional-order derivative of a square-integrable function that is expanded by a shifted Chebyshev series and integrated using the Chebyshev-Gauss-Lobatto quadrature.

Remark 2.1: For the shifted Chebyshev–Gauss–Lobatto quadrature, the Christoffel numbers are the same as those of the Chebyshev-Gauss-Lobatto quadrature. The shifted Gauss–Lobatto nodes are defined as ([21])

$$y_j=\frac{L}{2}\cos\left(\frac{\pi j}{N}\right)+\frac{L}{2}, \tag{14}$$

and the associated Christoffel weight number $w_{L,j}=\pi/c_i\ N$, $0\leq j\leq N$, where $c_0=c_N=2$ and $c_j=1$ for j=1,2,…, N-1.

Lemma 2.2: Assume that $u(y)$ is an integrable function defined on the domain$[0,L]$, then the function can be expanded in terms of shifted Chebyshev polynomials as a N+1 truncated series:

$$u_N(y) = \sum_{n=0}^{N} u_n T_{L,n}(y), \tag{15}$$

where, the coefficients u_n satisfy the orthogonality condition, which is given in discrete form as

$$u_n = \frac{1}{h_n} \sum_{j=0}^{N} \frac{\pi}{c_j N} u(y_j) T_{L,n}(y_j), \quad n = 0, \dots, N. \tag{16}$$

Lemma 2.3: Let $T_{L,n}(y)$ be a n–th order shifted Chebyshev polynomials, then the a–th order derivative based on the Caputo's definition is defined as [13, 14]

$$\mathrm{D}^{\alpha} T_{L,n}(y) = \sum_{k=0}^{N} \mathrm{D}_{n,k}^{(\alpha)} T_{L,k}(y), \tag{17}$$

where,

$$\mathrm{D}_{n,k}^{(\alpha)} = n \sum_{j=0}^{n} \frac{(-1)^{n-j}(n+j-1)!\, 2^{2j}}{(n-j)!\,(2j)!\, L^{j}} \frac{\Gamma(j+1)}{\Gamma(j-\alpha+1)} q_{j,k}, \tag{18}$$

and $q_{j,k}$ are entries of a matrix and these entries are defined as (Ahmadi - Darani and Saadatmandi [22], Ahmadi - Darani and Nasiri [23])

$$q_{j,k} = \begin{cases} 0 & j = 0,1, \dots, \lceil \alpha \rceil - 1, \\ \dfrac{k\sqrt{\pi}}{h_k} \displaystyle\sum_{r=0}^{k} \frac{(-1)^{k-r}(k+r-1)!\, 2^{2r}}{(k-r)!\,(2r)!} L^{j-\alpha} \frac{\Gamma\left(j-\alpha+r+\frac{1}{2}\right)}{\Gamma(j-\alpha+r+1)}, & j = \lceil \alpha \rceil, \lceil \alpha \rceil + 1, \dots, N; \\ & k = 0,1, \dots, N. \end{cases} \tag{19}$$

The proof of this lemma can be found in Atabakzadeh et al. [14] and Doha et al. [13].

Theorem 2.4: Assume $u(y)$ is a continuously bounded and integrable function defined on the truncated semi-infinite domain $[0,L]$. If $u(y)$ is approximated using the shifted Chebyshev polynomials and evaluated at the shifted Gauss-Lobatto collocation points, then any arbitrary order derivative of $u(y)$ is given by

$$\mathrm{D}^{\alpha} u_N(y) = \sum_{j=0}^{N} \mathrm{D}_{j,p}^{\alpha} u(y_j). \tag{20}$$

Here,

$$\mathrm{D}_{j,p}^{\alpha} = \frac{\pi}{c_j N} \sum_{n=0}^{N} \sum_{k=0}^{N} \frac{1}{h_n} T_{L,n}(y_j) \mathrm{D}_{n,k}^{(\alpha)} T_{L,k}(y_p), \quad j,p = 0,1, \dots, N. \tag{21}$$

Proof. If we consider the first $N+1$ shifted Chebyshev polynomials, and a combination of the results of Lemma 2.2 and Lemma 2.3, the proof is completed.

Hitherto, we have only focused on functions of one variable. We now focus on functions of two variables, precisely time and spatial variables. We will use the results of the lemmas and theorem stated above to obtain the approximated values of a bivariate function and its fractional-order partial derivatives. The most straightforward approach to expanding a function of two variables is to take the tensor product of the expansion in each variable [24]. For a function $u(y,t)$, the expansion by shifted Chebyshev polynomials is given as

$$u_{N_y,N_t}(y,t) = \sum_{n=0}^{N_y} \sum_{m=0}^{N_t} u_{n,m} T_{L,n}(y) T_{\mathrm{T},m}(t), \tag{22}$$

where, $u_{n,m}$ are entries of the matrix which consist of the coefficients of expansion.

Proposition 2.5: If $u(y,t)$ is a function defined on the rectangular domain $[0,L]\times[0,T]$, then it can be approximated at the shifted Gauss-Lobatto nodes in terms of N+1 shifted Chebyshev polynomials so that we have

$$vec(\vec{u}) = \left[I_t \otimes I_y\right] vec(\vec{u}). \tag{23}$$

Here, both I_y and I_t are interpolation matrices (Lemma 2.2) in y and t respectively, and $vec(\vec{u})$ is formed by piling columns of $\{u(y_i,t_j) \mid i=0,\dots, N_y, j=0,\dots,N_t\}$ into a vector.

Proposition 2.6: Any arbitrary order, say α>0 derivatives of $u(y,t)$ can also be expanded and approximated in terms of the shifted Chebyshev polynomials and shifted Gauss–Lobatto nodes. The α–th order derivatives in terms of both variables are given as

$$\begin{aligned} vec(\vec{u}_{\alpha}) &= \left[I_t \otimes \mathrm{D}_y^{\alpha}\right] vec(\vec{u}), \\ vec(\vec{u}^{\alpha}) &= \left[\mathrm{D}_t^{\alpha} \otimes I_y\right] vec(\vec{u}), \\ vec(\vec{u}_{\alpha}^{\alpha}) &= \left[\mathrm{D}_t^{\alpha} \otimes \mathrm{D}_y^{\alpha}\right] vec(\vec{u}), \end{aligned}$$

where, the superscript indicates the derivative with respect to the temporal variable and the subscript is the derivative with respect to the spatial variable and D^{α} is from Theorem 2.4.

3. ERROR ESTIMATION FOR THE APPROXIMATION

Assume that $u(y)$ is a square-integrable function and $w_L(y)$ is a Lebesgue integrable function defined in the interval $\mathbb{I} = [0, L]$. Then, we can define a $\mathbf{L}_{w_L}^2$ space in which $u(y)$ is measurable and the norm $\| u(y) \|_{w_L}$ is defined as

$$\| u(y) \|_{w_L} = \left(\int_{\mathbb{I}} |u(y)|^2 w_L(y) dy \right)^{1/2} < \infty, \tag{24}$$

such that the norm is induced by the inner product

$$\langle u(y), \hat{u}(y)\rangle = \int_0^L u(y)\hat{u}(y)w_L(y)dy. \tag{25}$$

If $u(y)$ is the exact solution and $u_N(y)$ is the approximated solution based on the Chebyshev polynomials given in Eq. (15) with the coefficients u_n obtained by the normalized inner product

$$u_n = \frac{\langle u_N(y), T_{L,n}(y)\rangle}{\| T_{L,n}(y) \|^2_{w_L}}, \tag{26}$$

We can define an error bound for the approximation in the $\mathbf{L}^2_{w_L}$ norm.

Theorem 3.1 (Error estimation for a single variable approximation): Given the shifted interpolation nodes defined in Eq. (14) and let $P_N u(y)$ be the approximation through these nodes given in Eq. (15), where $\boldsymbol{P_N}$ is the space of all Chebyshev polynomials of degree less than or equal to N. Assume that $d^{N+1}u/dy^{N+1}$ exist and is continuous on the interval $\mathbb{I}$, then the error bound is defined as

$$\begin{aligned}&\|u(y) - \mathbf{P}_N u(y)\| \\ &\leq \frac{1}{\left(\Gamma(N+2)\right)^2}\left(\max_{0<y\leq L}\left|\frac{d^{N+1}u(y)}{dy^{N+1}}\right|\right)^2 L^{2N+2}\sqrt{\pi}\frac{\Gamma\left(2N+\frac{5}{2}\right)}{\Gamma(2N+3)}.\end{aligned} \tag{27}$$

Proof. Consider the generalized Taylor's approximation of $u(y)$ in which the error bound is known as

$$|R_N(y)| \leq \frac{|y|^{N+1}}{\Gamma(N+2)}\max_{0<y\leq L}\left|\frac{d^{N+1}u(y)}{dy^{N+1}}\right|, \tag{28}$$

then for any y in the collocation points

$$\begin{aligned}&\|u(y) - \mathbf{P}_N u(y)\|^2_{w_L} \leq \|R_N(y)\|^2_{w_L} \\ &\leq \frac{1}{\left(\Gamma(N+2)\right)^2}\left(\max_{0<y\leq L}\left|\frac{d^{N+1}u(y)}{dy^{N+1}}\right|\right)^2 \int_0^L \frac{y^{2N+2}}{\sqrt{Ly-y^2}}dy\end{aligned} \tag{29}$$

$$= \frac{1}{\left(\Gamma(N+2)\right)^2}\left(\max_{0<y\leq L}\left|\frac{d^{N+1}u(y)}{dy^{N+1}}\right|\right)^2 L^{2N+2}\sqrt{\pi}\frac{\Gamma\left(2N+\frac{5}{2}\right)}{\Gamma(2N+3)}. \tag{30}$$

This leads to the desired result.

Theorem 3.2: Let $u: \mathbb{I}\times\mathbb{J}\to\mathbb{R}$ be a continuously differentiable function such that at least (N_y+1)th partial derivative with respect to y, (N_t+1)th partial derivative with respect to t, and (N_y+N_t+2)th mixed derivative with respect to y and t exist, then based on the mean value theorem, the following remainder formula holds ([25])

$$\begin{aligned}\left|R_{N_y,N_t}(y,t)\right| \leq{}& \frac{K_1 y^{N_y+1}}{\Gamma\left(N_y+2\right)} + \frac{K_2 t^{N_t+1}}{\Gamma(N_t+2)} \\ &+ \frac{K_3 y^{N_y+1}t^{N_t+1}}{\Gamma\left(N_y+2\right)\Gamma(N_t+2)},\end{aligned} \tag{31}$$

where, $\mathbb{I} = [0, L]$, $\mathbb{J} = [0, \mathrm{T}]$ and K_1, K_2, K_3 are constants, defined as

$$K_1 = \sup\left\{\left|\frac{\partial^{N_y+1}u(y,t)}{\partial y^{N_y+1}}\right| : y,t \in \mathbb{I}\times\mathbb{J}\right\}, \tag{32}$$

$$\begin{aligned}K_2 &= \sup\left\{\left|\frac{\partial^{N_t+1}u(y,t)}{\partial t^{N_t+1}}\right| : y,t \in \mathbb{I}\times\mathbb{J}\right\}, \\ K_3 &= \sup\left\{\left|\frac{\partial^{N_y+N_t+2}u(y,t)}{\partial y^{N_y+1}\partial t^{N_t+1}}\right| : y,t \in \mathbb{I}\times\mathbb{J}\right\},\end{aligned} \tag{33}$$

respectively.

Theorem 3.3 (Error bound for functions of 1+1 variables approximation): We define the error bound for the approximation of a function of two variables as

$$\begin{aligned}&\left\|R_{N_y,N_t}(y,t)\right\|_{w_L,w_\mathrm{T}} \\ &\leq \frac{K_1^2\pi\sqrt{\pi}L^{2N_y+2}}{(\Gamma(N_y+2))^2}\frac{\Gamma(2N_y+\frac{5}{2})}{\Gamma(2N_y+3)} \\ &+ \frac{K_2^2\pi\sqrt{\pi}\mathrm{T}^{2N_t+2}}{(\Gamma(N_t+2))^2}\frac{\Gamma(2N_t+\frac{5}{2})}{\Gamma(2N_t+3)} \\ &+ \frac{K_3^2\pi L^{2N_y+2}\mathrm{T}^{2N_t+2}}{(\Gamma(N_y+2))^2(\Gamma(N_t+2))^2}\frac{\Gamma\left(2N_t+\frac{5}{2}\right)}{\Gamma(2N_t+3)}\frac{\Gamma\left(2N_y+\frac{5}{2}\right)}{\Gamma\left(2N_y+3\right)}\end{aligned} \tag{34}$$

Proof. Given that $\mathbf{P}_{N_y,N_t}u(y,t)$ is the space of all Chebyshev polynomials which approximate $u(y,t)$. In a similar sense as in Theorem 3.1, for any points y, t in the collocation points and using the relation in Eq. (31), we define

$$\begin{aligned}&\left\|u(y,t) - \mathbf{P}_{N_y,N_t}u(y,t)\right\|^2_{w_L,w_\mathrm{T}} \\ &\qquad\leq \left\|R_{N_y,N_t}(y,t)\right\|^2_{w_L,w_\mathrm{T}}\end{aligned} \tag{35}$$

$$\begin{aligned}&\leq \int_{\mathbb{I}\times\mathbb{J}}\left(\left|\frac{K_1 y^{N_y+1}}{\Gamma(N_y+2)}\right|^2 + \left|\frac{K_2 t^{N_t+1}}{\Gamma(N_t+2)}\right|^2\right. \\ &\left.+ \left|\frac{K_3 y^{N_y+1}t^{N_t+1}}{\Gamma(N_y+2)\Gamma(N_t+2)}\right|^2\right)\frac{1}{\sqrt{\mathrm{T}t-t^2}}\frac{1}{\sqrt{Ly-y^2}}dydt\end{aligned} \tag{36}$$

$$\begin{aligned}&= \frac{K_1^2}{(\Gamma(N_y+2))^2}\int_{\mathbb{I}\times\mathbb{J}}\frac{1}{\sqrt{\mathrm{T}t-t^2}}\frac{y^{2N_y+2}}{\sqrt{Ly-y^2}}dydt \\ &+ \frac{K_2^2}{(\Gamma(N_t+2))^2}\int_{\mathbb{I}\times\mathbb{J}}\frac{t^{2N_t+2}}{\sqrt{\mathrm{T}t-t^2}}\frac{1}{\sqrt{Ly-y^2}}dydt \\ &+ \frac{K_3^2}{(\Gamma(N_t+2))^2(\Gamma(N_y+2))^2}\int_{\mathbb{I}\times\mathbb{J}}\frac{t^{2N_t+2}}{\sqrt{\mathrm{T}t-t^2}}\frac{y^{2N_y+2}}{\sqrt{Ly-y^2}}dydt\end{aligned} \tag{37}$$

The integrals in Eq. (37) are evaluated as

$$\begin{aligned}&\int_{\mathbb{I}\times\mathbb{J}}\frac{1}{\sqrt{\mathrm{T}t-t^2}}\frac{y^{2N_y+2}}{\sqrt{Ly-y^2}}dydt \\ &\qquad= \pi\sqrt{\pi}L^{2N_y+2}\frac{\Gamma(2N_y+\frac{5}{2})}{\Gamma(2N_y+3)}\end{aligned} \tag{38}$$

$$\begin{aligned}&\int_{\mathbb{I}\times\mathbb{J}}\frac{t^{2N_t+2}}{\sqrt{\mathrm{T}t-t^2}}\frac{1}{\sqrt{Ly-y^2}}dydt \\ &\qquad= \pi\sqrt{\pi}\mathrm{T}^{2N_t+2}\frac{\Gamma\left(2N_t+\frac{5}{2}\right)}{\Gamma(2N_t+3)}\end{aligned} \tag{39}$$

$$\int_{\mathbb{I}\times\mathbb{J}} \frac{t^{2N_t+2}}{\sqrt{\mathrm{T}t-t^2}} \frac{y^{2N_y+2}}{\sqrt{Ly-y^2}} dydt = \pi L^{2N_y+2}\mathrm{T}^{2N_t+2} \frac{\Gamma(2N_t+\frac{5}{2})}{\Gamma(2N_t+3)} \frac{\Gamma(2N_y+\frac{5}{2})}{\Gamma(2N_y+3)}. \quad (40)$$

Substituting Eq. (38) to Eq. (40) into Eq. (37) completes the proof. If we consider $u_{N_y,N_t}(y,t)$, the $\mathbf{L}^2_{w_L,w_\mathrm{T}}$ orthogonal projection of $u(y,t)$onto $\mathbf{P}_{N_y,N_t}$, then

$$\left|u(y,t)-u_{N_y,N_t}(y,t)\right| = \left|u(y,t)-\mathbf{P}_{N_y,N_t}u(y,t) + \mathbf{P}_{N_y,N_t}u(y,t)-u_{N_y,N_t}(y,t)\right| \quad (41)$$

$$\leq \left|u(y,t)-\mathbf{P}_{N_y,N_t}u(y,t)\right| + \left|u_{N_y,N_t}(y,t)-\mathbf{P}_{N_y,N_t}u(y,t)\right|. \quad (42)$$

Based on Theorem 3.3, Eq. (42) tends to zero as $N_y, N_t \to \infty$.

4. NUMERICAL ILLUSTRATION

In this section, we apply the numerical scheme using the Chebyshev–Gauss–Lobatto quadrature to the flow of an MHD and non–isothermal generalized Oldroyd–B fluid.

4.1 Flow of an MHD Oldroyd–B fluid

We investigate an unsteady unidirectional flow of an MHD Oldroyd-B fluid occupying the upper half-plane bounded by an impermeable wall at y=0. The y–axis is perpendicular to the rigid flat plate, and the plate oscillates parallel to itself. The fluid is assumed to be at rest until startup. The momentum and shear stress equations for this unsteady flow are given as [26]

$$Re\left[\frac{\partial}{\partial t}+We^{\alpha}\frac{\partial^{\alpha+1}}{\partial t^{\alpha+1}}\right]u-\left[\frac{\partial^2}{\partial y^2}+\lambda_r^{\beta}\frac{\partial^{\beta+2}}{\partial t^{\beta}\partial y^2}\right]u + Ha^2\left[1+We^{\alpha}\frac{\partial^{\alpha}}{\partial t^{\alpha}}\right]u=0 \quad (43)$$

$$\left[1+We^{\alpha}\frac{\partial^{\alpha}}{\partial t^{\alpha}}\right]\tau=\left[\frac{\partial}{\partial y}+\lambda_r^{\beta}\frac{\partial^{\beta+1}}{\partial t^{\beta}\partial y}\right]u, \quad (44)$$

with initial conditions

$$u(y,0)=\frac{\partial}{\partial t}u(y,0)=0, \quad \tau(y,0)=0, \quad (45)$$

and boundary conditions with a sine oscillation at the wall and dimensionless frequency of oscillation ω

$$u(0,t)=\sin(\omega t), \qquad u(y,t)=0 \text{ as } y\to\infty, \qquad t>0. \quad (46)$$

We seek a solution in the form of truncated Chebyshev polynomials

$$u(y,t)=\sum_{n=0}^{N_y}\sum_{m=0}^{N_t}u_{n,m}T_{L,n}(y)T_{\mathrm{T},m}(t), \qquad \tau(y,t)=\sum_{n=0}^{N_y}\sum_{m=0}^{N_t}\tau_{n,m}T_{L,n}(y)T_{\mathrm{T},m}(t), \quad (47)$$

where, the coefficients $\hat{u}_{n,m}$ and $\hat{\tau}_{n,m}$ are defined by Lemma 2.2. Using the results of Proposition 2.6, we resolve Eq. (43) and Eq. (44) into a system of discrete equations

$$Re\left[(\mathrm{D}_t^1\otimes I_y)+We^{\alpha}(\mathrm{D}_t^{\alpha+1}\otimes I_y)\right] - \left[(I_t\otimes \mathrm{D}_y^2)+\lambda_r^{\beta}(\mathrm{D}_t^{\beta}\otimes \mathrm{D}_y^2)\right]+Ha^2\left[(I_t\otimes I_x)+We^{\alpha}(\mathrm{D}_t^{\alpha}I_y)\right]vec(\vec{u})=vec(\vec{0}) \quad (48)$$

$$\left[(I_t\otimes I_y)+We^{\alpha}(\mathrm{D}_t^{\alpha}\otimes I_y)\right]vec(\vec{\tau}) = \left[(I_t\otimes \mathrm{D}_y^1)+\lambda_r^{\beta}(\mathrm{D}_t^{\beta}\otimes \mathrm{D}_y^1)\right]vec(\vec{u}), \quad (49)$$

where, $vec(\vec{0})$ is a vector of zeroes of size (N_y+1) times (N_t+1) and each system is solved independently by matrix inversion.

The accuracy of the solutions for different values of α, β, N_t, N_y are presented in Table 1 in terms of the maximum residual error and condition number. The condition number was computed using the python package '*numpy.linalg.cond'*. The results in Figure 1 are shown for two frequencies of oscillation and α=0.25, β=0.75, t=10, Re=0.1 and Ha=0.5. We consider the cases: We=1<λr=1.5, Jeffrey fluid (λr=1.2<We=1.5), Maxwell fluid (We=1.5, λr=0), second-grade fluid (We=0, λr=1.2) and Newtonian fluid. The figure shows the velocity and tangential shear stress profiles. In Figure 1a, the velocity profiles are plotted for special cases of the fractional Oldroyd–B fluid. In all cases, the oscillation of the fluid velocity decays as it approaches the boundary layer region. The fractional second-grade fluid has the lowest amplitude of oscillation, while the fractional Maxwell fluid has the highest amplitude. This result is in agreement with the study of Jamil et al. [26]. In Figure 1b, the shear stress profiles for fixed time t are plotted for special cases. This figure shows that the case We=0 (second-grade fluid) has the highest shear stress at the wall, while the case when λ_r=0 (Maxwell fluid) has the smallest shear stress. Figure 2 and Figure 3 illustrate the behaviour of the velocity and shear stress for different values of the fractional orders α and β. Figure 2 shows that as the order α increases, the shear stress decreases, while the net effect of increasing β is that the shear stress increases. In Figure 3, it can be seen that as β increases, the amplitude of oscillation becomes smaller while the amplitude becomes more significant as α increases. This result, in effect, shows that the likelihood of having a region of reverse flow close to the wall is less likely for fixed β, decreasing α and fixed α, increasing β. We remark that the degree of α is related to the relaxation time. Hence, the lack of reverse flow or small amplitude of oscillation for small values of α can be associated with the short memory of the fluid and slow response to shear stress.

Table 1. Residual and condition number for the problem in Section 4.1

(α,β)	(N_t,N_y)	Res_u	CN_u	Res_τ	CN_τ
(0.25,0.5)	(5,5)	4.1482e-16	203.5	1.3210e-15	17.35
	(10,10)	2.8511e-14	6.0310e+04	7.2893e-15	18.99
	(15,15)	1.3015e-07	6.1347e+11	1.7146e-07	8.6119e+04
(0.5,0.75)	(5,5)	9.0899e-16	313.1	1.1055e-15	24.02
	(10,10)	3.1403e-14	1.5079e+03	5.2698e-15	44.92
	(15,15)	3.5876e-07	5.6432e+11	1.2344e-06	4.1606e+06
(0.75,1)	(5,5)	5.7333e-16	477.8	2.0091e-15	36.39
	(10,10)	4.8934e-14	4.3557e+04	7.8238e-15	104.4
	(15,15)	1.2859e-07	2.2473e+11	3.4619e-07	2.7625e+06
(1,1)	(5,5)	7.8409e-16	625.5	1.4658e-15	60.11
	(10,10)	7.6247e-14	7.0962e+04	1.7502e-14	236.8
	(15,15)	1.1289e-08	2.6527e+10	3.9879e-07	4.1076e+06

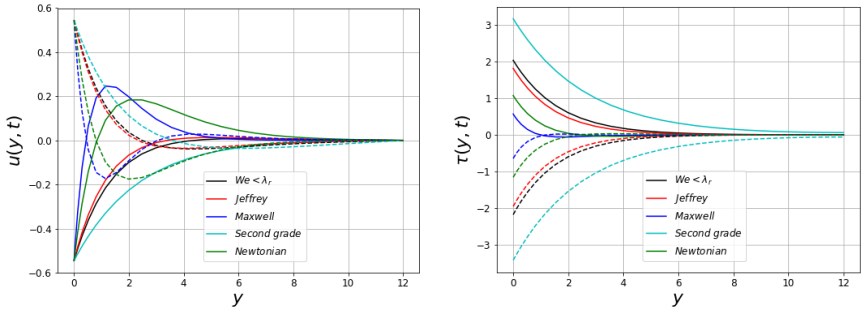

(a) (b)

Figure 1. Velocity and shear stress of special cases of the fractional Oldroyd-B fluid with ω=70+$n\pi$/2

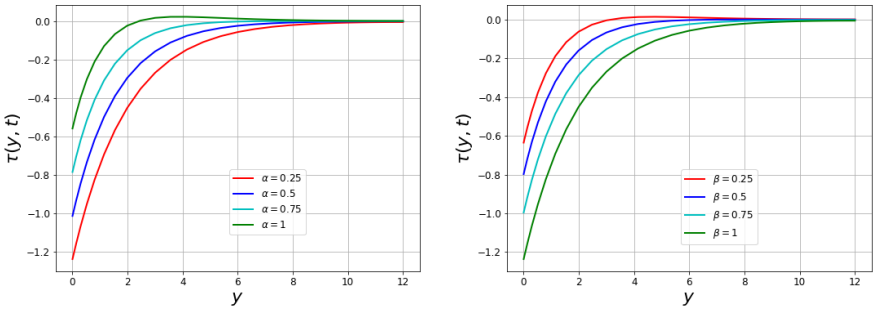

(a) (b)

Figure 2. Variation of the tangential shear stress profiles with ω=10+π/2 for **(a)** different α with β=1 and **(b)** different β with α=0.25

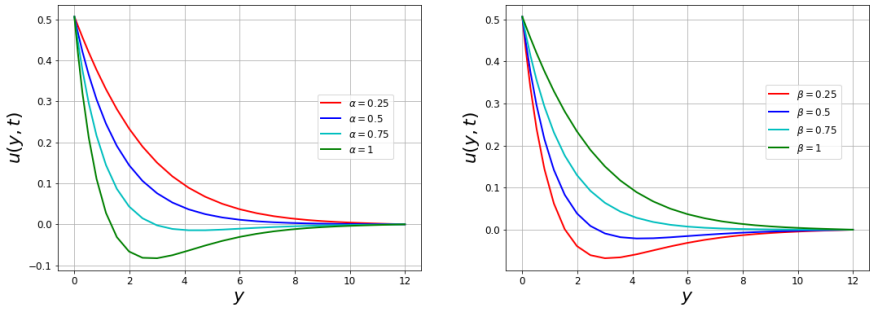

(a) (b)

Figure 3. Velocity profiles with ω=10+π/2 for: (a) different α with β=1 and (b) different β with α=0.25

4.2 The non-isothermal flow of an Oldroyd–B fluid

Here we consider the unsteady non–isothermal flow of a generalized Oldroyd–B fluid. The thermal property of the fluid (γ), the specific heat (c) and the thermal conductivity (k) are constant and isotropic, except the viscosity which is assumed to be temperature-dependent with reference viscosity, μ_0. We use [27]

$$\mu(T) = \frac{\mu_0}{1+\gamma(T-T_0)} \tag{50}$$

to model the non-isothermal viscosity. The system of equations describing the conservation of momentum Eq. (6) [Ha=0], the shear stress Eq. (7), and the energy equation are given as [28, 29]:

$$Re\left[\frac{\partial u}{\partial t}+We^{\alpha}\frac{\partial^{\alpha+1}u}{\partial t^{\alpha+1}}\right]-\left[\frac{\partial u}{\partial y}\frac{\partial}{\partial y}\left(\frac{1}{1+\theta_e\theta}\right)+\lambda_r^{\beta}\frac{\partial^{\beta+1}u}{\partial t^{\beta}\partial y}\frac{\partial}{\partial y}\left(\frac{1}{1+\theta_e\theta}\right)+\frac{1}{1+\theta_e\theta}\frac{\partial^2 u}{\partial y^2}+\frac{1}{1+\theta_e\theta}\frac{\partial^{\beta+2}u}{\partial t^{\beta}\partial y^2}\right]=0 \tag{51}$$

$$Re\left[\frac{\partial\theta}{\partial t}+We^{\alpha}\frac{\partial^{\alpha+1}\theta}{\partial t^{\alpha+1}}\right]-\frac{1}{Pr}\left[\frac{\partial^2\theta}{\partial y^2}+We^{\alpha}\frac{\partial^{\alpha+2}\theta}{\partial t^{\alpha}\partial y^2}\right]-Ec\left[\frac{1}{1+\theta_e\theta}\left(\frac{\partial u}{\partial y}\right)^2+\frac{\lambda_r^{\beta}}{1+\theta_e\theta}\frac{\partial^{\beta+1}u}{\partial t^{\beta}\partial y}\frac{\partial u}{\partial y}\right]=0 \tag{52}$$

$$\left[1+We^{\alpha}\frac{\partial^{\alpha}}{\partial t^{\alpha}}\right]\tau=\frac{1}{1+\theta_e\theta}\left[\frac{\partial u}{\partial y}+\lambda_r^{\beta}\frac{\partial^{\beta+1}u}{\partial t^{\beta}\partial y}\right], \tag{53}$$

where, θ_e=$\gamma\Delta T$, the temperature ratio, $Ec=\mathbf{U}_0^2(c\Delta T)^{-1}$, the Eckert number, Pr=$c\mu_0$ k^{-1}, the reference Prandtl number, θ=(T-T_0)ΔT^{-1}, the dimensionless temperature are dimensionless parameters. The initial and boundary conditions are given as in Eq. (45) and Eq. (46) and

$$\theta(y,0)=\frac{\partial}{\partial t}\theta(y,0)=0\ \ \forall\, y>0 \tag{54}$$

$$\theta(0,t)=1,\quad \theta(y,t)=0\ \ \text{as}\ \ y\to\infty, t>0. \tag{55}$$

We seek a solution in the form of Eq. (22) for each dependent variable and apply the quasi–linearization method to linearize the system of equations (see Bellman and Kalaba [30], Motsa et al. [31]):

$$\begin{aligned}&\left[Re\left[\left(\mathrm{D}_t^1\otimes I_y\right)+We^{\alpha}\left(\mathrm{D}_t^{\alpha+1}\otimes I_y\right)\right]+a_{0r}\left(I_t\otimes\mathrm{D}_y^2\right)\right.\\&\quad+a_{1r}\left(I_t\otimes\mathrm{D}_y\right)\\&\quad+a_{2r}\left(\mathrm{D}_t^{\beta}\otimes\mathrm{D}_y^2\right)+a_{3r}\left(\mathrm{D}_t^{\beta}\right.\\&\quad\left.\left.\otimes\mathrm{D}_y^1\right)\right]vec(\vec{u}_{r+1})\\&\quad+\left[a_{4r}\left(I_t\otimes\mathrm{D}_y^1\right)\right.\\&\quad\left.+a_{5r}\left(I_t\otimes I_y\right)\right]vec(\vec{\theta}_{r+1})\\&\quad=vec(\vec{R}_{1r})\end{aligned} \tag{56}$$

$$\begin{aligned}&\left[Re(\mathrm{D}_t^1\otimes I_y)+ReWe^{\alpha}(\mathrm{D}_t^{\alpha+1}\otimes I_y)-\frac{1}{Pr}(I_t\otimes\mathrm{D}_y^2)\right.\\&\quad-\frac{We^{\alpha}}{Pr}(\mathrm{D}_t^{\alpha}\otimes\mathrm{D}_y^2)+b_{2r}(I_t\\&\quad\left.\otimes I_y)\right]vec(\vec{\theta}_{r+1})\\&\quad+\left[b_{0r}(I_t\otimes\mathrm{D}_y^1)+b_{1r}(\mathrm{D}_t^{\beta}\right.\\&\quad\left.\otimes\mathrm{D}_y^1)\right]vec(\vec{u}_{r+1})=vec(\vec{R}_{2r})\end{aligned} \tag{57}$$

Table 2. Residuals for the dependent variables in the problem in Section 4.2

(α,β)	(N_t,N_y)	Res_u	Res_θ	Res_τ
(0.25,0.5)	(7,10)	2.1518e-14	1.0823e-13	9.8749e-16
	(10,15)	1.7957e-13	6.2928e-13	6.8437e-15
	(12,20)	2.0137e-12	5.9289e-12	3.9240e-14
(0.5,0.75)	(7,10)	3.2932e-14	1.7114e-13	1.0634e-15
	(10,15)	4.0798e-13	9.5568e-13	4.3160e-15
	(12,20)	5.1502e-12	8.9247e-12	4.9766e-14
(0.75,1)	(7,10)	4.4381e-14	1.3593e-13	2.2664e-15
	(10,15)	1.1795e-12	1.3475e-12	2.0567e-14
	(12 ,20)	1.4751e-11	1.9498e-11	3.6492e-14
(1,1)	(7,10)	7.6759e-14	1.3427e-13	3.5037e-15
	(10,15)	2.0559e-12	3.0306e-12	1.7538e-14

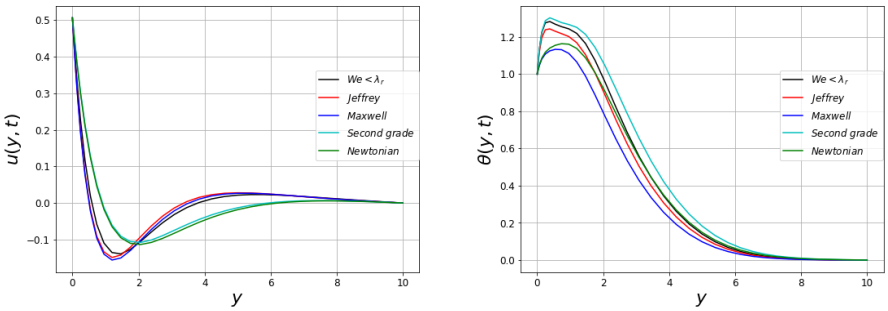

(a) (b)

Figure 4. Velocity and temperature profiles for non-isothermal flow of the special cases of the fractional Oldroyd-B fluid

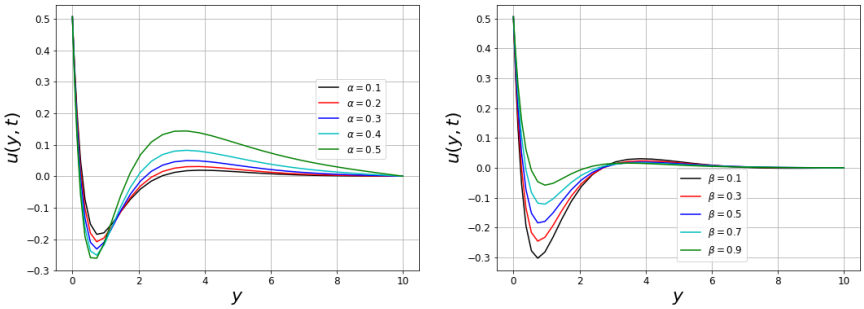

(a) (b)

Figure 5. Velocity profiles of the non-isothermal flow for (a) β= 0.5 and (b) α=0.1

Table 2 shows the maximum residual error for $0 \leqslant t \leqslant 10$ for different values of α and β. In Figure 4, the velocity and temperature profiles are illustrated for the special cases of the fractional Oldroyd – B fluid with α=0.25, β=0.5, Re=1.1, Pr=5, Ec=0.2, θe=0.33 and ω=10+π/2. We consider the cases: We=0.2<λr=1.5, Jeffrey fluid (λr=1.2<We=1.5), Maxwell fluid (We=1.5, λr=0), second-grade fluid (We=0, λr=1.2) and Newtonian fluid. It can be seen that, as in Section 4.1, the second-order fluid has the smallest amplitude while the Maxwell fluid has the highest oscillation amplitude. However, for the temperature profiles, the Maxwell fluid reaches its thermal boundary layer region quicker than the other fluids, and the second-grade fluid has the most extensive thermal boundary layer. Figure 4b also show increased temperature close to the wall. The study of Ishfaq et al. [28] attributes this behaviour to the accumulation of energy in the fluid particles in the vicinity of the wall because the viscous effect is profoundly felt in this region. The effects of different orders of derivatives are shown in Figure 5. Unlike the problem in Section 4.1, where velocity profiles are either strictly increasing or decreasing functions of α and β, in this flow, the velocity profiles intersect. We ascribe this behaviour to the coupling effect and non–isothermic nature of the fluid.

5. CONCLUSION

In this study, efficient and accurate numerical solutions for unsteady and unidirectional flows of generalized Oldroyd–B fluids have been obtained using the shifted Chebyshev polynomials of the first kind as the basis function. The two problems presented have a varying degree of complexity, which are mainly non–linearity and coupling. The accuracy of the solutions was investigated through the calculation of the residual error norm. The condition number of the discretization matrices was also presented for various values of the orders of derivatives and truncation of the Chebyshev series. The effects of the fractional-order derivatives in the constitutive equation of the Oldroyd–B fluid on shear stress and velocity are also discussed. We found that small values of the order of the relaxation term can be used to model the flow of viscoelastic fluid with short-term memory and slow response to shear force. Since many fluid dynamics problems exist on complex geometries, improvement can be made to accommodate problems with complex geometries.

REFERENCES

[1] Oldroyd, J. (1958). Non-Newtonian effects in steady motion of some idealized elastico-viscous liquids. Proceedings of the Royal Society London Series A, 245: 278-297.

[2] Maxwell, J.C. (2003). On the dynamical theory of gases: The Kinetic Theory of Gases: An anthology of classic papers with historical commentary. World Scientific, 197-261.

[3] Tarasov, V.E. (2013). Review of some promising fractional physical models. International Journal of Modern Physics B, 27(9): 1330005. http://dx.doi.org/10.1142/S0217979213300053

[4] Jamil, M., Khan, N., Zafar, A. (2011). Translational flows of an Oldroyd-B fluid with fractional derivatives. Computers & Mathematics with Applications, 62(3): 1540-1553. http://dx.doi.org/10.1016/j.camwa.2011.03.090

[5] Bazhlekova, E., Bazhlekov, I. (2017). Stokes' first problem for viscoelastic fluids with a fractional Maxwell model. Fractal and Fractional, 1(1): 7. http://dx.doi.org/10.3390/fractalfract1010007

[6] Le Roux, C. (2014). On flows of viscoelastic fluids of Oldroyd type with wall slip. Journal of Mathematical Fluid Mechanics, 16(2): 335-350. http://dx.doi.org/10.1007/s00021-013-0159-9

[7] Wang, Q. (2006). Numerical solutions for fractional KdV–Burgers equation by Adomian decomposition method. Applied Mathematics and Computation, 182(2): 1048-1055. http://dx.doi.org/10.1016/j.amc.2006.05.004

[8] Diethelm, K., Ford, N.J., Freed, A.D. (2002). A predictor-corrector approach for the numerical solution of fractional differential equations. Nonlinear Dynamics, 29: 3-22.

[9] Erjaee, G., Taghvafard, H., Alnasr M. (2011). Numerical solution of the high thermal loss problem presented by a fractional differential equation. Communications in Nonlinear Science and Numerical Simulation, 169(3): 1356-1362. http://dx.doi.org/10.1016/j.cnsns.2010.06.031

[10] El-Sayed, A., El-Kalla, I., Ziada, E. (2010). Analytical and numerical solutions of multiterm nonlinear fractional orders differential equations. Applied Numerical Mathematics, 60(8): 788-797. http://dx.doi.org/10.1016/j.apnum.2010.02.007

[11] Momani, S., Odibat, Z. (2007) Comparison between the homotopy perturbation method and the variational

iteration method for linear fractional partial differential equations. Computers & Mathematics with Applications, 54(7-8): 910-919. http://dx.doi.org/10.1016/j.camwa.2006.12.037

[12] Momani, S., Odibat, Z. (2007). Homotopy perturbation method for nonlinear partial differential equations of fractional order. Physics Letters A, 365(5-6): 345-350. http://dx.doi.org/10.1016/j.physleta.2007.01.046

[13] Doha, E., A. Bhrawy, A., Ezz-Eldien, S. (2011). Efficient Chebyshev spectral methods for solving multiterm fractional orders differential equations. Applied Mathematical Modelling, 35(12): 5662-5672. http://dx.doi.org/10.1016/j.apm.2011.05.011

[14] Atabakzadeh, M., Akrami, M., Erjaee, G. (2013). Chebyshev operational matrix method for solving multi-order fractional ordinary differential equations. Applied Mathematical Modelling, 37(20-21): 8903-8911. http://dx.doi.org/10.1016/j.apm.2013.04.019

[15] Liu, J., Li, X., Wu, L. (2016). An operational matrix of fractional differentiation of the second kind of Chebyshev polynomial for solving multiterm variable order fractional differential equation. Mathematical Problems in Engineering. http://dx.doi.org/10.1155/2016/7126080

[16] Benattia, M.E., Belghaba, K. (2017). Numerical solution for solving fractional differential equations using shifted Chebyshev wavelet. General Letters in Mathematics, 3: 101-110.

[17] Bhrawy, A.H., Alghamdi, M.A. (2013). The operational matrix of Caputo fractional derivatives of modified generalized Laguerre polynomials and its applications. Advances in Difference Equations, 307. http://dx.doi.org/10.1186/1687-1847-2013-307

[18] Baseri, A., Babolian, E., Abbasbandy, S. (2017). Normalized Bernstein polynomials in solving space-time fractional diffusion equation. Advances in Difference Equations, 346. http://dx.doi.org/10.1186/s13662-017-1401-1

[19] Podlubny, I. (1998). Fractional differential equations: an introduction to fractional derivatives, fractional differential equations, to methods of their solution and some of their applications. Elsevier.

[20] Atangana, A. (2017). Fractional operators with constant and variable order with application to geo-hydrology. Academic Press.

[21] Abramowitz, M., Stegun, I.A. (1965). Handbook of mathematical functions: with formulas, graphs, and mathematical tables, Courier Corporation.

[22] Ahmadi Darani, M., Saadatmandi, A. (2017). The operational matrix of fractional derivative of the fractional-order Chebyshev functions and its applications. Computational Methods for Differential Equations, 5: 67-87.

[23] Ahmadi Darani, M., Nasiri, M. (2013). A fractional type of the Chebyshev polynomials for approximation of solution of linear fractional differential equations. Computational Methods for Differential Equations, 1: 96-107.

[24] Shao, W., Wu, X., Chen, S. (2012). Chebyshev tau meshless method based on the integration–differentiation for biharmonic-type equations on irregular domain. Engineering Analysis with Boundary Elements, 36(12): 1787-1798. http://dx.doi.org/10.1016/j.enganabound.2012.06.005

[25] Bhrawy, A.H. (2016). A highly accurate collocation algorithm for 1+1 and 2+1 fractional percolation equations. Journal of Vibration and Control, 22(9): 2288-2310. http://dx.doi.org/10.1177/1077546315597815

[26] Jamil, M., Khan, A.N., Shahid, N. (2013). Fractional magnetohydrodynamics Oldroyd-B fluid over an oscillating plate. Thermal Science, 17(4): 997-1011. http://dx.doi.org/10.2298/TSCI110731140J

[27] Lai, F., Kulacki, F. (1990). The effect of variable viscosity on convective heat transfer along a vertical surface in a saturated porous medium. International Journal of Heat and Mass Transfer, 33(5): 1028-1031. http://dx.doi.org/10.1016/0017-9310(90)90084-8

[28] Ishfaq, N., Khan, W., Khan, Z. (2017). The Stokes' second problem for nanofluids. Journal of King Saud University-Science. 31(1): 61. http://dx.doi.org/10.1016/j.jksus.2017.05.001

[29] Zhao, J., Zheng, L., Zhang, X., Liu, F. (2016). Unsteady natural convection boundary layer heat transfer of fractional Maxwell viscoelastic fluid over a vertical plate. International Journal of Heat and Mass Transfer, 97: 760-766. http://dx.doi.org/10.1016/j.ijheatmasstransfer.2016.02.059

[30] Bellman, R.E., Kalaba, R.E. (1965). Quasilinearization and nonlinear boundary-value problems.

[31] Motsa, S.S., Magagula, V., Sibanda, P. (2014). A bivariate Chebyshev spectral collocation quasilinearization method for nonlinear evolution parabolic equations. The Scientific World Journal. http://dx.doi.org/10.1155/2014/581987

NOMENCLATURE

B_0	the applied magnetic field, $N \cdot s / C \cdot m$
c	specific heat capacity, $J/ K/ kg$
Ec	Eckert number
e_{ij}	stress tensor, N/m^2
Ha	Hartmann number
k	thermal conductivity, $W/ m \cdot K$
Pr	reference Prandtl number
Re	Reynolds number
U_0	reference velocity, m/s
We	Weissenberg number

Greek symbols

α,β	fractional orders
θ_e	temperature ratio
λ	relaxation time, s
λ_r	retardation time, s / dimensionless retardation time
μ	viscosity, $kg/m/s$
μ_0	reference viscosity, $kg/m/s$
ρ	fluid density, kg/m^3
σ	electrical conductivity, S/m
τ	shear stress, N/m^2
ω	frequency of oscillation, s^{-1}

APPENDIX

The vectors R_{1r} and R_{2r} in Eq. (56) and Eq. (57) are defined as

$$R_{1r} = a_{0r}\frac{\partial^2 u_r}{\partial y^2} + a_{1r}\frac{\partial u_r}{\partial y} + a_{2r}\frac{\partial^{\beta+2} u_r}{\partial t^\beta \partial y^2} + a_{3r}\frac{\partial^{\beta+1} u_r}{\partial t^\beta \partial y} + a_{4r}\frac{\partial \theta_r}{\partial y} + a_{5r}\theta_r - Nu_r, \tag{58}$$

where,

$$Nu_r = -\frac{\partial u_r}{\partial y}\frac{\partial}{\partial y}\left(\frac{1}{1+\theta_e\theta_r}\right) - \lambda_r^\beta \frac{\partial^{\beta+1} u_r}{\partial t^\beta \partial y}\frac{\partial}{\partial y}\left(\frac{1}{1+\theta_e\theta_r}\right) - \frac{1}{1+\theta_e\theta_r}\frac{\partial^2 u_r}{\partial y^2} - \frac{1}{1+\theta_e\theta_r}\frac{\partial^{\beta+2} u_r}{\partial t^\beta \partial y^2},$$

$$a_{0r} = -(1+\theta_e\theta_r)^{-1}, \quad a_{1r} = \theta_e(1+\theta_e\theta_r)^{-2}\frac{\partial \theta_r}{\partial y},$$

$$a_{2r} = -(1+\theta_e\theta_r)^{-1},$$

$$a_{3r} = \theta_e\lambda_r^\beta(1+\theta_e\theta_r)^{-2}\frac{\partial \theta_r}{\partial y},$$

$$a_{4r} = \theta_e(1+\theta_e\theta_r)^{-2}\left(\frac{\partial u_r}{\partial y} + \lambda_r^\beta \frac{\partial^{\beta+1} u_r}{\partial t^\beta \partial y}\right),$$

$$a_{5r} = -2\theta_e^2(1+\theta_e\theta_r)^{-3}\left(\frac{\partial \theta_r}{\partial y}\frac{\partial u_r}{\partial y} + \lambda_r^\beta \frac{\partial \theta_r}{\partial y}\frac{\partial^{\beta+1} u_r}{\partial t^\beta \partial y}\right) + \theta_e(1+\theta_e\theta_r)^{-2}\left(\frac{\partial^2 u_r}{\partial y^2} + \frac{\partial^{\beta+2} u_r}{\partial t^\beta \partial y^2}\right),$$

and

$$R_{2r} = b_{0r}\frac{\partial u_r}{\partial y} + b_{1r}\frac{\partial^{\beta+1} u_r}{\partial t^\beta \partial y} + b_{2r}\theta_r - N\theta r. \tag{59}$$

Here,

$$N\theta_r = -Ec\left[\frac{1}{1+\theta_e\theta_r}\left(\frac{\partial u_r}{\partial y}\right)^2 + \frac{\lambda_r^\beta}{1+\theta_e\theta_r}\frac{\partial^{\beta+1} u_r}{\partial t^\beta \partial y}\frac{\partial u_r}{\partial y}\right],$$

$$b_{0r} = -2Ec(1+\theta_e\theta_r)^{-1}\frac{\partial u_r}{\partial y} - \lambda_r^\beta(1+\theta_e\theta_r)^{-1}\frac{\partial^{\beta+1} u_r}{\partial t^\beta \partial y},$$

$$b_{1r} = -\lambda_r^\beta(1+\theta_e\theta_r)^{-1}\frac{\partial u_r}{\partial y},$$

$$b_{2r} = \theta_e(1+\theta_e\theta_r)^{-1}\left(Ec\left(\frac{\partial u_r}{\partial y}\right)^2 + \lambda_r^\beta \frac{\partial^{\beta+1} u_r}{\partial t^\beta \partial y}\frac{\partial u_r}{\partial y}\right).$$

Chapter 4

A Chebyshev pseudo–spectral method for the multi–dimensional fractional Rayleigh problem for a generalized Maxwell fluid with Robin boundary conditions

In Chapter 3, one–dimensional time–fractional partial differential equations were considered, and the solutions approximated using shifted Chebyshev polynomials of the first kind in both space and time. In this chapter, we consider multidimensional time–fractional partial differential equations that model the Rayleigh problem for a generalized Maxwell fluid. The model equations are solved with mixed boundary conditions. Unlike in Chapter 3, here, we approximate the solutions of the equations by writing them as a linear combination of shifted Chebyshev polynomials of the first kind in the time variables and Lagrange basis polynomials in the spatial variables. Both temporal and spatial differentiation matrices are presented. The temporal derivatives, which are of arbitrary order, are approximated using Chebyshev polynomials, while the space derivatives are approximated in terms of the Lagrange function. A convergence analysis of the numerical scheme is given, and numerical results are obtained for both one– and two–dimensional cases of the Rayleigh problem. When these results are compared with the closed–form solutions, good accuracy and convergence are obtained.

A Chebyshev pseudo–spectral method for the multi–dimensional fractional Rayleigh problem for a generalized Maxwell fluid with Robin boundary conditions

Shina D. Oloniiju[a,*], Sicelo P. Goqo[a], Precious Sibanda[a]

[a]*School of Mathematics, Statistics and Computer Science, University of KwaZulu-Natal, Private Bag X01, Scottsville, Pietermaritzburg, 3209, South Africa.*

Abstract

Many pseudospectral schemes have been developed for time fractional partial differential equations, most of which use the spectral tau method. In this study, we develop an accurate numerical scheme using a combination of Lagrange and Chebyshev polynomials of the first kind for the multi-dimensional fractional Rayleigh problem integrated using the Gauss–Lobatto quadrature. The Chebyshev expansion coefficients are evaluated using the orthogonality condition of the polynomials. Arbitrary temporal derivatives are approximated using shifted Chebyshev polynomials, while the spatial derivatives are approximated using Lagrange basis functions. To establish the accuracy of the proposed scheme, we present a convergence analysis of the absolute errors. The convergence analysis shows that the absolute error tends to zero for sufficiently large number of collocation points.

Keywords: Fractional Maxwell fluid, Spectral method, Chebyshev polynomials, Lagrange interpolating polynomials, Rayleigh problem, Robin boundary conditions.

1. Introduction

Fractional calculus has spawned renewed interest by mathematicians because of the broad prospects for modelling complex problems with multiple temporal and/or spatial scales. Fractional calculus generalizes the classical integral and differential calculus by accommodating integration and differentiation of arbitrary order. Over the last few decades, there has been a paradigm shift from mere mathematical investigations and formulations to numerous applied disciplines. By introducing arbitrary order derivatives, fractional partial differential equations are suited to better describe physical phenomena such as viscoelasticity, fluid

*corresponding author

Email addresses: shina@aims.edu.gh (Shina D. Oloniiju), goqos@ukzn.ac.za (Sicelo P. Goqo), sibandap@ukzn.ac.za (Precious Sibanda)

dynamics, electrodynamics and image and signal processing [4, 18, 19, 21]. The pioneering study of Bagley and Torvik [4] established a theoretical basis for which arbitrary order derivatives can be used in linear viscoelasticity with an experimental model that realistically depicted the mechanical properties of the viscoelastic material's regions of transition. Viscoelastic materials exhibit both viscous and elastic characteristics with dynamics that are intrinsically memory dependent. Therefore, it is ideal to construct constitutive relations with non-local derivatives. Mainardi [16] provides an exhaustive review of the connection between fractional calculus and linear viscoelasticity, viscoelastic models and wave propagation in linear viscoelastic media. A dynamical analysis of a fractional viscoelastic fluid using a general boundary element formulation was given by Makris et al. [17]. Following the study by Bagley and Torvik [4], a considerable number of studies have been carried out on fractional viscoelastic fluids. Sheikh et al. [27] presented an analysis of the free convection flow of a generalized second grade fluid in a porous medium using the Caputo–Fabrizio fractional operator. A fractional boundary layer flow of Maxwell fluid on an unsteady stretching sheet was investigated by Chen et al. [12]. The partial differential equations describing the boundary layer flow with both time and spatial fractional derivative was solved using the explicit finite difference method and the shifted Grünwald–Letnikov formula. In the study by Saqib et al. [25], an exact solution to the equations of free convection flow of a generalized Jeffrey fluid with Caputo–Fabrizio fractional derivatives was presented. A study of an unsteady flow of fractional Maxwell fluid in a channel was carried out by Qi and Xu [22]. Exact solutions were obtained using the finite Fourier cosine and Laplace transforms.

The Rayleigh problem, also referred to as Stokes' first problem describes the behaviour of a fluid occupying a semi–infinite domain bounded by an impermeable wall at $y = 0$ and initially at rest. The wall is then spontaneously accelerated and moves on its plane at a constant speed U_0. The problem, first described and formulated by Stokes [29] and later explored and solved by Rayleigh [24] has been reformulated for different kinds of fluids [1, 2, 8, 14, 20, 23, 30]. The fractional Rayleigh-Stokes' problem for non–Newtonian fluids is important in our understanding of the flow and behaviour of viscoelastic fluids. In this study, we are concerned with the multi–dimensional fractional Rayleigh problem for a generalized Maxwell fluid. If we consider a bounded spatial domain $\Upsilon \subset \mathbb{R}^{1,2}$ with boundary $\partial\Upsilon$ and time domain $\Phi = [0, T],\ T > 0$, then the fractional Rayleigh problem model for a generalized Maxwell fluid is given by the equation

$$(1 + \lambda^{\alpha} {}_0^C D_t^{\alpha}) \frac{\partial \mathbf{u}}{\partial t} = \nu \Delta \mathbf{u} \quad \text{in} \quad \Upsilon \times \Phi, \quad \alpha \in (0, 1], \tag{1}$$

where Δ is the Laplace operator and ${}_0^C D_t^{\alpha}$ is the Caputo fractional operator of order α defined in Miller and Ross [18], Podlubny [21] as

$$ {}_0^C D_t^\alpha \mathbf{u}(\mathbf{y},t) := \begin{cases} \frac{1}{\Gamma(1-\alpha)} \int_0^t (t-\tilde{t})^{-\alpha} \frac{\partial \mathbf{u}}{\partial \tilde{t}} d\tilde{t}, & 0 < \alpha < 1, \\ \\ \frac{\partial \mathbf{u}}{\partial t}, & \alpha = 1. \end{cases} \tag{2} $$

The corresponding fractional integral operator of order $0 < \alpha \leq 1, t > 0, \alpha, t \in \mathbb{R}$ is defined as

$$ {}_0 I_t^\alpha \mathbf{u}(\mathbf{y},t) = \frac{1}{\Gamma(\alpha)} \int_0^t (t-\tilde{t})^{\alpha-1} \mathbf{u}(\mathbf{y},\tilde{t}) d\tilde{t}. \tag{3} $$

The existence of a time–fractional derivative in the equation captures the inherent memory dynamics of the fluid flow. Significant attention has been drawn to this kind of problem. Both exact and numerical solutions have been obtained for the fractional Rayleigh problem for viscoelastic fluids. Sene [26] studied the fractional Rayleigh problem for a generalized second grade fluid using the Atangana–Baleanu fractional derivative and obtained the exact solution using the Fourier sine and fractional Laplace transforms. Shen et al. [28] obtained an exact solution for a heated fractional second grade fluid and Xue and Nie [32] presented an exact solution for the fractional Rayleigh problem of a second grade fluid in a porous medium. Exact solutions for multi–dimensional fractional Rayleigh problem are difficult to obtain, and when available, may require the use of special functions and/or infinite series. However, accurate numerical methods can be used to solve this kind of model. Zaky [33] developed a numerical algorithm using the Legendre–Tau method for a one– and two–dimensional fractional Rayleigh–Stokes' problem for a heated generalized second grade fluid. Chen et al. [11] developed an implicit finite difference algorithm and Lin and Jiang [15] used the method of reproducing kernel to develop a numerical scheme for Stokes' first problem for a heated generalized second grade fluid. Prevailing numerical approaches for classical differential equations have been broadened to differential equations of arbitrary order. The fundamental problem in the development of numerical methods for fractional partial differential equation is the huge computational cost due to the inherent non–local property associated with fractional derivatives. This suggests that non–local methods such as the spectral collocation method could be an appropriate tool in approximating solutions of fractional differential equations. The history of spectral collocation methods for fractional differential equations is relatively short, although promising studies have been presented in the literature. The spectral collocation method for fractional order differential equations has been used by Bhrawy and Zaky [5] and Bhrawy and Zaky [6]. Literature review shows that the spectral collocation method using a combination of Lagrange interpolating polynomials and first kind shifted Chebyshev polynomials has not been used to solve the fractional Rayleigh problem for a generalized Maxwell fluid with Robin boundary conditions. In this study, we develop a numerical scheme that approximates the spatial derivative with Lagrange polynomials and the temporal derivative with Chebyshev polynomials of the first kind, and interpolating using Gauss-Lobatto quadrature.

2. Basic Concepts

2.1. Constitutive equation

The constitutive relation of an incompressible Maxwell fluid is given by [12]

$$\sigma_{ij} = -pI + \tau_{ij}, \tag{4}$$

where I is the identity tensor, p is the mechanical pressure, σ_{ij} is the Cauchy stress tensor and τ_{ij} is the extra stress tensor defined by

$$\left(1 + \lambda \frac{\partial}{\partial t}\right) \tau_{ij} = \mu e_{ij}. \tag{5}$$

Here, $\mu \geq 0$ is the dynamic viscosity, λ is the relaxation time of the fluid and e_{ij} is the Rivlin–Ericksen tensor, defined as

$$e_{ij} = \frac{\partial \mathbf{u}_i}{\partial \mathbf{y}_j} + \frac{\partial \mathbf{u}_j}{\partial \mathbf{y}_i}. \tag{6}$$

For a fractional Maxwell fluid, we define the stress tensor as

$$(1 + \lambda {}_0^{\alpha C} D_t^{\alpha}) \tau_{ij} = \mu e_{ij}. \tag{7}$$

Stokes' first problem for an incompressible fluid with constant pressure and no body forces is defined as

$$\rho \frac{\partial u}{\partial t} = \nabla \cdot \tau_{ij}. \tag{8}$$

The fluid is motionless when $t < 0$, but for $t \geq 0$, it flows with velocity $\mathbf{u} = u(\mathbf{y}, t)i$, with shear stress applied at the boundaries. The shear stresses are given as

$$\tau_{xy} = \tau_{yx} = \mu (1 + \lambda {}_0^{\alpha C} D_t^{\alpha})^{-1} \frac{\partial u}{\partial y} \tag{9}$$

$$\tau_{xz} = \tau_{zx} = \mu (1 + \lambda {}_0^{\alpha C} D_t^{\alpha})^{-1} \frac{\partial u}{\partial z}. \tag{10}$$

The remaining shear stress components are all equal to zero. Substituting the shear stresses into eq. (8) gives

$$(1+\lambda^{\alpha}\,{}_{0}^{C}D_{t}^{\alpha})\frac{\partial u}{\partial t}=\nu\Delta u(\mathbf{y},t). \tag{11}$$

2.2. Differentiation and integration matrices

The shifted Chebyshev polynomials is used to approximate temporal derivative. The time interval is defined in the positive real domain $[0,T]$, where T is a truncation of the semi–infinite time domain. We define $\mathcal{T}_{T,n}(t)=\mathcal{T}_{n}\left(\frac{2t}{T}-1\right)$, the first kind shifted Chebyshev polynomials of degree $n\geq 0$ is defined in series form as

$$\mathcal{T}_{T,n}=n\sum_{j=0}^{n}\frac{(-1)^{n-j}(n+j-1)!2^{2j}}{(n-j)!(2j)!T^{j}}t^{j}, \tag{12}$$

where T^{j} comes from the fact that we are considering a domain $[0,T]$. The set of polynomials $\mathcal{T}_{T,n}(t)$ satisfy the orthogonality condition

$$\langle\mathcal{T}_{T,n}(t),\mathcal{T}_{T,m}(t)\rangle=\int_{0}^{T}\mathcal{T}_{T,n}(t)\mathcal{T}_{T,m}(t)w_{T}(t)dt=\delta_{mn}h_{n}, \tag{13}$$

where $w_{T}(t)$ is the weight function associated with the shifted Chebyshev polynomials defined as ${}^{1}/\sqrt{Tt-t^{2}}$, $h_{n}={}^{c_{n}\pi}/_{2}$ with $c_{0}=2,c_{n}=1\ \forall\ n\geq 1$ and δ_{mn} is the Kronecker delta symbol. For a square integrable function $u\in[0,T]$ expanded in terms of an $\mathcal{M}$–truncated shifted Chebyshev polynomials, we have

$$u_{\mathcal{M}}(t)=\sum_{n=0}^{\mathcal{M}}\hat{u}_{n}\mathcal{T}_{T,n}(t), \tag{14}$$

where $\hat{u}_{n}:0\leq n\leq\mathcal{M}$ satisfies the orthogonality condition

$$\hat{u}_{n}=\frac{1}{h_{n}}\int_{0}^{T}u(t)\mathcal{T}_{T,n}(t)w_{T}(t)dt, \tag{15}$$

Equation (15) can be expressed in discrete form as

$$\hat{u}_n = \frac{1}{h_n} \sum_{j=0}^{\mathcal{M}} w_{T,j} u(t_j) \mathcal{T}_{T,n}(t_j), \qquad n = 0, \ldots, \mathcal{M}, \tag{16}$$

where w_T is the associated Christoffel number of the shifted Chebyshev–Gauss–Lobatto quadrature defined as

$$w_{T,j} = \frac{\pi}{c_j \mathcal{M}},\ 0 \le j \le \mathcal{M},\ c_0 = c_{\mathcal{M}} = 2 \text{ and } c_j = 1\ \forall\ 1 \le j \le \mathcal{M} - 1. \tag{17}$$

Using the fractional differential and integral operators defined above, the following holds

$${}_0^C D_t^\alpha t^j = \begin{cases} 0 & \text{for } j \in \mathbb{N}_0 \text{ and } j < \lceil \alpha \rceil \\ \\ \frac{\Gamma(j+1)}{\Gamma(j+1-\alpha)} t^{j-\alpha} & \text{for } j \in \mathbb{N}_0, j \ge \lceil \alpha \rceil. \end{cases} \tag{18}$$

$${}_0 I_t^\alpha t^j = \frac{\Gamma(j+1)}{\Gamma(j+\alpha+1)} t^{j+\alpha}. \tag{19}$$

2.2.1. Integer order time derivative

For the evaluation of the integer order derivative of the function $u(t)$ using the truncated shifted Chebyshev polynomials, we have

$$\frac{d}{dt} u_{\mathcal{M}}(t) = \sum_{n=0}^{\mathcal{M}} \hat{u}_n \frac{d}{dt} \mathcal{T}_{T,n}(t) \tag{20}$$

$$= \sum_{n=0}^{\mathcal{M}} n \hat{u}_n \mathcal{S}_{T,n-1}(t_k), \quad k = 0, \ldots, \mathcal{M}. \tag{21}$$

where $\mathcal{S}_{T,n-1}$ is the shifted second kind Chebyshev polynomials of degree, $n \ge 1$ [3]. By substituting eq. (16) into eq. (21), the first order derivative of $u(t)$ is given as

$$\frac{d}{dt} u_{\mathcal{M}}(t) = \sum_{j=0}^{\mathcal{M}} d_{j,k} u(t_j), \qquad k = 0, \ldots, \mathcal{M}, \tag{22}$$

where

$$d_{j,k} = \sum_{n=0}^{\mathcal{M}} \frac{n}{h_n} \mathcal{T}_{T,n}(t_j) \mathcal{S}_{T,n-1}(t_k) w_{T,j} \qquad k, j = 0, \ldots, \mathcal{M}. \tag{23}$$

2.2.2. Fractional order time derivatives

The fractional order derivative of $u(t)$ is defined as

$$ {}_0^C D_t^{\alpha} u_{\mathcal{M}}(t) = \sum_{j=0}^{\mathcal{M}} D_{j,p}^{\alpha} u(t_j), \tag{24}$$

where $D_{j,p}^{\alpha}$ are entries of a $(\mathcal{M}+1) \times (\mathcal{M}+1)$ matrix defined as

$$D_{j,p}^{\alpha} = w_{T,j} \sum_{n=0}^{\mathcal{M}} \sum_{k=0}^{\mathcal{M}} \frac{1}{h_n} \mathcal{T}_{T,n}(t_j) D_{n,k}^{(\alpha)} \mathcal{T}_{T,k}(t_p), \qquad j, p = 0, \ldots, \mathcal{M}. \tag{25}$$

Here, $D_{n,k}^{(\alpha)}$ is obtained by taking the α–th order derivative of the shifted first kind Chebyshev polynomials and the entries are defined as [see [13]]

$$D_{n,k}^{(\alpha)} = n \sum_{j=0}^{n} \frac{(-1)^{n-k}(n+j-1)! 2^{2j}}{(n-j)!(2j)! T^j} \frac{\Gamma(j+1)}{\Gamma(j-\alpha+1)} q_{j,k}, \tag{26}$$

where $q_{j,k}$ is defined as

$$q_{j,k} = \begin{cases} 0 & j = 0, 1, \ldots, \lceil \alpha \rceil - 1, \\ \frac{k\sqrt{\pi}}{h_k} \sum_{r=0}^{k} \frac{(-1)^{k-r}(k+r-1)! 2^{2r}}{(k-r)!(2r)!} T^{j-\alpha} \frac{\Gamma(j-\alpha+r+1/2)}{\Gamma(j-\alpha+r+1)} & j = \lceil \alpha \rceil, \lceil \alpha \rceil + 1, \ldots, \mathcal{M}; \\ & k = 0, 1, \ldots, \mathcal{M}. \end{cases} \tag{27}$$

2.2.3. Fractional order integration matrix

We consider the integral of the expansion (14), such that any arbitrary integral of $u(t)$ is given by

$$ {}_0I_t^{\alpha} u_{\mathcal{M}}(t) = \sum_{n=0}^{\mathcal{M}} \hat{u}_n \, {}_0I_t^{\alpha} \mathcal{T}_{T,n}(t), \qquad 0 < \alpha \leq 1. \tag{28} $$

Theorem 2.3. *Let $\mathcal{T}_{T,n}(t)$ be shifted Chebyshev polynomials of degree n, then any arbitrary order integral is defined as [7]*

$$ {}_0I_t^{\alpha} \mathcal{T}_{T,n}(t) = \sum_{k=0}^{\mathcal{N}} {}_0I_{n,k}^{(\alpha)} \mathcal{T}_{T,k}(t), \qquad 0 < \alpha \leq 1, \tag{29} $$

where

$$ \begin{aligned} {}_0I_{n,k}^{(\alpha)} = n \sum_{j=0}^{n} \frac{(-1)^{n-j}(n+j-1)!2^{2j}}{(n-j)!(2j)!} T^{\alpha} \frac{\Gamma(j+1)}{\Gamma(j+\alpha+1)} \frac{2k}{\sqrt{\pi} c_k} \times \\ \sum_{r=0}^{k} \frac{(-1)^{k-r}(k+r-1)!2^{2r}\Gamma(j+r+\alpha+1/2)}{(k-r)!(2r)!\Gamma(j+\alpha+r+1)}. \end{aligned} \tag{30} $$

Proof. The fractional integral of the shifted Chebyshev polynomial is given by

$$ {}_0I_t^{\alpha} \mathcal{T}_{T,n}(t) = n \sum_{j=0}^{n} \frac{(-1)^{n-j}(n+j-1)!2^{2j}}{(n-j)!(2j)!T^j} {}_0I_t^{\alpha} t^j \tag{31} $$

$$ = n \sum_{j=0}^{n} \frac{(-1)^{n-j}(n+j-1)!2^{2j}}{(n-j)!(2j)!T^j} \frac{\Gamma(j+1)}{\Gamma(j+\alpha+1)} t^{j+\alpha}. \tag{32} $$

We now represent $t^{j+\alpha}$ in terms of series of the Chebyshev polynomials, so that

$$ t^{j+\alpha} = \sum_{k=0}^{\infty} \theta_{j,k} \mathcal{T}_{T,k}(t), \tag{33} $$

where $\theta_{j,k}$ satisfies the orthogonality condition (13) and is given as

$$\theta_{j,k} = \frac{2k}{\sqrt{\pi}} \sum_{r=0}^{k} \frac{(-1)^{k-r}(k+r-1)!2^{2r}T^{j+\alpha}}{(k-r)!(2r)!} \frac{\Gamma(j+\alpha+r+1/2)}{\Gamma(j+\alpha+r+1)}. \tag{34}$$

Substituting Equations (33) and (34) into Equation (32) proves the theorem. □

Therefore, we can now write the arbitrary order integral of the expansion (14) as

$${}_0I_t^{\alpha} u_{\mathcal{M}}(t) = \sum_{j=0}^{\mathcal{M}} \left[w_{T,j} \sum_{n=0}^{\mathcal{M}} \sum_{k=0}^{\mathcal{M}} \frac{2}{\pi c_n} \mathcal{T}_{T,n}(t_j) {}_0I_{n,k}^{(\alpha)} \mathcal{T}_{T,k}(t_p) \right] u(t_j), \qquad j,p = 0,\ldots,\mathcal{M}. \tag{35}$$

2.4. Spatial differentiation matrix with Lagrange polynomials

We use the Lagrange interpolating polynomial to approximate the spatial derivative. If $u(y)$ is a continuously differentiable function, then it can be approximated at the Gauss–Lobatto nodes as

$$u_{\mathcal{N}_y}(y) = \sum_{s=0}^{\mathcal{N}_y} u(y_s)\mathcal{L}_s(y), \tag{36}$$

where $\mathcal{L}_s(y)$ is the Lagrange interpolating polynomials defined as

$$\mathcal{L}_s(y) = \prod_{r=0}^{\mathcal{N}_y} \frac{y - y_r}{y_s - y_r} \quad \text{and} \quad \mathcal{L}_s(y_r) = \delta_{sr} = \begin{cases} 0 \; s \neq r \\ 1 \; s = r. \end{cases} \tag{37}$$

Here, y_r is the Gauss–Lobatto grid points defined by

$$\{y_r\} = \left\{ -\cos\left(\frac{\pi r}{\mathcal{N}_y}\right) \right\}_{r=0}^{\mathcal{N}_y}. \tag{38}$$

To approximate the first order derivative of $u(y)$, we differentiate the interpolating function to get

$$u_y(y_r) = \sum_{s=0}^{\mathcal{N}_y} u(y_s) \frac{d\mathcal{L}_s(y_r)}{dy} = \sum_{s=0}^{\mathcal{N}_y} D_{rs} u(y_s), \quad r = 0,\ldots,\mathcal{N}_y, \tag{39}$$

where D_{rs} are entries of the differentiation matrix defined by Trefethen [31]

Definition 2.5 (Sobolev space [10]). *We define the Sobolev space $H^m(\Upsilon)$, $m \geq 0$ as*

$$H^m(\Upsilon) = \left\{ u \in L^2(\Upsilon) : \frac{\partial^i u}{\partial y^i} \in L^2(\Upsilon), 0 \leq i \leq m \right\}, \tag{40}$$

such that the semi–norm and norm associated with the space $H^m(\Upsilon)$ are respectively defined as

$$|u|_{H^{m,\mathcal{N}_y}(\Upsilon)} = \left(\left\| \frac{\partial^m u}{\partial y^m} \right\|^2_{L^2(\Upsilon)} \right)^{1/2}, \quad \|u\|_{H^m(\Upsilon)} = \left(\sum_{i=0}^{m} \left\| \frac{\partial^i u}{\partial y^i} \right\|^2_{L^2(\Upsilon)} \right)^{1/2}. \tag{41}$$

Definition 2.6 ([10]). *We define the weighted norm over the interval Φ as*

$$\|u\|_{H^n_{w_T}(\Phi)} = \left(\sum_{j=0}^{n} \left\| \frac{\partial^j u}{\partial t^j} \right\|^2_{L^2_{w_T}(\Phi)} \right)^{1/2}, \tag{42}$$

where $H^n_{w_T}(\Phi)$ is the Hilbert space associated with the norm and the semi–norm is defined as

$$|u|_{H^n_{w_T}(\Phi)} = \left(\sum_{j=\min(n,\mathcal{M}+1)}^{n} \left\| \frac{\partial^j u}{\partial t^j} \right\|^2_{L^2_{w_T}(\Phi)} \right)^{1/2}. \tag{43}$$

Definition 2.7 ([9, 10]). *Denote the norm*

$$\|u\|_{L^2(\Omega)} = \left(\int_\Phi \int_\Upsilon |u(y,t)|^2_{w_T} dy dt \right)^{1/2}, \tag{44}$$

where $L^2_w(\Omega) = L^2_{w_T}(\Phi; L^2(\Upsilon))$. We define the Hilbert space

$$H^{m,n}_w(\Omega) = H^n_{w_T}(\Phi; H^m(\Upsilon)) = \left\{ u \in L^2_w(\Omega) : \frac{\partial^{i+j} u}{\partial y^i \partial t^j} \in L^2_w(\Omega), 0 \leq i \leq m, 0 \leq j \leq n \right\}, \tag{45}$$

and the associated norm

$$\|u\|_{H^{m,n}_w(\Omega)} = \left(\sum_{i=0}^{m} \sum_{j=0}^{n} \left\| \frac{\partial^{i+j} u}{\partial y^i \partial t^j} \right\|^2_{L^2_w(\Omega)} \right)^{1/2}. \tag{46}$$

3. The one–dimensional Rayleigh problem

We consider the one–dimensional Rayleigh problem for the fractional Maxwell fluid

$$\frac{\partial u(y,t)}{\partial t} + \lambda^{\alpha} {}_0^C D_t^{\alpha+1} u(y,t) = \nu \frac{\partial^2 u(y,t)}{\partial y^2} + Q(y,t), \qquad (y,t) \in \Upsilon \times \Phi, \tag{47}$$

with initial and the Robin boundary conditions defined as

$$u(y,0) = g_1(y), \quad \frac{\partial}{\partial t} u(y,0) = g_2(y), \qquad y \in \Upsilon \tag{48}$$

$$u(-1,t) + \frac{\partial u(-1,t)}{\partial y} = a_1(t) \qquad t \in \Phi \tag{49}$$

$$u(1,t) + \frac{\partial u(1,t)}{\partial y} = a_2(t) \tag{50}$$

The first step is to approximate $u(y,t)$ using a combination of $\mathcal{M}$–truncated Chebyshev polynomials and $\mathcal{N}_y$–truncated Lagrange polynomials as

$$u_{\mathcal{N}_y,\mathcal{M}}(y_r,t_j) = \sum_{s=0}^{\mathcal{N}_y} \sum_{j=0}^{\mathcal{M}} \left[\sum_{n=0}^{\mathcal{M}} \frac{1}{h_n} \mathcal{L}_s(y_r) \mathcal{T}_{T,n}(t_j) \mathcal{T}_{T,n}(t_j) w_{T,j} \right] u(y_s,t_j). \tag{51}$$

Using eqs. (22), (24) and (39), we obtain the following discrete representation of the derivatives

$$\frac{\partial^2 u_{\mathcal{N}_y,\mathcal{M}}(y_r,t_j)}{\partial y^2} = \sum_{s=0}^{\mathcal{N}_y} \sum_{j=0}^{\mathcal{M}} D_{r,s}^2 \left[\sum_{n=0}^{\mathcal{M}} \frac{1}{h_n} \mathcal{T}_{T,n}(t_j) \mathcal{T}_{T,n}(t_j) w_{T,j} \right] u(y_s,t_j), \tag{52}$$

$$\frac{\partial u_{\mathcal{N}_y,\mathcal{M}}(y_r,t_j)}{\partial t} = \sum_{s=0}^{\mathcal{N}_y} \sum_{j=0}^{\mathcal{M}} \mathcal{L}_s(y_r) d_{j,k} u(y_s,t_j), \qquad k = 0, \dots \mathcal{M}, \tag{53}$$

$${}_0^C D_t^{\alpha} u_{\mathcal{N}_y,\mathcal{M}}(y_r,t_j) = \sum_{s=0}^{\mathcal{N}_y} \sum_{j=0}^{\mathcal{M}} \mathcal{L}_s(y_r) D_{j,p}^{\alpha} u(y_s,t_j), \qquad p = 0, \dots \mathcal{M}. \tag{54}$$

Substituting the expressions for the approximations of the derivatives into eqs. (47), (49) and (50) results in

$$\sum_{s=1}^{\mathcal{N}_y-1}\sum_{j=0}^{\mathcal{M}}\mathcal{L}_s(y_r)d_{j,k}u(y_s,t_j)+\lambda^{\alpha}\sum_{s=1}^{\mathcal{N}_y-1}\sum_{j=0}^{\mathcal{M}}\mathcal{L}_s(y_r)D_{j,p}^{\alpha+1}u(y_s,t_j)$$
$$-\nu\sum_{s=1}^{\mathcal{N}_y-1}\sum_{j=0}^{\mathcal{M}}D_{r,s}^2\left[\sum_{n=0}^{\mathcal{M}}\frac{1}{h_n}\mathcal{T}_{T,n}(t_j)\mathcal{T}_{T,n}(t_j)w_{T,j}\right]u(y_s,t_j)=0, \tag{55}$$

$$u(y_0,t_j)+D_{r,0}u(y_0,t_j)=A_1(t_j), \tag{56}$$

$$u(y_{\mathcal{N}_y},t_j)+D_{r,\mathcal{N}_y}u(y_{\mathcal{N}_y},t_j)=A_2(t_j),\qquad r=0,\ldots,\mathcal{N}_y,\ j=0,\ldots,\mathcal{M}, \tag{57}$$

where A_1 and A_2 are defined respectively as

$$A_1(t_j)=\sum_{j=0}^{\mathcal{M}}\left[\sum_{n=0}^{\mathcal{M}}\frac{1}{h_n}\mathcal{T}_{T,n}(t_j)\mathcal{T}_{T,n}(t_j)w_{T,j}\right]a_1(t_j)\qquad\text{and} \tag{58}$$

$$A_2(t_j)=\sum_{j=0}^{\mathcal{M}}\left[\sum_{n=0}^{\mathcal{M}}\frac{1}{h_n}\mathcal{T}_{T,n}(t_j)\mathcal{T}_{T,n}(t_j)w_{T,j}\right]a_2(t_j). \tag{59}$$

To obtain the solutions of eqs. (47) to (50), we must solve the linear algebraic system of eqs. (55) to (57). The algebraic system was solved using the PYTHON NUMPY library.

4. Convergence analysis

We present in this section the convergence analysis of the spectral method for the Rayleigh problem for a generalized Maxwell fluid. We however confine the analysis to the one–dimensional flow given in Equation (47). We define the error function $\varepsilon_{\mathcal{N}_y,\mathcal{M}}(y,t)=u_{\mathcal{N}_y,\mathcal{M}}(y,t)-u(y,t)$, where $u(y,t)$ is the exact solution and $u_{\mathcal{N}_y,\mathcal{M}}$ is the polynomial approximation of $u(y,t)$. First, we provide some important lemmas needed for the analysis.

Lemma 4.1 (see [10]). *Assume that $u\in H^m(\Upsilon)$ and the $P_{\mathcal{N}_y}$ is the interpolation associated with $(\mathcal{N}_y+1)$ Gauss–Lobatto points, then the truncation error is estimated by the following*

$$\|P_{\mathcal{N}_y}u-u\|_{H_w^l(\Upsilon)}\le K\mathcal{N}_y^{2l-m}|u|_{H_w^{m,\mathcal{N}_y}(\Upsilon)},\quad 1\le l\le m \tag{60}$$

$$\|P_{\mathcal{N}_y}u-u\|_{L_w^2(\Upsilon)}\le K\mathcal{N}_y^{-m}|u|_{H_w^{m,\mathcal{N}_y}(\Upsilon)}. \tag{61}$$

Lemma 4.2 (see [7, 10]). *Let $u_{\mathcal{N}_y,\mathcal{M}}(y,t)$ denote the orthogonal projection of $u(y,t)$ onto $P_{\mathcal{N}_y,\mathcal{M}}$, then for all $m,n\ge 0$, we have*

$$\|\epsilon_{\mathcal{N}_y,\mathcal{M}}\|_{L_w^2(\Omega)}=\|P_{\mathcal{N}_y,\mathcal{M}}u-u\|_{L_w^2(\Omega)}\le K_1\mathcal{N}_y^{-m}\|u\|_{H_w^{m,0}(\Omega)}+K_2\mathcal{M}^{-n}\|u\|_{H_w^{0,n}(\Omega)}, \tag{62}$$

where the K's are positive constant independent of the number of collocation points.

Using the above lemmas, we will prove the convergence of the numerical scheme for the one–dimensional Rayleigh problem.

Theorem 4.3. *Suppose that the exact solution of Equations* (47) *to* (50) *is* $u \in L^2(\Omega)$ *and its approximation is* $u_{\mathcal{N}_y,\mathcal{M}}$. *For sufficiently large* $\mathcal{N}_y$ *and* $\mathcal{M}$, *we have* $\|u_{\mathcal{N}_y,\mathcal{M}} - u\|_{L^2_w(\Omega)}$ *tends to* 0, *provided that* u *is regular in* Ω.

Proof. Consider the integration of Equation (47) given as

$$u(y,t) = -\lambda^\alpha \, {}_0^C D_t^\alpha u + \nu \, {}_0 I_t^1 \frac{\partial^2 u}{\partial y^2} + \tilde{Q}(y,t), \tag{63}$$

where

$$\tilde{Q}(y,t) = q(y) + \int_\Phi Q(y,\xi) d\xi. \tag{64}$$

Define the approximation $u_{\mathcal{N}_y,\mathcal{M}}$ which uses $\mathcal{M}$–truncated Chebyshev approximation in time and $\mathcal{N}_y$–truncated Lagrange approximation in space, such that $u_{\mathcal{N}_y,\mathcal{M}}$ is given as

$$u_{\mathcal{N}_y,\mathcal{M}}(y,t) = -\lambda^\alpha \, P_{\mathcal{N}_y,\mathcal{M}} \, {}_0^C D_t^\alpha u_{\mathcal{N}_y,\mathcal{M}} + \nu \, P_{\mathcal{N}_y,\mathcal{M}} \, {}_0 I_t^1 \frac{\partial^2 u_{\mathcal{N}_y,\mathcal{M}}}{\partial y^2} + P_{\mathcal{N}_y,\mathcal{M}} \tilde{Q}(y,t). \tag{65}$$

Subtracting Equation (63) from Equation (65) results in

$$\begin{aligned}\varepsilon_{\mathcal{N}_y,\mathcal{M}} = u_{\mathcal{N}_y,\mathcal{M}} - u &= -\lambda^\alpha P_{\mathcal{N}_y,\mathcal{M}} {}_0^C D_t^\alpha [u_{\mathcal{N}_y,\mathcal{M}} - u] + \nu P_{\mathcal{N}_y,\mathcal{M}} {}_0 I_t^\alpha \frac{\partial^2}{\partial y^2}[u_{\mathcal{N}_y,\mathcal{M}} - u] \\ &\quad - \lambda^\alpha P_{\mathcal{N}_y,\mathcal{M}} {}_0^C D_t^\alpha u + \lambda^\alpha {}_0^C D_t^\alpha u + \nu P_{\mathcal{N}_y,\mathcal{M}} {}_0 I_t^\alpha \frac{\partial^2}{\partial y^2} u - \nu {}_0 I_t^\alpha \frac{\partial^2}{\partial y^2} u + [P_{\mathcal{N}_y,\mathcal{M}} \tilde{Q} - \tilde{Q}] \end{aligned} \tag{66}$$

$$= -\lambda^\alpha P_{\mathcal{N}_y,\mathcal{M}} {}_0^C D_t^\alpha \varepsilon_{\mathcal{N}_y,\mathcal{M}} + \nu P_{\mathcal{N}_y,\mathcal{M}} {}_0 I_t^\alpha \frac{\partial^2}{\partial y^2} \varepsilon_{\mathcal{N}_y,\mathcal{M}} + \epsilon_{\mathcal{N}_y,\mathcal{M}}. \tag{67}$$

Using Lemma 4.2 and the fractional operators 2 and 3, we have

$$\begin{aligned}\|\varepsilon_{\mathcal{N}_y,\mathcal{M}}\|_{L^2_w(\Omega)} \leq K_1 \left\| \int_\Phi (t-\tilde{t})^{-\alpha} \frac{\partial \varepsilon_{\mathcal{N}_y,\mathcal{M}}}{\partial t} d\tilde{t} \right\|_{L^2_w(\Omega)} + K_2 \left\| \int_\Phi \frac{\partial^2 \varepsilon_{\mathcal{N}_y,\mathcal{M}}}{\partial y^2} d\tilde{t} \right\|_{L^2(\Omega)} \\ + K_3 \mathcal{N}_y^{-m} \|u\|_{H^{m,0}_w(\Omega)} + K_4 \mathcal{M}^{-n} \|u\|_{H^{0,n}_w(\Omega)}. \end{aligned} \tag{68}$$

Using Young's inequality and the properties of Sobolev norm, we have

$$\|\varepsilon_{\mathcal{N}_y,\mathcal{M}}\|_{L^2_w(\Omega)} \leq K_1 \left\| \int_\Phi t^{-\alpha} d\tilde{t} \right\|_{L^1_w(\Omega)} \left\| \frac{\partial \varepsilon_{\mathcal{N}_y,\mathcal{M}}}{\partial t} d\tilde{t} \right\|_{L^2_w(\Omega)} + K_2 \left\| \frac{\partial^2 \varepsilon_{\mathcal{N}_y,\mathcal{M}}}{\partial y^2} \right\|_{L^2_w(\Omega)}$$
$$+ K_3 \mathcal{N}_y^{-m} \|u\|_{H^{m,0}_w(\Omega)} + K_4 \mathcal{M}^{-n} \|u\|_{H^{0,n}_w(\Omega)} \tag{69}$$
$$\leq K_1 \|\varepsilon_{\mathcal{N}_y,\mathcal{M}}\|_{H^{0,1}_w(\Omega)} + K_2 \|\varepsilon_{\mathcal{N}_y,\mathcal{M}}\|_{H^{2,0}_w(\Omega)}$$
$$+ K_3 \mathcal{N}_y^{-m} \|u\|_{H^{m,0}_w(\Omega)} + K_4 \mathcal{M}^{-n} \|u\|_{H^{0,n}_w(\Omega)}, \tag{70}$$

which tends to zero for sufficiently large $\mathcal{N}_y$ and $\mathcal{M}$, provided that u is regular in Ω, thus concluding the proof. □

5. The two–dimensional Rayleigh problem

We broaden the numerical scheme to the two–dimensional Rayleigh problem

$$\frac{\partial u(y,z,t)}{\partial t} + \lambda^{\alpha} {}_0^C D_t^{\alpha+1} u(y,z,t) = \nu \left[\frac{\partial^2 u(y,z,t)}{\partial y^2} + \frac{\partial^2 u(y,z,t)}{\partial z^2} \right] + R(y,z,t) \tag{71}$$

with initial and boundary conditions

$$u(y,z,0) = g_1(y,z), \quad \frac{\partial}{\partial t} u(y,z,0) = g_2(y,z), \qquad y,z \in \Upsilon \tag{72}$$
$$u(-1,z,t) + \frac{\partial u(-1,z,t)}{\partial y} = e_1(z,t) \qquad t \in \Phi \tag{73}$$
$$u(1,z,t) + \frac{\partial u(1,z,t)}{\partial y} = e_2(z,t) \tag{74}$$
$$u(y,-1,t) + \frac{\partial u(y,-1,t)}{\partial z} = f_1(y,t) \tag{75}$$
$$u(y,1,t) + \frac{\partial u(y,1,t)}{\partial z} = f_2(y,t), \tag{76}$$

where $\Upsilon = [-1,1] \times [-1,1]$ is a finite rectangular domain. The function $u(y,z,t)$ can be approximated as

$$u_{\mathcal{N}_y,\mathcal{N}_z,\mathcal{M}}(y_r,z_i,t_j) = \sum_{s=0}^{\mathcal{N}_y} \sum_{q=0}^{\mathcal{N}_z} \sum_{j=0}^{\mathcal{M}} \left[\sum_{n=0}^{\mathcal{M}} \frac{1}{h_n} \mathcal{L}_s(y_r) \mathcal{L}_q(z_i) \mathcal{T}_{T,n}(t_j) \mathcal{T}_{T,n}(t_j) w_{T,j} \right] u(y_s,z_q,t_j). \tag{77}$$

The discrete forms of the derivatives are given as

$$\frac{\partial^2 u_{\mathcal{N}_y,\mathcal{N}_z,\mathcal{M}}(y_r,z_i,t_j)}{\partial y^2} = \sum_{s=0}^{\mathcal{N}_y}\sum_{q=0}^{\mathcal{N}_z}\sum_{j=0}^{\mathcal{M}} D_{r,s}^{2,0}\mathcal{L}_q(z_i)\left[\sum_{n=0}^{\mathcal{M}}\frac{1}{h_n}\mathcal{T}_{T,n}(t_j)\mathcal{T}_{T,n}(t_j)w_{t\infty,j}\right]u(y_s,z_q,t_j), \tag{78}$$

$$\frac{\partial^2 u_{\mathcal{N}_y,\mathcal{N}_z,\mathcal{M}}(y_r,z_i,t_j)}{\partial z^2} = \sum_{s=0}^{\mathcal{N}_y}\sum_{q=0}^{\mathcal{N}_z}\sum_{j=0}^{\mathcal{M}} \mathcal{L}_s(y_r)D_{i,q}^{0,2}\left[\sum_{n=0}^{\mathcal{M}}\frac{1}{h_n}\mathcal{T}_{T,n}(t_j)\mathcal{T}_{T,n}(t_j)w_{t\infty,j}\right]u(y_s,z_q,t_j), \tag{79}$$

$$\frac{\partial u_{\mathcal{N}_y,\mathcal{N}_z,\mathcal{M}}(y_r,z_i,t_j)}{\partial t} = \sum_{s=0}^{\mathcal{N}_y}\sum_{q=0}^{\mathcal{N}_z}\sum_{j=0}^{\mathcal{M}} \mathcal{L}_s(y_r)\mathcal{L}_q(z_i)d_{j,k}u(y_s,z_q,t_j) \qquad k=0,\dots\mathcal{M}, \tag{80}$$

$${}_0^C D_t^\alpha u_{\mathcal{N}_y,\mathcal{N}_z,\mathcal{M}}(y_r,z_i,t_j) = \sum_{s=0}^{\mathcal{N}_y}\sum_{q=0}^{\mathcal{N}_z}\sum_{j=0}^{\mathcal{M}} \mathcal{L}_s(y_r)\mathcal{L}_q(z_i)D_{j,p}^{\alpha}u(y_s,z_q,t_j), \qquad p=0,\dots\mathcal{M} \tag{81}$$

Substituting eqs. (78) to (81) into eq. (71) results in a system of linear equations which are solved with the boundary conditions

$$u(y_0,z_q,t_j) + D_{r,0}u(y_0,z_q,t_j) = E_1(z_q,t_j) \tag{82}$$
$$u(y_{\mathcal{N}_y},z_q,t_j) + D_{r,\mathcal{N}_y}u(y_{\mathcal{N}_y},z_q,t_j) = E_2(z_q,t_j) \tag{83}$$
$$u(y_s,z_0,t_j) + D_{i,0}u(y_s,z_0,t_j) = F_1(y_s,t_j) \tag{84}$$
$$u(y_s,z_{\mathcal{N}_z},t_j) + D_{i,\mathcal{N}_z}u(y_s,z_{\mathcal{N}_z},t_j) = F_2(y_s,t_j), \tag{85}$$

where E_1, E_2, F_1, F_2 are obtained by approximating the functions e_1, e_2, f_1, f_2 using a combination of the Lagrange interpolation polynomials and shifted first kind Chebyshev polynomials, respectively.

6. Illustrative Examples

In this section we consider some numerical examples. We consider both one– and two–dimensional cases.

Example 6.1. *We consider the one–dimensional case*

$$\frac{\partial u}{\partial t} + {}_0^C D_t^{\alpha+1} u = \frac{\partial^2 u}{\partial y^2} + Q(y,t), \tag{86}$$

$$u(y,0) = \frac{\partial}{\partial t} u(y,0) = 0, \tag{87}$$

$$u(-1,t) + \frac{\partial u(-1,t)}{\partial y} = t^{1+\alpha}(\sin(-\pi) + \pi\cos(-\pi)) \tag{88}$$

$$u(1,t) + \frac{\partial u(1,t)}{\partial y} = t^{1+\alpha}(\sin(\pi) + \pi\cos(\pi)) \tag{89}$$

$$\tag{90}$$

The exact solution is given as $u(y,t) = t^{1+\alpha}\sin(\pi y)$ *and* $Q(y,t) = \sin(\pi y)[(1+\alpha)t^{\alpha} + \Gamma(2+\alpha) + \pi^2 t^{1+\alpha}]$.

Table 1 shows the maximum absolute error defined as

$$E_{max} = \max_{\substack{0\le t\le T \\ -1\le y\le 1}} |u_{\mathcal{N}_y,\mathcal{M}}(y,t) - u(y,t)|.$$

The errors indicate that the results are accurate even for some choices of $\mathcal{N}_y$ and $\mathcal{M}$. Figure 1 shows algebraic rate of convergence of the numerical scheme. The figure shows that the computational error decreases exponentially as the number of grid points is increased as the value of α is varied. The results are typical of a spectral method. Figure 2 shows the quarterline velocity of the one-dimensional flow. The figure shows that the flow of fractional Maxwell fluid with larger fractional order α starts up quicker at $t = 0$ and the effects on velocity become reversed at a critical point. This same phenomenon was observed by Zaky [33] for a fractional second grade fluid. Figures 3 and 4 show the velocity profiles for increasing time and increasing values of the fractional order α respectively. It can be seen that the magnitude of the velocity increases as both the time and fractional order increase.

Table 1: Computational errors for Example 6.1, with $T = 2$ and $\mathcal{N}_y = 40$.

α	$\mathcal{M} = 4$	$\mathcal{M} = 6$	$\mathcal{M} = 8$	$\mathcal{M} = 10$
0.1	1.4×10^{-3}	1.1×10^{-3}	2.5×10^{-3}	1.6×10^{-4}
0.3	3.1×10^{-2}	4.2×10^{-3}	1.2×10^{-3}	9.8×10^{-3}
0.5	3.2×10^{-2}	5.1×10^{-3}	2.9×10^{-3}	6.6×10^{-3}
0.7	1.4×10^{-2}	2.4×10^{-2}	3.2×10^{-3}	6.3×10^{-3}
0.9	4.3×10^{-2}	1.1×10^{-2}	1.8×10^{-3}	7.3×10^{-3}

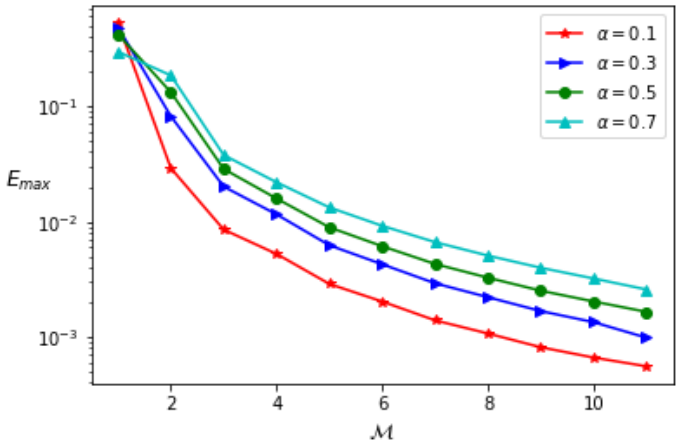

Figure 1: Maximum absolute error of the one–dimensional problem with $T = 1$, $\mathcal{N}_y = 40$.

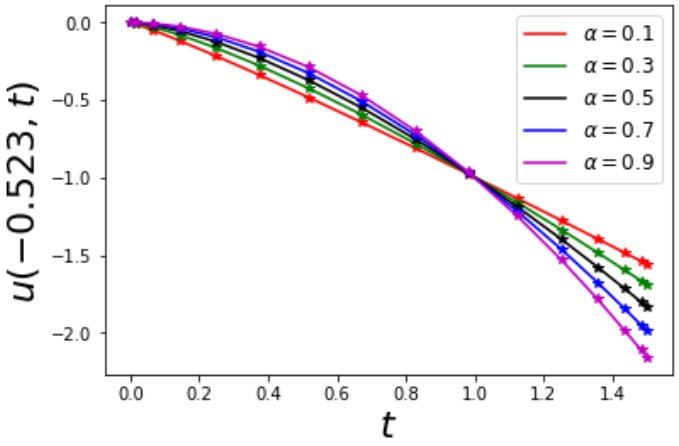

Figure 2: Quarterline region velocity profiles of the one–dimensional Rayleigh problem for the fractional Maxwell fluid, with $T = 1.6$, $\mathcal{N}_y = 40$ and $\mathcal{M} = 15$. Numerical: *solid lines*. Exact: *star*

Example 6.2. *Consider the two–dimensional problem defined on* $[-1, 1] \times [-1, 1] \times [0, T]$ *by*

$$\frac{\partial u}{\partial t} + {}_0^C D_t^{\alpha+1} u = \frac{\partial^2 u}{\partial y^2} + \frac{\partial^2 u}{\partial z^2} + R(y, z, t), \tag{91}$$

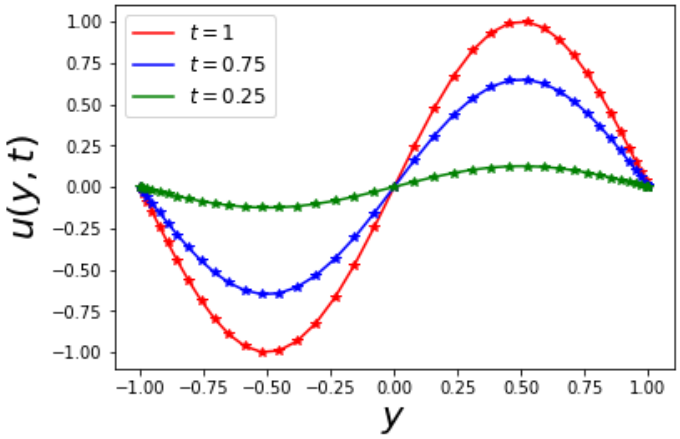

Figure 3: Comparison of the time progression of the fluid velocity of example 6.1 with $\alpha = 0.5$ with the exact solutions. Numerical: *solid lines*. Exact: *star*.

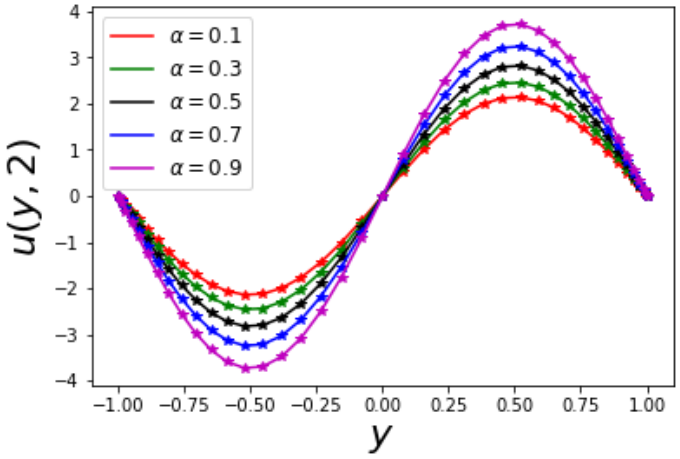

Figure 4: Comparison of the velocity profiles of example 6.1 at $t = 2$ for different values of α with the exact solutions. Numerical: *solid lines*. Exact: *star*.

with initial and boundary conditions

$$u(y,z,0) = \frac{\partial}{\partial t}u(y,z,0) = 0 \tag{92}$$

$$u(-1,z,t) + \frac{\partial u(-1,z,t)}{\partial y} = t^{1+\alpha}(\cos(1+z^2) + 2\sin(1+z^2)) \tag{93}$$

$$u(1,z,t) + \frac{\partial u(1,z,t)}{\partial y} = t^{1+\alpha}(\cos(1+z^2) - 2\sin(1+z^2)) \tag{94}$$

$$u(y,-1,t) + \frac{\partial u(y,-1,t)}{\partial z} = t^{1+\alpha}(\cos(y^2+1) + 2\sin(y^2+1)) \tag{95}$$

$$u(y,1,t) + \frac{\partial u(y,1,t)}{\partial z} = t^{1+\alpha}(\cos(y^2+1) - 2\sin(y^2+1)). \tag{96}$$

The exact solution is given as $u(y,z,t) = t^{1+\alpha}\cos(y^2+z^2)$ *and* $R(y,z,t) = \sin(y^2+z^2)[(1+\alpha)t^{\alpha} + \Gamma(2+\alpha) + 4t^{1+\alpha}(y^2+z^2)] + 4t^{1+\alpha}\sin(y^2+z^2)$.

Table 2: Computational errors for Example 6.2 for different values of the fractional order α and time t and $\mathcal{N}_y = \mathcal{N}_z = 40$.

α	$t = 0.5$	$t = 1.5$	$t = 2$
0.1	3.7×10^{-3}	8.9×10^{-3}	1.0×10^{-3}
0.3	1.2×10^{-3}	2.4×10^{-3}	4.7×10^{-3}
0.5	8.1×10^{-4}	1.6×10^{-3}	3.5×10^{-3}
0.7	4.7×10^{-3}	6.4×10^{-2}	1.2×10^{-3}
0.9	7.5×10^{-3}	7.8×10^{-3}	1.6×10^{-3}

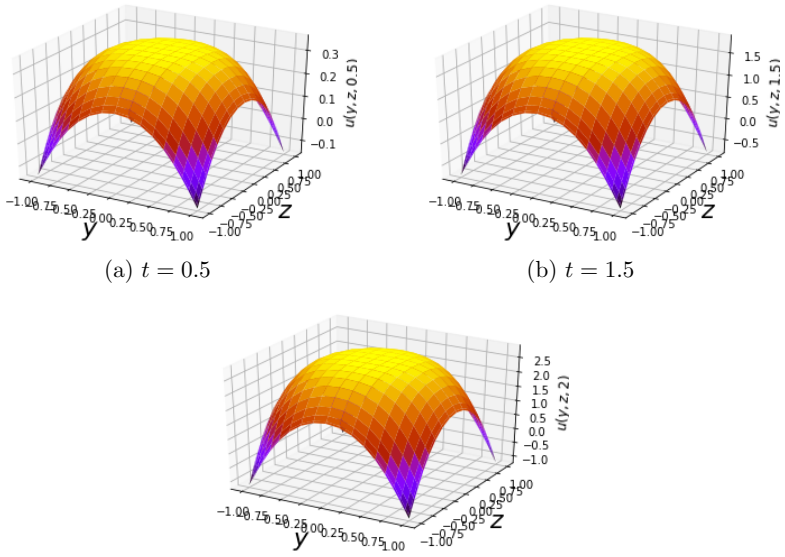

(a) $t = 0.5$ (b) $t = 1.5$

(c) $t = 2$

Figure 5: Approximate solutions of Example 6.2 for $\alpha = 0.5$, $\mathcal{N}_y = \mathcal{N}_z = 20$ and $\mathcal{M} = 15$ at different values of t.

With fractional order $\alpha = 0.5$, and $\mathcal{N}_y = \mathcal{N}_z = 20$ and $\mathcal{M} = 15$ collocation points, we present in Figure 5 the numerical solutions of the two dimensional problem for different values of t. It can be seen that the magnitude of the velocity increases as the time increases. This observation is similar to the one–dimensional case. We see in Figure 6 that the errors at different time values show some degrees of accuracy. In Table 2, the maximum errors at

different values of fractional order α and time t are presented, and some level of precision with the exact solutions can be seen. Owing to the inherent memory effect of fractional derivative, the maximum absolute error increases as the time interval $[0, T]$ grows as evident in Figure 7.

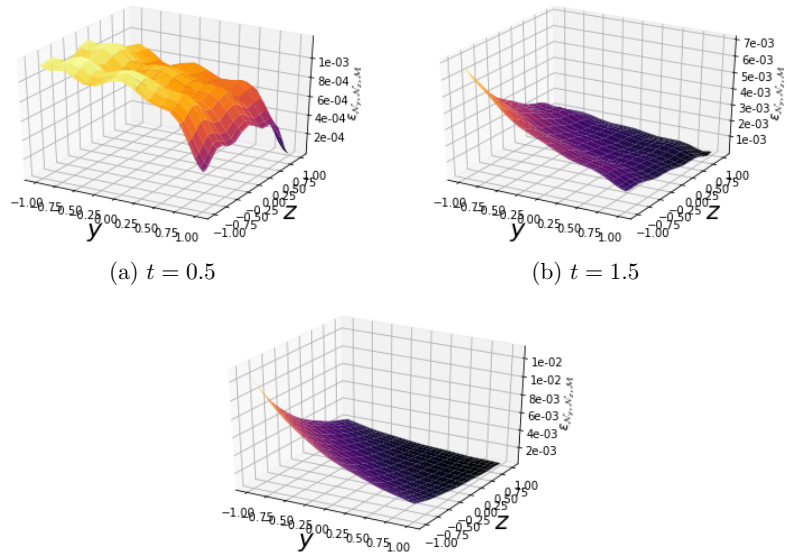

(a) $t = 0.5$

(b) $t = 1.5$

(c) $t = 2$

Figure 6: Spatial graphs of the absolute errors of the solutions of Example 6.2 for $\alpha = 0.5$, $\mathcal{N}_y = \mathcal{N}_z = 20$ and $\mathcal{M} = 15$ at different values of t.

7. Conclusion

The objective of this study was to develop a spectral algorithm for solving the multi-dimensional Rayleigh problem for a fractional Maxwell fluid. We developed a numerical scheme for approximating a function using a combination of truncated shifted first kind Chebyshev polynomials and Lagrange polynomials. In the numerical scheme, the spatial derivatives were approximated using the differentiation matrix based on Lagrange orthogonal basis functions and for temporal derivatives, we used the Chebyshev polynomials of the first kind. We presented some numerical results and compared these with exact solutions. Based on the size of the computational errors, we noted that the numerical solutions are in agreement with the exact solutions and thus can conclude that the numerical scheme is reliable and accurate. In future works, we hope to extend this scheme to higher dimensional problems, coupled differential equations and equations with non–linearity.

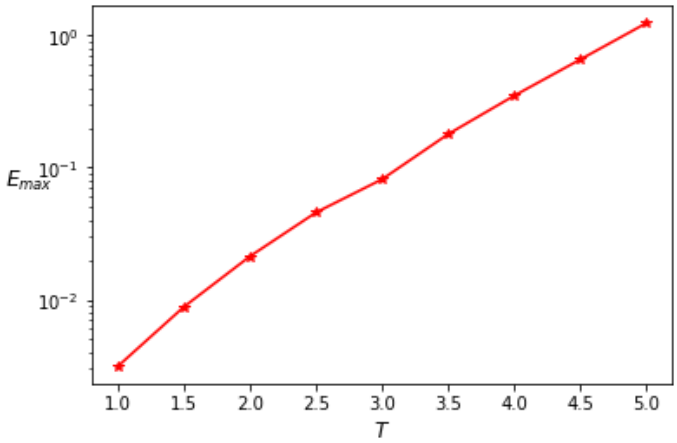

Figure 7: Maximum error for different time intervals $[0, T]$ for Example 6.2 with $\mathcal{N}_y = \mathcal{N}_z = 20$ and $\mathcal{M} = 10$.

References

[1] M. Abd-El-Malek, N.A. Badran, H.S. Hassan, Solution of the Rayleigh Problem for a Power Law Non-Newtonian Conducting Fluid via Group Method, eConf 107094 (2001) 49–56.

[2] S. Abelman, T. Hayat, E. Momoniat, On the Rayleigh problem for a Sisko fluid in a rotating frame, Appl. Math. and Comput. 215 (2009) 2515–2520.

[3] M. Abramowitz, I.A. Stegun, Handbook of mathematical functions: with formulas, graphs, and mathematical tables, volume 55, Courier Corporation, 1965.

[4] R.L. Bagley, P. Torvik, A theoretical basis for the application of fractional calculus to viscoelasticity, J. of Rheol. 27 (1983) 201–210.

[5] A. Bhrawy, M. Zaky, Shifted fractional-order Jacobi orthogonal functions: application to a system of fractional differential equations, Appl. Math. Modelling 40 (2016) 832–845.

[6] A. Bhrawy, M. Zaky, An improved collocation method for multi-dimensional space–time variable-order fractional Schrödinger equations, Appl. Num. Math. 111 (2017) 197–218.

[7] A. Bhrawy, M.A. Zaky, R.A. Van Gorder, A space-time Legendre spectral tau method for the two-sided space-time Caputo fractional diffusion-wave equation, Num. Algorithms 71 (2016) 151–180.

[8] R.B. Bird, Unsteady pseudoplastic flow near a moving wall, AIChE J. 5 (1959) 565–6D.

[9] C. Canuto, M.Y. Hussaini, A. Quarteroni, A. Thomas Jr, et al., Spectral methods in fluid dynamics, Springer Science & Business Media, 2012.

[10] C. Canuto, M.Y. Hussaini, A. Quarteroni, T.A. Zang, Spectral methods: Fundametals in Single domains, Springer, 2006.

[11] C.M. Chen, F. Liu, V. Anh, Numerical analysis of the Rayleigh–Stokes problem for a heated generalized second grade fluid with fractional derivatives, Appl. Math. and Comput. 204 (2008) 340–351.

[12] S. Chen, L. Zheng, B. Shen, X. Chen, Time–space dependent fractional boundary layer flow of Maxwell fluid over an unsteady stretching surface, Theor. and Appl. Mech. Lett. 5 (2015) 262–266.

[13] E. Doha, A. Bhrawy, S. Ezz-Eldien, Efficient Chebyshev spectral methods for solving multi-term fractional orders differential equations, Appl. Math. Modelling 35 (2011) 5662–5672.

[14] B.R. Duffy, D. Pritchard, S.K. Wilson, The shear-driven Rayleigh problem for generalised Newtonian fluids, J. of Non-Newton. Fluid Mech. 206 (2014) 11–17.

[15] Y. Lin, W. Jiang, Numerical method for Stokes' first problem for a heated generalized second grade fluid with fractional derivative, Num. Methods for Partial Differ. Equ. 27 (2011) 1599–1609.
[16] F. Mainardi, Fractional calculus and waves in linear viscoelasticity: an introduction to mathematical models, World Scientific, 2010.
[17] N. Makris, G. Dargush, M. Constantinou, Dynamic analysis of generalized viscoelastic fluids, J. of Eng. Mech. 119 (1993) 1663–1679.
[18] K.S. Miller, B. Ross, An introduction to the fractional calculus and fractional differential equations (1993).
[19] K. Oldham, J. Spanier, The fractional calculus theory and applications of differentiation and integration to arbitrary order, volume 111, Elsevier, 1974.
[20] S.D. Oloniiju, S.P. Goqo, P. Sibanda, Heat and mass transfer in an unsteady second grade nanofluid with viscous heating dissipation, Int. J. of Comput. Methods (2019) 1940005.
[21] I. Podlubny, Fractional differential equations: an introduction to fractional derivatives, fractional differential equations, to methods of their solution and some of their applications, volume 198, Elsevier, 1998.
[22] H. Qi, M. Xu, Unsteady flow of viscoelastic fluid with fractional maxwell model in a channel, Mech. Res. Commun. 34 (2007) 210–212.
[23] K. Rajagopal, A note on unsteady unidirectional flows of a non-Newtonian fluid, Int. J. of Non-Linear Mech. 17 (1982) 369–373.
[24] L. Rayleigh, LXXXII. On the motion of solid bodies through viscous liquid, The Lond., Edinb., and Dublin Philos. Mag. and J. of Sci. 21 (1911) 697–711.
[25] M. Saqib, F. Ali, I. Khan, N.A. Sheikh, S.A.A. Jan, et al., Exact solutions for free convection flow of generalized Jeffrey fluid: A Caputo-Fabrizio fractional model, Alex. Eng. J. 57 (2018) 1849–1858.
[26] N. Sene, Stokes' first problem for heated flat plate with Atangana–Baleanu fractional derivative, Chaos, Solitons & Fractals 117 (2018) 68–75.
[27] N.A. Sheikh, F. Ali, I. Khan, M. Saqib, A modern approach of Caputo–Fabrizio time-fractional derivative to MHD free convection flow of generalized second-grade fluid in a porous medium, Neural Comput. and Appl. 30 (2018) 1865–1875.
[28] F. Shen, W. Tan, Y. Zhao, T. Masuoka, The Rayleigh–Stokes problem for a heated generalized second grade fluid with fractional derivative model, Nonlinear Anal.: Real World Appl. 7 (2006) 1072–1080.
[29] G.G. Stokes, On the effect of the internal friction of fluids on the motion of pendulums, volume 9, Pitt Press Cambridge, 1851.
[30] R.I. Tanner, Note on the Rayleigh problem for a visco-elastic fluid, Zeitschrift für angewandte Mathematik und Physik ZAMP 13 (1962) 573–580.
[31] L.N. Trefethen, Spectral methods in MATLAB, volume 10, SIAM, 2000.
[32] C. Xue, J. Nie, Exact solutions of the Rayleigh–Stokes problem for a heated generalized second grade fluid in a porous half-space, Appl. Math. Modelling 33 (2009) 524–531.
[33] M.A. Zaky, An improved tau method for the multi-dimensional fractional Rayleigh–Stokes problem for a heated generalized second grade fluid, Comput. & Math. with Appl. 75 (2018) 2243–2258.

Chapter 5

Shifted Chebyshev spectral method for two–dimensional space–time fractional partial differential equations

In Chapters 2 to 4, fractional orders are considered only in one variable. In Chapters 5 and 6, we solve fractional differential equations with arbitrary real orders in more than one variable.

In this chapter, we consider linear and nonlinear two–dimensional space–time differential equations of arbitrary real orders. The numerical solutions of the differential equations are approximated as linear combinations of shifted Chebyshev polynomials of the first kind in all three variables, and are then evaluated using the shifted Chebyshev–Gauss–Lobatto points. In the nonlinear case, a quasilinearization approach is used to linearize the fractional partial differential equation. An error analysis is presented to demonstrate the convergence of the numerical scheme. Besides the convergence of the scheme, which is geometric, the results indicate that the method is accurate and computationally efficient. Although, some of the assumed exact solutions are not necessarily smooth, accurate numerical results are, nevertheless, obtained.

Azerbaijan Journal of Mathematics
V. ×, No 1, 20××, January
ISSN 2218-6816

Shifted Chebyshev spectral method for two–dimensional space–time fractional partial differential equations

Shina D. Oloniiju*, Nolwazi S. Nkomo, Sicelo P. Goqo, Precious Sibanda
School of Mathematics, Statistics and Computer Science, University of KwaZulu-Natal, Private Bag X01, Scottsville, Pietermaritzburg, 3209, South Africa.

Abstract. In this study, we present a numerical method for solving two–dimensional space–time fractional partial differential equations (FPDEs), where the solutions of the FPDEs are expanded in terms of the shifted Chebyshev polynomials. The numerical approximations are evaluated at the Chebyshev–Gauss–Lobatto points. In the case when the FPDE is nonlinear, we employ a Newton–Raphson approach to linearize the equation. Both the linear and nonlinear cases lead to a consistent system of linear algebraic equations. The scheme is tested on selected FPDEs and the numerical results show that the proposed numerical scheme is accurate and computationally efficient in terms of CPU times. To establish the accuracy of the method, we also present an error analysis which shows the convergence of the numerical method. These positive attributes make the proposed method a good approach for solving two–dimensional fractional partial differential equations with both space and time fractional orders.

Key Words and Phrases: Shifted Chebyshev polynomials, Chebyshev–Gauss–Lobatto quadrature, space–time FPDE

2010 Mathematics Subject Classifications: 65D05

1. Introduction

Fractional partial differential equations (FPDEs) are a generalization of classical partial differential equations to include derivatives of arbitrary order [27]. For the past three centuries, FPDEs were considered to be of little mathematical or practical interest [21, 23]. However, in the last few years, they have been used in applications such as fluid dynamics [5, 34], finance [26, 33] and physics [3, 20]. Fractional partial derivatives provide an excellent instrument for the description of physical systems with inherent memory [2, 8]. Fractional partial derivatives are more flexible in modelling real world dynamical systems.

*Corresponding author.

Email addresses: shina@aims.edu.gh, mankomolwazinkomo.ln@gmail.com, goqos@ukzn.ac.za, sibandap@ukzn.ac.za

In many problems of interest, FPDEs have no recognized analytical solution, so approximate and numerical techniques must be used [15]. Several numerical methods such as the finite difference method [24, 25], wavelet methods [17, 18], adomian decomposition method [11, 19], predictor–corrector method [22] and spectral methods [7, 32] have been developed for FPDEs. One of the earliest contributions to numerical solutions of FPDEs was by Lynch et al.[24], where they applied an approach based on the $L2$ method proposed by Oldham and Spanier[29] to solve an anomalous diffusion equation. In their study, the FPDEs were fractional in the spatial dimension and the second derivative was approximated by the standard three-point centred finite difference formula. Meerschaert and Tadjeran[28] gave a detailed study of a one-dimensional fractional diffusion equations using the finite difference method. They used a truncated Grunwald–Letnikov derivative evaluated on a shifted grid. Meerschaert and Tadjeran[27] later extended the method to one-dimensional space FPDEs.

The literature on spectral methods for solving FPDEs is comparatively short, although, interest has grown steadily in recent years. The spectral methods are an excellent tool for computing approximate solutions of differential equations because of high-order accuracy (see for instance Bhrawy[6] and Doha et al.[14]). With this high-order accuracy, spectral methods are useful for both temporal and spatial discretizations of FPDEs. Using spectral methods may significantly reduce the storage requirement because fewer time and space grid points are needed to compute smooth solutions. The basic concept of spectral methods is to express the solution of the differential equation as a sum of basis functions and estimate the coefficients of expansion such that approximation error is minimized [7]. Doha et al.[12] derived an operational matrix of the fractional derivatives and used the spectral tau method. The study of Doha et al.[12] was later extended to the more general Jacobi polynomials by Doha et al.[13], but was only applied to fractional ordinary differential equations.

In this study, a purely spectral based method is introduced and applied to solve $(2 + 1)$ dimensional FPDEs of the initial–boundary value problems type. The solution method involve approximating the variable and its fractional order partial derivatives in terms of the first kind shifted Chebyshev polynomials constructed on the Chebyshev–Gauss–Lobatto quadrature. In the case where the FPDE is nonlinear, we simplify using the quasilinearization method of Bellman and Kalaba[4]. The FPDE is discretized to yield a consistent system of linear algebraic equations. The method is tested using some FPDEs of the initial boundary value type and the numerical results obtained are compared with the exact solutions.

2. Preliminaries and Notations

In this section, we provide some preliminary results on fractional operators and the shifted Chebyshev polynomials of the first kind.

2.1. The fractional operators

Definition 2.2. *The Riemann–Liouville fractional integral of order $\alpha > 0$ is defined as [31]*

$$ {}_0I_x^\alpha g(x) = \frac{1}{\Gamma(\alpha)} \int_0^x (x-\tilde{x})^{\alpha-1} g(\tilde{x}) d\tilde{x}, \quad \alpha > 0,\ x > 0, \tag{1a} $$

$$ {}_0I_x^0 g(x) = g(x), \tag{1b} $$

where Γ is the Euler gamma function.

The fractional integral of a power function x^j is given as

$$ I^\alpha x^j = \frac{\Gamma(j+1)}{\Gamma(j+\alpha+1)} x^{j+\alpha}. \tag{2} $$

Definition 2.3. *We defined the corresponding differential operator of order α in the Caputo sense as [31]*

$$ {}_0D_x^\alpha g(x) = {}_0I_x^{n-\alpha} \left(\frac{d^n}{dx^n} g(x) \right) = \begin{cases} \frac{1}{\Gamma(n-\alpha)} \int_0^x \frac{d^n g(\tilde{x})}{d\tilde{x}^n} \frac{d\tilde{x}}{(x-\tilde{x})^{\alpha+1-n}}, & n-1 < \alpha < n, \\ \frac{d^n g(x)}{dx^n}, & \alpha = n. \end{cases} \tag{3} $$

We also define the fractional derivative of order α of x^j, which will be useful later in this study as

$$ {}_0D_x^\alpha x^j = \begin{cases} 0 & j \in \mathbb{N}_0,\ j < \lceil \alpha \rceil, \\ \frac{\Gamma(j+1)}{\Gamma(j+1-\alpha)} x^{j-\alpha}, & j \in \mathbb{N}_0,\ j \geq \lceil \alpha \rceil, \end{cases} \tag{4} $$

where $\lceil \alpha \rceil$ denotes the smallest integer greater than or equal to α.

2.4. The shifted Chebyshev polynomials

Consider the Sturm–Liouville eigenvalue problem

$$ \left(\sqrt{1-x^2} T_n'(x) \right)' + \frac{n^2}{\sqrt{1-x^2}} T_n(x) = 0, \quad -1 \leq x \leq 1,\ n = 0, 1, \ldots. \tag{5} $$

The Chebyshev polynomials are eigenvalue solutions of the eigenvalue problem, defined as [1]

$$ T_n(x) = \cos(n \arccos x), \quad n = 0, 1, \ldots, \quad x \in [-1, 1], \tag{6} $$

and are defined recurrently as

$$ T_{n+1}(x) = 2x T_n(x) - T_{n-1}(x), \quad n = 1, 2, \ldots, \tag{7} $$

where the zeroth and first order polynomials are respectively defined as $T_0(x) = 1$ and $T_1(x) = x$. We shall consider the interval $\tilde{x} \in [0, 1]$, hence we define the shifted Chebyshev polynomials by using the affine mapping $x = 2\hat{x} - 1$. Therefore the shifted Chebyshev polynomials can be generated through the recurring formula

$$\hat{T}_{n+1}(\hat{x}) = 2(2\hat{x} - 1)\hat{T}_n(\hat{x}) - \hat{T}_{n-1}(\hat{x}), \quad 0 \leq \hat{x} \leq 1, \quad n = 1, 2, \ldots, \tag{8}$$

where $\hat{T}_0(\hat{x}) = 1$ and $\hat{T}_1(\hat{x}) = 2\hat{x} - 1$, and the polynomials can be expanded in series form as (dropping the hat for brevity)

$$T_n(x) = n \sum_{j=0}^{n} \frac{(-1)^{n-j}(n + j - 1)!2^{2j}}{(n - j)!(2j)!} x^j. \tag{9}$$

The shifted Chebyshev polynomials of the first kind satisfy the orthogonality condition

$$\int_0^1 T_n(x)T_m(x)w(x)dx = \delta_{mn}h_n, \tag{10}$$

where $w(x)$ is a weight function defined as $1/\sqrt{x - x^2}$ and $h_n = c_n\pi/2$, with $c_0 = 2$ and $c_n = 1$ for $n \geq 1$. The shifted Chebyshev–Gauss–Lobatto points on which the interpolation is performed are extrema of $T_n(x)$ on the interval $x \in [0, 1]$ defined as

$$x_j = \frac{1}{2}\left(1 - \cos\left(\frac{j\pi}{N}\right)\right), \quad 0 \leq j \leq N. \tag{11}$$

The corresponding Christoffel numbers are the same as those of the standard Chebyshev–Gauss–Lobatto quadrature and are defined as $\varpi_j = \pi/c_jN$, $0 \leq j \leq N$, where $c_0 = c_N = 2$ and $c_j = 1$ for $j = 1, 2, \ldots, N - 1$.

3. Solution method

In this section, we describe the scheme for solving a $(2 + 1)$ dimensional fractional partial differential equations. For conveniency, we divide this section into three subsections. In Section 3.1, we propose the arbitrary derivative of a square integrable function in terms of the shifted Chebyshev polynomials. The resulting fractional differentiation matrix is used to approximate the derivatives of the dependent variable using Chebyshev–Gauss–Lobatto quadrature. In Section 3.4, we construct a scheme for solving linear fractional partial differential equations and in Section 3.5 we describe an iterative scheme for finding the solution of nonlinear fractional partial differential equations based on quasilinearization and Chebyshev collocation approaches.

3.1. Function and derivatives approximations

Consider a smooth function $u(x)$ defined on the interval $[0,1]$, then $u(x)$ can be approximated in terms of the truncated shifted Chebyshev polynomials as

$$u(x) \approx U_N(x) = \sum_{n=0}^{N} U_n T_n(x), \tag{12}$$

where the coefficients U_n are given to satisfy the orthogonality condition, and we write in discrete form as

$$U_n = \frac{1}{h_n} \sum_{j=0}^{N} U(x_j) T_n(x_j) \varpi_j, \quad n = 0, \ldots, N. \tag{13}$$

Therefore,

$$U_N(x_k) = \sum_{j=0}^{N} \left[\varpi_j \sum_{n=0}^{N} \frac{1}{h_n} T_n(x_j) T_n(x_k) \right] U(x_j), \qquad k = 0, 1, \ldots, N. \tag{14}$$

In order to approximate the arbitrary order derivative of $U_N(x)$, we first obtain the fractional derivative of the shifted Chebyshev polynomials.

Lemma 3.2. *The fractional derivative of the shifted Chebyshev polynomial is (see [12, 30])*

$${}_0D_x^{\alpha} T_n(x) = \sum_{k=0}^{N} D_{n,k}^{(\alpha)} T_k(x), \tag{15}$$

where

$$D_{n,k}^{(\alpha)} = n \sum_{j=0}^{n} \frac{(-1)^{n-j}(n+j-1)! 2^{2j}}{(n-j)!(2j)!} \frac{\Gamma(j+1)}{\Gamma(j-\alpha+1)} q_{j,k}, \tag{16}$$

and $q_{j,k}$ is given as

$$q_{j,k} = \begin{cases} 0 & j = 0, 1, \ldots \lceil \alpha \rceil - 1, \\ \frac{k\sqrt{\pi}}{h_k} \sum_{r=0}^{k} \frac{(-1)^{k-r}(k+r-1)! 2^{2r}}{(k-r)!(2r)!} \frac{\Gamma(j-\alpha+r+1/2)}{\Gamma(j-\alpha+r+1)}, & j = \lceil \alpha \rceil, \lceil \alpha \rceil + 1, \ldots, N, \\ & k = 0, 1, \ldots, N. \end{cases} \tag{17}$$

Theorem 3.3. *The arbitrary order derivative of $u(x)$ is given as*

$${}_0D_x^{\alpha} u(x_l) \approx D^{\alpha} U_N(x_l) = \sum_{j=0}^{N} \mathcal{D}_{j,l}^{\alpha} U(x_j) = \mathcal{D}^{\alpha} U, \tag{18}$$

where the entries of $\mathcal{D}^{\alpha}$ are defined as

$$\mathcal{D}^{\alpha}_{j,l} = \varpi_j \sum_{n=0}^{N}\sum_{k=0}^{N} \frac{1}{h_n} T_n(x_j) D^{(\alpha)}_{n,k} T_k(x_l), \quad j,l = 0,1,\ldots,N. \tag{19}$$

Proof. If we use the result of Lemma 3.2 and the expression in Equation (13), together with the expansion in terms of the shifted Chebyshev polynomials given in Equation (12), the theorem is proved.

3.4. Linear FPDEs

In this section, we describe the scheme for solving linear FPDEs. We consider a linear FPDE with variable coefficients of the form

$$\frac{\partial^{\alpha} u}{\partial t^{\alpha}} = u + \sum_{d=1} f_d(x,y)\frac{\partial^{\beta_d} u}{\partial x^{\beta_d}} + \sum_{e=1} g_e(x,y)\frac{\partial^{\gamma_e} u}{\partial y^{\gamma_e}} + q(x,y,t), \quad (x,y) \in (0,1)\times(0,1),\ t \in (0,1], \tag{20}$$

where $0 < \alpha < 1$, $\beta_1 < \beta_2 < \ldots$, $\gamma_1 < \gamma_2 < \ldots$ and $d-1 < \beta_d < d$ $(d = 1,2,\ldots,)$, $e-1 < \gamma_e < e$ $(e = 1,2,\ldots)$. Moreover, $f_d(x,y)$ $(d = 1,2,\ldots,)$ and $g_e(x,y)$ $(e = 1,2,\ldots,)$ are functions of x and y and $q(x,y,t)$ is dependent on all three variables. Equation (20) is solved subject to the initial condition

$$u(x,y,0) = \mathcal{I}(x,y), \tag{21}$$

and boundary conditions

$$\begin{aligned} u(0,y,t) &= \mathcal{B}^x_0(y,t), \quad u(1,y,t) = \mathcal{B}^x_1(y,t), \\ u(x,0,t) &= \mathcal{B}^y_0(x,t), \quad u(x,1,t) = \mathcal{B}^y_1(x,t), \end{aligned} \tag{22}$$

where $\mathcal{I}(x,y), \mathcal{B}^x_0(y,t), \mathcal{B}^x_1(y,t), \mathcal{B}^y_0(x,t), \mathcal{B}^y_1(x,t)$ are known functions. If $\alpha > 1$, additional initial condition will be needed to make the differential equation well–posed. We define the fractional order derivative with respect to x approximated at the interpolation points (x_i, y_j, t_k) for $i = 0,1,\ldots,N_x,\ j = 0,1,\ldots,N_y, k = 0,1,\ldots,N_t$ as follows

$$\frac{\partial^{\beta}}{\partial x^{\beta}} u(x,y,t) \approx \frac{\partial^{\beta}}{\partial x^{\beta}} U(x_i,y_j,t_k) = \mathcal{D}^{\beta} U_{j,k}, \tag{23}$$

where $U_{j,k} = [U(x_0,y_j,t_k), U(x_1,y_j,t_k), \ldots, U(x_{N_x},y_j,t_k)]^T, j = 0,1,\ldots,N_y,\ k = 0,1,\ldots,N_t$. Fractional order derivatives with respect to y and t are approximated in similarly manner. Therefore, we can approximate Equation (20) in terms of the shifted Chebyshev polynomial as

$$\sum_{k=1}^{N_t}\sum_{j=1}^{N_y-1} \mathcal{D}^{\alpha}_{k,n} U_{j,k} - \sum_{j=1}^{N_y-1}\left[\sum_{e=1} G_e \mathcal{D}^{\gamma_e}_{j,m}\right] U_{j,k} - \left[\sum_{d=1} F_d \mathcal{D}^{\beta_d}\right] U_{j,k} - U_{j,k} = Q_{j,k},$$

$$n = 0, 1, \ldots, N_t,\ m = 0, 1, \ldots, N_y, \tag{24}$$

where $Q_{j,k} = [Q(x_0, y_j, t_k), Q(x_1, y_j, t_k), \ldots, Q(x_{N_x}, y_j, t_k)]^T, j = 0, 1, \ldots, N_y,\ k = 0, 1, \ldots, N_t$ is the approximation of $q(x, y, t)$ on the Chebyshev–Gauss–Lobatto points (x_i, y_j, t_k). The above is a linear algebraic system which when combined with the initial and boundary conditions evaluated at the interpolation points as

$$U(x_0, y_j, t_k) = \mathcal{B}_0^x(y_j, t_k), \quad U(x_{N_x}, y_j, t_k) = \mathcal{B}_1^x(y_j, t_k), \tag{25}$$

$$U(x_i, y_0, t_k) = \mathcal{B}_0^y(x_i, t_k), \quad U(x_i, y_{N_y}, t_k) = \mathcal{B}_1^y(x_i, t_k), \tag{26}$$

and

$$U(x_i, y_j, t_0) = \mathcal{I}(x_i, y_j) \tag{27}$$

yields a consistent system.

3.5. Nonlinear FPDEs

In this section, we detail how to use the proposed method to solve nonlinear FPDEs. Consider the nonlinear FPDE

$$\frac{\partial^\alpha u}{\partial t^\alpha} = F\left(u, \frac{\partial^{\beta_1} u}{\partial x^{\beta_1}}, \frac{\partial^{\beta_2} u}{\partial x^{\beta_2}}, \ldots, \frac{\partial^{\gamma_1} u}{\partial y^{\gamma_1}}, \frac{\partial^{\gamma_2} u}{\partial y^{\gamma_2}}, \ldots\right) + q(x, y, t), \tag{28}$$

with the initial and boundary conditions in Equations (21) and (22) and F is a nonlinear operator. In order to solve Equation (28), we first linearize using the quasilinearization technique of [4]. This quasilinearization method is based on the Newton–Raphson approach and developed from the linear expansion in terms of the Taylor's series about an initial solution. Applying the approach on Equation (28), we obtain the iterative scheme

$$\begin{aligned}\frac{\partial^\alpha u_{r+1}}{\partial t^\alpha} - \left(\frac{\partial F_r}{\partial u}\right) u_{r+1} - \left(\frac{\partial F_r}{\partial D_x^{\beta_1} u}\right) \frac{\partial^{\beta_1} u_{r+1}}{\partial x^{\beta_1}} - \left(\frac{\partial F_r}{\partial D_x^{\beta_2} u}\right) \frac{\partial^{\beta_2} u_{r+1}}{\partial x^{\beta_2}} - \cdots \\ - \left(\frac{\partial F_r}{\partial D_y^{\gamma_1} u}\right) \frac{\partial^{\gamma_1} u_{r+1}}{\partial y^{\gamma_1}} - \left(\frac{\partial F_r}{\partial D_y^{\gamma_2} u}\right) \frac{\partial^{\gamma_2} u_{r+1}}{\partial y^{\gamma_2}} - \ldots = R_r + q(x, y, t),\end{aligned} \tag{29}$$

where

$$\begin{aligned}R_r = \left(\frac{\partial F_r}{\partial u}\right) u_r - \left(\frac{\partial F_r}{\partial D_x^{\beta_1} u}\right) D_x^{\beta_1} u_r - \left(\frac{\partial F_r}{\partial D_x^{\beta_2} u}\right) D_x^{\beta_2} u_r - \ldots - \left(\frac{\partial F_r}{\partial D_y^{\gamma_1} u}\right) D_y^{\gamma_1} u_r \\ - \left(\frac{\partial F_r}{\partial D_y^{\gamma_2} u}\right) D_y^{\gamma_2} u_r - \ldots - F_r,\end{aligned} \tag{30}$$

and r in this case signifies the previous iteration. Equation (29) can then be expanded in terms of shifted Chebyshev polynomials, when combined with the initial and boundary conditions form a consistent linear algebraic system.

4. Space of fractional derivative and convergence analysis

In this section, we establish some functional spaces of fractional derivatives and then present a convergence analysis of the spectral method for a space–time fractional partial differential equation of the form Equation (20). We introduce the domain $\Omega = \Phi \times \Upsilon$, where $\Phi = (0, 1]$ and $\Upsilon = [0, 1] \times [0, 1]$. Define $(\cdot, \cdot)_\Omega$ and $\|\cdot\|_{0,\Omega}$ the inner product and norm $L^2(\Omega)$ respectively and assume that $u(x, y, t), f_d(x, y)|_{d\geq 1}, g_e(x, y)|_{e\geq 1}$ and $q(x, y, t)$ are defined in the space of smooth functions.

Definition 4.1. *Define the space $H^m(\Phi), m \geq 0$, the Sobolev space [9, 10]*

$$H^m(\Phi) = \left\{ u \in L^2(\Phi) : \frac{\partial^j u}{\partial t^j} \in L^2(\Phi), 0 \leq j \leq m \right\}, \tag{31}$$

endowed with the respective weighted semi–norm and norm

$$|u|_{m,\Phi} = \left(\left\| \frac{\partial^m u}{\partial t^m} \right\|^2_{L^2(\Phi)} \right)^{1/2}, \qquad \|u\|_{m,\Phi} = \left(\sum_{j=0}^{m} \left\| \frac{\partial^j u}{\partial t^j} \right\|^2_{L^2(\Phi)} \right)^{1/2}. \tag{32}$$

Definition 4.2. *We define the fractional Sobolev space $H^\alpha(\Phi)$ for any $\alpha > 0$ as [9, 16]*

$$H^\alpha(\Phi) = \left\{ u \in L^2(\Phi) : {}_0D^\alpha u \in L^2(\Phi) \right\}, \tag{33}$$

such that the semi–norm and norm associated with the space are defined respectively as

$$|u|_{\alpha,\Phi} = \|{}_0D^\alpha u\|_{L^2(\Phi)}, \qquad \|u\|_{\alpha,\Phi} = \left(\|u\|^2_{L^2(\Phi)} + |u|^2_{\alpha,\Phi} \right)^{1/2}. \tag{34}$$

Lemma 4.3. *For $u \in H^\alpha(\Phi)$, if $0 < p < \alpha$, then there is a non–negative constant C such that [16]*

$$\|u\|_{p,\Phi} \leq C\|u\|_{\alpha,\Phi}. \tag{35}$$

Lemma 4.4. *Let $u \in H^m(\Phi)$ and T_N be the expansion in terms of $(N + 1)$ Chebyshev–Gauss–Lobatto nodes, then the error is estimated as [10]*

$$\|u - T_N u\|_{l,\Phi} \leq CN^{2l-m}\|u\|_{m,\Phi},\ l \leq m \tag{36}$$

$$\|u - T_N u\|_{L^2_w(\Phi)} \leq CN^{-m}\|u\|_{m,\Phi}. \tag{37}$$

Lemma 4.5. *Assume that U_{N,N_t}, with $N = (N_x + N_y + 2)$ be the orthogonal projection operator of $L^2(\Omega)$) onto $T_{N,N_t}(\Omega)$, then for all $m, n \geq 0$, there exist a positive constant C not dependent on N and N_t such that [9, 10]*

$$\|u - T_{N,N_t}u\|_{L^2_w(\Omega)} \leq C\left(N^{-m}\|u\|_{m,0} + N_t^{-n}\|u\|_{0,n}\right). \tag{38}$$

Theorem 4.6 (Convergence)**.** *Assume that u is the exact solution of Equation* (20) *and its approximation is given as U, and $q \in C(\Omega) \cap H^{0,p_2}(\Phi; H^{p_1,0}(\Upsilon))$, then*

$$\|u - U\|_{L^2_w(\Omega)} \to 0. \tag{39}$$

Proof. Considering the integration of Equation (20), we have

$$u = {}_0I_t^\alpha u + \sum_{d=1} f_d \; {}_0I_t^\alpha \frac{\partial^{\beta_d} u}{\partial x^{\beta_d}} + \sum_{e=1} g_e \; {}_0I_t^\alpha \frac{\partial^{\gamma_e} u}{\partial y^{\gamma_e}} + {}_0I_t^\alpha q, \tag{40}$$

and let U represents the approximation of u which uses N_x truncated Chebyshev approximation in x, N_y truncated Chebyshev expansion in y and N_t truncated expansion in t is given as

$$U = {}_0I_t^\alpha U + \sum_{d=1} f_d \; {}_0I_t^\alpha \frac{\partial^{\beta_d} U}{\partial x^{\beta_d}} + \sum_{e=1} g_e \; {}_0I_t^\alpha \frac{\partial^{\gamma_e} U}{\partial y^{\gamma_e}} + {}_0I_t^\alpha Q. \tag{41}$$

In view of Equations (40) and (41), we obtain

$$\begin{aligned}\|u - U\|_{L^2_w(\Omega)} \leq \|{}_0I_t^\alpha (u - U)\|_{L^2_w\Omega} + \left\|\sum_{d=1} f_d \; {}_0I_t^\alpha \frac{\partial^{\beta_d}(u-U)}{\partial x^{\beta_d}}\right\|_{L^2_w(\Omega)} + \left\|\sum_{e=1} g_e \; {}_0I_t^\alpha \frac{\partial^{\gamma_e}(u-U)}{\partial y^{\gamma_e}}\right\|_{L^2_w(\Omega)} \\ + \|{}_0I_t^\alpha (q - Q)\|_{L^2_w(\Omega)}. \end{aligned} \tag{42}$$

For a Chebyshev–Gauss–Lobatto quadrature and using the properties of a Sobolev norm and Young's inequality, we have

$$\begin{aligned}|({}_0I_t^\alpha (q - Q))|_{L^2_w(\Omega)} &= |({}_0I_t^\alpha (q - T_{N,N_t}q + T_{N,N_t}q - Q))| \\ &\leq |({}_0I_t^\alpha)||(q - T_{N,N_t}q + T_{N,N_t}q - Q)| \\ &\leq C|(q - T_{N,N_t}q + T_{N,N_t}q - Q)| \\ &\leq C(|(q - T_{N,N_t}q)| + |(T_{N,N_t}q - Q)|) \\ &\leq C(\|(q - T_{N,N_t}q\|_0 + \|T_{N,N_t}q - Q)\|_0)\end{aligned}$$

$$\leq C(N^{-p_1}\|q\|_{p_1,0} + N_t^{-p_2}\|q\|_{0,p_2}). \tag{43}$$

Therefore, Equation (42) becomes

$$\begin{aligned}\|u-U\|_{L^2_w(\Omega)} &\leq \left({}_0I_t^{\alpha}|u-U|_0 + \left|\sum_{d=1} f_d\ {}_0I_t^{\alpha}\right| |u-U|_{\beta_d} + \left|\sum_{e=1} g_e\ {}_0I_t^{\alpha}\right| |u-U|_{\gamma_e}\right) \\ &\quad + C(N^{-p_1}\|q\|_{p_1,0} + N_t^{-p_2}\|q\|_{0,p_2}) \qquad (44)\\ &\leq C\left(\|u-U\|_0 + \|u-U\|_{\beta_d} + \|u-U\|_{\gamma_e} + N^{-p_1}\|q\|_{p_1,0} + N_t^{-p_2}\|q\|_{0,p_2}\right). \qquad (45)\end{aligned}$$

In order to estimate $\|u-U\|_{\beta}$, we have

$$\begin{aligned}\|u-U\|_{\beta} &\leq \|u - T_{N,N_t}u\|_{\beta,0} + \|T_{N,N_t}u - U\|_{\beta,0}\\ &\leq N^{2\beta-m}\|u\|_{m,0} + N_t^{-n}\|u\|_{0,n}. \qquad (46)\end{aligned}$$

For any $\beta_d (d = 1, 2, \ldots)$ or $\gamma_e (e = 1, 2, \ldots)$, there exist non negative constants C_d or C_e such that (by Lemma 4.3)

$$\|u-U\|_{\beta_d} \leq C_d\|u-U\|_{\beta,0} \quad \text{or} \quad \|u-U\|_{\gamma_e} \leq C_e\|u-U\|_{\gamma,0}. \tag{47}$$

Therefore, we have

$$\begin{aligned}\|u-U\|_{L^2_w(\Omega)} \leq C\Big(&N^{-m}\|u\|_{m,0} + N_t^{-n}\|u\|_{0,n} + N^{2\beta-m}\|u\|_{m,0} + N_t^{-n}\|u\|_{0,n}\\ &+N^{2\gamma-m}\|u\|_{m,0} + N_t^{-n}\|u\|_{0,n} + N^{-p_1}\|q\|_{p_1,0} + N_t^{-p_2}\|q\|_{0,p_2}\Big), \qquad (48)\end{aligned}$$

where C is non–negative and not dependent on N_x, N_y and N_t.

5. Numerical examples

In this section, we applied the numerical scheme to selected linear and nonlinear two–dimensional time–space fractional partial differential equations of the initial–boundary value type. The accuracy and efficiency of the method is demonstrated by comparing the results with exact solutions.

Example 5.1. *We consider the two–dimensional time–space fractional diffusion equation with variable coefficients on a finite domain*

$$\frac{\partial^{0.8}u}{\partial t^{0.8}} = f(x,y)\frac{\partial^{1.8}u}{\partial x^{1.8}} + g(x,y)\frac{\partial^{1.5}u}{\partial y^{1.5}} + q(x,y,t), \tag{49}$$

where $f(x,y)$ and $g(x,y)$ are the diffusion coefficients. We investigate the case where

$$f(x,y) = \frac{x^{1.8}}{\Gamma(3.8)}, \quad g(x,y) = \frac{\Gamma(2.5)}{6}y^{1.5}, \tag{50}$$

and subject to the boundary conditions

$$u(0,y,t) = 0, \quad u(1,y,t) = y^3(1+t^2), \quad 0 \le y \le 1,\ 0 < t \le 1 \tag{51}$$

$$u(x,0,t) = 0, \quad u(x,1,t) = x^{2.8}(1+t^2), \quad 0 \le x \le 1,\ 0 < t \le 1. \tag{52}$$

The initial condition for this FPDE is given as

$$u(x,y,0) = x^{2.8}y^3, \quad 0 \le x \le 1,\ 0 \le y \le 1, \tag{53}$$

and the source term $q(x,y,t)$ is defined as

$$q(x,y,t) = -2\left(t^2 - \frac{t^{1.2}}{\Gamma(2.2)} + 1\right)x^{2.8}y^3. \tag{54}$$

The exact solution is given in [35] as

$$u(x,y,t) = x^{2.8}y^3(1+t^2). \tag{55}$$

Example 5.2. *Consider the two–dimensional generalized space–time fractional diffusion equation with variable coefficients (see Zheng and Zhang[35])*

$$\frac{\partial^{\alpha}u}{\partial t^{\alpha}} = f(x,y)\frac{\partial^{\beta}u}{\partial x^{\beta}} + g(x,y)\frac{\partial^{\gamma}u}{\partial y^{\gamma}} + q(x,y,t), \quad 0 < \alpha \le 1,\ 1 < \beta,\gamma \le 2. \tag{56}$$

In this test problem, the explicit solution is chosen as

$$u(x,y,t) = x^2y^3t^2, \tag{57}$$

such that when we substitute the solution into the equation, we obtain the diffusion coefficients as

$$f(x,y) = \frac{(3-2x)\Gamma(3-\beta)}{2}, \quad g(x,y) = \frac{(4-y)\Gamma(4-\gamma)}{6}, \tag{58}$$

and the source term as

$$q(x,y,t) = \frac{2}{\Gamma(3-\alpha)}x^2y^3t^{2-\alpha} + y^3t^2(2x^{3-\beta} - 3x^{2-\beta}) + x^2t^2(y^{4-\gamma} - 4y^{3-\gamma}). \tag{59}$$

The FPDE is solved subject to the initial condition

$$u(x, y, 0) = 0, \tag{60}$$

and boundary conditions

$$u(0, y, t) = 0, \quad u(1, y, t) = y^3 t^2, \quad 0 \leq y \leq 1,\ 0 < t \leq 1, \tag{61}$$
$$u(x, 0, t) = 0, \quad u(x, 1, t) = x^2 t^2, \quad 0 \leq x \leq 1,\ 0 < t \leq 1. \tag{62}$$

Example 5.3. *We consider the nonlinear two–dimensional space–time Fisher's partial differential equations [35]*

$$\frac{\partial^\alpha u}{\partial t^\alpha} = \frac{\partial^\beta u}{\partial x^\beta} + \frac{\partial^\gamma u}{\partial y^\gamma} + u(1-u) + q(x, y, t), \quad 0 < \alpha \leq 1,\ 1 < \beta, \gamma \leq 2, \tag{63}$$

with exact solution

$$u(x, y, t) = x^2 y^2 t. \tag{64}$$

The equation is solved subject to the boundary conditions

$$u(0, y, t) = 0, \quad u(1, y, t) = y^2 t, \quad 0 \leq y \leq 1,\ 0 < t \leq 1, \tag{65}$$
$$u(x, 0, t) = 0, \quad u(x, 1, t) = x^2 t, \quad 0 \leq x \leq 1,\ 0 < t \leq 1, \tag{66}$$

and the initial condition

$$u(x, y, 0) = 0. \tag{67}$$

The function $q(x, y, t)$ is defined as

$$q(x, y, t) = \frac{1}{\Gamma(2-\alpha)} x^2 y^2 t^{1-\alpha} - \frac{2}{\Gamma(3-\beta)} x^{2-\beta} y^2 t - \frac{2}{\Gamma(3-\gamma)} x^2 y^{2-\gamma} t - x^2 y^2 t + x^4 y^4 t^2. \tag{68}$$

6. Result and Discussion

This section discusses the numerical results obtained by applying the method to Examples 5.1–5.3. We focus on the accuracy of the scheme and the ease of implementation. The numerical simulations were made using the PYTHON programming language run on a computer with *Intel Core i5–7200U, CPU @ 2.50 GHz*, and *8 GB DDR4* installed memory. The results show how the orders of the shifted Chebyshev polynomials in each variable affect the accuracy of the numerical method. In order to determine the accuracy of the method, we define the infinity error norm which measures the maximum of the absolute values of the difference between the exact and numerical solutions

$$\|\varepsilon\|_\infty = \|u(x_i, y_j, t_k) - U(x_i, y_j, t_k)\|_\infty, \tag{69}$$

where u and U are respectively the exact and numerical solutions. This is a good measure for accuracy because we expect that the difference between the exact and numerical solutions at every grid points to be close to zero.

Figure 1 shows the numerical and exact solutions for Example 5.1. It can be seen that both solutions are in agreement. The errors presented in Tables 1 and 2 are associated with Example 5.1. In Table 1, the number of grid points in both the spatial and temporal domains are varied. The result show accurate results for different combinations of the numbers of grid points and/or orders of the shifted Chebyshev polynomials. We observe that the numerical solutions become better as the orders of the polynomials increase. The table also shows the condition number of the matrix, as well as the computational time. The condition numbers are obtained using the PYTHON package "*numpy.linalg.cond*". Both the condition number and the computational time increase as the combination of the grid points increases. This is explained by the higher number of algebraic equations that need to be solved with an increase in number of grid points. For instance, in the case when $N_x = N_y = 15$ and $N_t = 10$, there are 2816 coupled linear algebraic equations to be solved, and when $N_x = N_y = N_t = 7$, there are 512 linear algebraic equations. This well–conditioned system of equations was solved and accurate solutions obtained in less than 2 seconds, thus showing that the method is not only accurate but also efficient. The high number of coupled linear algebraic equations solved in few seconds establish the efficiency of the method. Given that fractional derivatives are non–local, we remark that this is a fairly good result. Table 2 shows the comparison between the exact solution and the approximate solution obtained at selected points (x, y, t). We observe that the magnitude of the error at these selected points is small.

The numerical solutions of Example 5.2 at $t = 0.5$ and $t = 1$ are shown in Figure 2. These solutions are in agreement with the exact solutions. In Tables 3 and 4, we present the error norm, condition number and computational time for Example 5.2 for different combinations of the numbers of terms in the polynomials and different combination of the fractional orders respectively. Again, we observe accuracy in the results which is evident from the magnitude of the error norms and efficiency, evident from the CPU time required to solve the system of algebraic equations. Table 4 shows the accuracy for different values of $\alpha \in (0, 1)$ and $\beta, \gamma \in (1, 2)$ for fixed numbers of grid points $N_x = N_y = N_t = 10$. In Table 5, we present the error norms for Example 5.3 which is a nonlinear space–time fractional differential equation. The results presented in Table 5 are obtained after the sixth iteration. A distinctive difference between the result obtained in Example 5.3 and that obtained in Examples 5.1 and 5.2 is the computational time to solve the resulting system of algebraic equation in Example 5.3. The CPU time in Example 5.3 is higher than that in Examples 5.1 and 5.2. This owes to the fact that Example 5.3 is solved through an iterative process. Figure 3 depicts the numerical solution and absolute error for Example 5.3 at $t = 0.5$ and $t = 1$ with $\alpha = 9/10$ and $\beta = \gamma = 1.9$. One obvious advantage of the method over many other methods that have been used to find solutions of FPDEs is the fact that it only requires small numbers of terms of the shifted Chebyshev polynomials, and as a result small numbers of grid points to achieve accuracy.

Although, we assumed that the solution $u(x, y, t)$ must be continuously differentiable for the

approximation to be convergent. However, a closer inspection of the examples in the previous section shows that the exact solutions may not be continuously differentiable. Nevertheless, as it has been shown, the method converges and perform well. It is quite ubiquitous in literature to construct approximations for equations whose solutions are non–smooth.

Table 1: Error norms of Example 5.1 for different combinations of the values of N_x, Ny, N_t.

(N_x, N_y, N_t)	$\|\varepsilon\|_\infty$	condition number	CPU time(sec)
$(5, 5, 5)$	$1.7367e-04$	$1.0050e+03$	0.0304
$(7, 7, 5)$	$2.5291e-05$	$4.9732e+03$	0.0463
$(7, 7, 7)$	$2.0069e-05$	$5.6195e+03$	0.0688
$(10, 10, 7)$	$7.9423e-06$	$5.1577e+04$	0.2336
$(10, 10, 10)$	$3.3726e-06$	$5.4943e+04$	0.2863
$(15, 15, 10)$	$3.2808e-06$	$2.2740e+09$	1.8369

Table 2: Comparison of the numerical and exact solutions at some random points of x, y, t: Example 5.1 $N_x = 10, N_y = 10, N_t = 10$

(x, y, t)	$u(x, y, t)$	$U(x, y, t)$	$abs(u - U)$
$(0.50, 0.50, 0.10)$	0.0181	0.0181	$3.0437e-07$
$(0.50, 0.90, 0.10)$	0.1072	0.1072	$6.4668e-07$
$(0.90, 0.90, 0.10)$	0.5638	0.5638	$1.5162e-07$
$(0.50, 0.50, 0.50)$	0.0224	0.0224	$3.0558e-07$
$(0.90, 0.50, 0.50)$	0.1180	0.1180	$4.9251e-07$
$(0.50, 0.90, 0.50)$	0.1328	0.1328	$8.2658e-07$
$(0.90, 0.90, 0.50)$	0.6984	0.6984	$3.1169e-06$
$(0.90, 0.50, 0.90)$	0.1716	0.1716	$1.9308e-07$
$(0.50, 0.90, 0.90)$	0.1932	0.1932	$3.3049e-07$
$(0.90, 0.90, 0.90)$	1.0158	1.0158	$9.3025e-07$

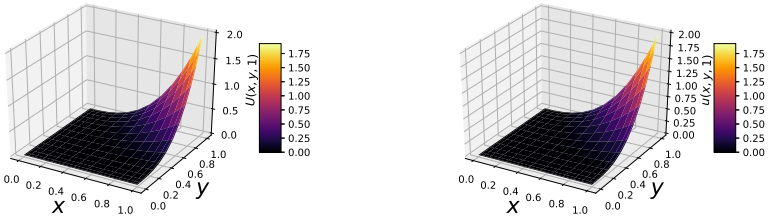

(a) Numerical solution (b) Exact solution

Figure 1: The numerical and exact solutions for Example 5.1 at $t = 1$.

Table 3: Absolute error norms of Example 5.2 for different values of N_x, N_y, N_t and $\alpha = 0.7, \beta = 1.5, \gamma = 1.6$

(N_x, N_y, N_t)	$\|\varepsilon\|_\infty$	condition number	CPU time(sec)
$(5, 5, 5)$	$1.4801e-04$	$1.5767e+03$	0.0248
$(7, 7, 5)$	$6.5902e-05$	$4.4287e+03$	0.0499
$(7, 7, 7)$	$6.2105e-05$	$4.7101e+03$	0.0713
$(10, 10, 7)$	$3.2852e-05$	$1.4321e+04$	0.2672
$(10, 10, 10)$	$3.2941e-05$	$1.4905e+04$	0.3124
$(15, 15, 10)$	$9.0358e-06$	$3.8865e+08$	1.7789

Table 4: Error norm values obtained when Example 5.2 is solved with $N_x = N_y = N_t = 10$ for different values of α, β, γ.

(α, β, γ)	$\|\varepsilon\|_\infty$	condition number	CPU time(sec)
$(0.1, 1.1, 1.2)$	$1.1259e-05$	$8.6909e+03$	0.2882
$(0.3, 1.3, 1.4)$	$2.7852e-05$	$9.1981e+03$	0.2972
$(0.5, 1.5, 1.6)$	$3.3015e-05$	$1.3738e+04$	0.3062
$(0.7, 1.7, 1.8)$	$3.1277e-05$	$2.1455e+04$	0.3032

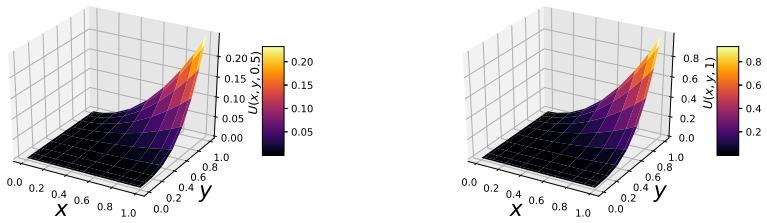

(a) $t = 1/2$ (b) $t = 1$

Figure 2: Numerical solutions of Example 5.2 for different t with $N_t = N_x = N_y = 10$, $\alpha = 1/2$ and $\beta = \gamma = 3/2$.

Table 5: Absolute error norms obtained for Example 5.3 for different values of α, β, γ after the sixth iteration: $N_x = N_y = N_t = 10$.

(α, β, γ)	$\|\varepsilon\|_\infty$	condition number	CPU time(sec)
$(0.1, 1.1, 1.2)$	$3.4572e-04$	$1.1729e+04$	1.2437
$(0.3, 1.3, 1.4)$	$1.3217e-04$	$9.0201e+03$	1.2407
$(0.5, 1.5, 1.6)$	$1.2695e-04$	$1.2389e+04$	1.2377
$(0.7, 1.7, 1.8)$	$1.1264e-04$	$2.0124e+04$	1.2277

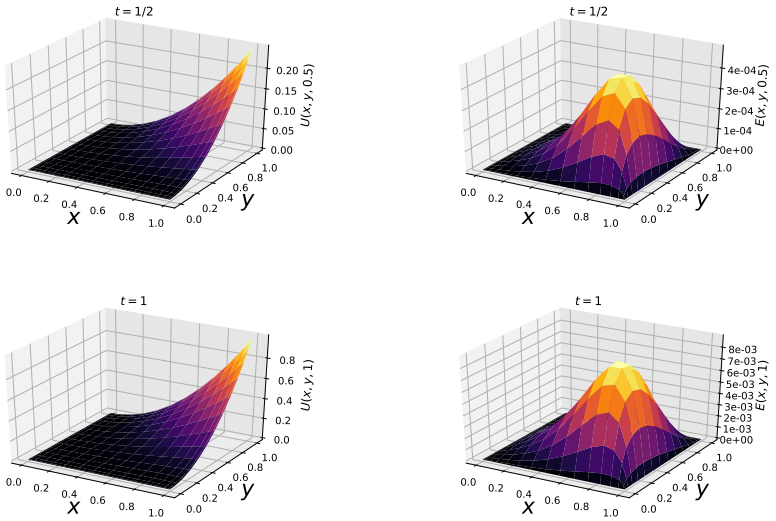

Figure 3: Surface plots of the numerical solution and absolute error for different values of t for Example 5.3 with $N_t = N_x = N_y = 15$ and $\alpha = 9/10$ and $\beta = \gamma = 1.9$.

7. Conclusion

In this study, we presented a numerical scheme for two–dimensional space–time fractional partial differential equations. The method is purely spectral and approximates the dependent variable and its fractional derivative (both spatial and temporal) using shifted Chebyshev polynomials and integrated using shifted Chebyshev–Gauss–Lobatto quadrature. In the case of nonlinear two–dimensional space–time FPDEs, we used quasilinearization to linearize the equation and then expanded the solution in terms of the shifted Chebyshev polynomials . The method was described and applied to some FPDEs of the initial–boundary value type. In the examples considered, we found that the method is accurate, reliable and efficient. The accuracy was confirmed through an analysis of the magnitude of the error norms. The accuracy of the method can be attributed to the fact that the approach is purely spectral, and spectral methods are non–local in nature. They generate an approximate solution over the entire grid points instead of using neighbouring points. The efficiency is evident in the computational time required to solve the system of algebraic equations resulting from the expansion in terms of shifted Chebyshev polynomials. In future, the method may be extended to a large time domain and irregular spatial domains.

References

[1] Milton Abramowitz and Irene A Stegun. *Handbook of mathematical functions with formulas, graphs, and mathematical tables*, volume 55. US Government Printing Office, 1948.

[2] CN Angstmann, BI Henry, and AV McGann. A fractional order recovery SIR model from a stochastic process. *Bulletin of Mathematical Biology*, 78(3):468–499, 2016.

[3] Eli Barkai, Ralf Metzler, and Joseph Klafter. From continuous time random walks to the fractional Fokker-Planck equation. *Physical Review E*, 61(1):132, 2000.

[4] Richard Ernest Bellman and Robert E Kalaba. Quasilinearization and nonlinear boundary-value problems. *Rand Corporation*, 1965.

[5] DA Benson, SW Wheatcraft, and MM Meerschaert. Application of a fractional advection-dispersion equation. *Water Resources Research*, 36(6):1403–1412, 2000.

[6] AH Bhrawy. A Jacobi–Gauss–Lobatto collocation method for solving generalized Fitzhugh–Nagumo equation with time-dependent coefficients. *Applied Mathematics and Computation*, 222:255–264, 2013.

[7] AH Bhrawy and MA Zaky. A method based on the Jacobi tau approximation for solving multi-term time–space fractional partial differential equations. *Journal of Computational Physics*, 281:876–895, 2015.

[8] Luise Blank. Numerical treatment of differential equations of fractional order. *Nonlinear World*, 4:473–492, 1997.

[9] Claudio Canuto, M Yousuff Hussaini, Alfio Quarteroni, and Thomas A Zang. *Spectral methods: Fundamentals in single domains*. Springer Science & Business Media, 2007.

[10] Claudio Canuto, M Yousuff Hussaini, Alfio Quarteroni, A Thomas Jr, et al. *Spectral methods in fluid dynamics*. Springer Science & Business Media, 2012.

[11] Varsha Daftardar-Gejji and Hossein Jafari. Adomian decomposition: a tool for solving a system of fractional differential equations. *Journal of Mathematical Analysis and Applications*, 301(2):508–518, 2005.

[12] EH Doha, AH Bhrawy, and SS Ezz-Eldien. A Chebyshev spectral method based on operational matrix for initial and boundary value problems of fractional order. *Computers & Mathematics with Applications*, 62(5):2364–2373, 2011.

[13] EH Doha, AH Bhrawy, and SS Ezz-Eldien. A new Jacobi operational matrix: An application for solving fractional differential equations. *Applied Mathematical Modelling*, 36(10):4931–4943, 2012.

[14] EH Doha, AH Bhrawy, MA Abdelkawy, and RA Van Gorder. Jacobi–Gauss–Lobatto collocation method for the numerical solution of 1+1 nonlinear Schrödinger equations. *Journal of Computational Physics*, 261:244–255, 2014.

[15] M Enelund and BL Josefson. Time-domain finite element analysis of viscoelastic structures with fractional derivatives constitutive relations. *American Institute of Aeronautics and Astronatics Journal*, 35(10):1630–1637, 1997.

[16] Vincent J Ervin and John Paul Roop. Variational formulation for the stationary fractional advection dispersion equation. *Numerical Methods for Partial Differential Equations: An International Journal*, 22(3):558–576, 2006.

[17] MH Heydari, Mohammad Reza Hooshmandasl, and Fakhrodin Mohammadi. Legendre wavelets method for solving fractional partial differential equations with dirichlet boundary conditions. *Applied Mathematics and Computation*, 234:267–276, 2014.

[18] MH Heydari, MR Hooshmandasl, and F Mohammadi. Two-dimensional legendre wavelets for solving time-fractional telegraph equation. *Advances in Applied Mathematics and Mechanics*, 6(2):247–260, 2014.

[19] Hossein Jafari and Varsha Daftardar-Gejji. Solving a system of nonlinear fractional differential equations using adomian decomposition. *Journal of Computational and Applied Mathematics*, 196(2):644–651, 2006.

[20] J Klafter, A Blumen, and MF Shlesinger. Stochastic pathway to anomalous diffusion. *Physical Review A*, 35(7):3081, 1987.

[21] H Kober. On fractional integrals and derivatives. *The Quarterly Journal of Mathematics*, (1):193–211, 1940.

[22] Manoj Kumar and Varsha Daftardar-Gejji. A new family of predictor-corrector methods for solving fractional differential equations. *Applied Mathematics and Computation*, 363: 124633, 2019.

[23] AV Letnikov. Theory of differentiation of fractional order. *Mathematics S B*, 3(1), 1868.

[24] VE Lynch, BA Carreras, D del Castillo-Negrete, KM Ferreira-Mejias, and HR Hicks. Numerical methods for the solution of partial differential equations of fractional order. *Journal of Computational Physics*, 192(2):406–421, 2003.

[25] Pin Lyu and Seakweng Vong. A high-order method with a temporal nonuniform mesh for a time-fractional benjamin–bona–mahony equation. *Journal of Scientific Computing*, 80(3):1607–1628, 2019.

[26] F Mainardi, M Raberto, R Gorenflo, and E Scalas. Fractional calculus and continuous-time finance II: The waiting-time distribution. *Physica A: Statistical Mechanics and its Applications*, 287(3-4):468–481, 2000.

[27] Mark M Meerschaert and Charles Tadjeran. Finite difference approximations for two-sided space-fractional partial differential equations. *Applied Numerical Mathematics*, 56 (1):80–90, 2006.

[28] MM Meerschaert and C Tadjeran. Finite difference approximations for fractional advection–dispersion flow equations. *Journal of Computational and Applied Mathematics*, 172(1):65–77, 2004.

[29] KB Oldham and J Spanier. *The Fractional Calculus*. Academic Press, New York, 1974.

[30] Shina Oloniiju, Sicelo Goqo, and Precious Sibanda. A Chebyshev spectral method for heat and mass transfer in MHD nanofluid flow with space fractional constitutive model. *Frontiers in Heat and Mass Transfer*, 13, 2019.

[31] Igor Podlubny. *Fractional differential equations: an introduction to fractional derivatives, fractional differential equations, to methods of their solution and some of their applications*, volume 198. Elsevier, 1998.

[32] Jincheng Ren, Dongyang Shi, and Seakweng Vong. High accuracy error estimates of a galerkin finite element method for nonlinear time fractional diffusion equation. *Numerical Methods for Partial Differential Equations*, 36(2):284–301, 2020.

[33] Lorenzo Sabatelli, Shane Keating, Jonathan Dudley, and Peter Richmond. Waiting time distributions in financial markets. *The European Physical Journal B-Condensed Matter and Complex Systems*, 27(2):273–275, 2002.

[34] R Schumer, DA Benson, MM Meerschaert, and B Baeumer. Multiscaling fractional advection-dispersion equations and their solutions. *Water Resources Research*, 39(1), 2003.

[35] Liancun Zheng and Xinxin Zhang. *Modeling and analysis of modern fluid problems*. Academic Press, 2017.

Chapter 6

A geometrically convergent pseudo–spectral method for multi–dimensional two–sided space fractional partial differential equations

In Chapter 5, a shifted Chebyshev pseudo–spectral method was presented for space–time fractional partial differential equations. This chapter extends the pseudo–spectral method to two–sided space fractional partial differential equations. As in Chapters 2, 3 and 5, the solutions of the differential equations are approximated as truncated series expansions using shifted Chebyshev polynomials of the first kind as basis function. The approximations are evaluated using the Chebyshev–Gauss–Lobatto collocation points. Left– and right–sided differentiation matrices, which serve as approximations of both the left– and right–sided fractional differential operators, are presented. Convergence analysis of the full discretization scheme is performed, and numerical examples are presented to illustrate the effectiveness of the numerical scheme. The results show that the numerical scheme is computationally efficient and accurate.

A geometrically convergent pseudo–spectral method for multi–dimensional two–sided space fractional partial differential equations

Shina D. Oloniiju*, Sicelo P. Goqo, Precious Sibanda

School of Mathematics, Statistics and Computer Science, University of KwaZulu-Natal, Private Bag X01, Scottsville, Pietermaritzburg, 3209, South Africa.

Abstract

In this study, we present a geometrically convergent numerical method for solving multi–dimensional two–sided space–time fractional differential equations. The approach allows for the representation of solutions of differential equations in terms of the shifted Chebyshev polynomials. The expansions are evaluated at the shifted Chebyshev–Gauss–Lobatto nodes. We present the left–sided integration matrix and the left– and right– sided differentiation matrices based on Caputo fractional operators. The performance of the method is demonstrated using selected two–sided space fractional partial differential equations in one and two dimensions. The numerical results obtained show that the method is accurate and computationally efficient. A theoretical analysis of the convergence of the method is presented, where it is shown that the numerical solution converges for sufficiently large number of grid points provided the solution is continuously differentiable.

Keywords: Shifted Chebyshev polynomials, Chebyshev–Gauss–Lobatto quadrature, two–sided space–time fractional partial differentials, fractional calculus, convergence analysis

1. Introduction

Interest in the description of physical processes using models with arbitrary order derivatives has grown tremendously over the last few decades. Physical models, including the diffusion equation [1, 2], the wave equation [3, 4], viscoelastic fluid models [5–8], flows in porous

*corresponding author

Email addresses: shina@aims.edu.gh (Shina D. Oloniiju), goqos@ukzn.ac.za (Sicelo P. Goqo), sibandap@ukzn.ac.za (Precious Sibanda)

medium [9, 10], hydrological models [11], have been generalized using fractional order derivatives. Arbitrary order differential equations can model intricate systems deftly and describe physical parameters precisely [12, 13]. The global nature of the time fractional derivative is fundamental to astutely describing long term memory characteristics of dynamical systems, where these are inherently present. In physical applications, particularly in diffusion and dispersion processes, space fractional derivatives are used to model anomalous diffusion, in which a nonlinear relationship exists between the mean squared displacement and time. Of interest, is the two–sided space fractional derivatives which allow the influence from either side of the physical domain of a process to be measured [14]. The literature shows that physical processes that are modelled with two–sided space fractional derivatives have been studied extensively. In fact, the Riesz fractional operator is defined to incorporate both the left–sided and right–sided Riemann–Liouville fractional operators [12, 14].

In this study, we describe a numerical scheme for the approximation of the solution of two–sided fractional differential equations. A two–sided space fractional partial differential equation can be reduced to either a left–sided or right–sided fractional differential equation, or reconstructed to form the space Riesz fractional differential equation. Due to the complexity of fractional differential equations, obtaining analytical solutions can be demanding, hence necessitating the use of numerical methods. Published articles on the numerical solution of two–sided fractional partial differential equations are relatively few. Meerschaert and Tadjeran [15] used an implicit Euler method with the shifted Grünwald formulae to solve two–sided space time dependent fractional partial differential equations. They used the shifted Grünwald formulae to circumvent the instability that is usually associated with the finite difference schemes based on the left– and right–sided Grünwald–Letnikov definitions. This numerical method was also used to solve space fractional differential equations in [4, 16–19]. In Chen and Deng [2], an alternating direction implicit method was proposed for two–sided space fractional convection diffusion equations. The numerical scheme was based on a linear spline approximation of both the right– and left–sided Riemann–Liouville fractional operators. A full discrete scheme was described in detail for one– and two– dimensional two–sided space fractional, time dependent convection diffusion equations. In Liu et al. [20], a semi implicit form of the method proposed by Chen and Deng [2] was used to solve a two–dimensional FitzHugh–Nagumo monodomain model defined using the Riesz space fractional derivative. Using the shifted Grünwald formulae proposed by Meerschaert and Tadjeran [15], Liu et al. [21] presented explicit and implicit difference schemes for the space–time fractional advection–diffusion equation. In Feng et al. [22], a finite volume method for the two–sided space fractional diffusion equation based on the nodal basis function was presented. An implicit finite volume method was used, and the resulting discrete system was solved in matrix form. Chen et al. [23] used a semi–implicit difference method, and an iterative procedure developed by decomposing the dense coefficient matrix into a combination of Toeplitz–like matrices, thus diminishing the storage requirement and high computational cost associated with difference methods.

One of the many challenges in numerical mathematics is the high computational costs

associated with obtaining accurate numerical solutions of fractional differential equations, on account of the global nature of fractional operators. Research into more efficient methods can mitigate this high computational expense. Owing to the non–local nature of fractional operators, non–local methods are useful in approximating solutions of fractional differential equations. One such non–local numerical method is the spectral method. Different versions of the spectral method have been developed and applied to solve one–sided fractional differential equations [see [24–28] and the references therein]. However, studies on spectral methods for two–sided fractional differential equation are comparatively uncommon. Among the few such studies are Mao and Shen [1], Bhrawy et al. [29], Mao and Karniadakis [30], Bhrawy et al. [31] and Bhrawy et al. [32].

In this study, we consider general two–sided space time fractional partial differential equations of the form

$$ {}_0D_t^{\gamma} u(\mathbf{x},t) = \sum_{\iota=1}^{d} \left[c_{+,\iota}(\mathbf{x}) {}_0D_{x_\iota}^{\alpha_\iota} u(\mathbf{x},t) + c_{-,\iota}(\mathbf{x}) {}_{x_\iota}D_{\mathsf{L}_\iota}^{\alpha_\iota} u(\mathbf{x},t) \right] + s(\mathbf{x},t), \quad 0 < t \leq \mathsf{T} \qquad (1) $$

on the finite domain $0 < x_\iota < \mathsf{L}_\iota$, such that $x_\iota \in \mathbb{R}^d$, where $c_{+,\iota}(\mathbf{x}), c_{-,\iota}(\mathbf{x})$ are variable coefficients and $s(\mathbf{x},t)$ is the source function.

Equation (1) is defined in its general form, with $d = 1, d = 2$ respectively corresponding to the one and two–dimensional cases. For two–dimensional cases, we redefine the spatial variables $x_1 = x$ and $x_2 = y$, and the fractional orders $\alpha_1 = \alpha$ and $\alpha_2 = \beta$. In the case of the one–dimensional two–sided space time fractional differential equation, all subscripts on α, x, L are dropped. The left–sided fractional derivative ${}_0D_x^{\alpha}$ of any function at a point x depends on all the values of the function to the left of x. In like manner, the right–sided fractional derivative ${}_xD_{\mathsf{L}}^{\alpha}$ of any function at a point x depends on all values of the function to the right of x. These two fractional operators are not identical, except, on the one hand, when α is an even integer; in which case, the derivatives are classical and equal. On the other hand, when α is an odd integer, the two operators are local and opposite in sign [15]. In this study, we introduce a spectral method to solve two–sided space–time fractional differential equations (1). The method involves approximating $u(\mathbf{x},t)$ in terms of shifted first kind Chebyshev polynomials integrated at the Gauss–Lobatto quadrature. We perform a convergence analysis of the method for the general two–sided fractional differential equation (1). We present several examples to illustrate the effectiveness of the method and compare the results obtained with those from closed form solutions, and where possible, with those obtained in past studies.

2. Preliminaries and Notations

In this section, we provide definitions of fractional operators, the properties of the shifted Chebyshev polynomial of the first kind and other important concepts that are relevant for this study.

2.1. Fractional operators

Definition 2.2. *Consider a function $f(x) : [0, \mathsf{L}] \to \mathbb{R}$, which is integrable and continuously differentiable in $\mathbb{R}$. The left– and right–sided Riemann–Liouville fractional integrals of $f(x)$ of any arbitrary order α are defined as [12, 13]*

$$ {}_0I_x^\alpha f(x) := \frac{1}{\Gamma(\alpha)} \int_0^x \frac{f(\tilde{x})}{(x-\tilde{x})^{1-\alpha}} d\tilde{x}, \quad \alpha > 0,\ x > 0 \tag{2} $$

and

$$ {}_\mathsf{L}I_x^\alpha f(x) := \frac{1}{\Gamma(\alpha)} \int_x^\mathsf{L} \frac{f(\tilde{x})}{(\tilde{x}-x)^{1-\alpha}} d\tilde{x}, \quad x < \mathsf{L}, \tag{3} $$

respectively, where Γ is the Euler gamma function. For the case $\alpha = 0$, we have

$$ {}_0I_x^0 f(x) := f(x). \tag{4} $$

We define the fractional integral of a power function x^j as

$$ {}_0I_x^\alpha x^j = \frac{\Gamma(j+1)}{\Gamma(j+\alpha+1)} x^{j+\alpha}. \tag{5} $$

Definition 2.3. *For any $\alpha \in \mathbb{R}^+$, such that $n-1 \leq \alpha < n$, with $n \in \mathbb{N}^+$, the left–sided Riemann–Liouville and left–sided Caputo fractional derivatives are defined as [12, 13]*

$$ {}_0^{RL}D_x^\alpha f(x) := \frac{1}{\Gamma(n-\alpha)} \frac{d^n}{dx^n} \int_0^x \frac{f(\tilde{x})}{(x-\tilde{x})^{\alpha+1-n}} d\tilde{x} \tag{6} $$

and

$$ {}_0^{C}D_x^\alpha f(x) := \frac{1}{\Gamma(n-\alpha)} \int_0^x \frac{f^n(\tilde{x})}{(x-\tilde{x})^{\alpha+1-n}} d\tilde{x}, \quad x > 0, \tag{7} $$

respectively. The corresponding right–sided Riemann–Liouville and right–sided Caputo fractional derivatives are defined as [12, 13]

$$ {}_x^{RL}D_\mathsf{L}^\alpha f(x) := \frac{1}{\Gamma(n-\alpha)} \frac{d^n}{dx^n} \int_x^\mathsf{L} \frac{f(\tilde{x})}{(\tilde{x}-x)^{\alpha+1-n}} d\tilde{x} \tag{8} $$

and

$$ {}_x^{C}D_\mathsf{L}^\alpha f(x) := \frac{1}{\Gamma(n-\alpha)} \int_x^\mathsf{L} \frac{f^n(\tilde{x})}{(\tilde{x}-x)^{\alpha+1-n}} d\tilde{x}, \quad x < \mathsf{L}, \tag{9} $$

respectively.

In both the Riemann–Liouville and Caputo definitions, the fractional operators ${}^{RL}_{0}D^{\alpha}_{x}, {}^{C}_{0}D^{\alpha}_{x} \to d^n/dx^n$ as $\alpha \to n$, thus recapturing the classical derivative with respect to x. As noted in Section 1, the Riesz fractional derivative incorporates both the left– and right–sided Riemann–Liouville fractional derivatives.

Definition 2.4. *For any $\alpha \in \mathbb{R}^+$, the Riesz fractional derivative of order α is defined as [14]*

$$ {}^{Riesz}D^{\alpha}_{x} f(x) := \frac{d^{\alpha} f(x)}{d|x|^{\alpha}} = -\frac{1}{2}\sec\left(\frac{\alpha\pi}{2}\right)\left[{}^{RL}_{0}D^{\alpha}_{x} f(x) + {}^{RL}_{x}D^{\alpha}_{\mathsf{L}} f(x)\right]. \tag{10} $$

The fractional operators defined above can be rewritten for multivariate functions. Additionally, from the Caputo derivatives, we have the following properties, which are important in the proposition of the numerical scheme

$$ {}^{C}_{0}D^{\alpha}_{x} x^{j} = \begin{cases} 0 & j \in \mathbb{N}_0,\ j < \lceil\alpha\rceil, \\ \\ \frac{\Gamma(j+1)}{\Gamma(j+1-\alpha)} x^{j-\alpha}, & j \in \mathbb{N}_0,\ j \geq \lceil\alpha\rceil, \end{cases} \tag{11} $$

and

$$ {}^{C}_{x}D^{\alpha}_{\mathsf{L}} (x-\mathsf{L})^{j} = \begin{cases} 0 & j \in \mathbb{N}_0,\ j < \lceil\alpha\rceil, \\ \\ (-1)^{j} \frac{\Gamma(j+1)}{\Gamma(j+1-\alpha)} (\mathsf{L}-x)^{j-\alpha}, & j \in \mathbb{N}_0,\ j \geq \lceil\alpha\rceil. \end{cases} \tag{12} $$

2.5. The shifted Chebyshev polynomials

The Chebyshev polynomials $T_n(x) = \cos(n \arccos x), n = 0, 1, \ldots$ are eigenvalue solutions of the Sturm–Liouville eigenvalue problem [33]

$$ \left(\sqrt{1-x^2}\,T_n'(x)\right)' + \frac{n^2}{\sqrt{1-x^2}} T_n(x) = 0, \quad -1 \leq x \leq 1,\ n = 0, 1, \ldots. \tag{13} $$

If we consider a change in variable $x = 2\tilde{x}/\mathsf{L} - 1$, such that $x \in [-1, 1] \mapsto x \in [0, \mathsf{L}]$, then we have the shifted Chebyshev polynomials generated through recursive formula

$$ \tilde{T}_{\mathsf{L},n+1}(\tilde{x}) = 2\left(\frac{2\tilde{x}}{\mathsf{L}} - 1\right)\tilde{T}_{\mathsf{L},n}(\tilde{x}) - \tilde{T}_{\mathsf{L},n-1}(\tilde{x}), \quad 0 \leq \tilde{x} \leq \mathsf{L},\ n = 1, 2, \ldots, \tag{14} $$

where $\tilde{T}_{\mathsf{L},0}(\tilde{x}) = 1$ and $\tilde{T}_{\mathsf{L},1}(\tilde{x}) = 2\tilde{x}/\mathsf{L} - 1$. The shifted Chebyshev polynomials is given in series form as (tilde dropped for simplicity) [27, 33]

$$ T_{\mathsf{L},n}(x) = n \sum_{j=0}^{n} \frac{(-1)^{n-j}(n+j-1)!\,2^{2j}}{(n-j)!(2j)!\mathsf{L}^{j}} x^{j} \tag{15} $$

$$ = n \sum_{j=0}^{n} \frac{(n+j-1)!\,2^{2j}}{(n-j)!(2j)!\mathsf{L}^{j}} (x-\mathsf{L})^{j}. \tag{16} $$

These sets of polynomials satisfy the weighted $L^2_{w_{\mathsf{L}}}(0,\mathsf{L})$ – orthogonality condition

$$\int_0^{\mathsf{L}} T_{\mathsf{L},n}(x)T_{\mathsf{L},m}(x)w_{\mathsf{L}}(x)dx = \delta_{mn}h_n, \tag{17}$$

where $w_{\mathsf{L}}(x) = 1/\sqrt{\mathsf{L}x - x^2}$ is the weight function of the shifted polynomial, $h_n = c_n\pi/2$, such that $c_0 = 2, c_n = 1$ for $n \geq 1$. In approximating on the Chebyshev–Gauss–Lobatto quadrature, we define the Christoffel number as $\varpi_j = \pi/c_j N,\ 0 \leq j \leq N$, with $c_0 = c_N = 2$ and $c_j = 1$ for $j = 1, 2, \ldots, N-1$.

3. Shifted Chebyshev spectral approximation

In this section, we describe the left and right sided fractional differential matrices. In approximating the fractional derivatives of any function, we use the differentiation matrices. The left–sided fractional differentiation matrix is used whenever we approximate the temporal derivative. In general, we seek a solution in terms of the shifted Chebyshev polynomials:

$$u(\mathbf{x},t) \approx U(\mathbf{x},t) = \sum_{n_1=0}^{N_{\mathbf{x}}}\sum_{n_2=0}^{N_t} \hat{U}_{n_1,n_2}T_{\mathsf{L},n_1}(\mathbf{x})T_{\mathsf{T},n_2}(t), \quad \mathbf{x} \in [0,\mathsf{L}],\ t \in [0,\mathsf{T}], \tag{18}$$

where $\hat{U}_{n_1,n_2} : 0 \leq n_1 \leq N_{\mathbf{x}}, 0 \leq n_2 \leq N_t$ satisfies the orthogonality condition

$$\hat{U}_{n_1,n_2} = \frac{1}{h_{n_1}}\frac{1}{h_{n_2}}\int_0^{\mathsf{L}}\int_0^{\mathsf{T}} U(\mathbf{x},t)T_{\mathsf{L},n_1}(\mathbf{x})T_{\mathsf{T},n_2}(t)w_{\mathsf{L}}(\mathbf{x})w_{\mathsf{T}}(t)d\mathbf{x}dt, \tag{19}$$

and can be represented in discrete form as

$$\hat{U}_{n_1,n_2} = \frac{1}{h_{n_1}}\frac{1}{h_{n_2}}\sum_{j_1=0}^{N_{\mathbf{x}}}\sum_{j_2=0}^{N_t} \varpi_{j_1}\varpi_{j_2}U(\mathbf{x}_{j_1},t_{j_2})T_{\mathsf{L},n_1}(\mathbf{x}_{j_1})T_{\mathsf{T},n_2}(t_{j_2}). \tag{20}$$

Therefore, the approximate solution for $u(\mathbf{x},t)$ is

$$U(\mathbf{x},t) = \sum_{j_1=0}^{N_{\mathbf{x}}}\sum_{j_2=0}^{N_t}\left[\varpi_{j_1}\varpi_{j_2}\sum_{n_1=0}^{N_{\mathbf{x}}}\sum_{n_2=0}^{N_t}\frac{1}{h_{n_1}}\frac{1}{h_{n_2}}T_{\mathsf{L},n_1}(\mathbf{x}_{j_1})T_{\mathsf{L},n_1}(\mathbf{x}_{p_1})T_{\mathsf{T},n_2}(t_{j_2})T_{\mathsf{T},n_2}(t_{p_2})\right]U(\mathbf{x}_{j_1},t_{j_2})$$
$$p_1 = 0,1,\ldots,N_{\mathbf{x}},\ p_2 = 0,1,\ldots,N_t. \tag{21}$$

Equation (21) can be rewritten to approximate a function of three variables by simply expanding it in terms of shifted Chebyshev polynomials in three variables.

Theorem 3.1. *Consider a smooth function $u(\mathbf{x},t)$ approximated in terms of the truncated shifted Chebyshev polynomials. The left–sided fractional integration of $u(\mathbf{x},t)$ with respect to t is given by*

$$
\begin{aligned}
{}_0I_t^{\gamma}U(\mathbf{x},t) = \sum_{j_1=0}^{N_{\mathbf{x}}}\sum_{j_2=0}^{N_t}\Bigg[\varpi_{j_1}\varpi_{j_2}\sum_{n_1=0}^{N_{\mathbf{x}}}\sum_{n_2=0}^{N_t}\sum_{k=0}^{N_t}\frac{1}{h_{n_1}}\frac{1}{h_{n_2}}T_{\mathsf{L},n_1}(\mathbf{x}_{j_1})T_{\mathsf{L},n_1}(\mathbf{x}_{p_1})T_{\mathsf{T},n_2}(t_{j_2}) \\
{}^{left}I_{n_2,k}^{(\gamma)}T_{\mathsf{T},k}(t_{p_2})\Bigg]U(\mathbf{x}_{j_1},t_{j_2}),
\end{aligned}
\tag{22}
$$

where

$$
\begin{aligned}
{}^{left}I_{n_2,k}^{(\gamma)} = n_2\sum_{j_2=0}^{n_2}\frac{(-1)^{n_2-j_2}(n_2+j_2-1)!2^{2j_2}\mathsf{T}^{\gamma}}{(n_2-j_2)!(2j_2)!}\frac{\Gamma(j_2+1)}{\Gamma(j_2+\gamma+1)} \\
\frac{2k}{\sqrt{\pi}c_k}\sum_{r=0}^{k}\frac{(-1)^{k-r}(k+r-1)!2^{2r}\Gamma(j_2+r+\gamma+1/2)}{(k-r)!(2r)!\Gamma(j_2+\gamma+r+1)}.
\end{aligned}
\tag{23}
$$

Proof. The derivation of ${}^{left}I_{n_2,k}^{(\gamma)}$ can be found in Oloniiju et al. [8]. □

We define the approximation of the left–sided integration of $u(\mathbf{x},t)$ as

$$
{}_0I_t^{\gamma}U(\mathbf{x},t) = \sum_{j_1=0}^{N_{\mathbf{x}}}\sum_{j_2=0}^{N_t}{}^{left}\mathbf{\Gamma}_{j2,p2}^{\gamma}U(\mathbf{x}_{j_1},t_{j_2}),\quad p_2=0,\ldots,N_t,
\tag{24}
$$

and the entries of the left–sided fractional integration matrix are defined as

$$
\begin{aligned}
{}^{left}\mathbf{\Gamma}_{j2,p2}^{\gamma} = \varpi_{j_1}\varpi_{j_2}\sum_{n_1=0}^{N_{\mathbf{x}}}\sum_{n_2=0}^{N_t}\sum_{k=0}^{N_t}\frac{1}{h_{n_1}}\frac{1}{h_{n_2}}T_{\mathsf{L},n_1}(\mathbf{x}_{j_1})T_{\mathsf{L},n_1}(\mathbf{x}_{p_1})T_{\mathsf{T},n_2}(t_{j_2})^{left}I_{n_2,k}^{(\gamma)}T_{\mathsf{T},k}(t_{p_2}) \\
p_1,j_1=0,1,\ldots N_{\mathbf{x}},\ p_2,j_2=0,1,\ldots,N_t.
\end{aligned}
\tag{25}
$$

Theorem 3.2. *The left–sided fractional derivative of $u(\mathbf{x},t)$ with respect to x, where $u(\mathbf{x},t)$ is a continuously bounded and integrable function is given as*

$$
\begin{aligned}
{}_0^CD_{\mathbf{x}}^{\alpha}U(\mathbf{x},t) = \sum_{j_1=0}^{N_{\mathbf{x}}}\sum_{j_2=0}^{N_t}\Bigg[\varpi_{j_1}\varpi_{j_2}\sum_{n_1=0}^{N_{\mathbf{x}}}\sum_{n_2=0}^{N_t}\sum_{k=0}^{N_{\mathbf{x}}}\frac{1}{h_{n_1}}\frac{1}{h_{n_2}}T_{\mathsf{L},n_1}(\mathbf{x}_{j_1})T_{\mathsf{T},n_2}(t_{j_2})T_{\mathsf{T},n_2}(t_{p_2}) \\
{}^{left}D_{n_1,k}^{(\alpha)}T_{\mathsf{L},k}(\mathbf{x}_{p_1})\Bigg]U(\mathbf{x}_{j_1},t_{j_2}),
\end{aligned}
\tag{26}
$$

where

$$
{}^{left}D_{n_1,k}^{(\alpha)} = n_1\sum_{j_1=0}^{n_1}\frac{(-1)^{n_1-j_1}(n_1+j_1-1)!2^{2j_1}}{(n_1-j_1)!(2j_1)!\mathsf{L}^{j_1}}\frac{\Gamma(j_1+1)}{\Gamma(j_1-\alpha+1)}q_{j_1,k},
\tag{27}
$$

and

$$q_{j_1,k} = \begin{cases} 0 & j_1 = 0, 1, \dots \lceil \alpha \rceil - 1, \\ \frac{k\sqrt{\pi}}{h_k} \sum_{r=0}^{k} \frac{(-1)^{k-r}(k+r-1)!2^{2r}}{(k-r)!(2r)!} \mathsf{L}^{j_1-\alpha} \frac{\Gamma(j_1-\alpha+r+1/2)}{\Gamma(j_1-\alpha+r+1)}, & j_1 = \lceil \alpha \rceil, \lceil \alpha \rceil + 1, \dots, N, \\ & k = 0, 1, \dots, N. \end{cases} \tag{28}$$

Proof. See [8, 27, 28] for the derivation of $q_{j_1,k}$ and ${}^{left}D^{(\alpha)}_{n_1,k}$. □

The left–sided derivative of $u(\mathbf{x}, t)$ with respect to $\mathbf{x}$, approximated on the shifted Chebyshev–Gauss–Lobatto quadrature, is defined as

$${}^{C}_{0}D^{\alpha}_{\mathbf{x}} U(\mathbf{x}, t) = \sum_{j_1=0}^{N_{\mathbf{x}}} \sum_{j_2=0}^{N_t} {}^{left}\mathbf{D}^{\alpha}_{j_1,p_1} U(\mathbf{x}_{j_1}, t_{j2}), \quad p_1 = 0, \dots, N_{\mathbf{x}}, \tag{29}$$

such that the entries of the left–sided fractional differential matrix with respect to the variable $\mathbf{x}$ are given as

$${}^{left}\mathbf{D}^{\alpha}_{j_1,p_1} = \varpi_{j_1} \varpi_{j_2} \sum_{n_1=0}^{N_{\mathbf{x}}} \sum_{n_2=0}^{N_t} \sum_{k=0}^{N_{\mathbf{x}}} \frac{1}{h_{n_1}} \frac{1}{h_{n_2}} T_{\mathsf{L},n_1}(\mathbf{x}_{j_1}) T_{\mathsf{T},n_2}(t_{j_2}) T_{\mathsf{T},n_2}(t_{p_2}) {}^{left}D^{(\alpha)}_{n_1,k} T_{\mathsf{L},k}(\mathbf{x}_{p_1}). \tag{30}$$

Theorem 3.3. *Let $T_{\mathsf{L},n}(x)$ be a shifted Chebyshev polynomial of order n, then any arbitrary order derivative based on the right–sided Caputo's operator is defined as*

$${}^{C}_{x}D^{\alpha}_{\mathsf{L}} T_{\mathsf{L},n}(x) = \sum_{k=0}^{N} {}^{right}D^{(\alpha)}_{n,k} T_{\mathsf{L},k}(x), \tag{31}$$

where

$${}^{right}D^{(\alpha)}_{n,k} = n \sum_{j=0}^{n} \frac{(-1)^j (n+j-1)! 2^{2j}}{(n-j)!(2j)! \mathsf{L}^{\alpha}} \frac{\Gamma(j+1)}{\Gamma(j-\alpha+1)} \frac{2k}{\pi c_k} \sum_{r=0}^{k} \frac{(-1)^r (k+r-1)! 2^{2r}}{(k-r)!(2r)!} \frac{\sqrt{\pi}\Gamma(j-\alpha+r+1/2)}{\Gamma(j-\alpha+r+1)}. \tag{32}$$

Proof. Consider the series form of the shifted Chebyshev polynomials $T_{\mathsf{L},n}(x)$ of order n, given in Equation (16). By taking the right–sided Caputo derivative, we have

$$
\begin{aligned}
{}_{x}^{C}D_{\mathsf{L}}^{\alpha}T_{\mathsf{L},n}(x) &= n\sum_{j=0}^{n}\frac{(n+j-1)!2^{2j}}{(n-j)!(2j)!\mathsf{L}^{j}}{}_{x}^{C}D_{\mathsf{L}}^{\alpha}(x-\mathsf{L})^{j} && (33)\\
&= n\sum_{j=\lceil\alpha\rceil}^{n}\frac{(n+j-1)!2^{2j}}{(n-j)!(2j)!\mathsf{L}^{j}}\frac{\Gamma(j+1)}{\Gamma(j-\alpha+1)}(\mathsf{L}-x)^{j-\alpha}, \quad n=\lceil\alpha\rceil,\lceil\alpha\rceil+1,\ldots. && (34)
\end{aligned}
$$

where $(\mathsf{L}-x)^{j-\alpha}$ can be expressed in terms of the truncated shifted Chebyshev polynomials as

$$
(\mathsf{L}-x)^{j-\alpha}=\sum_{k=0}^{N}\phi_{j,k}T_{\mathsf{L},k}(x), \tag{35}
$$

and $\phi_{j,k}$ satisfies the orthogonality condition of the shifted Chebyshev polynomials. This is given as

$$
\begin{aligned}
\phi_{j,k} &= \frac{2}{\pi c_k}\int_{0}^{\mathsf{L}}(\mathsf{L}-x)^{j-\alpha}T_{\mathsf{L},k}(x)w_{\mathsf{L}}(x)dx && (36)\\
&= \frac{2k}{\pi c_k}\sum_{r=0}^{k}\frac{(k+r-1)!2^{2r}}{(k-r)!(2r)!\mathsf{L}^{r}}\int_{0}^{\mathsf{L}}\frac{(\mathsf{L}-x)^{j-\alpha}}{\sqrt{\mathsf{L}x-x^{2}}}(x-\mathsf{L})^{r}dx. && (37)
\end{aligned}
$$

After evaluating the integral in Equation (37) above, we have

$$
\phi_{j,k}=\frac{2k}{\pi c_k}\sum_{r=0}^{k}\frac{(k+r-1)!2^{2r}}{(k-r)!(2r)!\mathsf{L}^{r}}\frac{\mathsf{L}^{j-\alpha+r}\sqrt{\pi}\Gamma(j-\alpha+r+1/2)}{\Gamma(j-\alpha+r+1)}. \tag{38}
$$

Therefore,

$$
(\mathsf{L}-x)^{j-\alpha}=\sum_{k=0}^{N}\frac{2k}{\pi c_k}\sum_{r=0}^{k}\frac{(k+r-1)!2^{2r}}{(k-r)!(2r)!}\frac{\mathsf{L}^{j-\alpha}\sqrt{\pi}\Gamma(j-\alpha+r+1/2)}{\Gamma(j-\alpha+r+1)}T_{\mathsf{L},k}(x). \tag{39}
$$

Substituting Equation (39) in Equation (34) completes the proof. □

Theorem 3.4. *Assume that $u(\mathbf{x},t)$ is a continuously bounded and smooth function, approximated in terms of the truncated shifted Chebyshev polynomials, and integrated over the Gauss–Lobatto quadrature, then its right–sided derivative of arbitrary order in the Caputo sense is approximated as*

$$
{}_{\mathbf{x}}^{C}D_{\mathsf{L}}^{\alpha}U(\mathbf{x},t)=\sum_{j_1=0}^{N_{\mathbf{x}}}\sum_{j_2=0}^{N_t}{}^{right}\mathbf{D}_{j_1,p_1}^{\alpha}U(\mathbf{x}_{j_1},t_{j_2}), \quad p_1=0,\ldots,N_{\mathbf{x}} \tag{40}
$$

where

$$ {}^{right}\mathbf{D}^{\alpha}_{j_1,p_1} = \varpi_{j_1}\varpi_{j_2}\sum_{n_1=0}^{N_{\mathbf{x}}}\sum_{n_2=0}^{N_t}\sum_{k=0}^{N_{\mathbf{x}}}\frac{1}{h_{n_1}}\frac{1}{h_{n_2}}T_{\mathsf{L},n_1}(\mathbf{x}_{j_1})T_{\mathsf{T},n_2}(t_{j_2})T_{\mathsf{T},n_2}(t_{p_2})^{right}D^{(\alpha)}_{n_1,k}T_{\mathsf{L},k}(\mathbf{x}_{p_1}). \tag{41} $$

Proof. Using the result of Theorem 3.3 and Equation (21), the theorem is proven. □

Remark 3.5. *Each approximation leads to a system of algebraic equations that are approximated at the shifted Chebyshev–Gauss–Lobatto nodes. The approximations here are presented for functions of two variables, this analysis can easily be extended to trivariate functions.*

Using the results in this section, we can easily obtain the discretization for the two–sided space–time fractional differential Equation (1) in both the $(1+1)$ and $(2+1)$ dimensions.

4. Convergence analysis

This section discusses the general convergence of the numerical scheme for two–sided fractional differential equation. We demonstrate the convergence in the weighted $L^2_{w_{\mathsf{T}}}(\Omega_t; L^2_{w_{\mathsf{L}}}(\Omega_{\mathbf{x}}))$ norm, where $\Omega_t = [0,\mathsf{T}]$ and $\Omega_{\mathbf{x}} = [0,\mathsf{L}]$. We restrict the discussion to the general two–sided fractional partial differential equation (1). It is however important to establish certain results first.

Definition 4.1. *We define $H^p_{w_{\mathsf{L}}}(\Omega_{\mathbf{x}}), p \geq 0$, the weighted Sobolev space of a function $u(\mathbf{x})$ [34]*

$$ H^p_{w_{\mathsf{L}}}(\Omega_{\mathbf{x}}) = \left\{ u \in L^2_{w_{\mathsf{L}}}(\Omega_{\mathbf{x}}) : \frac{\partial^i u(\mathbf{x})}{\partial \mathbf{x}^i} \in L^2_{w_{\mathsf{L}}}(\Omega_{\mathbf{x}}), 0 \leq i \leq p \right\}, \tag{42} $$

such that the semi–norm and norm associated with the space are, respectively,

$$ |u|_{H^p_{w_{\mathsf{L}}}}(\Omega_{\mathbf{x}}) = \left(\left\| \frac{\partial^p u}{\partial \mathbf{x}^p} \right\|^2_{L^2_{w_{\mathsf{L}}}(\Omega_{\mathbf{x}})} \right)^{1/2}, \ \|u\|_{H^p_{w_{\mathsf{L}}}}(\Omega_{\mathbf{x}}) = \left(\sum_{i=0}^{p} \left\| \frac{\partial^i u}{\partial \mathbf{x}^i} \right\|^2_{L^2_{w_{\mathsf{L}}}(\Omega_{\mathbf{x}})} \right)^{1/2}. \tag{43} $$

Definition 4.2. *We define the weighted norm [34, 35]*

$$ \|u\|_{L^2_w(\Omega)} = \left(\int_0^{\mathsf{T}} \int_0^{\mathsf{L}} |u(\mathbf{x},t)|^2 \, w_{\mathsf{L}}(\mathbf{x}) w_{\mathsf{T}}(t) d\mathbf{x} dt \right)^{1/2}, \tag{44} $$

where $L^2_w(\Omega) = L^2_{w_{\mathsf{T}}}(\Omega_t; L^2_{w_{\mathsf{L}}}(\Omega_{\mathbf{x}}))$. We define the weighted Hilbert space

$$ H^{p,q}_w(\Omega) = H^q_{w_{\mathsf{T}}}(\Omega_t; H^p_{w_{\mathsf{L}}}(\Omega_{\mathbf{x}})) = \left\{ u(\mathbf{x},t) \in L^2_w(\Omega) : \frac{\partial^{i+j} u}{\partial \mathbf{x}^i \partial t^j} \in L^2_w(\Omega), i \in [0,p], j \in [0,q] \right\}. \tag{45} $$

The associated norm is defined as

$$\|u\|_{H_w^{p,q}(\Omega)} = \left(\sum_{i=0}^{p} \sum_{j=0}^{q} \left\| \frac{\partial^{i+j} u}{\partial \mathbf{x}^i \partial t^j} \right\|_{L_w^2(\Omega)}^2 \right)^{1/2}. \tag{46}$$

Lemma 4.3. *Let $T_{N_\mathbf{x},N_t} u(\mathbf{x},t)$ be the orthogonal projection of $u(\mathbf{x},t)$ onto $T_{N_\mathbf{x},N_t}$ and assume that the Gauss–Lobatto points relative to the shifted Chebyshev weights are used for integration. Then, for all $p, q \geq 0$, the truncation error estimate holds [29, 34]*

$$\|u(\mathbf{x},t) - T_{N_\mathbf{x},N_t} u(\mathbf{x},t)\|_{L_w^2(\Omega)} \leq C_1 N_\mathbf{x}^{-p} \|u\|_{H_w^{p,0}(\Omega)} + C_2 N_t^{-q} \|u\|_{H_w^{0,q}(\Omega)}. \tag{47}$$

Here, the C's are independent of $N_\mathbf{x}$ and N_t and are positive constants.

Theorem 4.4. *Consider the 1–d case of Equation (1). Assume that $u(x,t)$ is the exact solution of Equation (1) and $T_{N_x,N_t} u(x,t) = U(x,t)$ is the solution obtained through approximation in terms of the shifted Chebyshev polynomials. Then, for sufficiently large N_x, N_t,*

$$\|u(x,t) - U(x,t)\|_{L_w^2(\Omega)} \to 0, \tag{48}$$

provided $c_+(x), c_-(x), s(x,t)$ from Equation (1) are smooth functions.

Proof. Consider the one–dimensional case of Equation (1). By direct integration, the exact solution is given by

$$u(x,t) = c_+(x) {}_0I_t^\gamma {}_0^C D_x^\alpha u(x,t) + c_-(x) {}_0I_t^\gamma {}_x^C D_\mathsf{L}^\alpha u(x,t) + {}_0I_t^\gamma s(x,t), \tag{49}$$

and we define the general approximation using the N_x–truncated Chebyshev expansion in x and N_t–truncated Chebyshev expansion in t as

$$U(x,t) = T_{N_x,N_t} C_+(x) {}_0I_t^\gamma {}_0^C D_x^\alpha U(x,t) + T_{N_x,N_t} C_-(x) {}_0I_t^\gamma {}_x^C D_\mathsf{L}^\alpha U(x,t) + T_{N_x,N_t 0} I_t^\gamma S(x,t). \tag{50}$$

If we define $E(x,t) = u(x,t) - U(x,t)$ and subtract Equation (50) from (49), we have

$$\begin{aligned} u(x,t) - U(x,t) &= c_+(x) {}_0I_t^\gamma {}_0^C D_x^\alpha u(x,t) - T_{N_x,N_t} C_+(x) {}_0I_t^\gamma {}_0^C D_x^\alpha U(x,t) \\ &\quad + c_-(x) {}_0I_t^\gamma {}_x^C D_\mathsf{L}^\alpha u(x,t) - T_{N_x,N_t} C_-(x) {}_0I_t^\gamma {}_x^C D_\mathsf{L}^\alpha U(x,t) \\ &\quad + {}_0I_t^\gamma s(x,t) - T_{N_x,N_t 0} I_t^\gamma S(x,t) \qquad (51) \\ &= c_+(x) {}_0I_t^\gamma {}_0^C D_x^\alpha u(x,t) - T_{N_x,N_t} c_+(x) {}_0I_t^\gamma {}_0^C D_x^\alpha u(x,t) \\ &\quad + c_-(x) {}_0I_t^\gamma {}_x^C D_\mathsf{L}^\alpha u(x,t) - T_{N_x,N_t} c_-(x) {}_0I_t^\gamma {}_x^C D_\mathsf{L}^\alpha u(x,t) \\ &\quad + {}_0I_t^\gamma s(x,t) - T_{N_x,N_t 0} I_t^\gamma s(x,t) + R(x,t), \qquad (52) \end{aligned}$$

where $R(x,t)$ is the residual. Taking the weighted norm of Equation (52), we have

$$\begin{aligned}\|u(x,t)-U(x,t)r\|_{L^2_w(\Omega)} &\leq \|c_+(x){}_0I_t^{\gamma}\,{}_0^C D_x^{\alpha}u(x,t) - T_{N_x,N_t}c_+(x){}_0I_t^{\gamma}\,{}_0^C D_x^{\alpha}u(x,t)\|_{L^2_w(\Omega)} \\ &\quad + \|c_-(x){}_0I_t^{\gamma}\,{}_x^C D_{\mathsf{L}}^{\alpha}u(x,t) - T_{N_x,N_t}c_-(x){}_0I_t^{\gamma}\,{}_x^C D_{\mathsf{L}}^{\alpha}u(x,t)\|_{L^2_w(\Omega)} \\ &\quad + \|{}_0I_t^{\gamma}s(x,t) - T_{N_x,N_t}{}_0I_t^{\gamma}s(x,t)\|_{L^2_w(\Omega)} + \|R(x,t)\|_{L^2_w(\Omega)} \quad (53)\\ &\leq C_l\left(N_x^{2\alpha-p}\|u\|_{H_w^{p,0}(\Omega)} + N_t^{-q}\|u\|_{H_w^{0,q}(\Omega)}\right) \\ &\quad + C_r\left(N_x^{2\alpha-p}\|u\|_{H_w^{p,0}(\Omega)} + N_t^{-q}\|u\|_{H_w^{0,q}(\Omega)}\right) \\ &\quad + C\left(N_x^{-p}\|s\|_{H_w^{p,0}(\Omega)} + N_t^{-q}\|s\|_{H_w^{0,q}(\Omega)}\right) \\ &\quad + C_2\left(N_x^{-p}\|u\|_{H_w^{p,0}(\Omega)} + N_t^{-q}\|u\|_{H_w^{0,q}(\Omega)}\right) \quad (54)\\ &\leq C_l\left(N_x^{2\alpha-p}\|u\|_{H_w^{p,0}(\Omega)} + N_t^{-q}\|u\|_{H_w^{0,q}(\Omega)}\right) \\ &\quad + C_r\left(N_x^{2\alpha-p}\|u\|_{H_w^{p,0}(\Omega)} + N_t^{-q}\|u\|_{H_w^{0,q}(\Omega)}\right) \\ &\quad + C\left(N_x^{-p}\|s\|_{H_w^{p,0}(\Omega)} + N_t^{-q}\|s\|_{H_w^{0,q}(\Omega)}\right) \quad (55)\end{aligned}$$

Each term in Equation (55), given that $0 \leq \alpha \leq p$, tends to zero for sufficiently large N_x and N_t, therefore, the proof is complete. □

The convergence of the numerical solution $U(x,t)$ to the exact solution $u(x,t)$ is dependent on the number of times that $u(x,t)$ is continuously differentiable with respect to x and t.

5. Numerical Examples

Having demonstrated the convergence of the numerical scheme in the previous section, we now present some numerical examples to test the numerical scheme. In this section, we solve selected one– and two–dimensional two–sided fractional differential equations to demonstrate the performance, accuracy and efficiency of the proposed numerical method.

Example 5.1. *We consider a one–dimensional two–sided space fractional partial differential equation (FPDE) [15]*

$$\frac{\partial u}{\partial t} = c_+\,{}_0^C D_x^{1.8}u + c_-\,{}_x^C D_2^{1.8}u + s(x,t) \quad (56)$$

on a finite domain $\Omega_x = 0 < x < 2$ and $t > 0$, with the coefficient functions defined as

$$c_+(x) = \Gamma(1.2)x^{1.8}, \qquad c_-(x) = \Gamma(1.2)(2-x)^{1.8}. \quad (57)$$

If we consider the forcing function

$$s(x,t) = 32e^{-t}\left[\frac{1}{8}x^2(2-x)^2 + x^2 + (2-x)^2 - 2.5(x^3+(2-x)^3) + \frac{25}{22}(x^4+(2-x)^4)\right], \quad (58)$$

the closed form of Equation (56) *is obtained as* $u(x,t) = 4e^{-t}x^2(2-x)^2$. *The initial condition is given as*

$$u(x,0) = 4x^2(2-x)^2, \tag{59}$$

and boundary condition as

$$u(x,t)|_{\partial\Omega_x} = 0. \tag{60}$$

In general, we seek a solution of the form in Equation (21). The left– and right–sided derivatives are approximated accordingly. Upon approximating the function and its derivatives using the proposed method, the expansions as well as the initial and boundary conditions result in a consistent system of algebraic equations evaluated on the shifted Chebyshev–Gauss–Lobatto points, and written in matrix form as

$$\mathbf{A}U = \mathbf{S}, \tag{61}$$

where $\mathbf{A}$ is a matrix of size $((N_x+1)(N_t+1)) \times ((N_x+1)(N_t+1))$ and $\mathbf{S}$ is a $((N_x+1)(N_t+1))$ column vector. Table 1 examines the performance of the proposed scheme in terms of the weighted error norm for Example 5.1. We compute the error norm at $t = 1.0$ and the error norm is compared with the maximum error observed in Meerschaert and Tadjeran [15]. As the order of the shifted polynomials in time/space is increased geometrically, there is an geometric reduction in the L_w^2 error norm, which is an attribute that is synonymous with spectral based methods, unlike the linear reduction in error reported in the finite difference scheme of Meerschaert and Tadjeran [15]. The convergence of the error of the proposed scheme also gives credence to the convergence error estimate presented in Theorem 4.4.

Example 5.2. *In this example, we consider a one–dimensional space–time FPDE of the form*

$${}_0^C D_t^\gamma u = c_+ \, {}_0^C D_x^\alpha u + c_- \, {}_x^C D_1^\alpha u + s(x,t), \; 0 < \gamma \leq 1, \; 1 < \alpha \leq 2 \tag{62}$$

on the domain $\Omega_x = 0 < x < 1$, $t > 0$ *and the variable coefficients given as*

$$c_+(x) = \frac{x^\alpha}{2}, \quad c_-(x) = \frac{(1-x)^\alpha}{2}, \tag{63}$$

and the source function defined as

$$\begin{aligned} s(x,t) = 2x^2(1-x)^2 \left[\frac{t^{2-\gamma}}{\Gamma(3-\gamma)} - \frac{t^{1-\gamma}}{\Gamma(2-\gamma)} \right] - (t-1)^2 \left[\frac{1}{\Gamma(3-\alpha)}(x^2 + (1-x)^2) \right. \\ \left. - \frac{6}{\Gamma(4-\alpha)}(x^3 + (1-x)^3) + \frac{12}{\Gamma(5-\alpha)}(x^4 + (1-x)^4) \right]. \end{aligned} \tag{64}$$

The exact solution is obtained as $u(x,t) = (t-1)^2x^2(1-x)^2$, *such that the initial condition is given by* $u(x,0) = x^2(1-x)^2$ *and the boundary condition as*

$$u(x,t)|_{\partial\Omega_x} = 0. \tag{65}$$

Again, we seek a solution of the form in Equation (21), and all derivatives are approximated as discussed in Section 3. In Table 2, we present the weighted error norm using approximations in terms of different orders of the shifted Chebyshev polynomials in the two variables (x, t) for different values of the fractional orders (γ, α) at $t = 1.0$. Again, we observe the geometric convergence of the error norms, as well as the accuracy of the method.

Example 5.3. *Consider the general two–dimensional two–sided space fractional partial differential equation of the form [36]*

$$\frac{\partial^2 u}{\partial t^2} = c_{+,1}\,{}_0^C D_x^{\alpha} u + c_{-,1}\,{}_x^C D_1^{\alpha} u + c_{+,2}\,{}_0^C D_y^{\beta} u + c_{-,2}\,{}_y^C D_1^{\beta} u + e u_x + f u_y + s(x, y, t), \quad 1 < \alpha, \beta \leq 2, \tag{66}$$

defined on $\Omega = \Omega_x \times \Omega_y = [0, 1] \times [0, 1]$, $t > 0$. *The variable coefficients are given as*

$$\begin{aligned} &c_{+,1}(x) = \Gamma(3-\alpha), x^{\alpha},\ c_{-,1}(x) = \Gamma(3-\alpha)(1-x)^{\alpha}, \\ &c_{+,2}(y) = \Gamma(3-\beta) y^{\beta},\ c_{-,2}(y) = \Gamma(3-\beta)(1-y)^{\beta}, \\ &e(x) = \frac{x}{2},\ f(y) = \frac{y}{2}, \end{aligned} \tag{67}$$

and the analytical solution is obtained as

$$u(x, y, t) = \sin(\pi t) x^2 (1-x)^2 y^2 (1-y)^2, \tag{68}$$

for which the forcing function can be obtained by simply substituting the exact solution and the coefficients into the Equation (66). *The initial conditions are given as*

$$u(x, y, 0) = 0, \quad u_t(x, y, 0) = \pi x^2 (1-x)^2 y^2 (1-y)^2, \tag{69}$$

and boundary condition as

$$u(x, y, t)|_{\partial\Omega} = 0. \tag{70}$$

We seek a solution as an expansion in terms of the shifted Chebyshev polynomials in three variables of the form

$$\begin{aligned} U(x, y, t) = \sum_{j_1=0}^{N_x} \sum_{j_2=0}^{N_y} \sum_{j_3=0}^{N_t} \Bigg[\varpi_{j_1} \varpi_{j_2} \varpi_{j_3} \sum_{n_1=0}^{N_x} \sum_{n_2=0}^{N_y} \sum_{n_3=0}^{N_t} \frac{1}{h_{n_1}} \frac{1}{h_{n_2}} \\ \frac{1}{h_{n_3}} T_{1,n_1}(x_{j_1}) T_{1,n_1}(x_{p_1}) T_{1,n_2}(y_{j_2}) T_{1,n_2}(y_{p_2}) T_{\mathsf{T},n_3}(t_{j_3}) T_{\mathsf{T},n_3}(t_{p_3}) \Bigg] U(x_{j_1}, y_{j_2}, t_{j_3}) \\ p_1 = 0, 1, \ldots, N_x,\ p_2 = 0, 1, \ldots, N_y,\ p_3 = 0, 1, \ldots, N_t, \end{aligned} \tag{71}$$

and the derivatives are approximated accordingly.

In Table 3, we present the weighted error norms and CPU times for different points in x, y, which demonstrate the accuracy and efficiency of the proposed numerical scheme. The error

norms and CPU time obtained are compared with average absolute errors and computational time obtained in Cheng et al. [36] through the improved moving least square approximation. While the Cheng et al. [36] approximation and the method proposed in this study perform well in terms of accuracy, as is evident from the order of the errors, the approximation in this study fare better in terms of computational time used, despite both approximations having been carried out on computers with similar processors and speed. From the table, the geometric convergence associated with spectral based methods is obvious as the orders of the shifted Chebyshev polynomials increase.

Table 1: Weighted error norm (L_w^2–error) for Example 5.1 compared with the maximum error norm in Meerschaert and Tadjeran [15].

	Current results			Meerschaert and Tadjeran [15]			
$N_x = N_t$	4	8	16	10	20	40	80
Error	0.8291	0.0342	2.5244×10^{-5}	0.1417	0.0571	0.0249	0.0113

Table 2: L_w^2 error norm for Example 5.2 for different values of the arbitrary orders of derivatives (γ, α).

		$N_x = N_t$		
γ	α	4	8	16
0.1	1.1	0.0331	0.0025	4.3034×10^{-6}
	1.5	0.0079	0.0010	2.4993×10^{-6}
	2	0.0079	1.4579×10^{-5}	2.3669×10^{-6}
0.5	1.1	0.0175	0.0019	5.9794×10^{-5}
	1.5	0.0078	0.0009	7.3358×10^{-6}
	2	0.0077	0.0002	1.2629×10^{-6}
1	1.1	0.0152	0.0014	1.4488×10^{-6}
	1.5	0.0083	0.0009	2.5627×10^{-7}
	2	0.0079	1.4015×10^{-8}	2.1101×10^{-12}

Table 3: L_w^2 error norm for Example 5.3 at $t = 0.5, \alpha = \beta = 1.5, N_t = 16$ compared with the average absolute errors obtained in Cheng et al. [36]

	Current results				Cheng et al. [36]			
$N_x \times N_y$	4×4	8×8	12×12	16×16	11×11	16×16	21×21	26×26
Error	0.0034	9.9636×10^{-5}	1.3783×10^{-6}	5.1381×10^{-7}	4.337×10^{-5}	2.345×10^{-5}	1.409×10^{-5}	8.78×10^{-6}
CPU time (secs)	0.053	0.370	1.900	6.835	26.25	15.45	8.08	3.46

Example 5.4. *Consider the general two–dimensional two–sided space–time differential*

equations of arbitrary order

$$ {}_0^C D_t^\gamma u = c_{+,1}\, {}_0^C D_x^\alpha u + c_{-,1}\, {}_x^C D_1^\alpha u + c_{+,2}\, {}_0^C D_y^\beta u + c_{-,2}\, {}_y^C D_1^\beta u + s(x,y,t), \tag{72} $$

$$ 0 < \gamma \leq 1,\ 1 < \alpha, \beta \leq 2, \tag{73} $$

whose exact solution is given as $u(x,y,t) = (t^3+1)x^2(1-x)^2y^2(1-y)^2$. *The differential equation satisfies the boundary condition*

$$ u(x,y,t)|_{\partial\Omega} = 0, \tag{74} $$

where $\Omega = \Omega_x \times \Omega_y = [0,1] \times [0,1]$, *and initial condition is given by*

$$ u(x,y,0) = x^2(1-x)^2y^2(1-y)^2. \tag{75} $$

The variable coefficients are defined as

$$ c_{+,1}(x) = x^\alpha,\ c_{-,1}(x) = (1-x)^\alpha,\ c_{+,2}(y) = y^\beta,\ c_{-,2}(y) = (1-y)^\beta \tag{76} $$

and the source term is defined to satisfy the differential equation.

Table 4: Weighted error norm for Example 5.4 at $t = 2, N_t = 12$ for different sizes of x, y grid points and fractional orders.

		$N_x \times N_y$		
γ	$\alpha = \beta$	4×4	8×8	16×16
0.5	1.5	0.0048	0.0009	1.7575×10^{-7}
	1.9	0.0048	8.5615×10^{-5}	8.2109×10^{-8}
0.9	1.5	0.0048	0.0004	1.3885×10^{-7}
	1.9	0.0047	8.4207×10^{-5}	2.0854×10^{-7}

We seek a solution of the form in Equation (71). Table 4 shows the weighted error norm between the approximation and exact solution at $t = 1$ for different values of the fractional orders $(\gamma, \alpha = \beta)$. It can be seen that the approximated solution is in agreement with the exact solution and the geometric convergence of the solution is also obvious. This result is consistent with the theoretical analysis of the convergence error norm.

6. Conclusion

In this study, we have presented a geometrically convergent numerical method in terms of the shifted Chebyshev polynomials for two–sided partial differential equations with arbitrary temporal and/or spatial orders. The fractional derivatives were defined in the Caputo sense and the approximations of fractional differentiations follow the Caputo fractional

operators. The approximations in terms of the shifted Chebyshev polynomials were evaluated at the Gauss–Lobatto quadrature. To demonstrate the applicability of the method, we solved several partial differential equations of arbitrary orders, which included one– and two–dimensional two–sided space fractional equations and one– and two–dimensional two–sided space time fractional partial differential equations. In addition to the accurate results obtained, the convergence of the scheme was shown to be geometrically convergent similar to other spectral based methods. The method is computationally efficient which is evident in the computational time.

References

[1] Z. Mao, J. Shen, Spectral element method with geometric mesh for two-sided fractional differential equations, Advances in Computational Mathematics 44 (2018) 745–771.

[2] M. Chen, W. Deng, A second-order numerical method for two-dimensional two-sided space fractional convection diffusion equation, Applied Mathematical Modelling 38 (2014) 3244–3259.

[3] H. Bulut, H. M. Baskonus, Y. Pandir, The modified trial equation method for fractional wave equation and time fractional generalized Burgers equation, Abstract and Applied Analysis (2013). Article ID 636802.

[4] N. H. Sweilam, M. M. Khader, A. Nagy, Numerical solution of two-sided space-fractional wave equation using finite difference method, Journal of Computational and Applied Mathematics 235 (2011) 2832–2841.

[5] F. Mainardi, Fractional calculus and waves in linear viscoelasticity: An introduction to mathematical models, World Scientific, 2010.

[6] N. Makris, G. Dargush, M. Constantinou, Dynamic analysis of generalized viscoelastic fluids, Journal of Engineering Mechanics 119 (1993) 1663–1679.

[7] H. Qi, M. Xu, Unsteady flow of viscoelastic fluid with fractional Maxwell model in a channel, Mechanics Research Communications 34 (2007) 210–212.

[8] S. D. Oloniiju, S. P. Goqo, P. Sibanda, A Chebyshev pseudo-spectral method for the multi-dimensional fractional Rayleigh problem for a generalized Maxwell fluid with Robin boundary conditions, Applied Numerical Mathematics 152 (2020) 253–266.

[9] Ł. Płociniczak, Analytical studies of a time-fractional porous medium equation. Derivation, approximation and applications, Communications in Nonlinear Science and Numerical Simulation 24 (2015) 169–183.

[10] F. del Teso, Finite difference method for a fractional porous medium equation, Calcolo 51 (2014) 615–638.

[11] D. A. Benson, M. M. Meerschaert, J. Revielle, Fractional calculus in hydrologic modeling: A numerical perspective, Advances in Water Resources 51 (2013) 479–497.

[12] I. Podlubny, Fractional differential equations: an introduction to fractional derivatives, fractional differential equations, to methods of their solution and some of their applications, volume 198, Elsevier, 1998.

[13] K. S. Miller, B. Ross, An introduction to the fractional calculus and fractional differential equations, Wiley-Interscience (1993).

[14] K. Oldham, J. Spanier, The fractional calculus theory and applications of differentiation and integration to arbitrary order, volume 111, Elsevier, 1974.

[15] M. M. Meerschaert, C. Tadjeran, Finite difference approximations for two-sided space-fractional partial differential equations, Applied Numerical Mathematics 56 (2006) 80–90.

[16] M. M. Meerschaert, C. Tadjeran, Finite difference approximations for fractional advection–dispersion flow equations, Journal of Computational and Applied Mathematics 172 (2004) 65–77.

[17] M. M. Meerschaert, H.-P. Scheffler, C. Tadjeran, Finite difference methods for two-dimensional fractional dispersion equation, Journal of Computational Physics 211 (2006) 249–261.
[18] C. Tadjeran, M. M. Meerschaert, H.-P. Scheffler, A second-order accurate numerical approximation for the fractional diffusion equation, Journal of Computational Physics 213 (2006) 205–213.
[19] C. Tadjeran, M. M. Meerschaert, A second-order accurate numerical method for the two-dimensional fractional diffusion equation, Journal of Computational Physics 220 (2007) 813–823.
[20] F. Liu, P. Zhuang, I. Turner, V. Anh, K. Burrage, A semi-alternating direction method for a 2-D fractional FitzHugh–Nagumo monodomain model on an approximate irregular domain, Journal of Computational Physics 293 (2015) 252–263.
[21] F. Liu, P. Zhuang, V. Anh, I. Turner, K. Burrage, Stability and convergence of the difference methods for the space–time fractional advection–diffusion equation, Applied Mathematics and Computation 191 (2007) 12–20.
[22] L. Feng, P. Zhuang, F. Liu, I. Turner, Stability and convergence of a new finite volume method for a two-sided space-fractional diffusion equation, Applied Mathematics and Computation 257 (2015) 52–65.
[23] S. Chen, F. Liu, X. Jiang, I. Turner, V. Anh, A fast semi-implicit difference method for a nonlinear two-sided space-fractional diffusion equation with variable diffusivity coefficients, Applied Mathematics and Computation 257 (2015) 591–601.
[24] A. Bhrawy, M. Zaky, Shifted fractional-order Jacobi orthogonal functions: application to a system of fractional differential equations, Applied Mathematical Modelling 40 (2016) 832–845.
[25] A. Bhrawy, M. Zaky, An improved collocation method for multi-dimensional space–time variable-order fractional Schrödinger equations, Applied Numerical Mathematics 111 (2017) 197–218.
[26] M. A. Zaky, An improved tau method for the multi-dimensional fractional Rayleigh–Stokes problem for a heated generalized second grade fluid, Computer & Mathematics with Application 75 (2018) 2243–2258.
[27] E. Doha, A. Bhrawy, S. Ezz-Eldien, Efficient Chebyshev spectral methods for solving multi-term fractional orders differential equations, Applied Mathematical Modelling 35 (2011) 5662–5672.
[28] S. Oloniiju, S. Goqo, P. Sibanda, A Chebyshev spectral method for heat and mass transfer in MHD nanofluid flow with space fractional constitutive model, Frontiers in Heat and Mass Transfer 13 (2019).
[29] A. Bhrawy, M. A. Zaky, R. A. Van Gorder, A space-time Legendre spectral tau method for the two-sided space-time Caputo fractional diffusion-wave equation, Numerical Algorithms 71 (2016) 151–180.
[30] Z. Mao, G. E. Karniadakis, A spectral method (of exponential convergence) for singular solutions of the diffusion equation with general two-sided fractional derivative, SIAM Journal on Numerical Analysis 56 (2018) 24–49.
[31] A. Bhrawy, M. Zaky, J. Tenreiro Machado, Efficient Legendre spectral tau algorithm for solving the two-sided space–time Caputo fractional advection–dispersion equation, Journal of Vibration and Control 22 (2016) 2053–2068.
[32] A. H. Bhrawy, M. A. Zaky, J. A. T. Machado, Numerical solution of the two-sided space–time fractional telegraph equation via Chebyshev tau approximation, Journal of Optimization Theory and Applications 174 (2017) 321–341.
[33] M. Abramowitz, I. A. Stegun, Handbook of mathematical functions: with formulas, graphs, and mathematical tables, volume 55, Courier Corporation, 1965.
[34] C. Canuto, M. Y. Hussaini, A. Quarteroni, T. A. Zang, Spectral methods: Fundametals in single domains, Springer, 2006.
[35] C. Canuto, M. Y. Hussaini, A. Quarteroni, A. Thomas Jr, et al., Spectral methods in fluid dynamics, Springer Science & Business Media, 2012.
[36] R. Cheng, F. Sun, J. Wang, Meshless analysis of two-dimensional two-sided space-fractional wave equation based on improved moving least-squares approximation, International Journal of Computer Mathematics 95 (2018) 540–560.

Chapter 7

A Chebyshev pseudo–spectral method for the numerical solutions of distributed order fractional ordinary differential equations

In Chapters 2 to 6, numerical solutions of fractional differential equations with fixed real orders were presented. In Chapters 7 and 8, we consider fractional differential equations with distributed orders. Unlike in fixed real order fractional differential equations, the orders of the derivatives are distributed over a range of real values. Distributed order fractional differential equations are robust in modelling physical processes. However, in solving this form of differential equations, additional computational cost is incurred. In most cases, as in fixed real order fractional differential equations, closed–form solutions cannot be obtained. This makes seeking numerical or approximate solutions essential.

In this chapter, we present a spectral method for finding the solutions of distributed order fractional ordinary differential equations. The solution process involves using a Newton–Cotes quadrature formula and a series expansion in terms of shifted Chebyshev polynomials of the first kind. The approximations are then integrated using the Gauss–Lobatto quadrature. Numerical examples are presented to illustrate the convergence and accuracy of the numerical method.

Applied Mathematics E-Notes, xx(20xx), xx-xx ©
Available free at mirror sites of http://www.math.nthu.edu.tw/∼amen/
ISSN 1607-2510

A Chebyshev pseudo–spectral method for the numerical solutions of distributed order fractional ordinary differential equations*

Shina D. Oloniiju, Sicelo P. Goqo, P. Sibanda †

Received 20 July 2000

Abstract

Distributed order differential equations offer new perspectives in the modelling of multi–scale physical problems. In distributed order fractional differential equations (DO–FDEs), the order of the derivatives is distributed over a range of real numbers. In this study, we present a numerical scheme for obtaining solutions of DO–FDEs. The method is a hybrid technique, comprising the composite trapezoidal rule and the Chebyshev pseudo spectral method. In the pseudo spectral method, the premise is that solutions of DO–FDEs may be written as a linear combination of shifted Chebyshev polynomials of the first kind, and integrated using Gauss–Lobatto quadrature. Numerical examples are presented to demonstrate the accuracy and convergence of the method. The accuracy is determined through comparison with exact solutions presented in earlier studies in the literature.

1 Introduction

Evidence of memory retention and anomalous behaviour abound in complex physical phenomena. Fractional differential and integral equations provide new possibilities for the rigorous modelling of such phenomena. The theory of fractional calculus has been extensively applied to physical problems such as those of viscoelasticity [1], diffusion [2] and growth models [3].

Fractional differential models are usually non–local and defined in terms of classical integrals, these make obtaining closed form solutions difficult. For this reason, numerous studies have been dedicated to developing accurate and effective numerical schemes for arbitrary order differential equations. Among these schemes are the finite difference method [4], finite volume method [5] and spectral methods [6, 7]. Recent studies have been geared towards exploring the global property of spectral methods to approximate the solutions of differential equations of arbitrary orders. The development of spectral methods such as the tau, Galerkin and collocation methods for fractional differential equations with single order has been relatively well treated in literature. For instance, [8] presented spectral tau method with Chebyshev polynomials for arbitrary order differential equations. [9] developed a spectral collocation method using the eigenvalue solution of the fractional Sturm–Liouville problem as basis functions. In the study by [10], a spectral Galerkin method was proposed for the time fractional diffusion equation.

In this study, we consider a distributed order fractional differential equation (DO–FDE) of the form

$$\int_{\alpha_l}^{\alpha_u} \rho(\alpha)\, {}_0^C D_x^{\alpha} y(x)\, d\alpha = f(x), \quad x > 0, \tag{1}$$

where $\alpha \in \mathbb{R}^+$ and $f(x)$ is a real valued function. The Caputo fractional derivative of $y(x)$, a sufficiently

*Mathematics Subject Classifications: 65D05

†School of Mathematics, Statistics and Computer Science, University of KwaZulu-Natal, Private Bag X01, Scottsville, Pietermaritzburg, 3209, South Africa.

smooth function is defined as [11]

$$ {}_0^C D_x^\alpha y(x) := \begin{cases} \frac{1}{\Gamma(n-\alpha)} \int_0^x \frac{y^n(\tilde{x})}{(x-\tilde{x})^{\alpha+1-n}} d\tilde{x}, & n-1 < \alpha < n,\ n \in \mathbb{N}, \\ \frac{d^n y(x)}{dx^n}, & \alpha = n \in \mathbb{N}, \end{cases} \tag{2} $$

where Γ is the Euler gamma function. From the properties of the Caputo fractional differential operator, it is easy to show that the fractional derivative of a power function is

$$ {}_0^C D_x^\alpha x^j = \begin{cases} 0 & j \in \mathbb{N}_0,\ j < \lceil \alpha \rceil, \\ \frac{\Gamma(j+1)}{\Gamma(j+1-\alpha)} x^{j-\alpha}, & j \in \mathbb{N}_0,\ j \geq \lceil \alpha \rceil. \end{cases} \tag{3} $$

This differential equation of arbitrary order offers new perspectives in the mathematical modelling of multi–scale systems. Unlike in the case of the conventional fractional differential equations where fractional orders are single with fixed real values, in DO–FDE, arbitrary differential orders are spread over a range of real values. Most published work on numerical methods for distributed order fractional differential equation are derived from difference schemes. Obtaining the numerical solutions of single order fractional differential equations can be computationally demanding, owing to the global property of differential operators. Additional computational cost can be incurred for the numerical integration of distributed order fractional differential equations, because differential orders are distributed over a set of real values. Among the few studies on the numerical solutions of DO–FDEs are studies by [13, 12, 14].

In this study, we present an accurate numerical scheme for differential equations (1). The method involves approximating the integral using Newton–Cotes formulas. The resulting linear multi–term fractional differential equation is then approximated in terms of the shifted Chebyshev polynomials of the first kind and Gauss–Lobatto quadrature. We present several examples to illustrate the use of the method and compare numerical solutions with the exact solutions where possible.

2 Method of solution

In this section, we present the method for solving the DO–FDE (1). The solution process is divided into two phases, the first involving approximating the integral as a finite sum using a quadrature rule. This transforms the DO–FDE into a multi–term fractional differential equation. We then approximate the numerical solution of the multi–term fractional differential equations in terms of the first kind shifted Chebyshev polynomials. We present the fractional differentiation matrix in terms of the shifted Chebyshev polynomials and use the Gauss–Lobatto quadrature. We remark here that the numerical method inherits all the properties (accuracy, stability and convergence) of both the quadrature rule and numerical integration method.

2.1 The first kind shifted Chebyshev polynomials

The class of polynomials $\{T_n(x) = \cos(n \cos^{-1} x), n = 0, 1, \ldots\}$ called Chebyshev polynomials of the first kind are eigenvalue solutions of the Sturm–Liouville problem [15]. Consider a mapping of the variable $x : [-1, 1] \mapsto [0, L]$ through the affine mapping $x = 2\tilde{x}/\mathsf{L} - 1$, then we have the recurrence relation of the shifted form of the first kind Chebyshev polynomials given as

$$ \tilde{T}_{\mathsf{L},n+1}(\tilde{x}) = 2\left(\frac{2\tilde{x}}{\mathsf{L}} - 1\right) \tilde{T}_{\mathsf{L},n}(\tilde{x}) - \tilde{T}_{\mathsf{L},n-1}(\tilde{x}), \quad 0 \leq \tilde{x} \leq \mathsf{L},\ n = 1, 2, \ldots, \tag{4} $$

where the zeroth and first order of the shifted polynomials are given respectively as $\tilde{T}_{\mathsf{L},0}(\tilde{x}) = 1$ and $\tilde{T}_{\mathsf{L},1}(\tilde{x}) = 2\tilde{x}/\mathsf{L} - 1$. In series form, Equation (4) is given as (tilde dropped for brevity) [15]

$$T_{\mathsf{L},n}(x) = n\sum_{j=0}^{n} \frac{(-1)^{n-j}(n+j-1)!2^{2j}}{(n-j)!(2j)!\mathsf{L}^j} x^j, \quad n = 0, 1, 2, \ldots, \tag{5}$$

which satisfy the orthogonality condition

$$\int_0^{\mathsf{L}} T_{\mathsf{L},n}(x) T_{\mathsf{L},m}(x) w_{\mathsf{L}}(x) dx = \delta_{mn} h_n, \tag{6}$$

where the weight function $w_{\mathsf{L}}(x) = 1/\sqrt{\mathsf{L}x - x^2}$, $h_n = c_n\pi/2$, $c_0 = 2, c_n = 1$ for $n \geq 1$. For approximations constructed on the Chebyshev–Gauss–Lobatto quadrature, we use the Christoffel number $\varpi_j = \pi/c_j N$, $0 \leq j \leq N$, with $c_0 = c_N = 2$ and $c_j = 1 \; \forall \; 1 \leq j \leq N-1$.

2.2 Quadrature rule

We approximate the integral in Equation (1) using the composite trapezoidal rule. If we express the integral as a finite sum using the composite trapezoidal rule with Q intervals, we have

$$\frac{\Delta\alpha}{2}\left[\rho_0 \, {}_0^C D_x^{\alpha_0} y(x) + 2\sum_{e=1}^{Q-1} \rho_e \, {}_0^C D_x^{\alpha_e} y(x) + \rho_Q \, {}_0^C D_x^{\alpha_Q} y(x)\right] + \mathcal{O}((\Delta\alpha)^2) = f(x), \tag{7}$$

where $[\rho_0, \rho_e, \rho_Q] \equiv [\rho(\alpha_0), \rho(\alpha_e), \rho(\alpha_Q)]$, $\Delta\alpha = (\alpha_u - \alpha_l)/Q$, with ${}_0^C D_x^{\alpha_0} \equiv {}_0^C D_x^{\alpha_l}$ and ${}_0^C D_x^{\alpha_Q} \equiv {}_0^C D_x^{\alpha_u}$, provided $y(x)$ is regular with respect to all $\alpha \in [\alpha_0, \alpha_Q]$.

The abscissas are evenly spaced points $\alpha_e = \alpha_l + e\Delta\alpha$, for $e = 0, 1, 2, \ldots, Q-1, Q$. The approximation of the integral is an essential part of the numerical integration of Equation (1). If $\alpha_l = 0$, then ${}_0^C D_x^{\alpha_l} y(x) \equiv y(x)$.

2.3 Approximation of $y(x)$ and its derivatives

Assume that $y(x)$ is a continuously differentiable function defined on the interval $[0, L]$, and approximate $y(x)$ as series expansion in terms of the shifted form of first kind Chebyshev polynomials as

$$y(x) \approx Y_N(x) = \sum_{n=0}^{N} Y_n T_{\mathsf{L},n}(x), \tag{8}$$

where the coefficients Y_n satisfy the orthogonality condition written in discrete form as

$$Y_n = \frac{1}{h_n}\sum_{j=0}^{N} Y(x_j) T_{\mathsf{L},n}(x_j)\varpi_j, \qquad n = 0, 1, \ldots, N. \tag{9}$$

Therefore, the approximation of $y(x)$ is given as

$$Y_N(x) = \sum_{j=0}^{N}\left[\varpi_j \frac{1}{h_n} T_{\mathsf{L},n}(x_j) T_{\mathsf{L},n}(x_k)\right] Y(x_j) = Y, \qquad k = 0, 1, \ldots, N. \tag{10}$$

Theorem 1 *The arbitrary derivative of a continuously differentiable function $y(x)$ is given as*

$${}_0^C D_x^{\alpha} y(x) \approx D^{\alpha} Y_N(x) = \sum_{j=0}^{N} D_{j,l}^{\alpha} Y(x_j) = D^{\alpha} Y, \tag{11}$$

where the entries $D^{\alpha}_{j,l}$ *are given as*

$$D^{\alpha}_{j,l} = \varpi_j \sum_{n=0}^{N}\sum_{k=0}^{N} \frac{1}{h_n} n \sum_{j=0}^{n} T_{\mathsf{L},n}(x_j) \frac{(-1)^{n-j}(n+j-1)!2^{2j}}{(n-j)!(2j)!} \frac{\Gamma(j+1)}{\Gamma(j-\alpha+1)} q_{j,k} T_{\mathsf{L},k}(x_l), \quad j,l = 0,1,\ldots,N, \tag{12}$$

and $q_{j,k}$ *is defined as*

$$q_{j,k} = \begin{cases} 0 & j = 0,1,\ldots \lceil\alpha\rceil - 1, \\ \frac{k\sqrt{\pi}}{h_k} \displaystyle\sum_{r=0}^{k} \frac{(-1)^{k-r}(k+r-1)!2^{2r}}{(k-r)!(2r)!} \frac{\Gamma(j-\alpha+r+1/2)}{\Gamma(j-\alpha+r+1)} \mathsf{L}^{j-\alpha}, & \substack{j=\lceil\alpha\rceil,\lceil\alpha\rceil+1,\ldots,N,\\ k=0,1,\ldots,N}. \end{cases} \tag{13}$$

The proof of this result can be found in [16].

Using this theorem, we can easily approximate the derivatives in Equation (7).

2.4 Numerical integration of Equation (1)

The numerical integration method is a combination of the quadrature rule described in Section 2.2 and the truncated Chebyshev polynomials approximation described in Section 2.3. Equation (1) is solved subject to initial conditions that are dependent on the values of α. If $\alpha_l = 0$ and $\alpha_u = 1$, the equation is solved subject to the condition $y(0) = y_0$, and when $\alpha_u = 2$, an additional condition is required. When the composite trapezoidal rule is used, the numerical integration of Equation (1) is given as

$$\frac{\Delta\alpha}{2}\left[\rho_0\, D^{\alpha_0} + 2\sum_{e=1}^{Q-1} \rho_e\, D^{\alpha_e} + \rho_Q\, D^{\alpha_Q}\right] Y = F. \tag{14}$$

where Y and F are defined using Equation (10) and evaluated on the Chebyshev–Gauss–Lobatto points $x_j = \mathsf{L}/2(1-\cos(\pi j/N))$, $0 \le j \le N$. If $\alpha_l = 0$ and $\alpha_u = 2$, Equation (14) can be written as a linear algebraic system

$$\frac{\Delta\alpha}{2}\sum_{j=2}^{N}\left[\left[\rho_0 D^{\alpha_0}_{j,l} + 2\sum_{e=1}^{Q-1} \rho_e D^{\alpha_e}_{j,l} + \rho_Q D^{\alpha_Q}_{j,l}\right] Y(x_j)\right] = F(x_j), \quad l = 0,1,2,\ldots,N, \tag{15}$$

which when combined with the initial condition $y(x_0) = y_0$, $y'(x_0) = y'_0$ respectively evaluated at the collocation points as

$$Y(x_0) = y_0, \qquad \sum_{j=0}^{N} D_{j,0} Y(x_j) = y'_0, \tag{16}$$

leads to a consistent system.

3 Convergence Analysis

In this section, we demonstrate the convergence of the numerical scheme. To do this, we introduce the $L^2([0,\mathsf{L}])$ norm defined as $\|\cdot\|_{L^2_w([0,\mathsf{L}])}$. We define the fractional Sobolev space $H^{\alpha}_w([0,\mathsf{L}])$, $\alpha \ge 0$ as

$$H^{\alpha}_w([0,\mathsf{L}]) = \{y \in L^2_w([0,\mathsf{L}]) \text{ s.t. } {}^{C}_{0}D^{\alpha}_x y(x) \in L^2_w([0,\mathsf{L}])\}, \tag{17}$$

endowed with the semi–norm

$$|y|_{l,\alpha} = \|{}_0^C D_x^\alpha y\|_{L_w^2([0,\mathsf{L}])}, \tag{18}$$

and the associated norm

$$\|y\|_{l,\alpha} = \left(\|y\|^2_{L_w^2([0,\mathsf{L}])} + |y|^2_{l,\alpha}\right)^{1/2}. \tag{19}$$

Lemma 2 *Let $y \in H_w^\alpha([0,\mathsf{L}])$, and $0 < r < \alpha$, then there exist a positive constant such that [17]*

$$\|y\|_{H_w^r([0,\mathsf{L}])} \leq C\|y\|_{H_w^\alpha([0,\mathsf{L}])}. \tag{20}$$

For the distributed order derivative, we have

$$\int_{\alpha_l}^{\alpha_u} \rho(\alpha)\, {}_0^C D_x^\alpha y(x)\, d\alpha = \frac{\Delta\alpha}{2}\left[\rho_0\, {}_0^C D_x^{\alpha_0} y(x) + 2\sum_{e=1}^{Q-1} \rho_e\, {}_0^C D_x^{\alpha_e} y(x) + \rho_Q\, {}_0^C D_x^{\alpha_Q} y(x)\right] + \mathcal{O}((\Delta\alpha)^2), \tag{21}$$

so we define the norm $\|y\|_{H_w^m}$ as

$$\|y\|_{H_w^m} = \left(\|y\|^2_{H_w^{\alpha_0}} + \sum_{e=1}^{Q-1}\|y\|^2_{H_w^{\alpha_e}} + \|y\|^2_{H_w^{\alpha_Q}}\right)^{1/2}. \tag{22}$$

Lemma 3 *Assume that T_N is the $L_w^2([0,\mathsf{L}])$ orthogonal projection onto the space of Chebyshev polynomials with degree up to $N+1$, and k and m are real numbers such that $0 \leq k \leq m$, then for positive constant C and for any function $y \in C([0,\mathsf{L}]) \cap H_w^m([0,\mathsf{L}])$, the following error estimates hold [18]*

$$\|y - T_N y\|_{H_w^k([0,\mathsf{L}])} \leq CN^{2k-m}\|y\|_{H_w^m([0,\mathsf{L}])} \tag{23}$$

$$\|y - T_N y\|_{L_w^2([0,\mathsf{L}])} \leq CN^{-m}\|y\|_{H_w^m([0,\mathsf{L}])}. \tag{24}$$

We now present the convergence analysis of the numerical scheme.

Theorem 4 *Assume that y and Y_N are solutions of Equations (7) and (14) respectively, satisfying $y \in C([0,\mathsf{L}]) \cap H_w^m([0,\mathsf{L}])$. Then, there exist a non–negative constant C independent of $\Delta\alpha$ and N such that*

$$\|y - Y_N\|_{L_w^2([0,\mathsf{L}])} \leq C_1\left(\sum_{e=0}^{Q} N^{2\alpha_e - m}\|y\|_{H_w^m} + (\Delta\alpha)^2\right) + C_2 N^{-m}\|y\|_{H_w^m}. \tag{25}$$

Proof. For the proof, define $\tilde{y} = T_N y$. Noting that $f = F$ and subtracting Equation (14) from Equation (7) gives the following error equation

$$y - Y_N = \frac{\Delta\alpha}{2}\rho_0 D^{\alpha_0}(y - \tilde{y}) + \Delta\alpha\sum_{e=1}^{Q-1}\rho_e D^{\alpha_e}(y - \tilde{y}) + \frac{\Delta\alpha}{2}\rho_Q D^{\alpha_Q}(y - \tilde{y}) + \mathcal{O}((\Delta\alpha)^2) + \epsilon, \tag{26}$$

where

$$\epsilon = \frac{\Delta\alpha}{2}\rho_0 D^{\alpha_0}(\tilde{y} - Y_N) + \Delta\alpha\sum_{e=1}^{Q-1}\rho_e D^{\alpha_e}(\tilde{y} - Y_N) + \frac{\Delta\alpha}{2}\rho_Q D^{\alpha_Q}(\tilde{y} - Y_N) \tag{27}$$

is the residual. To estimate $\|y - Y_N\|_{L^2_w([0,\mathrm{L}])}$, we have

$$\|y - Y_N\|_{L^2_w([0,\mathrm{L}])} \leq \left\| \frac{\Delta\alpha}{2}\rho_0 D^{\alpha_0}(y-\tilde{y}) \right\|_{L^2_w([0,\mathrm{L}])} + \left\| \Delta\alpha \sum_{e=1}^{Q-1} \rho_e D^{\alpha_e}(y-\tilde{y}) \right\|_{L^2_w([0,\mathrm{L}])}$$
$$+ \left\| \frac{\Delta\alpha}{2}\rho_Q D^{\alpha_Q}(y-\tilde{y}) \right\|_{L^2_w([0,\mathrm{L}])} + (\Delta\alpha)^2 + \|\epsilon\|_{L^2_w([0,\mathrm{L}])} \tag{28}$$
$$\leq C_1 \left(N^{2\alpha_0 - m}\|y\|_{H^m_w} + \sum_{e=1}^{Q-1} N^{2\alpha_e - m}\|y\|_{H^m_w} + N^{2\alpha_Q - m}\|y\|_{H^m_w} + (\Delta\alpha)^2 \right) + C_2 N^{-m}\|y\|_{H^m_w} \tag{29}$$
$$\leq C_1 \left(\sum_{e=0}^{Q} N^{2\alpha_e - m}\|y\|_{H^m_w} + (\Delta\alpha)^2 \right) + C_2 N^{-m}\|y\|_{H^m_w}, \tag{30}$$

where C_1 and C_2 are independent of N. ■

4 Numerical Examples

In this section, we demonstrate the efficiency and accuracy of the method on selected DO–FDEs. The numerical results, where possible, are compared with exact solutions. These examples are motivated by the range of applications of distributed order models studied in [19]. Numerical computations are performed using the *PYHTON* programming language on the *SPYDER IDE*.

Example 4.1 *Consider the DO–FDE defined on the domain* $[0, 0.99]$

$$\int_0^2 \frac{\Gamma(6-\alpha)}{120} {}_0^C D_x^\alpha y(x) d\alpha = \frac{x^5 - x^3}{\log x}, \tag{31}$$

with initial conditions $y(0) = y'(0) = 0$*, and whose unique solution is given as* $y(x) = x^5$ *[12, 14].*

We approximate Equation (31) using the numerical scheme described in Section 2 to obtain the following system of algebraic equations

$$\frac{1}{Q}\sum_{j=2}^{N}\left[\left[1 + 2\sum_{e=1}^{Q-1}\frac{\Gamma\left(6-2e/Q\right)}{120} D_{j,l}^{2e/Q} + \frac{1}{20}D_{j,l}^2\right] Y(x_j)\right] = F(x_j), \tag{32}$$

$$Y(x_0) = 0, \qquad \sum_{j=0}^{N} D_{j,0} Y(x_j) = 0, \qquad l = 0, 1, 2, \ldots, N, \tag{33}$$

where the function on the right hand is evaluated at the Chebyshev–Gauss–Lobatto points.

The solution was obtained numerically in [12] using a combination of a weighted quadrature formula and fractional Adams' method, and in [14] using the trapezoidal rule and an analogue equation method. Table 1 shows the convergence of the solution using the infinity error norm. The convergence is given in terms of the number of collocations points N and the number of intervals in the quadrature formula Q. It is expected that as both N and Q grow, the maximum error vanishes. In comparison with the absolute errors presented in [12] and [14], the maximum errors in this study are much smaller. Figure 1 depicts the logscale L–infinity and L^2 error norms for different values of N. The solution errors decay geometrically with an increase in the number of collocation points N.

Example 4.2 *Consider the DO–FDE*

$$\int_{0.2}^{1.5} \Gamma(3-\alpha)\,{}_0^C D_x^{\alpha} y(x)\,d\alpha = 2\frac{x^{1.8}-x^{0.5}}{\ln x}, \tag{34}$$

whose exact solution is given as $y(x) = x^2$ *in [14]. The equation is solved on the domain* $[0, 0.9]$ *with the initial condition* $y(0) = y'(0) = 0$.

Like Example 4.1, the approximation of Equation (34) leads to the linear algebraic system

$$\frac{13}{20Q}\sum_{j=2}^{N}\left[\left[\Gamma(2.8)D_{j,l}^{0,2} + 2\sum_{e=1}^{Q-1}\Gamma\left(3-\alpha_e\right)D_{j,l}^{\alpha_e} + \Gamma(1.5)D_{j,l}^{1,5}\right]Y(x_j)\right] = F(x_j), \tag{35}$$

$$Y(x_0) = 0, \qquad \sum_{j=0}^{N} D_{j,0}Y(x_j) = 0, \qquad l = 0, 1, 2, \ldots, N, \tag{36}$$

where $\alpha_e = 0.2 + 13e/10Q,\ e = 1, \ldots, Q-1$.

Numerical results were presented for this example using fractional Adams' method and analogue equation method by [12] and [14] respectively. In Table 2, we show the maximum absolute errors in the solution. One distinguishing feature of DO–FDE is the distributed order of the derivatives, and for this reason, we do not expect to obtain the same level of accuracy as in the case of fixed order FDEs. However, the results presented in Table 2 show that the numerical solution improves as the number of terms in the Chebyshev expansion and the number of intervals in the trapezoidal rule increase. In [12] and [14], 640 grid points were required to achieve the same level of accuracy in Table 2.

Table 1: Maximum absolute error norms for the approximation of Example 4.1 using different values of Q and N.

N	Q					
	2	4	8	16	32	64
2	0.99691	1.10720	1.14586	1.16029	1.16621	1.16884
4	0.03859	0.04828	0.05183	0.05312	0.05363	0.05384
6	0.00776	0.00189	0.00047	0.00012	3.14562×10^{-5}	9.41815×10^{-6}
8	0.00764	0.00187	0.00047	0.00012	2.97335×10^{-5}	7.94795×10^{-6}
10	0.00778	0.00189	0.00047	0.00012	2.98145×10^{-5}	7.82399×10^{-6}

Table 2: Absolute error norms in L^{∞} for the approximation of Example 4.2 using different values of Q and N.

N	Q					
	2	4	8	16	32	64
2	0.10225	0.10181	0.10171	0.10168	0.10168	0.10168
4	0.01058	0.00178	0.00110	0.00143	0.00152	0.00154
6	0.01493	0.00324	0.00047	0.00064	0.00072	0.00072
8	0.01618	0.00377	0.00073	0.00035	0.00039	0.00040
10	0.01642	0.00393	0.00084	0.00023	0.00025	0.00025

Example 4.3 *Consider the equation [14]*

$$\int_{0}^{2} \Gamma(4-\alpha)\sinh(\alpha)\,{}_0^C D_x^{\alpha} y(x)\,d\alpha = \frac{6x(x^2 - \cosh 2 - \sinh 2\ln x)}{(\ln x)^2 - 1}, \tag{37}$$

with the initial conditions $y(0) = y'(0) = 0$*, whose exact solution is given as* $y(x) = x^3$*. The equation is defined in the domain* $[0, 1]$*. The numerical solution was obtained in [14] using a hybrid composite trapezoidal rule and analogue equation method.*

The discretization of Equation (37) yields the system of linear algebraic equations

$$\frac{1}{Q}\sum_{j=2}^{N}\left[\left[2\sum_{e=1}^{Q-1}\Gamma\left(4-2e/Q\right)\sinh(2e/Q)D_{j,l}^{2e/Q}+\sinh(2)D_{j,l}^{2}\right]Y(x_j)\right]=F(x_j), \tag{38}$$

$$Y(x_0)=0, \qquad \sum_{j=0}^{N}D_{j,0}Y(x_j)=0, \qquad l=0,1,2,\ldots,N. \tag{39}$$

Table 3 shows the maximum absolute error in the solution for Equation (37). Again the rate of convergence is typical of spectral methods, although the solution is less accurate when compared with fractional differential equations with fixed or single real orders. Figure 2 shows the error $|y(x) - Y_N(x)|$ in the domain $x \in [0, 1]$ for $N = 15$ and $Q = 64$, while Figure 3 shows the convergence of the numerical solution in terms of L^∞ and L^2 errors with respect to N. Although, the exact solution may not be continuously differentiable in $[0, 1]$, the numerical approximation is accurate. We note that it is possible that the accuracy may deteriorate as N increases if the solution $y(x)$ is no longer in the space of smooth functions $C^N([0, 1])$.

Table 3: L^∞ error norms for the numerical approximation of Example 4.3 using different values of N and Q.

N	Q					
	2	4	8	16	32	64
2	0.99013	0.92874	0.91644	0.91374	0.91310	0.91294
4	0.22315	0.06628	0.01935	0.00717	0.00408	0.00331
6	0.20182	0.06035	0.01708	0.00572	0.00284	0.00212
8	0.19946	0.05899	0.01727	0.00774	0.00606	0.00579
10	0.19901	0.05864	0.01325	0.00300	0.00032	0.00045

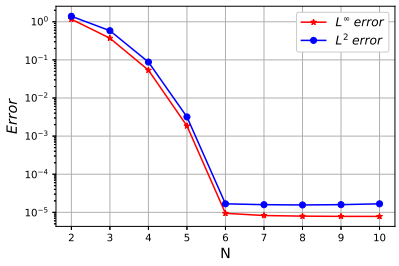

Figure 1: L^∞ and L^2 errors for Example 4.1 different values of N and $Q = 64$.

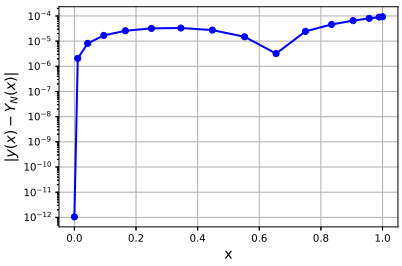

Figure 2: Error $|y(x) - Y_N(x)|$ for Example 4.3 using $N = 15, Q = 64$.

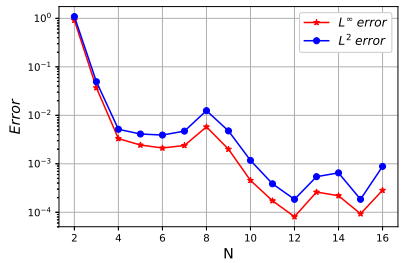

Figure 3: Convergence error norms for Example 4.3 in both L^∞ and L^2 norms for different number of terms in the Chebyshev expansion. $Q = 64$, $x \in [0, 1]$.

5 Conclusion

In this study, we presented a numerical method for solving a general distributed order fractional differential equation. The distributed order fractional differential equation was first approximated using a quadrature formula, which transform it to a multi–term fractional differential equation. The resulting multi–term fractional differential equation is then solved using a pseudo–spectral collocation method. The method of solution assumed that the solution of the distributed order fractional differential equation could be written as linear combination of the shifted first kind Chebyshev polynomials integrated using Gauss–Lobatto quadrature. We note that the scheme inherits the properties of the quadrature and numerical integration formulas. We demonstrated the accuracy and convergence of the method. The scheme has the advantage that it is easy to use and code. In future, the numerical scheme would be extended to higher dimensional distributed order fractional differential equations.

References

[1] F. Mainardi, Fractional calculus and waves in linear viscoelasticity: An introduction to mathematical models, World Scientific, 2010.

[2] R. Metzler, J. Klafter, The random walk's guide to anomalous diffusion: A fractional dynamics approach, Phys. Rep., 339(2000), 1–77.

[3] G. Jumarie, New stochastic fractional models for Malthusian growth, the Poissonian birth process and optimal management of populations, Math. Comput. Model., 44(2006), 231–254.

[4] N. H. Sweilam, M. M. Khader, A. Nagy, Numerical solution of two-sided space-fractional wave equation using finite difference method, J. Comput. Appl. Math., 235(2011), 2832–2841.

[5] L. Feng, P. Zhuang, F. Liu, I. Turner, Stability and convergence of a new finite volume method for a two-sided space-fractional diffusion equation, Appl. Math. Comput., 257(2015), 52–65.

[6] Z. Mao, J. Shen, Spectral element method with geometric mesh for two-sided fractional differential equations, Adv. Comput. Math., 44(2018), 745–771.

[7] A. Bhrawy, M. A. Zaky, R. A. Van Gorder, A space-time Legendre spectral tau method for the two–sided space–time Caputo fractional diffusion–wave equation, Numer. Algorithms, 71(2016), 151–180.

[8] E. H. Doha, A. Bhrawy, S. S. Ezz-Eldien, A Chebyshev spectral method based on operational matrix for initial and boundary value problems of fractional order, Comput. Math. Appl., 62(2011), 2364–2373.

[9] M. Zayernouri, G. E. Karniadakis, Fractional spectral collocation method, SIAM J. Sci. Comput., 36 (2014), A40–A62.

[10] X. Li, C. Xu, A space-time spectral method for the time fractional diffusion equation, SIAM J. Numer. Anal., 47(2009), 2108–2131.

[11] I. Podlubny, Fractional differential equations: an introduction to fractional derivatives, fractional differential equations, to methods of their solution and some of their applications, volume 198, Elsevier, 1998.

[12] K. Diethelm, N. J. Ford, Numerical analysis for distributed–order differential equations, J. Comput. Appl. Math., 225(2009), 96–104.

[13] G. Gao, Z. Sun, Two alternating direction implicit difference schemes with the extrapolation method for the two–dimensional distributed-order differential equations, Comput. Math. Appl., 69(2015), 926–948.

[14] J. T. Katsikadelis, Numerical solution of distributed order fractional differential equations, J. Comput. Phy., 259(2014), 11–22.

[15] M. Abramowitz, I. A. Stegun, Handbook of mathematical functions: with formulas, graphs, and mathematical tables, volume 55, Courier Corporation, 1965.

[16] S. Oloniiju, S. Goqo, P. Sibanda, A Chebyshev spectral method for heat and mass transfer in MHD nanofluid flow with space fractional constitutive model, Frontiers Heat Mass Transf., 13(2019).

[17] V. J. Ervin, J. P. Roop, Variational formulation for the stationary fractional advection dispersion equation, Numer. Methods Partial Diff. Eq., 22(2006), 558–576.

[18] C. Canuto, M. Y. Hussaini, A. Quarteroni, T. A. Zang, Spectral methods: Fundamentals in single domains, Springer Science & Business Media, 2007.

[19] T. Atanackovic, M. Budincevic, S. Pilipovic, On a fractional distributed–order oscillator, J. Phys. A, 38(2005), 6703.

Chapter 8

A pseudo–spectral method for time distributed two–sided space fractional partial differential equations

Building on the work of Chapter 6, where we presented numerical solutions of two–sided space fractional partial differential equations, and that of Chapter 7, where we introduced the concept of distributed order fractional differential equations, this chapter combines both concepts.

We present numerical solutions of two–sided space, time distributed order fractional differential equations. The time distributed differential operator is approximated using Simpson's quadrature formula. The resulting time multi–term, two–sided space differential equation is written as a truncated series expansion of shifted Chebyshev polynomials of the first kind in all variables. We present an analysis of the error norms, and use the numerical scheme to solve two–sided space, time distributed partial differential equations, including the fractional diffusion and advection–dispersion equations. Numerical results illustrate the accuracy and computational efficiency of the method.

A pseudo–spectral method for time distributed order two–sided space fractional differential equations

Shina D. Oloniiju*, Sicelo P. Goqo, Precious Sibanda

School of Mathematics, Statistics and Computer Science, University of KwaZulu-Natal, Private Bag X01, Scottsville, Pietermaritzburg, 3209, South Africa.

Abstract

Time distributed order two–sided space differential equations of arbitrary order offer a robust approach to modelling complex dynamical systems. In this study, we describe a scheme for obtaining the numerical solutions of time distributed order multidimensional two–sided space fractional differential equations. The numerical discretization scheme is a hybrid scheme, comprising a Newton–Cotes quadrature formula and a spectral collocation method. The time distributed order fractional differential operator is approximated using the composite Simpson's rule, and the solution of the resulting differential equation is expressed as a linear combination of shifted Chebyshev polynomials in all variables. Convergence analysis of the numerical scheme is presented. Some one– and two–dimensional time distributed order two–sided space fractional differential equations, such as the fractional advection–dispersion and diffusion equations, are presented to demonstrate the accuracy and computational efficiency of the numerical scheme, and numerical solutions are compared with the exact solutions, where these are available.

Keywords: Numerical method, Chebyshev–Gauss–Lobatto quadrature, two–sided space, time distributed order, fractional PDE

1. Introduction

In the past few decades, the number of studies on fractional calculus has grown tremendously owing to the vast amount of physical phenomena that can be modelled using fractional differential, integral and integrodifferential equations. Several mathematical models such as diffusion [3, 19, 20], viscoelasticity [2, 12, 15, 18], growth model [10] and flow in porous media [6] have been generalized to include fractional derivatives. Fractional models are, in general

*corresponding author

Email addresses: shina@aims.edu.gh (Shina D. Oloniiju), goqos@ukzn.ac.za (Sicelo P. Goqo), sibandap@ukzn.ac.za (Precious Sibanda)

non–local, which make them ideal for modelling multi–scale phenomena. Some physical systems are complex and cannot be modelled by a fixed order law, and so using multiple fixed orders leads to distributed order fractional models. Distributed order fractional models have been regarded as a robust tool for modelling sophisticated dynamical systems.

In this study, we consider a time distributed order two–sided space fractional differential equation of the form

$$\int_{\beta_l}^{\beta_u} \rho(\beta) {}_0^C D_t^\beta u(\mathbf{x},t) d\beta = {}_0^C D_{\mathbf{x}}^\alpha u(\mathbf{x},t) + {}_{\mathbf{x}}^C D_{\mathsf{L}}^\alpha u(\mathbf{x},t) + g(\mathbf{x},t), \tag{1}$$

with appropriate initial and boundary conditions on the finite spatial interval $[0, \mathsf{L}]$ and temporal domain $[0, \mathsf{T}]$, where $\alpha, \beta \in \mathbb{R}^+$. Here, ${}_0^C D_{\mathbf{x}}^\alpha$ and ${}_{\mathbf{x}}^C D_{\mathsf{L}}^\alpha$ respectively denote the left and right sided Caputo fractional differential operators defined as [15, 18]

$${}_0^C D_{\mathbf{x}}^\alpha u(\mathbf{x},t) = \frac{1}{\Gamma(n-\alpha)} \int_0^{\mathbf{x}} \frac{u^n(\tilde{\mathbf{x}},t)}{(\mathbf{x}-\tilde{\mathbf{x}})^{\alpha+1-n}} d\tilde{\mathbf{x}}, \quad \mathbf{x} > 0,\ n \in \mathbb{N}, \tag{2}$$

and

$${}_{\mathbf{x}}^C D_{\mathsf{L}}^\alpha u(\mathbf{x},t) = \frac{1}{\Gamma(n-\alpha)} \int_{\mathbf{x}}^{\mathsf{L}} \frac{u^n(\tilde{\mathbf{x}},t)}{(\tilde{\mathbf{x}}-\mathbf{x})^{\alpha+1-n}} d\tilde{\mathbf{x}}, \quad \mathbf{x} < \mathsf{L},\ n \in \mathbb{N}, \tag{3}$$

provided $u(\mathbf{x}, t)$ is a continuously differentiable function.

One of the many challenges in solving distributed order differential equations is the huge computational cost involved compared to fixed order fractional differential equations. Among the few studies that have been dedicated to obtaining numerical solutions of time distributed order fractional partial differential equations are [8, 11, 13, 14]. In [9], an implicit difference method was used to solve a one–dimensional differential equation of the form (1). A literature search reveals no studies where a pseudo–spectral method has been applied to time distributed order multidimensional two–sided space fractional differential equations.

This study presents a numerical scheme to approximate the solution of Equation (1) by approximating the integral using Simpson's rule. This leads to time multi–term fractional order two–sided space fractional differential equation which is approximated in terms of first kind shifted Chebyshev polynomials interpolated using Gauss–Lobatto quadrature. We illustrate the method using carefully chosen examples and compare the numerical results with exact solutions where available.

2. The numerical method

This section presents the numerical method of solution for Equation (1). The section is divided into several subsections which describe the the quadrature rule and the numerical

discretization method used in approximating arbitrary order derivatives in the time multi–term two–sided space fractional differential equations.

2.1. Quadrature rule: Simpson's 1/3 rule

We approximate the distributed order derivative as a finite sum by discretizing the interval $[\beta_l, \beta_u]$ using the points $\beta_l = \beta_0 < \beta_1 < \ldots < \beta_Q = \beta_u$ and define $\Delta\beta = (\beta_u - \beta_l)/Q$, where the points are evenly spaced defined as $\beta_e = \beta_l + e\Delta\beta,\ e = 0, 1, 2, \ldots, Q-1, Q$. Then using the Simpson's 1/3 quadrature formula, we have

$$\int_{\beta_l}^{\beta_u} \rho(\beta) {}_0^C D_t^{\beta} u(\mathbf{x}, t) d\beta = \frac{\Delta\beta}{3} \left[\rho(\beta_0) {}_0^C D_t^{\beta_0} u(\mathbf{x}, t) + 4 \sum_{e=1}^{Q/2} \rho(\beta_{2e-1}) {}_0^C D_t^{\beta_{2e-1}} u(\mathbf{x}, t) \right. \tag{4}$$
$$\left. + 2 \sum_{e=1}^{Q/2-1} \rho(\beta_{2e}) {}_0^C D_t^{\beta_{2e}} u(\mathbf{x}, t) + \rho(\beta_Q) {}_0^C D_t^{\beta_Q} u(\mathbf{x}, t) \right].$$

The time distributed order two–sided space fractional differential equation (1) is now transformed into a time multi–term two–sided space fractional differential equation

$$\frac{\Delta\beta}{3} \left[\rho(\beta_0) {}_0^C D_t^{\beta_0} u(\mathbf{x}, t) + \rho(\beta_Q) {}_0^C D_t^{\beta_Q} u(\mathbf{x}, t) + 4 \sum_{e=1}^{Q/2} \rho(\beta_{2e-1}) {}_0^C D_t^{\beta_{2e-1}} u(\mathbf{x}, t) \right.$$
$$\left. + 2 \sum_{e=1}^{Q/2-1} \rho(\beta_{2e}) {}_0^C D_t^{\beta_{2e}} u(\mathbf{x}, t) \right] + \mathcal{O}((\Delta\beta)^2) = {}_0^C D_{\mathbf{x}}^{\alpha} u(\mathbf{x}, t) + {}_{\mathbf{x}}^C D_{\mathsf{L}}^{\alpha} u(\mathbf{x}, t) + g(\mathbf{x}, t). \tag{5}$$

Next, we approximate the functions in Equation (5) and their derivatives in terms of the first kind shifted Chebyshev polynomials.

2.2. First kind Chebyshev approximation

Definition 2.3. *The first kind Chebyshev polynomials are eigenvalue solutions of the Sturm–Liouville problem with weight function* $1/\sqrt{1-x^2}$ *[1]. Considering a change of variable* $[-1, 1] \mapsto [0, \mathsf{L}]$*, the shifted form of the polynomials is defined in series form as*

$$T_{\mathsf{L},n}(x) = n \sum_{j=0}^{n} \frac{(-1)^{n-j}(n+j-1)!2^{2j}}{(n-j)!(2j)!\mathsf{L}^j} x^j = n \sum_{j=0}^{n} \frac{(n+j-1)!2^{2j}}{(n-j)!(2j)!\mathsf{L}^j} (x-\mathsf{L})^j. \tag{6}$$

We approximate the solution of Equation (5) as a linear combination of the shifted first kind Chebyshev polynomials in both variables as

$$u(\mathbf{x},t) \approx U(\mathbf{x},t) = \sum_{n_1=0}^{N_{\mathbf{x}}} \sum_{n_2=0}^{N_t} \hat{U}_{n_1,n_2} T_{\mathsf{L},n_1}(\mathbf{x}) T_{\mathsf{T},n_2}(t), \quad \mathbf{x} \in [0,\mathsf{L}],\ t \in [0,\mathsf{T}], \tag{7}$$

where $\hat{U}_{n_1,n_2}$ satisfies the L^2 orthogonality condition written in discrete form as

$$\hat{U}_{n_1,n_2} = \frac{1}{h_{n_1}} \frac{1}{h_{n_2}} \sum_{j_1=0}^{N_{\mathbf{x}}} \sum_{j_2=0}^{N_t} \varpi_{j_1} \varpi_{j_2} U(\mathbf{x}_{j_1}, t_{j_2}) T_{\mathsf{L},n_1}(\mathbf{x}_{j_1}) T_{\mathsf{T},n_2}(t_{j_2}). \tag{8}$$

Here, $h_n = c_n \pi/2$ with $c_0 = 2, c_n = 1\ \forall\ n \geq 1$ and the Christoffel number $\varpi_j = \pi/c_j N$, with $c_0 = c_N = 2, c_j = 1\ \forall\ 1 \leq j \leq N-1$. Therefore $U(\mathbf{x},t)$ is given as

$$U(\mathbf{x},t) = \sum_{j_1=0}^{N_{\mathbf{x}}} \sum_{j_2=0}^{N_t} \left[\varpi_{j_1} \varpi_{j_2} \sum_{n_1=0}^{N_{\mathbf{x}}} \sum_{n_2=0}^{N_t} \frac{1}{h_{n_1}} \frac{1}{h_{n_2}} T_{\mathsf{L},n_1}(\mathbf{x}_{j_1}) T_{\mathsf{L},n_1}(\mathbf{x}_{p_1}) T_{\mathsf{T},n_2}(t_{j_2}) T_{\mathsf{T},n_2}(t_{p_2}) \right] U(\mathbf{x}_{j_1}, t_{j_2}),$$
$$p_1 = 0,1,\ldots,N_{\mathbf{x}},\ p_2 = 0,1,\ldots,N_t. \tag{9}$$

Lemma 2.4. *Let $\alpha > 0$ and $\mathbf{x} > 0$. Suppose that $u(\mathbf{x},t)$ is a continuously differentiable function, then the approximation of the left sided derivative with respect to $\mathbf{x}$ is given as [7, 16, 17]*

$$ {}_0^C D_{\mathbf{x}}^{\alpha} U(\mathbf{x},t) = \sum_{j_1=0}^{N_{\mathbf{x}}} \sum_{j_2=0}^{N_t} \left[\varpi_{j_1} \varpi_{j_2} \sum_{n_1=0}^{N_{\mathbf{x}}} \sum_{n_2=0}^{N_t} \sum_{k=0}^{N_{\mathbf{x}}} \frac{1}{h_{n_1}} \frac{1}{h_{n_2}} T_{\mathsf{L},n_1}(\mathbf{x}_{j_1}) T_{\mathsf{T},n_2}(t_{j_2}) T_{\mathsf{T},n_2}(t_{p_2}) \times \right.$$
$$\left. {}^{l}D_{n_1,k}^{(\alpha)} T_{\mathsf{L},k}(\mathbf{x}_{p_1}) \right] U(\mathbf{x}_{j_1}, t_{j_2}), \tag{10}$$

where

$$ {}^{l}D_{n_1,k}^{(\alpha)} = n_1 \sum_{j_1=0}^{n_1} \frac{(-1)^{n_1-j_1}(n_1+j_1-1)! 2^{2j_1}}{(n_1-j_1)!(2j_1)! \mathsf{L}^{j_1}} \frac{\Gamma(j_1+1)}{\Gamma(j_1-\alpha+1)} q_{j_1,k}, \tag{11}$$

and

$$q_{j_1,k} = \begin{cases} 0, & j_1 = 0,1,\ldots \lceil \alpha \rceil - 1, \\ \\ \frac{k\sqrt{\pi}}{h_k} \sum_{r=0}^{k} \frac{(-1)^{k-r}(k+r-1)! 2^{2r}}{(k-r)!(2r)!} \mathsf{L}^{j_1-\alpha} \frac{\Gamma(j_1-\alpha+r+1/2)}{\Gamma(j_1-\alpha+r+1)}, & \substack{j_1=\lceil \alpha \rceil, \lceil \alpha \rceil+1,\ldots,N, \\ k=0,1,\ldots,N.} \end{cases} \tag{12}$$

The approximation in the above lemma can also be used for the temporal fractional derivatives.

Lemma 2.5. *For $\alpha > 0$ and $\mathbf{x} < \mathsf{L}$, and if $u(\mathbf{x}, t)$ is a smooth function, the right sided derivative of arbitrary order is discretized as*

$$ {}^{C}_{\mathbf{x}}D^{\alpha}_{\mathsf{L}}U(\mathbf{x},t) = \sum_{j_1=0}^{N_{\mathbf{x}}}\sum_{j_2=0}^{N_t}\Bigg[\varpi_{j_1}\varpi_{j_2}\sum_{n_1=0}^{N_{\mathbf{x}}}\sum_{n_2=0}^{N_t}\sum_{k=0}^{N_{\mathbf{x}}}\frac{1}{h_{n_1}}\frac{1}{h_{n_2}}T_{\mathsf{L},n_1}(\mathbf{x}_{j_1})T_{\mathsf{T},n_2}(t_{j_2})T_{\mathsf{T},n_2}(t_{p_2})\times {}^{r}D^{(\alpha)}_{n_1,k}T_{\mathsf{L},k}(\mathbf{x}_{p_1})\Bigg]U(\mathbf{x}_{j_1},t_{j_2}). \tag{13} $$

Here,

$$ {}^{r}D^{(\alpha)}_{n_1,k} = n_1\sum_{j_1=0}^{n_1}\frac{(-1)^{j_1}(n_1+j_1-1)!2^{2j_1}}{(n_1-j_1)!(2j_1)!\mathsf{L}^{\alpha}}\frac{\Gamma(j_1+1)}{\Gamma(j_1-\alpha+1)}\times \frac{2k}{\pi c_k}\sum_{r=0}^{k}\frac{(-1)^r(k+r-1)!2^{2r}}{(k-r)!(2r)!}\frac{\sqrt{\pi}\Gamma(j_1-\alpha+r+1/2)}{\Gamma(j_1-\alpha+r+1)}. \tag{14} $$

The discretizations in Equation (5), Lemma 2.4 and Lemma 2.5 lead to a linear algebraic system which is evaluated using shifted Gauss–Lobatto quadrature. This can be extended to fractional differential equations in three variables.

3. Space of fractional derivatives and convergence analysis

Here, we give the convergence analysis of the numerical discretization scheme described above. To this end, we define the domain $\vartheta = \tau \times \chi$, where $\tau = [0, \mathsf{T}]$ and $\chi = [0, \mathsf{L}] \times [0, \mathsf{L}]$, and the $L^2_w(\vartheta)$ norm defined as $\|\cdot\|_{\vartheta}$. We introduce the fractional Sobolev space $H^{\beta}_w(\vartheta), \beta \geq 0$ defined as

$$ H^{\beta}_w(\vartheta) = \{u \in L^2_w(\vartheta) : {}^{C}D^{\beta}u \in L^2_w(\vartheta)\}. \tag{15} $$

Given $\alpha > 0$, we define the semi–norm $|u|_{l,\alpha}$ and associated norm $\|u\|_{l,\alpha}$ respectively as [21]

$$ |u|_{l,\alpha} = \left(\|{}^{C}_{0}D^{\alpha}_{\mathbf{x}}\|^2_{L^2_w(\vartheta)}\right)^{1/2} \qquad \text{and} \qquad \|u\|_{l,\alpha} = \left(\|u\|^2_{L^2_w(\vartheta)} + |u|^2_{l,\alpha}\right)^{1/2}, \tag{16} $$

and the semi–norm $|u|_{r,\alpha}$ and associated norm $\|u\|_{r,\alpha}$ respectively as

$$ |u|_{r,\alpha} = \left(\|{}^{C}_{\mathbf{x}}D^{\alpha}_{\mathsf{L}}\|^2_{L^2_w(\vartheta)}\right)^{1/2} \qquad \text{and} \qquad \|u\|_{r,\alpha} = \left(\|u\|^2_{L^2_w(\vartheta)} + |u|^2_{r,\alpha}\right)^{1/2}. \tag{17} $$

Lemma 3.1. *Let $u \in H_w^n(\tau)$ and P_N be the orthogonal projector into space of shifted Chebyshev polynomials up to degree $N+1$, then we have the following estimates [4, 5]*

$$\|u - P_N u\|_{H_w^k(\tau)} \leq C N^{2k-n} \|u\|_{H_w^n(\tau)} \tag{18}$$
$$\|u - P_N u\|_{L_w^2(\tau)} \leq C N^{-m} \|u\|_{H_w^n(\tau)}, \tag{19}$$

for k and n real numbers, such that $0 \leq k \leq n$ and C, a positive constant independent of N.
Lemma 3.2. *For $u \in H_w^{m,n}(\vartheta)$, $m, n \geq 0$, we have [5]*

$$\|u - P_{N,N_t} u\|_{L_w^2(\vartheta)} \leq C \left(N_t^{-n} \|u\|_{H_w^{0,n}(\vartheta)} + N^{-m} \|u\|_{H_w^{m,0}(\vartheta)} \right). \tag{20}$$

The exact solution of Equation (1) is

$$\frac{\Delta\beta}{3} \left[\rho(\beta_0) {}_0^C D_t^{\beta_0} u(\mathbf{x},t) + \rho(\beta_Q) {}_0^C D_t^{\beta_Q} u(\mathbf{x},t) + 4 \sum_{e=1}^{Q/2} \rho(\beta_{2e-1}) {}_0^C D_t^{\beta_{2e-1}} u(\mathbf{x},t) \right.$$
$$\left. + 2 \sum_{e=1}^{Q/2-1} \rho(\beta_{2e}) {}_0^C D_t^{\beta_{2e}} u(\mathbf{x},t) \right] + \mathcal{O}((\Delta\beta)^2) = {}_0^C D_{\mathbf{x}}^{\alpha} u(\mathbf{x},t) + {}_{\mathbf{x}}^C D_{\mathsf{L}}^{\alpha} u(\mathbf{x},t) + g(\mathbf{x},t), \tag{21}$$

provided $u(\mathbf{x},t)$ is regular with respect to all $\beta \in [\beta_0, \beta_Q]$. The numerical approximation scheme is

$$\frac{\Delta\beta}{3} \left[\rho(\beta_0) {}_0^C D_t^{\beta_0} U(\mathbf{x},t) + \rho(\beta_Q) {}_0^C D_t^{\beta_Q} U(\mathbf{x},t) + 4 \sum_{e=1}^{Q/2} \rho(\beta_{2e-1}) {}_0^C D_t^{\beta_{2e-1}} U(\mathbf{x},t) \right.$$
$$\left. + 2 \sum_{e=1}^{Q/2-1} \rho(\beta_{2e}) {}_0^C D_t^{\beta_{2e}} U(\mathbf{x},t) \right] = {}_0^C D_{\mathbf{x}}^{\alpha} U(\mathbf{x},t) + {}_{\mathbf{x}}^C D_{\mathsf{L}}^{\alpha} U(\mathbf{x},t) + G(\mathbf{x},t). \tag{22}$$

Theorem 3.3. *Let $u(\mathbf{x},t)$ be the exact solution of Equation (1) and $U(\mathbf{x},t)$ be the solution given by the numerical scheme, such that $u \in H_w^{m,n}(\vartheta)$. Then, there exists a positive constant C independent of $\Delta\beta$, N and N_t such that*

$$\|u - U\|_{L_w^2(\vartheta)} \leq C \left((\Delta\beta)^4 + N_t^{2\beta_0 - n} \|\xi\|_{0,n} + N_t^{2\beta_Q - n} \|\xi\|_{0,n} + \sum_{e=1}^{Q/2} N_t^{2\beta_{2e-1} - n} \|\xi\|_{0,n} \right.$$
$$\left. + \sum_{e=1}^{Q/2-1} N_t^{2\beta_{2e} - n} \|\xi\|_{0,n} + N^{2\alpha - m} \|\xi\|_{m,0} + N^{-m} \|u\|_{m,0} + N_t^{-n} \|u\|_{0,n} \right). \tag{23}$$

Proof. To prove this result, define $\tilde{u} = P_{N,N_t}u$, $\xi = \tilde{u} - U$ and note that $g = G$. Subtracting Equation (22) from Equation (21) yields the following error equation

$$\frac{\Delta\beta}{3}\Bigg[\rho(\beta_0){}_0^C D_t^{\beta_0}(u-U) + \rho(\beta_Q){}_0^C D_t^{\beta_Q}(u-U) + 4\sum_{e=1}^{Q/2}\rho(\beta_{2e-1}){}_0^C D_t^{\beta_{2e-1}}(u-U) + 2\sum_{e=1}^{Q/2-1}\rho(\beta_{2e}){}_0^C D_t^{\beta_{2e}}(u-U)\Bigg] + \mathcal{O}((\Delta\beta)^2) = {}_0^C D_{\mathbf{x}}^{\alpha}(u-U) + {}_{\mathbf{x}}^C D_{\mathsf{L}}^{\alpha}(u-U). \quad (24)$$

Projecting Equation (24) into the space of shifted Chebyshev polynomials gives

$$\frac{\Delta\beta}{3}\rho(\beta_0){}_0^C D_t^{\beta_0}\xi + \frac{\Delta\beta}{3}\rho(\beta_Q){}_0^C D_t^{\beta_Q}\xi + \frac{4\Delta\beta}{3}\sum_{e=1}^{Q/2}\rho(\beta_{2e-1}){}_0^C D_t^{\beta_{2e-1}}\xi + \frac{2\Delta\beta}{3}\sum_{e=1}^{Q/2-1}\rho(\beta_{2e}){}_0^C D_t^{\beta_{2e}}\xi = ({}_0^C D_{\mathbf{x}}^{\alpha} + {}_{\mathbf{x}}^C D_{\mathsf{L}}^{\alpha})\xi + \epsilon + \mathcal{O}((\Delta\beta)^2), \quad (25)$$

where

$$\epsilon = -\frac{\Delta\beta}{3}\Bigg[\rho(\beta_0){}_0^C D_t^{\beta_0}(u-\tilde{u}) + \rho(\beta_Q){}_0^C D_t^{\beta_Q}(u-\tilde{u}) + 4\sum_{e=1}^{Q/2}\rho(\beta_{2e-1}){}_0^C D_t^{\beta_{2e-1}}(u-\tilde{u}) + 2\sum_{e=1}^{Q/2-1}\rho(\beta_{2e}){}_0^C D_t^{\beta_{2e}}(u-\tilde{u})\Bigg] + ({}_0^C D_{\mathbf{x}}^{\alpha} + {}_{\mathbf{x}}^C D_{\mathsf{L}}^{\alpha})(u-\tilde{u}). \quad (26)$$

Applying Young's inequality and properties of the Sobolev norm on the left hand side of Equation (25), we have

$$\left\| \frac{\Delta\beta}{3}\rho(\beta_0){}_0^C D_t^{\beta_0}\xi + \frac{\Delta\beta}{3}\rho(\beta_Q){}_0^C D_t^{\beta_Q}\xi + \frac{4\Delta\beta}{3}\sum_{e=1}^{Q/2}\rho(\beta_{2e-1}){}_0^C D_t^{\beta_{2e-1}}\xi + \frac{2\Delta\beta}{3}\sum_{e=1}^{Q/2-1}\rho(\beta_{2e}){}_0^C D_t^{\beta_{2e}}\xi \right\|_{L_w^2(\vartheta)} \tag{27}$$

$$\leq \left\| \frac{\Delta\beta}{3}\rho(\beta_0){}_0^C D_t^{\beta_0}\xi \right\|_{L_w^2(\vartheta)} + \left\| \frac{\Delta\beta}{3}\rho(\beta_Q){}_0^C D_t^{\beta_Q}\xi \right\|_{L_w^2(\vartheta)} + \left\| \frac{4\Delta\beta}{3}\sum_{e=1}^{Q/2}\rho(\beta_{2e-1}){}_0^C D_t^{\beta_{2e-1}}\xi \right\|_{L_w^2(\vartheta)} + \left\| \frac{2\Delta\beta}{3}\sum_{e=1}^{Q/2-1}\rho(\beta_{2e}){}_0^C D_t^{\beta_{2e}}\xi \right\|_{L_w^2(\vartheta)} \tag{28}$$

$$\leq C\left(N_t^{2\beta_0-n}\|\xi\|_{0,n} + N_t^{2\beta_Q-n}\|\xi\|_{0,n} + \sum_{e=1}^{Q/2} N_t^{2\beta_{2e-1}-n}\|\xi\|_{0,n} + \sum_{e=1}^{Q/2-1} N_t^{2\beta_{2e}-n}\|\xi\|_{0,n} \right). \tag{29}$$

Estimating the first term on the right hand side of Equation (25) gives

$$\left\|({}_0^C D_{\mathbf{x}}^{\alpha} + {}_{\mathbf{x}}^C D_{\mathsf{L}}^{\alpha})\xi\right\|_{L_w^2(\vartheta)} \leq C N^{2\alpha-m}\|\xi\|_{m,0}, \tag{30}$$

and for the second term, we get

$$\|\epsilon\|_{L_w^2(\vartheta)} \leq C\left(N^{-m}\|u\|_{m,0} + N_t^{-n}\|u\|_{0,n}\right). \tag{31}$$

Applying the triangle inequality and substituting Equations (29) to (31) into Equation (25) yields

$$\|u - U\|_{L_w^2(\vartheta)} = \|\xi + \epsilon\|_{L_w^2(\vartheta)} \leq \|\xi\|_{L_w^2(\vartheta)} + \|\epsilon\|_{L_w^2(\vartheta)} \tag{32}$$

$$\leq C\left((\Delta\beta)^4 + N_t^{2\beta_0-n}\|\xi\|_{0,n} + N_t^{2\beta_Q-n}\|\xi\|_{0,n} + \sum_{e=1}^{Q/2} N_t^{2\beta_{2e-1}-n}\|\xi\|_{0,n} + \sum_{e=1}^{Q/2-1} N_t^{2\beta_{2e}-n}\|\xi\|_{0,n} + N^{2\alpha-m}\|\xi\|_{m,0} + N^{-m}\|u\|_{m,0} + N_t^{-n}\|u\|_{0,n} \right), \tag{33}$$

which completes the proof. □

4. Numerical examples

In this section, we experiment with the numerical scheme described earlier with some time distributed order two–sided space fractional partial differential equations. We consider both

one– and two–spatial dimensional two–sided space differential equations of arbitrary orders. In the examples, we consider the fractional advection–dispersion and fractional diffusion equations. The accuracy of the method is investigated by comparing the exact solution of these equations with obtained numerical solutions.

Example 4.1. *We consider the one dimensional time distributed order two–sided space fractional advection–dispersion equation [9]*

$$\int_0^1 \Gamma(3-\beta)\,{}_0^C D_t^\beta u(x,t)d\beta = -\frac{\partial u(x,t)}{\partial x} + \frac{1}{2}\,{}_0^C D_x^\alpha u(x,t) + \frac{1}{2}\,{}_x^C D_1^\alpha u(x,t) + g(x,t), \tag{34}$$

with $1 \le \alpha < 2$ *and boundary conditions*

$$u(x,t)|_{\partial\Omega} = 0; \qquad \Omega = [0,1], \quad t \in [0,\mathsf{T}], \tag{35}$$

and initial condition $u(x,0) = 0$. *If we assume that the exact solution that satisfies the equation is* $u(x,t) = t^2x^2(1-x)^2$, *then*

$$g(x,t) = g_1(x,t) + g_2(x,t) + g_3(x,t) + g_4(x,t), \tag{36}$$

where

$$g_1(x,t) = \frac{2x^2(1-x)^2(t^2-t)}{\ln t} \tag{37}$$

$$g_2(x,t) = 2x^2(1-x)(1-2x)t^2 \tag{38}$$

$$g_3(x,t) = -\frac{x^{2-\alpha}t^2[(3-\alpha)(4-\alpha) - 6(4-\alpha)x + 12x^2]}{\Gamma(5-\alpha)} \tag{39}$$

$$g_4(x,t) = -\frac{(1-x)^{2-\alpha}t^2[(3-\alpha)(4-\alpha) - 6(4-\alpha)(1-x) + 12(1-x)^2]}{\Gamma(5-\alpha)}. \tag{40}$$

Example 4.2. *Consider the two–sided space fractional diffusion equation with time fractional distributed order*

$$\int_0^2 \frac{\Gamma(6-\beta)}{120}\,{}_0^C D_t^\beta u(x,t)d\beta = \frac{1}{2}\,{}_0^C D_x^\alpha u(x,t) + \frac{1}{2}\,{}_x^C D_1^\alpha u(x,t) + g(x,t), \quad 1 \le \alpha \le 2, \tag{41}$$

with exact solution $u(x,t) = t^5x^2(1-x)^2$, *such that the boundary conditions are given as*

$$u(x,t)|_{\partial\Omega} = 0; \qquad \Omega = [0,1], \quad t \in [0,\mathsf{T}], \tag{42}$$

initial conditions given by

$$u(x,0) = u_t(x,0) = 0, \quad x \in \Omega, \tag{43}$$

and

$$g(x,t) = g_1(x,t) + g_2(x,t) + g_3(x,t) \tag{44}$$

$$g_1(x,t) = \frac{x^2(1-x)^2(t^5 - t^3)}{\ln t} \tag{45}$$

$$g_2(x,t) = -\frac{x^{2-\alpha}t^5[(3-\alpha)(4-\alpha) - 6(4-\alpha)x + 12x^2]}{\Gamma(5-\alpha)} \tag{46}$$

$$g_3(x,t) = -\frac{(1-x)^{2-\alpha}t^5[(3-\alpha)(4-\alpha) - 6(4-\alpha)(1-x) + 12(1-x)^2]}{\Gamma(5-\alpha)}. \tag{47}$$

Example 4.3. *In this example, we consider a two dimensional time distributed order two–sided space fractional diffusion equation with constant coefficients*

$$\int_0^1 \Gamma(3-\beta)\,{}_0^C D_t^\beta u \, d\beta = \frac{1}{2}\left[{}_0^C D_x^{\alpha_1} u + {}_x^C D_1^{\alpha_1} u + {}_0^C D_y^{\alpha_2} u + {}_y^C D_1^{\alpha_2} u\right] + g(x,y,t), \tag{48}$$

whose exact solution is assumed to be $u(x,y,t) = t^2x^2(1-x)^2y^2(1-y)^2$*, such that the boundary condition is given as*

$$u(x,y,t)|_{\partial\Omega} = 0, \tag{49}$$

and initial condition

$$u(x,y,0) = 0, \tag{50}$$

where Ω *is the rectangular domain* $[0,1] \times [0,1]$*. In this case the function*

$$g(x,y,t) = g_1(x,y,t) + g_2(x,y,t) + g_3(x,y,t) + g_4(x,y,t) + g_5(x,y,t), \tag{51}$$

where

$$g_1(x,y,t) = \frac{2x^2(1-x)^2y^2(1-y)^2(t^2-t)}{\ln t} \tag{52}$$

$$g_2(x,y,t) = -\frac{x^{2-\alpha_1}t^2y^2(1-y)^2[(3-\alpha_1)(4-\alpha_1)-6(4-\alpha_1)x+12x^2]}{\Gamma(5-\alpha_1)} \tag{53}$$

$$g_3(x,y,t) = -\frac{(1-x)^{2-\alpha_1}t^2y^2(1-y)^2[(3-\alpha_1)(4-\alpha_1)-6(4-\alpha_1)(1-x)+12(1-x)^2]}{\Gamma(5-\alpha_1)} \tag{54}$$

$$g_4(x,y,t) = -\frac{y^{2-\alpha_2}t^2x^2(1-x)^2[(3-\alpha_2)(4-\alpha_2)-6(4-\alpha_2)y+12y^2]}{\Gamma(5-\alpha_2)} \tag{55}$$

$$g_5(x,y,t) = -\frac{(1-y)^{2-\alpha_2}t^2x^2(1-x)^2[(3-\alpha_2)(4-\alpha_2)-6(4-\alpha_2)(1-y)+12(1-y)^2]}{\Gamma(5-\alpha_2)}. \tag{56}$$

Example 4.4. *Consider the two dimensional time distributed order two–sided space fractional diffusion equation*

$$\int_0^1 \Gamma(7/2-\beta){}_0^C D_t^\beta u \, d\beta = \frac{1}{2}\left[{}_0^C D_x^{\alpha_1}u + {}_x^C D_1^{\alpha_1}u + {}_0^C D_y^{\alpha_2}u + {}_y^C D_1^{\alpha_2}u\right] + g(x,y,t), \tag{57}$$

with exact solution $u(x,y,t) = t^{\frac{5}{2}}x^2(1-x)^2y^2(1-y)^2$. *The initial condition is given as*

$$u(x,y,0) = 0, \qquad x,y \in [0,1]\times[0,1], \tag{58}$$

and boundary conditions as

$$u(x,y,t)|_{\partial\Omega} = 0, \qquad t \in [0,\mathsf{T}], \quad \Omega = [0,1]\times[0,1]. \tag{59}$$

The function $g(x,y,t)$ *is defined by*

$$g(x,y,t) = g_1(x,y,t) + g_2(x,y,t) + g_3(x,y,t) + g_4(x,y,t) + g_5(x,y,t) \tag{60}$$

$$g_1(x,y,t) = \frac{15\sqrt{\pi}x^2(1-x)^2y^2(1-y)^2(t-1)t^{\frac{3}{2}}}{8\ln t} \tag{61}$$

$$g_2(x,y,t) = -\frac{x^{2-\alpha_1}t^{\frac{5}{2}}y^2(1-y)^2[(3-\alpha_1)(4-\alpha_1) - 6(4-\alpha_1)x + 12x^2]}{\Gamma(5-\alpha_1)} \tag{62}$$

$$g_3(x,y,t) = -\frac{(1-x)^{2-\alpha_1}t^{\frac{5}{2}}y^2(1-y)^2[(3-\alpha_1)(4-\alpha_1) - 6(4-\alpha_1)(1-x) + 12(1-x)^2]}{\Gamma(5-\alpha_1)} \tag{63}$$

$$g_4(x,y,t) = -\frac{y^{2-\alpha_2}t^{\frac{5}{2}}x^2(1-x)^2[(3-\alpha_2)(4-\alpha_2) - 6(4-\alpha_2)y + 12y^2]}{\Gamma(5-\alpha_2)} \tag{64}$$

$$g_5(x,y,t) = -\frac{(1-y)^{2-\alpha_2}t^{\frac{5}{2}}x^2(1-x)^2[(3-\alpha_2)(4-\alpha_2) - 6(4-\alpha_2)(1-y) + 12(1-y)^2]}{\Gamma(5-\alpha_2)}. \tag{65}$$

Table 1: Maximum errors and CPU time for different values of N_x with $\alpha = 1.3,\ \alpha = 1.9,\ N_t = 10,\ Q = 32$ and $T = 0.99$ for Example 4.1.

	$\alpha = 1.3$		$\alpha = 1.9$	
N_x	E_∞	CPU time (secs)	E_∞	CPU time (secs)
2	0.04026	0.8238	0.00869	0.8298
4	0.00739	0.8617	0.00703	0.8567
6	0.00035	1.0366	0.00023	1.1051
8	0.00012	1.0662	9.5289×10^{-5}	1.1107
10	5.3146×10^{-5}	1.2531	4.1654×10^{-5}	1.1043

Table 2: Maximum errors and CPU time for different values of N_t with $\alpha = 1.3,\ \alpha = 1.9,\ N_x = 10,\ Q = 32$ and $T = 0.99$ for Example 4.1

	$\alpha = 1.3$		$\alpha = 1.9$	
N_t	$\|E\|_\infty$	CPU time (secs)	$\|E\|_\infty$	CPU time (secs)
2	0.00278	0.0778	0.00184	0.0654
4	5.4704×10^{-5}	0.2430	4.2668×10^{-5}	0.1729
6	5.3122×10^{-5}	0.2276	4.1648×10^{-5}	0.2679
8	5.3082×10^{-5}	0.7049	4.1622×10^{-5}	0.6553
10	5.3146×10^{-5}	1.1849	4.1654×10^{-5}	1.1606

Table 3: Maximum errors and CPU time for different values of Q with $\alpha = 1.3,\ \alpha = 1.9,\ N_x = 10,\ N_t = 10$ and $T = 0.99$ for Example 4.1

	$\alpha = 1.3$		$\alpha = 1.9$	
Q	$\|E\|_\infty$	CPU time (secs)	$\|E\|_\infty$	CPU time (secs)
2	5.3148×10^{-5}	0.1311	4.1692×10^{-5}	0.1589
4	5.3146×10^{-5}	0.1904	4.1656×10^{-5}	0.2746
8	5.3146×10^{-5}	0.3028	4.1654×10^{-5}	0.3129
16	5.3146×10^{-5}	0.5816	4.1654×10^{-5}	0.8234
32	5.3146×10^{-5}	1.2644	4.1654×10^{-5}	1.0751

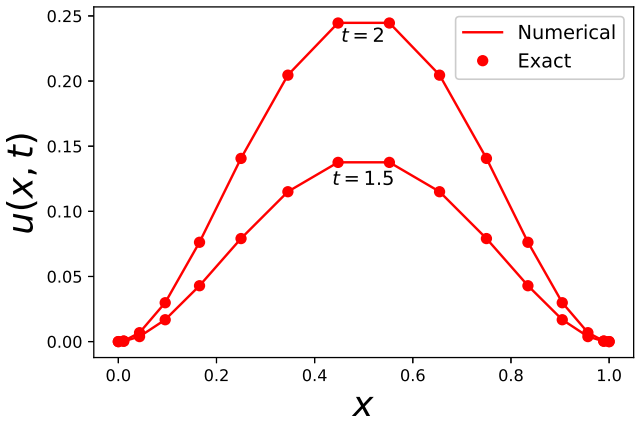

Figure 1: Numerical and exact solutions of Example 4.1 at $t = 1.5, 2$ with $N_t = N_x = 15$, $Q = 32$ and $\alpha = 1.5$

Table 4: Maximum errors and CPU time for different values of N_x with $\alpha = 1.2,\ \alpha = 1.8,\ N_t = 10,\ Q = 32$ and $T = 1.2$ for Example 4.2.

	$\alpha = 1.2$		$\alpha = 1.8$	
N_x	$\|E\|_\infty$	CPU time (secs)	$\|E\|_\infty$	CPU time (secs)
2	0.11373	1.0153	0.04094	0.9425
4	0.02022	0.9774	0.01702	1.1729
6	0.00055	1.0023	0.00079	1.0911
8	0.00016	1.0674	0.00035	1.0083
10	8.1689×10^{-5}	1.0253	0.00014	1.2128

Table 5: Maximum errors and CPU time for different values of N_t with $\alpha = 1.2,\ \alpha = 1.8,\ N_x = 10,\ Q = 32$ and $T = 1.2$ for Example 4.2

	$\alpha = 1.2$		$\alpha = 1.8$	
N_t	$\|E\|_\infty$	CPU time (secs)	$\|E\|_\infty$	CPU time (secs)
2	0.04700	0.2015	0.01346	0.0658
4	0.00239	0.1227	0.00093	0.1107
6	8.1716×10^{-5}	0.4807	0.00014	0.1845
8	8.1689×10^{-5}	0.4049	0.00014	0.4408
10	8.1689×10^{-5}	0.8637	0.00014	0.9845

Table 6: Maximum errors and CPU time for different values of Q with $\alpha = 1.2,\ \alpha = 1.8,\ N_x = 10,\ N_t = 10$ and $T = 1.2$ for Example 4.1

	$\alpha = 1.2$		$\alpha = 1.8$	
Q	$\|E\|_\infty$	CPU time (secs)	$\|E\|_\infty$	CPU time (secs)
2	8.1659×10^{-5}	0.1626	0.00014	0.1526
4	8.1684×10^{-5}	0.1766	0.00014	0.2244
8	8.1689×10^{-5}	0.2683	0.00014	0.2773
16	8.1689×10^{-5}	0.5156	0.00014	0.8082

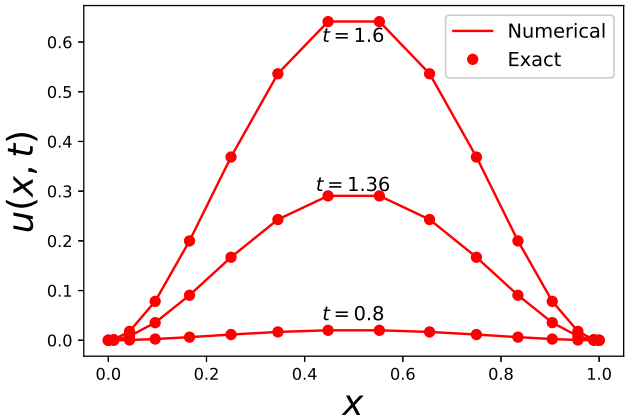

Figure 2: Approximate and exact solutions of Example 4.2 at $t = 0.8, 1.36, 1.6$ with $N_t = 16, N_x = 15$, $Q = 32$ and $\alpha = 1.4$

Table 7: Absolute error norms and CPU time obtained from the approximation of Example 4.3 for different time intervals $[0, \mathsf{T}]$ with $N_x = N_y = 15,\ N_t = 10$ and $Q = 32$.

	$\alpha_1 = \alpha_2 = 1.5$		$\alpha_1 = \alpha_2 = 1.9$	
T	$\|E\|_\infty$	CPU time (secs)	$\|E\|_\infty$	CPU time (secs)
0.5	5.0793×10^{-7}	3.3520	5.3510×10^{-8}	3.3909
1.2	3.1589×10^{-6}	3.3291	3.1941×10^{-7}	3.4827
1.9	8.1299×10^{-6}	3.4079	8.1058×10^{-7}	3.5286
2.6	1.5442×10^{-5}	3.4996	1.5284×10^{-6}	3.4398
3.3	2.5106×10^{-5}	3.4538	2.4736×10^{-6}	3.3391
4.0	3.7131×10^{-5}	3.4428	3.6467×10^{-6}	3.4458

Table 8: Maximum error norms and CPU time obtained from the approximation of Example 4.4 for different time intervals $[0, \mathsf{T}]$ with $N_x = N_y = 15,\ N_t = 10$ and $Q = 32$.

	$\alpha_1 = \alpha_2 = 1.2$		$\alpha_1 = \alpha_2 = 1.7$	
T	$\|E\|_\infty$	CPU time (secs)	$\|E\|_\infty$	CPU time (secs)
0.5	1.6666×10^{-7}	3.4308	2.1362×10^{-7}	3.5734
1.2	1.8109×10^{-6}	3.2503	2.1005×10^{-6}	3.5425
1.9	6.1596×10^{-6}	3.3480	6.8529×10^{-6}	3.2892
2.6	1.4079×10^{-5}	3.4857	1.5287×10^{-5}	3.4667
3.3	2.6287×10^{-5}	3.1785	2.8072×10^{-5}	3.2513
4.0	4.3405×10^{-5}	3.5116	4.5789×10^{-5}	3.6692

5. Results and discussion

In this section, we present the numerical results obtained after solving the equations in Examples 4.1 to 4.4 using the numerical scheme described in this study. The results are presented in form of tables and graphs. The results emphasize computational efficiency in terms of CPU time and accuracy which is measured in terms of the absolute difference between the exact and numerical solutions. The error is defined as

$$E = |u(\mathbf{x}_i, t_k) - U(\mathbf{x}_i, t_k)|, \tag{66}$$

where u and U respectively represent the exact and numerical solutions. The numerical scheme was implemented using the Python 3.6 programming language on the Spyder ide run on a computer with *Intel Core i5, 7th gen, CPU @ 2.50 GHz* and *8 GB DDR4 installed RAM.*

Tables 1 to 3 show the maximum absolute errors and computational time (in seconds) for Example 4.1 for different values of N_x, N_t and Q respectively. The results show that

the method is computationally accurate and efficient. In Tables 1 and 2, we can see that accuracy improves as the number of terms (both space and time) in the Chebyshev expansion increases. However, in Table 3, it can be seen that with 2 equal subintervals in Simpson's rule, accurate results are obtained. Obviously, it is expected that computation would become more expensive as the number of intervals in the quadrature formula and number of spatial and temporal grid points increase. This can be seen from the increasing CPU time as the quantities (N_x, N_t, Q) increase. Figure 1 shows the exact and numerical solutions of Example 4.1 at $t = 1.5$ and 2. It can be noted that the exact solutions are in agreement with the numerical approximations.

In Tables 4 to 6, we present the maximum error and computational time for Example 4.2 for different values of N_x, N_t and Q respectively. The results show that the numerical method gives accurate results. The computational efficiency of the numerical scheme in terms of CPU time is also given. The maximum computational time is approximately $1.2s$, which is the time required to solve the fractional differential equation with $N_x = N_t = 10$ terms of the shifted Chebyshev polynomials and approximate the distributed order with 32 intervals of Simpson's rule. In Figure 2, the numerical and exact solutions of Example 4.2 for $t = 0.8, 1.36, 1.6$ are in agreement.

In Table 7, we show the dynamics of the infinity error norms when the length of the time domain $[0, \mathsf{T}]$ is varied. The number of grid points in the spatial variables (N_x and N_y) are kept constant at $N_x = N_y = 15$ and the temporal grid points at $N_t = 10$. We used 32 equal subintervals for the quadrature formula. We also report the computational time, which was used as a measure of the efficiency of the numerical scheme. Table 7 shows that the orders of magnitude of the errors are small indicating that accurate results are obtained for this example. However, the accuracy diminishes as the length of the time interval $[0, \mathsf{T}]$ increases. Although, the accuracy of the scheme diminishes for increasing length of time interval, the effect on CPU time is negligible, putting the CPU time at approximately 3.4142 s and 3.4378 s for $\alpha_1 = \alpha_2 = 1.5$ and $\alpha_1 = \alpha_2 = 1.9$ respectively. Figure 3 shows the numerical solution of Example 4.3 for $t = 5, 10$ and $\alpha_1 = \alpha_2 = 1.5$ with $N_x = N_y = 15, N_t = 10$ and $Q = 32$. The corresponding error distribution over the spatial domain $[0, 1] \times [0, 1]$ are shown in Figure 4. These surface plots show that the numerical scheme is accurate on the entire spatial domain.

Figure 5 shows the evolution of the numerical solutions and corresponding error distribution on the spatial domain for Example 4.4 for different time levels with $\alpha_1 = \alpha_2 = 1.4$, $N_x = N_y = 15$, $N_t = 12$ and $Q = 32$. The surface plots of the error on the domain $x, y \in [0, 1] \times [0, 1]$ show that the numerical solutions are accurate at every points of x and y for all values of t presented. Table 8 shows the variation of the maximum error norm for different length of time interval $[0, \mathsf{T}]$. The computational time for each time interval are also obtained. The table shows that the numerical results are accurate for all time interval considered. However, as in the case of Example 4.3 (Table 7), the order of magnitude of the errors reduces as the length of the time interval increases, but the effect on computational time is trivial. The CPU times are respectively averaged at 3.3675 s and 3.4654 s for $\alpha_1 = \alpha_2 = 1.2$ and $\alpha_1 = \alpha_2 = 1.7$.

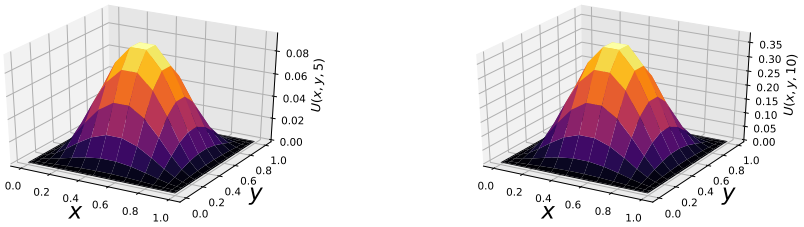

(a) $t = 5$ (b) $t = 10$

Figure 3: Approximate solutions obtained for Example 4.3 for $\alpha_1 = \alpha_2 = 1.5$, $N_x = N_y = 15$ and $N_t = 10$ at different values of t.

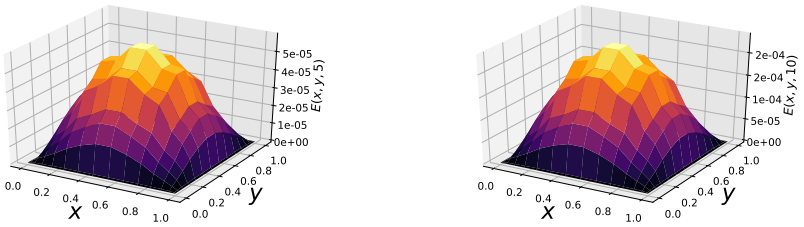

(a) $t = 5$ (b) $t = 10$

Figure 4: Error distribution for Example 4.3 on the spatial domain $[0, 1] \times [0, 1]$ for $\alpha_1 = \alpha_2 = 1.5$ with $N_x = N_y = 15$ and $N_t = 10$ at different values of t.

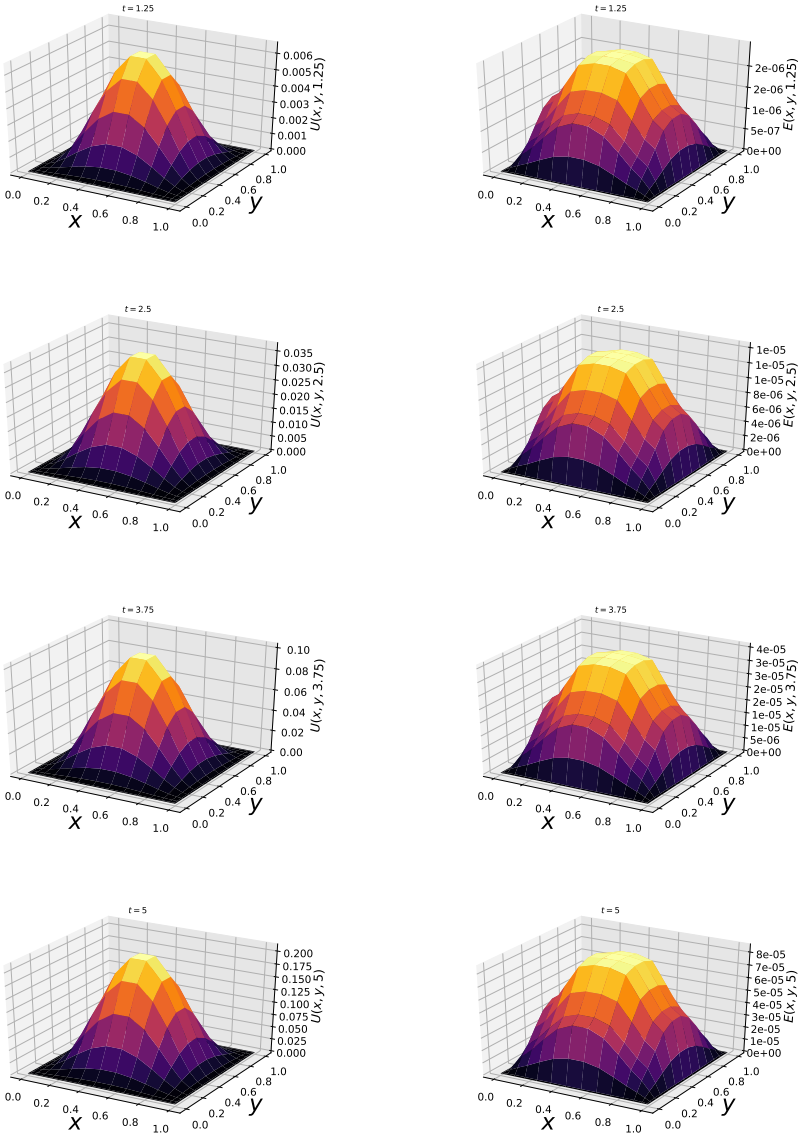

Figure 5: Graphs of numerical solution and error distribution on the spatial domain $[0,1] \times [0,1]$ for Example 4.4 with $\alpha_1 = \alpha_2 = 1.4$, $N_x = N_y = 15$ and $N_t = 12$ at different values of t.

6. Conclusion

Fractional partial differential equations are a special and important class of differential equations. It is well known that fractional differential equations with distributed order are a robust mathematical instrument for describing complex dynamical systems, especially systems that occur at multiscale stages. Thus, constructing accurate numerical schemes for this class of differential equations is essential. In this study, we have presented a numerical method for the discretization of a general time distributed order two–sided multi–dimensional fractional differential equations. The time distributed order fractional differential operator was approximated using a Newton–Cotes formula. We presented both the left and right sided fractional differentiation matrices using approximation in terms of shifted Chebyshev polynomials and shifted Chebyshev–Gauss–Lobatto quadrature. The convergence of the numerical scheme for the aforementioned class of differential equation was shown. We demonstrated the numerical discretization method on some one– and two–dimensional time distributed order two–sided space fractional differential equations such as the fractional advection–dispersion and fractional diffusion equations. The numerical results showed that the method is computationally efficient and accurate.

References

[1] M. Abramowitz and I. A. Stegun, *Handbook of mathematical functions: with formulas, graphs, and mathematical tables*, vol. 55, Courier Corporation, 1965.

[2] T. M. Atanackovic, S. Pilipovic, B. Stankovic, and D. Zorica, *Fractional Calculus with Applications in Mechanics: Wave Propagation, Impact and Variational Principles*, John Wiley & Sons, New York, 2014.

[3] L. Beghin, *Fractional Diffusion-type Equations with Exponential and Logarithmic Differential Operators*, Stochastic Process. Appl., 128 (2018), pp. 2427–2447.

[4] C. Canuto, M. Y. Hussaini, A. Quarteroni, and A. Thomas Jr, *Spectral methods in fluid dynamics*, Springer Science & Business Media, 2012.

[5] C. Canuto, M. Y. Hussaini, A. Quarteroni, and T. A. Zang, *Spectral methods: Fundametals in single domains*, Springer, 2006.

[6] M. Caputo, *Diffusion of fluids in porous media with memory*, Geothermics, 28 (1999), pp. 113–130.

[7] E. Doha, A. Bhrawy, and S. Ezz-Eldien, *Efficient Chebyshev spectral methods for solving multi-term fractional orders differential equations*, Appl. Math. Model., 35 (2011), pp. 5662–5672.

[8] S. Guo, L. Mei, Z. Zhang, and Y. Jiang, *Finite difference/spectral–galerkin method for a two–dimensional distributed–order time–space fractional reaction–diffusion equation*, Appl. Math. Lett., 85 (2018), pp. 157–163.

[9] X. Hu, F. Liu, I. Turner, and V. Anh, *An implicit numerical method of a new time distributed–order and two–sided space–fractional advection–dispersion equation*, Numer. Algorithms, 72 (2016), pp. 393–407.

[10] G. Jumarie, *New stochastic fractional models for Malthusian growth, the Poissonian birth process and optimal management of populations*, Math. Comput. Modelling, 44 (2006), pp. 231–254.

[11] X. Li and B. Wu, *A numerical method for solving distributed order diffusion equations*, Appl. Math. Lett., 53 (2016), pp. 92–99.

[12] K. S. Miller and B. Ross, *An introduction to the fractional calculus and fractional differential equations*, Wiley-Interscience, (1993).

[13] M. L. Morgado and M. Rebelo, *Nummerical approximation of distributed order reaction–diffusion equations*, J. Comput. Appl. Math., 275 (2015), pp. 216–227.

[14] M. L. Morgado, M. Rebelo, L. L. Ferras, and N. J. Ford, *Numerical solution for diffusion equations with distributed order in time using Chebyshev collocation method*, Appl. Numer. Math., 114 (2017), pp. 108–123.
[15] K. Oldham and J. Spanier, *The fractional calculus theory and applications of differentiation and integration to arbitrary order*, vol. 111, Elsevier, 1974.
[16] S. Oloniiju, S. Goqo, and P. Sibanda, *A Chebyshev spectral method for heat and mass transfer in MHD nanofluid flow with space fractional constitutive model*, Frontiers in Heat and Mass Transfer, 13 (2019).
[17] S. D. Oloniiju, S. P. Goqo, and P. Sibanda, *A Chebyshev pseudo-spectral method for the multi-dimensional fractional Rayleigh problem for a generalized Maxwell fluid with Robin boundary conditions*, Appl. Numer. Math., 152 (2020), pp. 253–266.
[18] I. Podlubny, *Fractional differential equations: an introduction to fractional derivatives, fractional differential equations, to methods of their solution and some of their applications*, vol. 198, Elsevier, 1998.
[19] W. R. Schneider and W. Wyss, *Fractional Diffusion and Wave Equations*, J. Math. Phys., 30 (1989), pp. 134–144.
[20] W. Wyss, *The Fractional Diffusion Equation*, J. Math. Phys., 27 (1986), pp. 2782–2785.
[21] F. Zeng, F. Liu, C. Li, K. Burrage, I. Turner, and V. Anh, *A Crank–Nicolson ADI spectral method for a two–dimensional Riesz space fractional nonlinear reaction–diffusion equation*, SIAM J. Numer. Anal., 52 (2014), pp. 2599–2622.

Chapter 9

Conclusion

The focus of this study was on the development of numerical schemes to solve mathematical models of arbitrary order. This study served to make contributions to this subject. We investigated the application of pseudo-spectral methods that use shifted Chebyshev polynomials to solve fractional differential equations; such as, fractional ordinary differential equations (Chapter 2), multi–dimensional time–fractional partial differential equations (Chapters 3 and 4), time–space fractional differential equations (Chapter 5), two–sided space fractional differential equations (Chapter 6) and distributed order fractional differential equations (Chapters 7 and 8). The numerical scheme was first developed to solve fractional ordinary differential equations, and then extended to fractional differential equations with higher dimensionality and other classes of differential equations of arbitrary orders. The accuracy and efficiency of the schemes were determined through conventional performance metrics for numerical method such as error norms and computational time. The results show that the error norms and computational time are small. Some of the conclusions drawn from this study are highlighted below.

In Chapter 2, we used a spatially non–local velocity gradient to model heat and mass transfer in a MHD nanofluid flow with space fractional constitutive equation. The conservation equations were transformed using Lie's group of transformations, resulting in a system of ordinary differential equations with fractional order. A numerically stable and accurate method that used shifted Chebyshev polynomials in the independent variable was proposed. A bound estimation of the numerical error was calculated, and the results obtained were shown to agree with those from the classical model. The residual error

norms of the solutions were found to be approximately 10^{-13}, thereby establishing the accuracy of the method. Further, it was found that heat and mass transfer rates increase as the fractional order increases.

In Chapter 3, we used the memory inherent non–local property of a fractional differential operator to describe the boundary layer flow of an Oldroyd–B fluid. We considered two different flow regimes; specifically, an unsteady unidirectional flow of a MHD fractional Oldroyd–B fluid occupying an upper half plane oscillating parallel to itself and an unsteady non–isothermal flow of a generalized Oldroyd–B fluid. The non–isothermal viscous property was considered in order to introduce nonlinearity and coupling into the system of time fractional differential equations. Efficient and accurate numerical discretizations through expansion of shifted Chebyshev polynomials in two independent variables were presented. The accuracy of the solutions was calculated using the residual error norms. Also, the effects of the fractional orders on the shear stress and velocity were investigated. It was found that small values of relaxation fractional order can be used to model viscoelastic fluid with short term memory and slow response to shear force.

In Chapter 4, we considered the Rayleigh flow of a fractional Maxwell fluid with mixed boundary conditions. The differential equations were a class of multidimensional time fractional partial differential equations with Robin boundary conditions. The numerical scheme was a linear combination of shifted Chebyshev polynomials of the first kind in time and Lagrange polynomials in space. The theoretical and numerical results of the numerical scheme indicated that it converges and is accurate. However, due to the inherent memory property of a fractional derivative, the accuracy of the numerical scheme reduces as the time interval $[0, T]$ grows. Additionally, there is a quick start–up for flow with fractional order close to unity and the effect on the velocity profile become reversed at a critical time value.

Linear and nonlinear multidimensional space–time fractional partial differential equations were considered in Chapter 5. We presented a highly accurate numerical scheme for this class of fractional differential equations. In the nonlinear case, we used the quasilinearization approach to linearize the differential equations. The magnitude of the error norms, the computational time, and the condition number of the differentiation matrix indicated that the method is accurate and computationally efficient. The convergence analysis showed that the convergence of the numerical scheme is dependent on both the fractional orders and number of collocation points in each variable.

In Chapter 6, we used the Chebyshev polynomials pseudo–spectral method for two–sided space fractional differential equations. We introduced the right–sided fractional differential matrix and combined it with the left–sided differentiation matrix to approximate both the left and right sided fractional differential operators. The results indicated that the method was geometrically convergent and computationally efficient. The computational efficiency is evident in the computational time, which was approximately 7 seconds for a 16×16 spatial grid.

Chapter 7 introduced the numerical scheme for distributed order fractional differential equations. The scheme is a hybrid of the Newton–Cotes quadrature formula and shifted Chebyshev pseudo–spectral methods. Convergence results indicated that the numerical convergence depends mainly on the number of subintervals in the Newton–Cotes formula, the number of terms in the Chebyshev expansion and the fractional order. Further, the numerical scheme inherits all the properties, which include, accuracy and convergence, of the quadrature formula and the pseudo–spectral method.

In Chapter 8, the numerical scheme in Chapter 7 was extended to time distributed order two–sided space fractional differential equations. In addition, to study the computational efficiency and accuracy of the numerical scheme, time distributed two–sided space

fractional advection–dispersion and diffusion equations and their numerical solutions were presented. The results obtained are consistent with those of the closed form solutions and show the geometric convergence and computational efficiency of the numerical approach.

In general, the numerical schemes presented in this study are robust and effective for a variety of classes of arbitrary order differential equations. The accuracy and computational efficiency of the approach have been established. An essential observation is that the schemes give geometric convergence; a feature that is generally associated with spectral methods. For further research, we suggest focusing on applications of fractional differential and integral operators to problems in the areas of fluid dynamics and heat and mass transfer. The practice of reformulating constitutive equations in terms of fractional differential and integral operators is gaining significant research interest and raises questions in, for example, the strain hardening effect and stress evolution of non–Newtonian fluids described using fractional calculus.

References

1. H. F. De Baggis and K. S. Miller. *Foundations of the Calculus*. W.B. Saunders. XIII, Philadelphia, 1966.

2. I. Podlubny. *Fractional Differential Equations: An Introduction to Fractional Derivatives, Fractional Differential Equations, to Methods of their Solution and some of their Applications*. Elsevier, San Diego, 1998.

3. B. Ross. The Development of Fractional Calculus 1695–1900. *Historia Mathematica*, 4(1):75–89, 1977.

4. K. Oldham and J. Spanier. *The Fractional Calculus Theory and Applications of Differentiation and Integration to Arbitrary Order*. Elsevier, San Diego, 1974.

5. J. Liouville. Mémoire sur l'Intégration de l'Équation $(mx^2 + nx + p)\frac{d^2y}{dx^2} + (qx + r)\frac{dy}{dx} + sy = 0$ à l'Aide des Différentielles à Indices Quelconques. *Journal de l'École Polytechnique – Mathématiques*, 13:163, 1832.

6. B. Riemann. Versuch einer Allgemeinen Auffassung der Integration und Differentiation. *Gesammelte Werke*, 62, 1876.

7. V. S. Kiryakova. *Generalized Fractional Calculus and Applications*. CRC Press, London, 1993.

8. Y. N. Sonin. On Differentiation with Arbitrary Index. *Moscow Matematicheskii Sbornik*, 6(1):1–38, 1869.

9. A. V. Letnikov. An Explanation of the Concepts of the Theory of Differentiation of Arbitrary Index. *Moscow Matematicheskii Sbornik*, 6:413–445, 1872.

10. H. Laurent. Sur le Calcul des Dérivées à Indices Quelconques. *Nouvelles Annales de Mathématiques: Journal des Candidats aux Écoles Polytechnique et Normale*, 3: 240–252, 1884.

11. P. A. Nekrassov. General Differentiation. *Matematicheskii Sbornik*, 14:45–168, 1888.

12. A. Krug. Theorie der Derivationen. *Denkschriften der Kaiserlichen Akademie der Wissenschaften / Mathematisch-Naturwissenschaftliche Classe.*, 57:151–228, 1890.

13. O. Heaviside. *Electrical Papers*, volume 2. Cambridge University Press, Cambridge, 2011.

14. M. Caputo. *Elasticita e Dissipazione*. Zanichelli, Bologna, 1969.

15. M. Caputo. Linear Models of Dissipation Whose Q is Almost Frequency Independent—II. *Geophysical Journal International*, 13(5):529–539, 1967.

16. C. V. Pao. Asymptotic Behavior of Solutions of Reaction–Diffusion Equations with nonlocal Boundary Conditions. *Journal of Computational and Applied Mathematics*, 88(1):225–238, 1998.

17. Y. Liu. Numerical Solution of the Heat Equation with nonlocal Boundary Conditions. *Journal of Computational and Applied Mathematics*, 110(1):115–127, 1999.

18. M. Caputo and M. Fabrizio. Applications of New Time and Spatial Fractional Derivatives with Exponential Kernels. *Progress in Fractional Differentiation and Applications*, 2(2):1–11, 2016.

19. M. Caputo and M. Fabrizio. A New Definition of Fractional Derivative without Singular Kernel. *Progress in Fractional Differentiation and Applications*, 1(2):1–13, 2015.

20. A. Atangana and D. Baleanu. New Fractional Derivatives with nonlocal and non–singular Kernel: Theory and Application to Heat Transfer Model. *arXiv preprint arXiv:1602.03408*, 2016.

21. A. Atangana and I. Koca. Chaos in a Simple nonlinear System with Atangana–Baleanu Derivatives with Fractional Order. *Chaos, Solitons & Fractals*, 89:447–454, 2016.

22. M. Caputo. Diffusion of Fluids in Porous Media with Memory. *Geothermics*, 28(1): 113–130, 1999.

23. L. Boltzmann. Zur Integration der Diffusionsgleichung bei Variabeln Diffusionscoefficienten. *Annalen der Physik*, 289(13):959–964, 1894.

24. C. M. Zener and S. Siegel. Elasticity and Anelasticity of Metals. *The Journal of Physical Chemistry*, 53(9):1468–1468, 1949.

25. K. S. Cole and R. H. Cole. Dispersion and Absorption in Dielectrics I. Alternating Current Characteristics. *The Journal of Chemical Physics*, 9(4):341–351, 1941.

26. M. Caputo and F. Mainardi. A New Dissipation Model Based on Memory Mechanism. *Pure and Applied Geophysics*, 91(1):134–147, 1971.

27. K. B. Oldham and J. Spanier. The Replacement of Fick's Laws by a Formulation Involving Semidifferentiation. *Journal of Electroanalytical Chemistry and Interfacial Electrochemistry*, 26(2-3):331–341, 1970.

28. G. Jumarie. New Stochastic Fractional Models for Malthusian Growth, the Poissonian Birth Process and Optimal Management of Populations. *Mathematical and Computer Modelling*, 44(3-4):231–254, 2006.

29. A. Atangana and S. I. Araz. Atangana-Seda Numerical Scheme for Labyrinth Attractor with New Differential and Integral Operators. *Fractals*, 2020. doi: 10.1142/S0218348X20400447.

30. M. B. Riaz, A. Atangana, and T. Abdeljawad. Local and nonlocal Differential Operators: A Comparative Study of Heat and Mass Transfer in MHD Oldroyd–B Fluid with Ramped Wall Temperature. *Fractals*, 2020. doi: 10.1142/S0218348X20400332.

31. A. Atangana and R. T. Alqahtani. New Numerical Method and Application to Keller–Segel Model with Fractional Order Derivative. *Chaos, Solitons & Fractals*, 116:14–21, 2018.

32. E. F. D. Goufo, A. Atangana, and M. Khumalo. On the Chaotic Pole of Attraction with Nonlocal and Nonsingular Operators in Neurobiology. In J. F. Gómez, L. Torres, and R. F. Escobar (Editors), *Fractional Derivatives with Mittag-Leffler Kernel*, pages 117–134. Springer, 2019.

33. E. F. D. Goufo and A. Atangana. Modulating Chaotic Oscillations in Autocatalytic Reaction Networks using Atangana–Baleanu Operator. In J. F. Gómez, L. Torres, and R. F. Escobar (Editors), *Fractional Derivatives with Mittag-Leffler Kernel*, pages 135–158. Springer, 2019.

34. A. Allwright and A. Atangana. Upwind–Based Numerical Approximation of a Space–Time Fractional Advection–Dispersion Equation for Groundwater Transport Within Fractured Systems. In J. F. Gómez, L. Torres, and R. F. Escobar (Editors), *Fractional Derivatives with Mittag-Leffler Kernel*, pages 309–341. Springer, 2019.

35. K. Muhammad Altaf and A. Atangana. Dynamics of Ebola Disease in the Framework of Different Fractional Derivatives. *Entropy*, 21(3):303, 2019.

36. S. Qureshi and A. Atangana. Mathematical Analysis of Dengue Fever Outbreak by Novel Fractional Operators with Field Data. *Physica A: Statistical Mechanics and its Applications*, 526:121127, 2019.

37. W. Wyss. The Fractional Diffusion Equation. *Journal of Mathematical Physics*, 27 (11):2782–2785, 1986.

38. L. Beghin. Fractional Diffusion-type Equations with Exponential and Logarithmic Differential Operators. *Stochastic Processes and their Applications*, 128(7): 2427–2447, 2018.

39. W. R. Schneider and W. Wyss. Fractional Diffusion and Wave Equations. *Journal of Mathematical Physics*, 30(1):134–144, 1989.

40. E. C. De Oliveira and J. A. Tenreiro Machado. A Review of Definitions for Fractional Derivatives and Integral. *Mathematical Problems in Engineering*, 2014, Article ID 238459, 6 pages, 2014.

41. B. A. Jacobs and C. Harley. Application of Nonlinear Time–Fractional Partial Differential Equations to Image Processing via Hybrid Laplace Transform Method. *Journal of Mathematics*, 2018, Article ID 8924547, 9 pages, 2018.

42. R. Metzler and J. Klafter. The Random Walk's Guide to Anomalous Diffusion: A Fractional Dynamics Approach. *Physics Reports*, 339(1):1–77, 2000.

43. K. S. Miller and B. Ross. *An Introduction to the Fractional Calculus and Fractional Differential Equations*. Wiley, New York, 1993.

44. T. M. Atanackovic, S. Pilipovic, B. Stankovic, and D. Zorica. *Fractional Calculus with Applications in Mechanics: Wave Propagation, Impact and Variational Principles*. John Wiley & Sons, New York, 2014.

45. A. El-Kahlout, T. O. Salim, and S. El-Azab. Exact Solution of Time Fractional Partial Differential Equation. *Applied Mathematical Sciences*, 2(52):2577–2590, 2008.

46. R. S. Damor, S. Kumar, and A. K. Shukla. Solution of Fractional Bioheat Equation in terms of Fox's H–function. *SpringerPlus*, 5(1):111, 2016.

47. Y. Pandir and Y. Gurefe. New Exact Solutions of the Generalized Fractional Zakharov–Kuznetsov Equations. *Life Science Journal*, 10(2):2701–2705, 2013.

48. Y. Pandir, Y. Gurefe, and E. Misirli. New Exact Solutions of the Time–Fractional nonlinear Dispersive KdV Equation. *International Journal of Modeling and Optimization*, 3(4):349, 2013.

49. A. Arikoglu and I. Ozkol. Solution of Fractional Differential Equations by using Differential Transform Method. *Chaos, Solitons & Fractals*, 34(5):1473–1481, 2007.

50. S. Momani, Z. Odibat, and V. S. Erturk. Generalized Differential Transform Method for Solving a Space– and Time–Fractional Diffusion–Wave Equation. *Physics Letters A*, 370(5-6):379–387, 2007.

51. Z. Odibat, S. Momani, and V. S. Erturk. Generalized Differential Transform Method: Application to Differential Equations of Fractional Order. *Applied Mathematics and Computation*, 197(2):467–477, 2008.

52. Z. Odibat and S. Momani. A Generalized Differential Transform Method for Linear Partial Differential Equations of Fractional Order. *Applied Mathematics Letters*, 21 (2):194–199, 2008.

53. V. S. Erturk, S. Momani, and Z. Odibat. Application of Generalized Differential Transform Method to Multi–Order Fractional Differential Equations. *Communications in Nonlinear Science and Numerical Simulation*, 13(8):1642–1654, 2008.

54. S. Momani and Z. Odibat. A Novel Method for nonlinear Fractional Partial Differential Equations: Combination of DTM and Generalized Taylor's Formula. *Journal of Computational and Applied Mathematics*, 220(1-2):85–95, 2008.

55. Z. Odibat, S. Momani, and A. Alawneh. Analytic Study on Time–Fractional Schrödinger Equations: Exact Solutions by GDTM. In *Journal of Physics: Conference Series*, volume 96, page 012066. IOP Publishing, 2008.

56. H. Jafari and V. Daftardar-Gejji. Positive Solutions of nonlinear Fractional Boundary Value Problems using Adomian Decomposition Method. *Applied Mathematics and Computation*, 180(2):700–706, 2006.

57. Z. M. Odibat and S. Momani. Application of Variational Iteration Method to nonlinear Differential Equations of Fractional Order. *International Journal of Nonlinear Sciences and Numerical Simulation*, 7(1):27–34, 2006.

58. J.-H. He. Approximate Analytical Solution for Seepage Flow with Fractional Derivatives in Porous Media. *Computer Methods in Applied Mechanics and Engineering*, 167(1-2):57–68, 1998.

59. Z.-B. Li and J.-H. He. Fractional Complex Transform for Fractional Differential Equations. *Mathematical and Computational Applications*, 15(5):970–973, 2010.

60. A. Bekir, Ö. Güner, and A. C. Cevikel. Fractional Complex Transform and Exp–Function Methods for Fractional Differential Equations. In *Abstract and Applied Analysis*, volume 2013, Article ID 426462, 8 pages, 2013.

61. H. Jafari and H. K. Jassim. Application of Local Fractional Variational Iteration Method to Solve System of Coupled Partial Differential Equations Involving Local Fractional Operator. *Applied Mathematics Information Sciences Letters*, 5:1–6, 2017.

62. H. Jafari, K. H. Jassim, and J. Vahidi. Reduced Differential Transform and Variational Iteration Methods for 3–D Diffusion Model in Fractal Heat Transfer within Local Fractional Operators. *Thermal Science*, 22(Suppl. 1):301–307, 2018.

63. H. Jafari. Numerical Solution of Time–Fractional Klein–Gordon Equation by using the Decomposition Methods. *Journal of Computational and Nonlinear Dynamics*, 11(4):041015, 5 pages, 2016.

64. B. A. Jacobs. High-order compact Finite Difference and Laplace Transform Method for the Solution of Time–Fractional Heat Equations with Dirchlet and Neumann Boundary Conditions. *Numerical Methods for Partial Differential Equations*, 32(4): 1184–1199, 2016.

65. B. A. Jacobs and C. Harley. A Comparison of Two Hybrid Methods for Applying the Time–Fractional Heat Equation to a Two Dimensional Function. In *AIP Conference Proceedings*, volume 1558, pages 2119–2122. American Institute of Physics, 2013.

66. B. A. Jacobs and C. Harley. Two Hybrid Methods for Solving Two–Dimensional Linear Time–Fractional Partial Differential Equations. In *Abstract and Applied Analysis*, volume 2014, Article ID 757204, 10 pages, 2014.

67. J. Weideman and L. Trefethen. Parabolic and Hyperbolic Contours for Computing the Bromwich Integral. *Mathematics of Computation*, 76(259):1341–1356, 2007.

68. A. Kuznetsov. On the Convergence of the Gaver–Stehfest Algorithm. *SIAM Journal on Numerical Analysis*, 51(6):2984–2998, 2013.

69. R. Jacquot, J. Steadman, and C. Rhodine. The Gaver–Stehfest Algorithm for Approximate Inversion of Laplace Transforms. *IEEE Circuits & Systems Magazine*, 5(1):4–8, 1983.

70. Y. Zhang. A Finite Difference Method for Fractional Partial Differential Equation. *Applied Mathematics and Computation*, 215(2):524–529, 2009.

71. W. Tian, H. Zhou, and W. Deng. A Class of Second Order Difference Approximations for Solving Space Fractional Diffusion Equations. *Mathematics of Computation*, 84 (294):1703–1727, 2015.

72. X. Chen, F. Zeng, and G. E. Karniadakis. A Tunable Finite Difference Method for Fractional Differential Equations with non–Smooth Solutions. *Computer Methods in Applied Mechanics and Engineering*, 318:193–214, 2017.

73. B. A. Jacobs. A New Grünwald–Letnikov Derivative Derived from a Second–Order Scheme. In *Abstract and Applied Analysis*, volume 2015, Article ID 952057, 9 pages, 2015.

74. R. B. Albadarneha, I. M. Batihab, and M. Zurigatb. Numerical Solutions for Linear Fractional Differential Equations of Order $1 < \alpha < 2$ using Finite Difference Method (FFDM). *International Journal of Mathematics and Computer Science*, 16(1):103–111, 2016.

75. E. Sousa. Numerical Approximations for Fractional Diffusion Equations via Splines. *Computers & Mathematics with Applications*, 62(3):938–944, 2011.

76. C. Tadjeran, M. M. Meerschaert, and H.-P. Scheffler. A Second–Order Accurate Numerical Approximation for the Fractional Diffusion Equation. *Journal of Computational Physics*, 213(1):205–213, 2006.

77. S. Shen, F. Liu, V. Anh, and I. Turner. The Fundamental Solution and Numerical Solution of the Riesz Fractional Advection–Dispersion Equation. *IMA Journal of Applied Mathematics*, 73(6):850–872, 2008.

78. G. J. Fix and J. P. Roop. Least Squares Finite–Element Solution of a Fractional Order Two–Point Boundary Value Problem. *Computers & Mathematics with Applications*, 48(7-8):1017–1033, 2004.

79. W. Deng. Finite Element Method for the Space and Time Fractional Fokker–Planck Equation. *SIAM Journal on Numerical Analysis*, 47(1):204–226, 2009.

80. B. Ghanbari and A. Atangana. An Efficient Numerical Approach for Fractional Diffusion Partial Differential Equations. *Alexandria Engineering Journal*, 2020. doi: 10.1016/j.aej.2020.01.042.

81. L. B. Feng, P. Zhuang, F. Liu, and I. Turner. Stability and Convergence of a New Finite Volume Method for a Two–Sided Space–Fractional Diffusion Equation. *Applied Mathematics and Computation*, 257:52–65, 2015.

82. K. Diethelm, N. J. Ford, and A. D. Freed. A Predictor–Corrector Approach for the Numerical Solution of Fractional Differential Equations. *Nonlinear Dynamics*, 29 (1-4):3–22, 2002.

83. Y. Li and N. Sun. Numerical Solution of Fractional Differential Equations using the Generalized Block Pulse Operational Matrix. *Computers & Mathematics with Applications*, 62(3):1046–1054, 2011.

84. K. Diethelm and A. D. Freed. On the Solution of nonlinear Fractional–Order Differential Equations used in the Modeling of Viscoplasticity. In F. Keil, W. Mackens, H. Voß, and J. Werther (Editors), *Scientific Computing in Chemical Engineering II*, pages 217–224. Springer, 1999.

85. C. Canuto, Y. M. Hussaini, A. Quarteroni, and T. A. Zang. *Spectral Methods: Fundamentals in Single Domains*. Springer Science & Business Media, Berlin, 2007.

86. J. P. Boyd. *Chebyshev and Fourier Spectral Methods*. Courier Corporation, New York, 2001.

87. C. Canuto, Y. M. Hussaini, A. Quarteroni, A. Thomas Jr, et al. *Spectral Methods in Fluid Dynamics*. Springer Science & Business Media, Berlin, 2012.

88. E. H. Doha, A. H. Bhrawy, and S. S. Ezz-Eldien. A new Jacobi Operational Matrix: an Application for Solving Fractional Differential Equations. *Applied Mathematical Modelling*, 36(10):4931–4943, 2012.

89. E. H. Doha, A. H. Bhrawy, and S. S. Ezz-Eldien. Efficient Chebyshev Spectral Methods for Solving Multi–Term Fractional Orders Differential Equations. *Applied Mathematical Modelling*, 35(12):5662–5672, 2011.

90. E. H. Doha, A. H. Bhrawy, and S. S. Ezz-Eldien. A Chebyshev Spectral Method Based on Operational Matrix for Initial and Boundary Value Problems of Fractional Order. *Computers & Mathematics with Applications*, 62(5):2364–2373, 2011.

91. A. H. Bhrawy, A. S. Alofi, and S. S. Ezz-Eldien. A Quadrature Tau Method for Fractional Differential Equations with Variable Coefficients. *Applied Mathematics Letters*, 24(12):2146–2152, 2011.

92. M. A. Zaky. An Improved Tau Method for the Multi–Dimensional Fractional Rayleigh–Stokes Problem for a Heated Generalized Second Grade Fluid. *Computers & Mathematics with Applications*, 75(7):2243–2258, 2018.

93. E. H. Doha, A. H. Bhrawy, and S. S. Ezz-Eldien. An Efficient Legendre Spectral Tau Matrix Formulation for Solving Fractional Subdiffusion and Reaction Subdiffusion Equations. *Journal of Computational and Nonlinear Dynamics*, 10(2):021019, 8 pages, 2015.

94. A. H. Bhrawy, E. H. Doha, D. Baleanu, and S. S. Ezz-Eldien. A Spectral Tau Algorithm Based on Jacobi Operational Matrix for Numerical Solution of Time Fractional Diffusion–Wave Equations. *Journal of Computational Physics*, 293: 142–156, 2015.

95. A. H. Bhrawy, E. H. Doha, J. A. Tenreiro Machado, and S. S. Ezz-Eldien. An Efficient Numerical Scheme for Solving Multi–Dimensional Fractional Optimal Control Problems with a Quadratic Performance Index. *Asian Journal of Control*, 17(6):2389–2402, 2015.

96. E. H. Doha, A. H. Bhrawy, D. Baleanu, S. S. Ezz-Eldien, and R. M. Hafez. An Efficient Numerical Scheme Based on the Shifted Orthonormal Jacobi Polynomials for Solving Fractional Optimal Control Problems. *Advances in Difference Equations*, 2015(1):15, 2015.

97. A. H. Bhrawy, E. H. Doha, S. S. Ezz-Eldien, and M. A. Abdelkawy. A Numerical Technique Based on the Shifted Legendre Polynomials for Solving the Time–Fractional Coupled KdV Equations. *Calcolo*, 53(1):1–17, 2016.

98. X. Li and C. Xu. A Space–Time Spectral Method for the Time Fractional Diffusion Equation. *SIAM Journal on Numerical Analysis*, 47(3):2108–2131, 2009.

99. X. Li and C. Xu. Existence and Uniqueness of the Weak Solution of the Space–Time Fractional Diffusion Equation and a Spectral Method Approximation. *Communications in Computational Physics*, 8(5):1016, 2010.

100. H. Jafari, H. Tajadodi, and D. Baleanu. A Numerical Approach for Fractional Order Riccati Differential Equation using B–Spline Operational Matrix. *Fractional Calculus and Applied Analysis*, 18(2):387, 2015.

101. M. Mahmoudi, M. Ghovatmand, and H. Jafari. An Adaptive Collocation Method for Solving Delay Fractional Differential Equations. *International Journal of Applied and Computational Mathematics*, 5(6):157, 2019.

102. P. Pandey, S. Kumar, H. Jafari, and S. Das. An Operational Matrix for Solving Time–Fractional Order Cahn–Hilliard Equation. *Thermal Science*, 23:2045–2052, 2019.

103. M. Zayernouri and G. E. Karniadakis. Fractional Spectral Collocation Method. *SIAM Journal on Scientific Computing*, 36(1):A40–A62, 2014.

104. M. Zayernouri and G. E. Karniadakis. Fractional Spectral Collocation Methods for Linear and Nonlinear Variable Order FPDEs. *Journal of Computational Physics*, 293: 312–338, 2015.

105. M. M. Khader. On the Numerical Solutions for the Fractional Diffusion Equation. *Communications in Nonlinear Science and Numerical Simulation*, 16(6):2535–2542, 2011.

106. A. Baseri, S. Abbasbandy, and E. Babolian. A Collocation Method for Fractional Diffusion Equation in a Long Time with Chebyshev Functions. *Applied Mathematics and Computation*, 322:55–65, 2018.

107. S. Esmaeili and M. Shamsi. A Pseudo–Spectral Scheme for the Approximate Solution of a Family of Fractional Differential Equations. *Communications in Nonlinear Science and Numerical Simulation*, 16(9):3646–3654, 2011.

108. N. H. Sweilam, A. M. Nagy, and M. M. Mokhtar. On the Numerical Treatment of a Coupled Nonlinear System of Fractional Differential Equations. *Journal of Computational and Theoretical Nanoscience*, 14(2):1184–1189, 2017.

109. M. Samiee, M. Zayernouri, and M. M. Meerschaert. A Unified Spectral Method for FPDEs with Two–Sided Derivatives; Part I: A Fast Solver. *Journal of Computational Physics*, 385:225–243, 2019.

110. J. F. Kelly, H. Sankaranarayanan, and M. M. Meerschaert. Boundary Conditions for Two–Sided Fractional Diffusion. *Journal of Computational Physics*, 376:1089–1107, 2019.

111. H. Hejazi, T. Moroney, and F. Liu. A Finite Volume Method for Solving the Two-Sided Time–Space Fractional Advection–Dispersion Equation. *Central European Journal of Physics*, 11(10):1275–1283, 2013.

112. T. Atanackovic, S. Pilipovic, and D. Zorica. Existence and Calculation of the Solution to the Time Distributed Order Diffusion Equation. *Physica Scripta*, 2009, T136: 014012, 2009.

113. T. Srokowski. Lévy Flights in nonhomogeneous Media: Distributed–Order Fractional Equation Approach. *Physical Review E*, 78(3):031135, 2008.

114. K. Diethelm and N. J. Ford. Numerical Analysis for Distributed-Order Differential Equations. *Journal of Computational and Applied Mathematics*, 225(1):96–104, 2009.

115. G.-H. Gao and Z.-Z. Sun. Two Alternating Direction Implicit Difference Schemes with the Extrapolation Method for the Two–Dimensional Distributed–Order Differential Equations. *Computers & Mathematics with Applications*, 69(9): 926–948, 2015.

116. J. T. Katsikadelis. Numerical Solution of Distributed Order Fractional Differential Equations. *Journal of Computational Physics*, 259:11–22, 2014.

117. M. Abramowitz and I. A. Stegun. *Handbook of Mathematical Functions: with Formulas, Graphs, and Mathematical Tables*. Courier Corporation, Massachusetts, 1965.